

WestminsterResearch

<http://www.westminster.ac.uk/westminsterresearch>

**Effect of age and pregnancy on the murine melanocortin system
in the female reproductive system**

Berruien, N.

This is an electronic version of a PhD thesis awarded by the University of Westminster.
© Miss Nasrin Berruien, 2019.

The WestminsterResearch online digital archive at the University of Westminster aims to make the research output of the University available to a wider audience. Copyright and Moral Rights remain with the authors and/or copyright owners.

Whilst further distribution of specific materials from within this archive is forbidden, you may freely distribute the URL of WestminsterResearch: (<http://westminsterresearch.wmin.ac.uk/>).

In case of abuse or copyright appearing without permission e-mail repository@westminster.ac.uk

**Effect of age and pregnancy on the murine
melanocortin system in the female
reproductive system**

Nasrin Nuri A. Berruien

A thesis submitted in partial fulfilment of the requirements of the
University of Westminster for the degree of Doctor of
Philosophy

January 2019

Abstract

The five melanocortin receptors (MC₍₁₋₅₎) are part of the G-coupled protein receptor (GPCR) family and have been reported to have a role in controlling appetite, modulating inflammation and stress response. The melanocortin receptor accessory proteins (MRAP1 and 2) influence MC receptor transport and signalling. The MCs are activated by proopiomelanocortin (POMC) derivatives: alpha-, beta-, and gamma-melanocyte stimulating hormones and adrenocorticotrophic hormone; while agouti signalling peptide (ASP) and agouti-related protein (AgRP) antagonise the peptide activity. The MCs were previously detected in the male mouse reproductive system, and their expression levels were found to be influenced by age. This thesis aims to investigate the expression of the MC system in the female mouse reproductive system and to determine the influence of age and pregnancy on the expression levels of MCs, accessory proteins, POMC and AgRP.

The gene expression of the MC system in the reproductive axis using RT-qPCR revealed the differential MC expression in the female mouse hypothalamus, pituitary gland, ovary and uterus. Age influenced the expression of MC₅ and POMC, whilst pregnancy altered the expression of MC₂, MC₄ and MC₅. This research reports, for the first time, the characterisation of MRAP1 expression in the hypothalamus and the pituitary gland. The chromogenic RNA *in situ* hybridisation method (RNAscope[®]) enabled MC₃, MC₅ and MRAP2 localisation in the hypothalamus, in the preoptic (rostral and medial) areas and arcuate nucleus. Those areas are known to contain the gonadotropin-releasing hormone (GnRH) neuronal network in the female mouse hypothalamus. The RNAscope[®] studies also detected the expression of MC₃ and MRAP2 in the gonadotrophs and the somatotrophs of the mouse anterior pituitary gland; these findings imply a modulatory role of MC₃ in the anterior pituitary cellular network. The expression of MC₃, MC₅ and MRAP2 was influenced by age and pregnancy. The co-expression of MC₃ and MRAP2 in the hypothalamus and the anterior pituitary gland, implicate the potential regulation of MC₃ responsiveness by MRAP2.

An *in vitro* cell culture model of GPCR signalling “PRESTO-Tango” assay investigated the regulation of MC₃ by the MRAPs and revealed a significant increase in the potency of MC₃ to ACTH₍₁₋₃₉₎, and NDP- α -MSH MC₃ in the presence of MRAP1. These studies also show a reduction in sensitivity of MC₃ to ACTH₍₁₋₃₉₎ with 1:1 co-expression of MC₃: MRAP2 whilst a 1:10 MC₃: MRAP2 expression ratio increased the sensitivity of MC₃ to both ACTH₍₁₋₃₉₎ and NDP- α -MSH. The data obtained in this thesis indicates that the members of the MC system are in close association within areas controlling female reproduction and that the MC system expression is affected by age and pregnancy. Finally, this research reports the regulation of MC₃ by both MRAP1 and MRAP2 *in vitro*.

Acknowledgement

I would like to extend my deepest gratitude to my Director of studies Dr Caroline L. Smith for the support and guidance throughout my PhD research and thesis writing. I would like to thank Caroline for her exemplary mentoring, knowledge and encouragement through my MSc and PhD studies and for all the opportunity and the incredible research experience in her lab. Without Caroline's invaluable help, completing my research would have been impossible.

My sincere thanks also go to my supervisors Dr Joanne F Murray and Dr Paul Le Tissier for generously supplying my research with all the required animal tissues, sections and plasmids and for having me in their lab at the University of Edinburgh which was generously sponsored by the Society of Endocrinology. Their help and guidance with the thesis writing always encouraged me to complete my PhD research. Special thanks to Dr Cynthia Andoniadou for generous contribution and for hosting me in her lab at King's College London; and also, thanks to Alice and John for assisting me with my work and image scanning and for making my visit to their lab quite enjoyable. I would like to express my very great appreciation to Dr Pamela Greenwell for her enthusiasm, for being the best MSc mentor anyone could wish for and for her endless RT-qPCR advice. Also, would like to thank Dr Monika Dowejko, who helped me through my MSc and get started with my PhD research.

Thank you to the Libyan Ministry of Higher Education and Research and the University of Benghazi for Providing me with the opportunity to pursue my postgraduate studies through the MSc and PhD full sponsorship and the support of the Libyan Cultural Department staff. I would like to extend my thanks to the University of Westminster laboratory and research staff for their support and help throughout my PhD journey.

I would like to thank all my friends and colleagues in the PhD Office for making this PhD journey the most enjoyable and for being able to work in the friendliest environment. My thanks are also extended to Karima for always taking care of me through my ups and downs, all the help and advice and the opportunity to do my cell culture work in her lab. Louise and Rachith for the help with thesis writing and help with the microbiology and cell culture advice. Thank you also to Nicola, for making working in the lab fun and also for being the best vocabulary and writing style editor.

Most importantly, a huge thank you to all of my family: Mama and Baba, as always, with their Dua'a and full support I knew I could do this. Both of them were my role models in perseverance and getting the job done. Mohammed, although the youngest, was the big brother who took care of me and making sure my panics at their normal levels. Finally, Arwa and Ranwah, holidays' chilling and forgetting that I had a PhD running back here would not have been possible without them.

Author's Declaration

I declare that the presented research is the author's own work and is original except where referenced in the text. The research project was conducted in accordance with the Guidelines and the Regulations of the University of Westminster.

Table of Contents

Abstract.....	2
Acknowledgement	3
Author’s Declaration	4
List of Tables	8
List of Figures	10
1 The Female Reproductive System	17
1. 1 Background.....	18
1. 1. 1 The reproductive life cycle of the female human	18
1. 1. 2 The reproductive life cycle of the female mouse.....	21
1. 1. 3 Regulation of the reproductive cycle in females.....	24
2 The Melanocortin system.....	26
2. 1 Background.....	27
2. 1. 1 Proopiomelanocortin (POMC)	27
2. 1. 2 The melanocortin peptides.....	29
2. 1. 3 Melanocortin receptors and their expression sites	30
2. 1. 4 Endogenous antagonists	34
2. 1. 5 Melanocortin receptors accessory proteins (MRAPs).....	34
2. 1. 6 The melanocortin system and reproduction	35
3 Materials and Methods.....	36
3. 2 Materials	37
3. 2 Methods	38
3. 2. 1 Tissue Collection	38
3. 2. 2 RNA Extraction.....	39
3. 2. 3 Complementary DNA (cDNA) synthesis.....	40
3. 2. 4 Reverse transcription - quantitative polymerase chain reaction (RT-qPCR).....	41
3. 2. 5 Chromogenic RNA in situ hybridisation, RNAscope®	49
4 Molecular and cellular characterisation of the MC system in the female mouse hypothalamus	62
4. 1 Background.....	63
4. 1. 1 GnRH neurons distribution and axonal projections	63
4. 1. 2 Postnatal GnRH.....	64
4. 1. 3 GnRH and puberty	65
4. 1. 4 GnRH pulsatile release	66
4. 1. 5 GnRH surge and the estrous cycle of mice	66
4. 1. 6 Hypothalamic control of pregnancy.....	67
4. 1. 7 The different approaches on hypothalamic organisation	69
4. 2 Methods	70
4. 3 Results	72
4.4 Discussion:.....	99

5 Molecular and cellular characterisation of the MC system in the female mouse pituitary gland	107
5.1 Background.....	108
5. 1. 1 Components of the anterior pituitary gland.....	108
5. 1. 2 Regulation of gonadotroph function.....	111
5. 2 Methods	116
5. 3 Results	118
5. 3 Discussion	143
6 Molecular and cellular characterisation of the MC system in the female mouse ovary.....	152
6.1 Background.....	153
6. 1. 1 Murine Oogenesis.....	153
6. 1. 2 Folliculogenesis.....	154
6. 1. 3 Ovulation.....	155
6. 1. 4 Ovarian luteinisation and luteolysis.....	156
6. 1. 5 Implication of the MC system in the functions of the mouse ovary	158
6. 2 Methods	158
6. 3 Results	160
6. 4 Discussion	169
7 Molecular and cellular characterisation of the MC system in the female mouse uterus.....	173
7. 1 Background.....	174
7. 1. 1 Postnatal uterine development	174
7. 1. 2 Uterine changes during the estrous cycle	175
7. 1. 3 Uterine preparation for implantation, decidualisation and maintenance of pregnancy.....	177
7. 1. 4 The possible role of the melanocortin system in the mouse uterus.....	181
7. 2 Methods	182
7. 3 Results	183
7. 4 Discussion	193
8 Melanocortin 3 receptor (MC₃) regulation by MRAP1 and MRAP2 using the PRESTO-Tango platform	198
8. 1 Background.....	199
8. 1. 1 Melanocortin receptors signalling pathways.....	200
8. 1. 2 The regulation of MCs by the MRAPs.....	201
8. 1. 3 The design of the PRESTO-Tango assay.....	203
8. 2 Methods	206
8. 2. 1 HTLA cells	206
8. 2. 2 Transforming E. coli (DH5 α) with the different plasmids.....	206
8. 2. 3 Co-transfecting HTLA cells with pCherry and Green fluorescent proteins (eGFP) plasmids.....	208
8. 2. 4 The MC ₃ -Tango transfection.....	212
8. 2. 5 MC ₃ -Tango and MRAP1 or MRAP2 transfection	215
8. 2. 6 PRESTO-Tango data analysis.....	215
8. 2. 7 HTLA cells Viability test (MTT assay)	216
8. 3 Results	217

8. 4 Discussion	230
9 Discussion and future recommendations.....	234
9. 1 General Discussion.....	235
9. 2 Recommendations for future work.....	240
References	241
Appendices	271
Appendix 1: Example of the RT-qPCR expression analysis the MC system (POMC in pituitary gland)	271
Appendix 2: RNAscope® pre-treatment optimisation for the hypothalamus.....	272
Appendix 3. A: Reference genes expression stability- C57BL/6 female mouse hypothalamus.....	273
Appendix 3. B: Reference genes expression stability- C57BL/6 female mouse pituitary gland	274
Appendix 3. C: Reference genes expression stability- C57BL/6 female mouse ovary	275
Appendix 3. D: Reference genes expression stability- C57BL/6 female mouse uterus	276
Appendix 4: The RNAscope® 2.5HD brown assay: the expression of MC3, MC5 and MRAP2 in the intermediate lobe of the female mouse pituitary gland.....	277
Appendix 5: The Full Sequence Map for 1436 pcDNA3 Flag HA.....	278
Appendix 6: PRESTO-Tango: choosing a transfection concentration for MC ₃ -Tango	279
Appendix 7: PRESTO-Tango: Determination of HTLA incubation period post-transfection and addition of stimulants	280
Appendix 8: PRESTO-Tango: Determining MRAP1 concentrations to be used in the co-transfection with MC3-Tango	281

List of Tables

Table 1-1: Illustrates the main developmental and hormonal milestones in female humans and mice.....	22
<i>Table 3-1: Mouse ages and their physiological status.....</i>	<i>39</i>
Table 3-2: Reference genes names, function, accession numbers and product length.....	42
Table 3-3: Primers used for determining primer pair amplification efficiency.....	46
Table 3-4: RNAscope® probes used in the RNAscope® Brown assays.....	52
Table 3-5: RNAscope® probes used in the RNAscope® Duplex assays.....	55
<i>Table 3-6: Scoring guidelines for RNAscope® staining by ACD Diagnostics.....</i>	<i>59</i>
Table 4-1: Amplification efficiency of CANX and YWHAZ in the hypothalamus.....	74
<i>Table 4-2: Primer pair amplification efficiencies for the MC₍₁₋₅₎, MRAP1, MRAP2, POMC and AgRP.....</i>	<i>76</i>
Table 4-3: MC system expression in the female hypothalamus.....	80
Table 5-1: Anterior pituitary cells and their percentage, distribution, hormones and functions.....	109
<i>Table 5-2: Hypothalamic regulators of the anterior pituitary hormone-producing cells.....</i>	<i>110</i>
Table 5-3: Amplification efficiency of CANX and YWHAZ in the pituitary gland.....	120
Table 5-4: MC system expression in the female pituitary gland.....	123
Table 5-5: The percentage of MC ₃ expression in the RNAscope® brown assay in the mouse anterior pituitary gland.....	128
Table 5-6: The percentage of MC ₅ expression in the RNAscope® brown assay in the mouse anterior pituitary gland.....	130
Table 5-7: The percentage of MRAP2 expression in the RNAscope® brown assay in the mouse anterior pituitary gland.....	132
Table 5-8: The percentage of MC ₃ / MRAP2 expression in the RNAscope® Duplex assay in the mouse anterior pituitary gland.....	136
Table 6-1: Amplification efficiency of ACTB, ATP5B and YWHAZ in the female ovary.....	162
Table 6-2: MC system expression in the mouse ovary.....	165
Table 7-1: E ₂ and P ₄ Concentrations in relation to changes in uterus in mouse estrous cycle.....	176
Table 7-2: Amplification efficiency of ACTB, ATP5B and YWHAZ in the female uterus.....	185
Table 7-3: MC system expression in the uterus.....	188
Table 8-1: The melanocortin receptors and their melanocortin natural and synthetic analogues.....	199
Table 8-2: The ligands used to treat the MC ₃ -Tango in the PRESTO-Tango assay.....	214

Table 8-3: PRESTO-Tango of MC ₃ response to the melanocortin peptides.....	219
Table 8-4: PRESTO-Tango of MC ₃ response to antagonistic SHU9119 treatment.....	220
Table 8-5: PRESTO-Tango of MC ₃ response with or without MRAP1-pCDNA3.1 co-transfection.....	225
Table 8-6: PRESTO-Tango of MC ₃ response with or without MRAP2-pCDNA3.1- myc co-transfection..	228

List of Figures

Figure 1.1: Hormones concentrations during the menstrual cycle in women.....	20
Figure 2.1: Gene structure and post-translational processing of the pro-opiomelanocortin molecule (POMC).....	28
Figure 2.2: The structure of class A G protein coupled receptor (GPCR).....	30
Figure 3.1: RT-qPCR melt curve and amplification curves.....	47
Figure 3.2: The RNAscope® in situ hybridisation workflow.....	51
Figure 3.3: RNAscope® HD 2.5 Brown assay in the uterus of 2 weeks old mouse.....	58
Figure 3.4: Selecting an area for quantification analysis in female mouse pituitary gland.....	60
Figure 3.5: Dividing the area to be quantified for expression into small squares for cells/ Expression counting.....	60
Figure 4.1: GnRH neurons locations within the mouse hypothalamus.....	64
Figure 4.2: Hypothalamic sections showing the regions of interest studied with RNAscope®.....	71
Figure 4.3: GeNorm ranking order of reference genes' stability in the female mouse hypothalamus.....	72
Figure 4.4: Variation score (V- score) by GeNorm.....	73
Figure 4.5: A representative example of the data acquired for the calculation of primer pair efficiency (MC ₅ standard curve).....	75
Figure 4.6: MC ₁ and MC ₂ expression in the female mouse hypothalamus.....	77
Figure 4.7: MC ₃₋₅ , MRAP1 and MRAP2 expression in the female mouse hypothalamus.....	78
Figure 4.8: POMC and AgRP expression in the female mouse hypothalamus.....	79
Figure 4.9: Gel electrophoresis of RT-qPCR of MC system in the hypothalamus.....	81
Figure 4.10: The RNAscope® 2.5HD Brown assay in the female mouse hypothalamus.....	82
Figure 4.11: The RNAscope® 2.5HD Duplex assay in the female mouse hypothalamus.....	83
Figure 4.12: RNAscope® 2.5HD Brown assay of MC ₃ in rPOA of female mouse hypothalamus.....	85
Figure 4.13: RNAscope® 2.5HD Brown assay of MC ₅ in rPOA of female mouse hypothalamus.....	86
Figure 4.14: RNAscope® 2.5HD Brown assay of MRAP2 in rPOA of female mouse hypothalamus.....	87
Figure 4.15: RNAscope® 2.5HD Duplex assay showing MRAP2 (C1-green)-MC ₃ (C2-red) expression in rPOA of female mouse hypothalamus.....	88
Figure 4.16: RNAscope® 2.5HD Brown assay of MC ₃ in mPOA of female mouse hypothalamus.....	90
Figure 4.17: RNAscope® 2.5HD Brown assay of MC ₅ in mPOA of female mouse hypothalamus.....	91

Figure 4.18: RNAscope® 2.5HD Brown assay of MRAP2 in mPOA of female mouse hypothalamus.....	92
Figure 4.19: RNAscope® 2.5HD Duplex assay showing MRAP2 (C1-green)-MC ₃ (C2-red) expression in mPOA of female mouse hypothalamus.....	93
Figure 4.20: RNAscope® 2.5HD Brown assay of MC ₃ in the arcuate nucleus of female mouse hypothalamus.....	95
Figure 4.21: RNAscope® 2.5HD Brown assay of MC ₅ in the arcuate nucleus of female mouse hypothalamus.....	96
Figure 4.22: RNAscope® 2.5HD Brown assay of MRAP2 in the arcuate nucleus of female Mouse hypothalamus.....	97
Figure 4.23: RNAscope® 2.5HD Duplex assay showing MRAP2 (C1-green)-MC ₃ (C2-red) expression in the arcuate nucleus of female mouse hypothalamus.....	98
Figure 5.1: Hormonal pituitary content of MC ₃ ^{-/-} and wild type male (A) and female (B) adult mice.....	115
Figure 5.2: GeNorm ranking order of reference genes stability in the female mouse pituitary gland.....	118
Figure 5.3: Variation score (V- score) by GeNorm.....	119
Figure 5.4: <i>POMC</i> expression in the female mouse pituitary gland.....	120
Figure 5.5: <i>MC₃</i> and <i>AgRP</i> expression in the female mouse pituitary gland.....	121
Figure 5.6: <i>MRAP1</i> and <i>MRAP2</i> expression in the female mouse pituitary gland.....	122
Figure 5.7: <i>MC₄</i> and <i>MC₅</i> expression in the female mouse pituitary gland.....	123
Figure 5.8: Gel electrophoresis of RT-qPCR of MC system in the pituitary gland.....	124
Figure 5.9: RNAscope® 2.5HD single-plex (brown) assay in the female mouse pituitary gland.....	125
Figure 5.10: RNAscope® 2.5HD Brown assay of MC ₃ in female mouse anterior pituitary gland.....	127
Figure 5.11: RNAscope® 2.5HD Brown assay of MC ₅ in female mouse anterior pituitary gland.....	129
Figure 5.12: RNAscope® 2.5HD Brown assay of MRAP2 in female mouse anterior pituitary gland.....	131
Figure 5.13: Comparison between MC ₃ , MC ₅ and MRAP2 expression in RNAscope® 2.5HD brown of the female mouse pituitary gland.....	133
Figure 5.14: RNAscope® 2.5HD duplex assay in female mouse pituitary gland.....	134
Figure 5.15: RNAscope® 2.5HD Duplex assay showing MC ₃ (C1)-MRAP2 (C2) expression in the female mouse pituitary gland.....	135
Figure 5.16: RNAscope® 2.5HD Duplex assay showing MC ₃ (C1)-GH (C2) expression in the	

female mouse pituitary gland.....	138
Figure 5.17: RNAscope® 2.5HD Duplex assay showing MC ₃ (C1)-LHβ (C2) expression in the female mouse pituitary gland.....	139
Figure 5.18: RNAscope® 2.5HD Duplex assay showing MRAP2 (C1)-GH (C2) expression after channel swap in the female mouse pituitary gland.....	141
Figure 5.19: RNAscope® 2.5HD Duplex assay showing MRAP2 (C1)- LHβ (C2) expression after channel swap in the female mouse pituitary gland.....	142
Figure 6.1: GeNorm ranking order of reference genes stability in the female mouse ovary.....	160
Figure 6.2: Variation score (V- score) by GeNorm.....	161
Figure 6.3: MC ₂ , MC ₄ and MC ₅ expression in the female mouse ovary.....	163
Figure 6.4: MRAP1 and MRAP2 expression in the female mouse ovary.....	164
Figure 6.5: POMC (truncated transcript) and AgRP expression in the female mouse ovary.....	165
Figure 6.6: Gel electrophoresis of RT-qPCR of MC system in the female mouse ovary.....	166
Figure 6.7: RNAscope®2.5HD single-plex (brown) assay in the female mouse ovary.....	167
Figure 6.8: RNAscope® 2.5HD single-plex (brown) assay of MC ₃ , MC ₅ and MRAP2 in the female mouse ovary.....	168
Figure 7.1: GeNorm ranking order of reference genes stability in the female mouse uterus.....	184
Figure 7.2: Variation score (V- score) by GeNorm.....	185
Figure 7.3: MC ₂ , MC ₄ and MC ₅ expression in the female mouse uterus.....	187
Figure 7.4: POMC (truncated transcript) and AgRP expression in the female mouse uterus.....	188
Figure 7.5: Gel electrophoresis of RT-qPCR of MC system in the female mouse uterus.....	189
Figure 7.6: RNAscope® 2.5HD single-plex (brown) assay in the female mouse uterus.....	190
Figure 7.7: RNAscope® 2.5HD single-plex (brown) assay of MC ₃ and MRAP2 in the female mouse uterus.....	191
Figure 7.8: RNAscope® 2.5HD single-plex (brown) assay of MC ₅ in the female mouse uterus.....	192
Figure 8.1: The PRESTO-Tango schematic design.....	204
Figure 8.2: Transfection efficiency of the pmCHERRY-N1 plasmid in HTLA cells.....	210
Figure 8.3: Co-transfection efficiency of the pCDNA3-EGFP and pmCHERRY-N1 plasmid in HTLA cells.....	210

Figure 8.4: Mammalian expression vector.....	211
Figure 8.5: The Sequences map of the MC ₃ -Tango.....	213
Figure 8.6: Bar chart of PRESTO-Tango assay of MC ₃ in HTLA cells.....	217
Figure 8.7: PRESTO-Tango dose-response curve of MC ₃ in the HTLA cells.....	218
Figure 8.8: PRESTO-Tango dose-response curve of MC ₃ in the HTLA cells.....	220
Figure 8.9: PRESTO-Tango dose-response curve of MC ₃ in the HTLA cells.....	221
Figure 8.10: Bar chart of PRESTO-Tango assay of MC ₃ -Tango/MRAP1-pCDNA3.1 or MC ₃ -Tango/ MRAP2-myc co-transfected HTLA cells.....	222
Figure 8.11: PRESTO-Tango dose-response curve MC ₃ -Tango and MRAP1- pCDNA3.1 co- transfection in HTLA cells.....	224
Figure 8.12: PRESTO-Tango dose-response curve of MC ₃ -TangoHTLA cells co-transfected with different concentrations of MRAP2-myc.....	226
Figure 8.13: PRESTO-Tango dose-response curve MC ₃ -Tango and 0.5 ng of MRAP2- myc co- transfection in HTLA cells.....	227
Figure 8.14: Cell viability of transfected and co-transfected HTLA cells.....	229

Abbreviations

18S	18S ribosomal RNA
3V	Third ventricle
AC	Anterior commissure
ACTH	Adrenocorticotrophic hormone
ACTB	Beta-actin
AgRP	<i>Agouti</i> related protein
AHA	Anterior hypothalamic area
ANOVA	Analysis of variance
ASP	<i>Agouti</i> signalling protein
ATP5B	Adenosine triphosphate (ATP) synthase
AVPV	Anteroventral periventricular area
B2M	Beta- 2- microglobulin
Ca ⁺⁺	Calcium ions
cAMP	Cyclic adenosine monophosphate
CANX	Calnexin
cDNA	Complementary deoxyribonucleic acid
CLIP	Corticotropin-like intermediate peptide
CL	Corpus luteum
COC	Cumulus-oocyte-complex
CRF -1/2	Corticotropin releasing factor receptor 1/2
CRH	Corticotropin releasing hormone
CT	Threshold crossing point
CYC1	Cytochrome C isoform 1
D1/D2R	Dopamine receptor 1 and 2
DAB	3,3'-diaminobenzidine
DAPB	Dihydrodipicolinate reductase B
DMEM	Dulbecco's modified eagle's medium
DNA	Deoxyribonucleic acid
dNTPs	Deoxynucleotides triphosphates
DPC	Days post coitus
dsDNA	Double stranded
E	Amplification efficiency
E ₂	Estrogen
E-GFP	Enhanced –green fluorescent protein and plasmid
EIF4A2	Eukaryotic translation initiation factor 4A2
ER/ER α /ER β	Estrogen receptor alpha or beta.
FFPE	Formalin-fixed paraffin embedded
FGD	Familial glucocorticoid deficiency
FGFs/FGFR	Fibroblast growth factors and receptor
FIGLA	Factor in the germline alpha
FSH/ FSH- β	Follicular stimulating hormone/ beta subunit
GABA	Gamma-aminobutyric acid
GAGs	Glycosaminoglycans
GAPDH	Glyceraldehyde- 3- phosphate dehydrogenase
GH	Growth hormone
GHSR1-a	Growth hormone secretagogue receptor or ghrelin receptor
GHRH/GHRHR	Growth hormone releasing hormone and receptor
GnRH/ GnRHR	Gonadotropin releasing hormone and receptor
GPCR	Guanine-protein coupled receptor
α -GSU	Alpha-glycoprotein subunit
hCG	Human choriogonadotropin
HPA	Hypothalamic-pituitary- adrenal
HPG	Hypothalamic-pituitary-gonadal
HPO	Hypothalamic-pituitary-ovarian axis
3 β -HSD	3 beta-hydroxysteroid hydrogenases
IFG-I	Insulin-like growth factor-I
IL-1/ IL-1 β /IL-10	Interleukin-1/ interleukin-1 beta/interleukin 10
INF- γ	Interferon gamma

IP ₃	Inositol triphosphate
JAK2	Janus kinase 2
Kiss ^{ARC} / Kiss ^{AVPV}	Kisspeptin neurons in the arcuate and anteroventral periventricular areas
KitL	Tyrosine kinase receptor and ligand
LB agar	Luria broth nutrient agar
LH / LH-β	luteinising hormone / beta subunit
β- and γ -LPH	Beta- and gamma-lipotropic hormone
M	Standard curve slope
MTI	Melanotan or NDP- α-MSH (α-MSH analogue)
MBH	Mediobasal hypothalamus
MC- MC ⁽¹⁻⁵⁾	Melanocortin- melanocortin receptors (1-5)
MCH and MCH-R1	Melanin-concentrating hormone and receptor
μg	Microgram
mg	Milligram
mIU or IU	Milli-international unit or international unit
μl	Micro litre
ml	Millilitre
μm ²	Squared micro metre
mPOA	Medial preoptic area
MRAP 1 and 2	Melanocortin receptor accessory proteins 1 and 2
mRNA	Messenger ribonucleic acid
MS	Medial septum
α-, β-, and γ-MSH	Alpha-, beta- and gamma- melanocyte stimulating hormone
MTT	3-(4,5-dimethyl-2-thiazolyl)-2,5-diphenyl-2H-tetrazolium bromide reagent
NBF	Neutral buffered formalin
NFκB	Nuclear factor kappa-B
ng	Nanogram
NHS	National Health Services
NICE	National Institute for Care Excellence
nm	Nanometre
NOBOX	Newborn ovary Homeobox
NO-RT	No- reverse transcriptase
NTC	Non-template control
NPY	Neuropeptide Y
OVLTL	Organum vasculosum of lamina terminalis
P ₄	Progesterone
PC 1/2	Prohormone convertases 1 and 2
PBS	Phosphate buffered saline
pg	Pico gram
PGF2α	Prostaglandin F2α
Pi3K/ERK	Phosphatidylinositol-3-Kinase/ Extracellular Signal-Regulated Kinase
PND	Postnatal day
POMC	Proopiomelanocortin
POLR2A	DNA-directed RNA polymerase II subunit RPB1
PPIB	Peptidylprolyl Isomerase B
PR	Progesterone receptor
R ²	Coefficient of determination
RPL13A	Ribosomal protein L 13a
rPOA	Rostral preoptic area
RT	Reverse transcriptase
RT-qPCR	Reverse transcription-quantitative polymerase chain reaction
SDHA	Succinate dehydrogenase complex flavoprotein subunit A
SNP	Single nucleotide polymorphism
SSC	Saline-sodium-citrate
SSTR2	Somatostatin receptor 2
STAT1	Signal transducer and activator of transcription signalling pathway

ST.DEV	Standard deviation
TBE	Tris/Borate/EDTA (Ethylenediaminetetraacetic acid)
TGF-β1	Transforming growth factor-beta1
TNFα /TNF-γ	Tumour necrosis factor alpha / Tumour necrosis factor - gamma
TRH	Thyroid-releasing hormone
TSH	Thyroid-stimulating hormone
UBC	Ubiquitin C
UV	Ultra violet
W/V	Weight/Volume
V	Volts
VIP	Vasoactive intestinal peptide
VEGF	Vascular endothelial growth factor
YWHAZ	Tyrosine-3-monooxygenase/tryptophan 5- monooxygenase activation protein zeta

1 The Female Reproductive System

1. 1 Background

Effective reproductive activity in all mammalian females requires the coordinated activity of the hypothalamic-pituitary-ovarian (HPO) axis. The female reproductive system comprises the ovaries, oviducts, uterus, external genitalia and the breast. It also includes the hypothalamus and the pituitary gland to form an axis that controls the primary functions of the reproductive system. The primary functions are gametogenesis, folliculogenesis, steroidogenesis, the initiation and maintenance of pregnancy and preparing for parturition and lactation. The HPO axis is responsible for coordinating the synchronised cyclicity of the hormonal events of the menstrual cycle in humans, primates, bats and elephant shrews; and the estrous cycle in other mammals. The HPO axis control is complex, since the 1930s, it was grossly postulated that the control involved a feedback mechanism which requires different elements within different cells, primarily the gonadotropin-releasing hormone (GnRH) from the hypothalamus, luteinizing hormone (LH) and follicular stimulating hormone (FSH) from the anterior pituitary gland and the sex steroid secreted mostly by the ovarian cells (Hohlweg and Junkmann, 1932).

1. 1. 1 The reproductive life cycle of the female human

From birth until puberty, primordial follicles commence growth but do not grow past the antral stage because there is not the correct endocrine milieu to support further growth. Until puberty, the hypothalamic control is inhibited, and hence, the secretion of both FSH and LH is also suppressed. The onset of puberty is associated with the onset of pulses of hypothalamic hormone gonadotropin-releasing hormone (GnRH): these pulses tend to occur at night, and the frequency of release is initially erratic. As puberty progresses, the pattern of release becomes more regular over the entire 24 h a day. Each pulse of GnRH from the hypothalamus elicits a pulse of LH from the anterior pituitary gland (Plant *et al.*, 2014). Different pathways have been found to be involved in stimulating the GnRH pulse generator in the hypothalamus, this will be discussed in more detail in Chapter 4. Although it is not possible to identify the exact day of the onset of puberty, the first day of menses defines the first day of the menstrual cycle.

The menstrual cycle in women lasts for 28 ± 5 days. It is divided into three phases: menstrual (days 1-5), proliferative (days 6-14) and secretory (days 15-28). These three

phases reflect changes that are occurring within the uterus. The cycle can also be divided into two phases if referring to ovarian activity: the follicular phase (days 1-14) and the luteal phase (days 15-28). The changes in hormones are illustrated in Figure 1.1.

Follicular phase: estrogen and progesterone are at low concentration due to loss of corpus luteum of previous cycle (about 150 pg/ml and almost 0 ng/ml respectively). The low estrogen concentration leads to the removal of the negative feedback on the FSH production causing a rise in the latter's concentration (> 20 mIU/ml) while LH remains at concentrations lower than 10 mIU/ml (Espey and Richards, 2006). Approaching next menses, FSH starts to decline as it undergoes inhibition by the rising estrogen concentration (about 300 pg/ml), secreted by the maturing follicles. This dramatic rise in estrogen causes a sharp increase in LH concentration causing a LH surge (40 mIU/ml) and henceforth, ovulation (Espey and Richards, 2006).

Luteal phase: following ovulation, the corpus luteum is formed and starts producing progesterone (reaching a concentration of 20 ng/ml). In case of pregnancy, progesterone concentrations remains high due to formation of the placenta which also secretes progesterone (Espey and Richards, 2006). If there is no pregnancy, the corpus luteum undergoes programmed atresia leading to the decline of progesterone at the end of the luteal phase. Estrogen is also secreted by the ovulatory corpus luteum but at lower concentration than that seen during ovulation (about 200 pg/ml) and also declines due to the loss of corpus luteum at the end of the cycle. Due to the effect of luteal estrogen and progesterone concentrations, LH drops sharply after the surge to about 5 mIU/ml while FSH gradually decrease reaching 7 mIU/ml. The latter starts to increase again at the end of the luteal phase due to the decrease in luteal estrogen and the start of the next menstrual cycle (Espey and Richards, 2006).

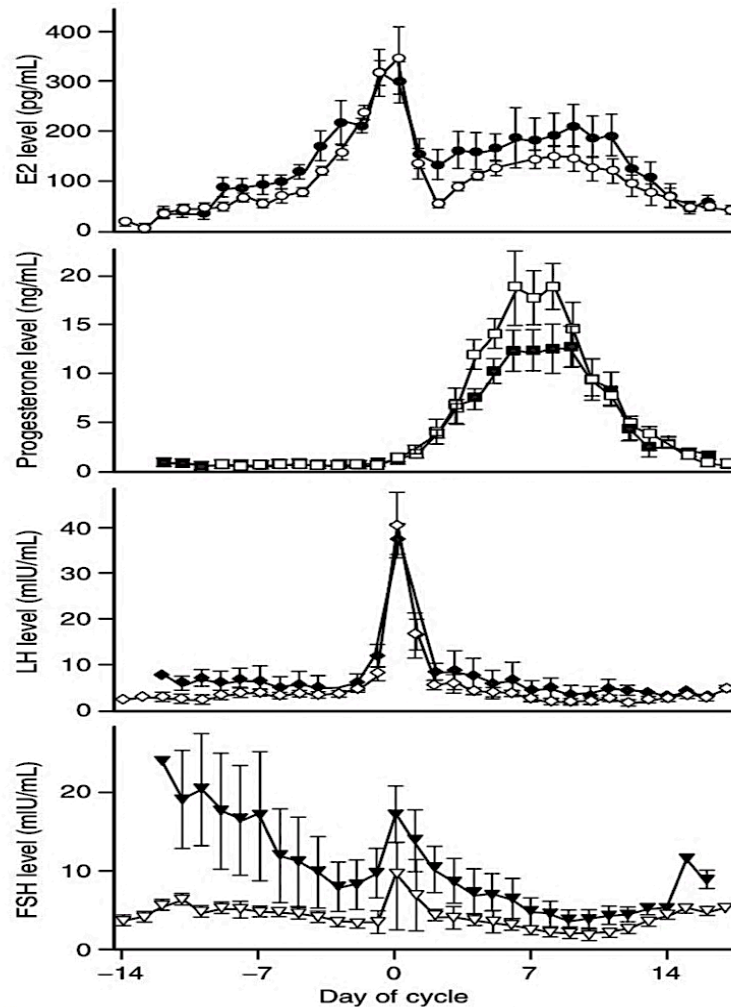


Figure 1.1: Hormone concentrations during the menstrual cycle in women. The menstrual cycle is 28 ± 5 days. It is divided to ovarian phases: follicular (days 1-14) and luteal (days 15- 28). Reprinted from Espey (2006) with permission from Elsevier.

If conception occurs, pregnancy in women lasts about 290 days. Different tissues are involved in maintaining pregnancy. During the first 6-8 weeks, the progesterone and estrogen synthesised and secreted from the corpus luteum are responsible for the maintenance of the pregnancy until the placenta is formed and becomes fully functional, replacing the corpus luteum in secreting progesterone. Progesterone concentrations gradually increase, then remain constant throughout pregnancy once it reaches a plateau as it is produced by the placenta. Just before the onset of labour, progesterone concentrations fall dramatically (Griffin and Ojeda, 2004).

Menopause is the cessation of menses which occurs due to the ovarian failure that is mediated by neuroendocrine hormonal fluctuations. The transition to menopause

occurs gradually and is characterised by shorter follicular phase leading to shorter cycles. Within the ovary, there are few, if any, mature follicles as well as reduced numbers of primary and secondary follicles. Peri-menopausal women with a regular menstrual cycle have lower circulating estradiol concentrations (Burger, 2002). Progesterone concentrations remain normal due to normal secretory phase. However, progesterone eventually declines in older women. There is also an increase in the circulating concentrations of FSH as a result of a decrease in ovarian estrogen synthesis and release and therefore a decrease in negative feedback (Sherman and Korenman, 1975).

Different types of studies use different species. In this research, the female mouse (strain C57BL/6) was the species of choice because of the large body of work which has been carried out on mice and the availability of transgenic and tissue specific knockouts.

1. 1. 2 The reproductive life cycle of the female mouse

The female inbred mouse (such as A/J, BALB/c and C57BL/6) has a lifespan of approximately 2-3 years. The mature female mouse is a spontaneous ovulator, and ovulation occurs every 4-5 days as part of the estrous cycle. The murine estrous cycle is divided into four phases with the length of the phase indicated parenthesis: proestrus (12-14 hours), estrus (25-27 hours), metestrus (6-8 hours), and diestrus (55-57 hours). The female mouse is a fast breeder (producing 5-10 offspring per pregnancy) with a gestational period that lasts 19-21 days. Post-partum ovulation occurs; however, if this does not result in pregnancy then regular estrous cycles and hence ovulation will not occur again until lactation has ceased (usually about 3 weeks) as reviewed by Bronson *et al.* (1968). The following sections will concentrate on the regulatory mechanisms that occur during the oestrous cycle of mice. Table 1.1 compares the reproductive cycles of female humans and mice.

Table 1. 1: Illustrates the main developmental and hormonal milestones in female humans and mice.

Developmental stage	Human	Mouse
Reproductive lifespan	30-38 years	16-20 months
Formation of female ovaries	16 weeks of gestation	9.5 days of gestation
The timing of peak number of oogonia	20 weeks of pregnancy (reaching 6-7 million); most undergoes atresia before birth and only 1-2 million follicles persist after birth	9-13 days of gestation (reaching 20,000 on day 14 of gestation); most undergoes atresia leaving 12,000 primordial follicles at birth
The appearance of first primary follicles	26 weeks of gestation	Day 3 after birth
The appearance of first secondary follicles	26 weeks of gestation	Day 21 after birth
Onset of puberty	12-14 years (first menstrual flow) but could occur as early as 9 years as ovaries are responsive to HPO axis 2-4 years earlier.	30-35 days (vaginal opening and cornified epithelium on smear). Ovaries are responsive 16-20 days earlier.
Cycle	Menstrual	Estrous
Length	23-33 days	4-5 days
Implantation of a fertilised ovum	Day 7 after fertilisation	Day 5 post-coitus (dpc)
Gestation Period	270-290 days (38 weeks)	19-21 days
Corpus luteum of pregnancy	Time CL of pregnancy required to maintain pregnancy: first 6 to 8 weeks until placenta is formed.	Required for the entire gestation period
Fertility postpartum	First fertilisation is about 6 weeks after parturition if no lactation. If lactation occurs, then return to fertility is a function of the lactation stimulus and maternal nutritional status.	First ovulation is 12-18 hours after giving birth. If conception does not occur then first estrus will be 3-4 days after lactation ceases.

CL: corpus luteum, dpc: days post coitus, HPO: hypothalamic-pituitary-ovarian axis. The content of the table informed by Bronson *et al.* (1968) and Johnson (2013).

1. 1. 2. 1 Hypothalamic regulation of fertility in the mouse

The hypothalamus contributes to the regulation of the HPO axis through the release of gonadotropin-releasing hormone (GnRH) which stimulates the gonadotropin secretion (FSH and LH) from the anterior lobe of the pituitary glands. The pattern of the gonadotropin secretion depends mainly on the pattern through which GnRH is released. There are two patterns of GnRH release: the pulsatile GnRH release and GnRH surge. The regulation of GnRH release and its effect on gonadotropins secretion will be discussed in further detail in chapter 4.

1. 1. 2. 2 Pituitary gland regulation of fertility in the mouse

In the pituitary gland, GnRH stimulates gonadotrophs to synthesise and secrete two glycoproteins, FSH and LH. Stimulated FSH receptors on the granulosa cells of the ovaries activate a signal pathway that promotes follicular development in the form of cell differentiation and increased gene expression of the enzymes involved in estrogen and progesterone synthesis (Levine, 2014). During the later stage of the follicular phase of the ovulatory cycle, higher circulating concentrations of estradiol act upon the hypothalamic-pituitary axis which leads to the LH surge. This surge results in the production of more androgens by theca cells; it also stimulates the maturation of the oocyte and induces ovulation and the formation of the corpus luteum (Levine, 2014).

1. 1. 2. 3 Ovarian roles in mouse female fertility

The ovary is composed of three compartments, the follicular tissue, the interstitial stroma and the corpus luteum; the latter is formed from the follicle after the release of the ovum. All three compartments, upon gonadotropin stimulation, synthesise steroids, estrogen, progesterone and testosterone. When a steroid ligand binds to its receptor, usually in the cytoplasm, the bound receptor becomes a transcription factor. The bound receptor is translocated to the nucleus and binds to response elements on target genes to cause gene transcription. The regulation of the ovarian function is reviewed in chapter 6.

1. 1. 2. 4 Uterine roles in female mouse fertility

In the murine uterus, the role of estradiol is pronounced during the proliferative phase of the estrous cycle leading to a proliferation of the luminal and glandular endometrial epithelia. Progesterone's role is mainly detected in the luteal phase of the cycle (Wood *et al.*, 2007). Progesterone causes a profound increase in the glandular epithelium, stroma and the myometrium. Progesterone also stimulates the gland to synthesise and release their secretions into their lumina preparing the uterine tissue for implantation and pregnancy (Johnson, 2013). The regulation of the uterine function is reviewed in chapter 7. In the mammary gland, there is a rise in progesterone receptor expression before ovulation, increased progesterone signalling, therefore leads to proliferation, branching and differentiation of the ductal and glandular system of the mammary gland preparing the mammary gland for pregnancy and lactation (McNeilly, 2006).

1. 1. 3 Regulation of the reproductive cycle in females

Different physiological and pathological conditions could affect various aspects of the reproductive axis in all female species. In the hypothalamus, it has been demonstrated that the GnRH neurons and axons have communications with neuropeptide Y (NPY) and its role in stimulating food intake and inhibiting the GnRH release as revealed by NPY knockout female mice (Hill *et al.*, 2008). Other neuropeptides could influence the three components of the reproductive axis, hypothalamus, pituitary gland and the ovaries; these include prolactin and growth hormone (GH). Both of which were found to stimulate male and female fertility. Prolactin maintains functional corpus luteum, increases expression of LH receptors and stimulates FSH and LH release. Prolactin was also found to effect the gonads, although the abnormally high level was shown to cause infertility (Bartke, 1999). The GH knockout studies on mice disclosed different mechanisms that resulted in infertility. The GH receptor knockout mice were found to have impaired oestrous cyclicity, and in males, there was decreased secretion of testosterone by the testes which were lighter in weight when compared with those of wild-type males (Bartke, 1999). This finding implies that GH is involved in fertility and growth of the male reproductive system. One other hormone was also found to be essential for the development of the reproductive system of female mice is the insulin-

like growth factor (IGF-I). IGF-I receptor-deficient mice were found to be completely infertile and have a juvenile phenotype reproductive system (Bartke, 1999).

The melanocortin (MC) systems were suggested to be involved in different functions of the reproductive system: such as, eliciting sexual behaviour in both males and females (Abdel-Malek, 2001) and restoring LH pulsatile secretion in lean animals (Backholer *et al.*, 2010). MC system also, has a role in the growth of the ovarian follicles and corpora lutea in mice as suggested by melanocortin receptor 4 knockout mouse studies (Sandrock *et al.*, 2009). According to the National health services (NHS) in the UK, there are about 3.5 million people having difficulty conceiving; of those, 25% have an unidentified cause of infertility. Different neuroendocrine elements could be affected on either level of the HPO axis causing infertility. The melanocortin system could be one of these neuroendocrine factors. The next section will discuss in detail the components and functions of the melanocortin system; it will also give a brief review of the suggested role of this system in female reproduction.

2 The Melanocortin system

2. 1 Background

The melanocortin system is found in both the central nervous system and peripheral tissues. It has important roles in both glucocorticoid and melanin synthesis, as well as functions in inflammation and appetite control. The melanocortin system consists of the melanocortin peptides, endogenous antagonists, melanocortin receptors and the melanocortin receptor accessory proteins.

2. 1. 1 Proopiomelanocortin (POMC)

The concept of the existence of a polypeptide precursor for adrenocorticotrophic hormone (ACTH) and beta-lipotropin (β -LPH) was considered in the early 1960s. The suggestion was made after sequencing these small peptides, and after studying them, different groups had found that these small peptides shared a link (Roberts and Herbert, 1977). Evidence to support this hypothesis was provided when the Nakanishi group used immunoprecipitation with anti-ACTH, anti-beta-endorphin and anti- β -LPH on newly translated proteins of messenger ribonucleic acid (mRNA) taken from bovine pituitaries. The protein was precipitated by more than one antibody proving that they all come from the same precursor polypeptide (Nakanishi *et al.*, 1979)

This precursor peptide was named proopiomelanocortin (POMC). The *Pomc* gene is made of 5 exons in mouse with most of the coding region contained in the third largest exon; this region is highly conserved between species (Clark, 2016). Most of POMC expression is predominantly in the pituitary gland within the corticotrophs of the anterior lobe and the melanotrophs of the intermediate lobe in mice (humans have a rudimentary intermediate lobe). POMC mRNA is also expressed in the brain and other tissues such as the thyroid, pancreas, placenta and digestive system as reviewed by Smith and Funder (1988). The proteolytic cleavage of POMC occurs in a tissue-specific manner depending on the presence of one or both of two prohormone convertases (PC1 and PC2). POMC is made of three domains: the amino terminus that comprises gamma-melanocyte stimulating hormone (γ -MSH) (Bicknell, 2008); the central domain includes adrenocorticotrophic hormone (ACTH), α -MSH and corticotropin-like intermediate peptide (CLIP); and the last domain is the carboxyl terminus which is cleaved into β -MSH, β -endorphin, β - and γ -lipotropic hormone (LPH) (as reviewed by Bicknell (2008): Figure 2. 1).

Pro-opiomelanocortin (POMC) gene

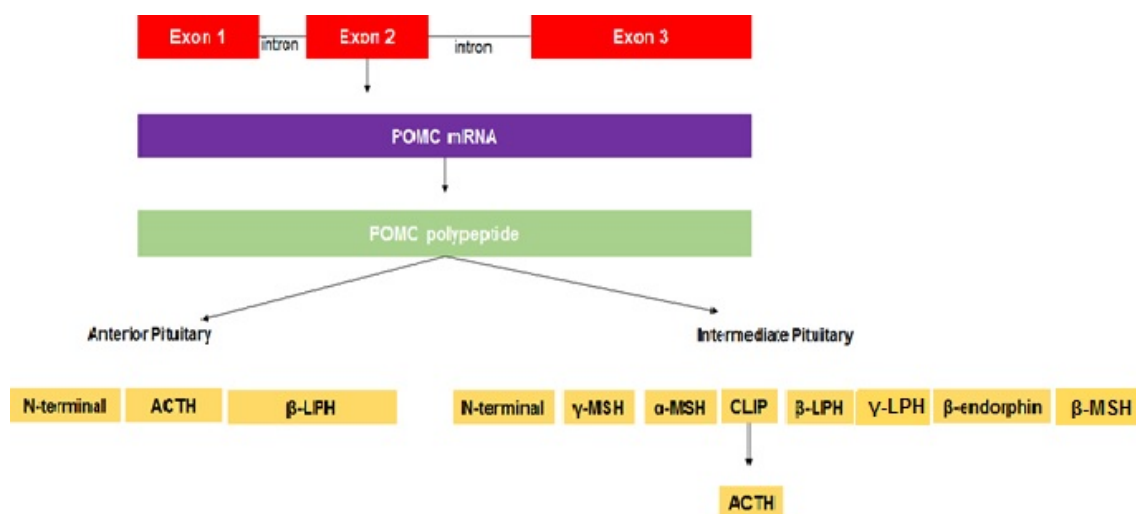


Figure 2.1: Gene structure and post-translational processing of the pro-opiomelanocortin molecule (POMC). In the corticotrophs of the anterior pituitary lobe, PC1 mediate the cleavage of POMC to N-terminus fragment, adrenocorticotrophic hormone (ACTH) and the beta – lipotropin (β -LPH) which in turn cleaved into beta-endorphin. In the melanotrophs of the intermediate pituitary lobe, PC1 and PC2 mediate the cleavage of POMC into N-terminus; alpha-, beta- and gamma-melanocyte stimulating hormone (α -, β -, and γ -MSH); Corticotropin-like Intermediate Peptide (CLIP) which is cleaved further to ACTH₍₁₋₃₉₎; β -LPH and beta-endorphin. Image adapted from Bicknell (2008) with permission granted by John Wiley and sons.

Through its end products [adrenocorticotrophic hormone (ACTH) and alpha-, beta- and gamma-melanocyte stimulating hormone (α -, β -, and γ -MSH)], POMC is involved in diverse roles: including analgesia and cardiovascular protective functions (Krude and Grüters, 2000). Mutations within or deletion of the POMC gene manifests as a triad of early obesity, red hair and pale skin, and low circulating cortisol concentrations due to adrenal insufficiency (Clark, 2016). Genotyping analyses have identified five single nucleotide polymorphisms (SNPs), and three of these were responsible for visceral and cutaneous adiposity in Hispanic descendants (Sutton *et al.*, 2005). Quite recently, a case report described mental retardation and ataxia alongside the triad due to a mutation in c.64delA of the *POMC* gene (Özen *et al.*, 2015). Some of the other mutations affecting specific regions of the *POMC* gene were found to have milder effects due to compensatory mechanisms; for instance, mutation in the ACTH coding region on POMC gene did not cause significant effects as it was found to be

compensated through the first 13 ACTH residues within the α -MSH sequence (Krude and Grüters, 2000).

The original functions of the melanocortins were thought to be limited to stimulating melanin synthesis in the epidermis of the skin and glucocorticoid production from the zona glomerulosa in the cortex of the adrenal glands (Abdel-Malek, 2001). However, other pathways, which are related to inflammation, energy homeostasis, sexual behaviour, learning behaviour and memory, have now been described (De Wied, 1999; Abdel-Malek, 2001; Gantz and Fong, 2003).

2. 1. 2 The melanocortin peptides

α -MSH is detected in various tissues: in the brain, it is synthesised in the arcuate nucleus where it behaves as an inhibitory neurotransmitter suppressing food intake and lowering body temperature (Xu *et al.*, 2014). Peripherally, α -MSH analogues are thought to be useful therapeutic candidates for treatment of inflammatory and allergic conditions, as well as autoimmune diseases (Catania *et al.*, 2004; Getting, 2006; Ahmed, 2014) because α -MSH inhibits the release of different cytokines (such as, IL-1, TNF α and IFN γ) from monocytes and macrophages (Catania *et al.*, 2004). α -MSH also counteracts inflammation by suppressing transcription factors (such as nuclear factor kappa B, NF κ B) in antigen presenting cells (Catania *et al.*, 1998). α -MSH, β -MSH, γ -MSH and ACTH contribute to anti-inflammatory responses (Muceniece *et al.*, 2004). The roles of ACTH were initially characterised as stimulating glucocorticoid synthesis in the adrenals and pigmentation in the skin (Ducrest *et al.*, 2008). However, ACTH also mediates an anti-inflammatory response, and the ACTH synthetic analogue (ACTH₍₁₋₃₉₎), Synacthen, has been used in the treatment of gouty arthritis (Getting, 2006). During the investigation of melanocortins in the central nervous system, studies also uncovered an indirect role for melanocortins in reproduction (Schiöth and Watanobe, 2002). The melanocortins were found to indirectly stimulate the release of GnRH through the interaction with estradiol, melanin concentrating hormone (MCH) and dopamine in the female rats (Wilson *et al.*, 1991; Gonzalez *et al.*, 1997; Murray *et al.*, 2000). GnRH stimulates the gonadotrophs of the pituitary gland, through activating different hypothalamic neurotransmitters such as leptin, prolactin, kisspeptin and orexin; thereby, enabling the hypothalamic-pituitary-gonadal (HPG) axis (Schiöth and Watanobe, 2002; Backholer *et al.*, 2009). ACTH, through its activity

in the hypothalamic-pituitary-adrenal (HPA) pathway, is known to have an inhibitory effect on the hypothalamic-pituitary-gonadal (HPG) axis in various physiological and pathological conditions: such as stress, Cushing's disease and pregnancy (Magiakou *et al.*, 1997). The role of melanocortin peptides and their synthetic analogues will be discussed further in the following sections.

2. 1. 3 Melanocortin receptors and their expression sites

The melanocortin receptors (MC₍₁₋₅₎) are five receptors belonging to the G-protein coupled receptor (GPCR) family. They have the same structure as the GPCRs belonging to the class A rhodopsin-like family; each receptor consists of a single polypeptide that is presented as seven short domains spanning the cell membrane with the amide end located at extracellular compartment and the carboxyl end located intracellularly (Figure 2. 2).

The amide end contains N-glycosylation sites while the carboxyl end comprises palmitoylation sites; phosphorylation sites are in the transmembrane first and third domains (Yang, 2011). MC₍₁₋₅₎ share the same ligands which is not surprising given the homology between the receptors. There are sequence similarities of 45-60% between MC₁ and MC₃ and between MC₄ and MC₅ respectively; whilst MC₂ and MC₄ share 38% sequence similarities making MC₂ the most distinctive receptor of all the MCs (Yang, 2011). The most common signalling pathway activated by these receptors is the activation of adenylate cyclase and increased cAMP production through the G_s subunit of the G protein complex. However, other signalling pathways are also activated by the MCs, these include inositol triphosphate (IP3), which leads to a rise in Ca⁺⁺ influx, and the phosphorylation cascade initiated by the Janus kinase 2 (JAK2) and signal transducers and activators of transcription (STAT1) tyrosine (Getting *et al.*, 2009). This is attributed to the differential binding affinity of the melanocortin peptides to the receptors and activating different G protein subunits. This could also explain the varied functions mediated by the same receptor binding to the same melanocortin peptide (Yang, 2011). The following sections will include a detailed account of each melanocortin receptor.

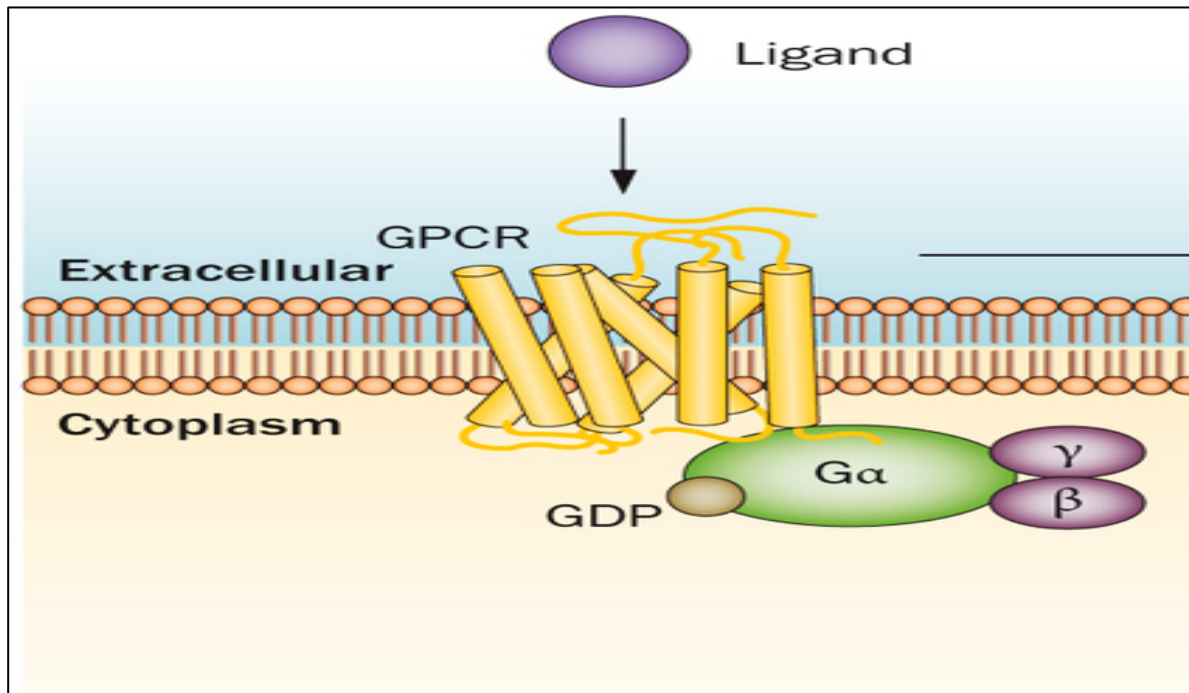


Figure 2.2: The structure of class A G protein coupled receptor (GPCR). GPCR is made of transmembrane molecule those 7 spans across the membrane. The short carboxyl terminus is located intracellularly and attached to the G protein 3 subunits. The short amide terminus is located extracellularly and contains N-glycosylation sites. Cysteine residues in parts of the transmembrane domain and the extracellular loop are responsible for GPCR as well as MC dimerization. Image reprinted from Neumann *et al.* (2014) (Permission to reuse image was granted by Nature Reviews Rheumatology).

2. 3. 3. 1 Melanocortin 1 receptor (MC₁)

The first melanocortin 1 receptor (MC₁), also known as an α -MSH receptor, was discovered in human melanoma cells (Chhajlani and Wikberg, 1992; Beleche *et al.*, 2012). The expression of MC₁ was detected in the periaqueductal neurons, glial cells, neutrophils, macrophages, fibroblasts, Leydig cells, placenta and the corpus luteum (Xia *et al.*, 1995; Wikberg *et al.*, 2000). This receptor has an affinity to all the melanocortin peptides but has the highest affinity for α -MSH. Melanin synthesis was found to be mediated by MC₁: following UV exposure the receptor and the melanocortin peptides are upregulated (Abdel-Malek, 2001). Additionally, MC₁ mediates an anti-inflammatory response through preventing neutrophil migration, stimulating the release of cytokines and inhibiting macrophage functions (Abdel-Malek, 2001). While preliminary studies report that the receptor's mRNA has been detected in all the tissues of the HPG axis, with higher levels in older male mice

(Dowejko, 2014), a role in the male and female reproductive axes remains to be characterised.

2. 1. 3. 2 Melanocortin 2 receptor (MC₂)

The MC₂ mRNA was first detected in the adrenal gland (Mountjoy *et al.*, 1992; Chhajlani *et al.*, 1993). The receptor is 100% selective for ACTH and when activated is responsible for glucocorticoid synthesis. The receptor is not exclusively expressed in the adrenal gland. The MC₂ receptor is also found in mouse adipocytes where it is proposed to have lipolytic activity (Boston and Cone, 1996). In foetal mice, MC₂ has been detected in the lungs, genital ridge, testes and ovaries. In the testis, MC₂ was detected in Leydig cells while in the ovaries, the MC₂ protein was localised within the oocyte hence a role for the receptor in oogenesis has been hypothesized (Nimura *et al.*, 2006). MC₂ is expressed in the corpus luteum of bovine ovaries and pseudopregnant rabbits and exposure to an ACTH agonist (ACTH₁₋₂₄) *in vitro* led to an increase in the production of sex steroids in the cells of the corpus luteum (Amweg *et al.*, 2011; Guelfi *et al.*, 2011). Immuno-positive staining for MC₂ has been found in the glands of the endometrium suggesting a role for stimulating uterine secretions (Lantang *et al.*, 2015).

2. 1. 3. 3 Melanocortin 3 receptor (MC₃)

The distribution of MC₃ was found to be wider than MC₂ as it was detected in the thalamus, hypothalamus, hippocampus, stomach, pancreas and the placenta (Gantz *et al.*, 1993; Roselli-Rehfuss *et al.*, 1993). Similar to MC₁, MC₃ has an affinity for all the melanocortin peptides with the highest affinity for γ -MSH. The primary functions of MC₃ appear to be the control of feeding behaviour and energy expenditure in mice (Butler and Cone, 2002). The uterus expresses MC₃ in the glandular epithelium of the endometrium of mice and natural killer cells of the uterus near the vasculature suggesting an indirect role for the receptor in controlling vascular stability through ACTH (Lantang *et al.*, 2015). In male mice, MC₃ was found to be expressed in all tissues of the HPG axis with lower amounts in the mouse testes (Dowejko, 2014). Dowejko's studies showed higher expression in female pituitary than males, and this

expression is significantly higher in pregnancy, suggesting a potential role for the MC₃ in pregnancy.

2. 1. 3. 4 Melanocortin 4 receptor (MC₄)

The expression of MC₄ was detected in several areas of the brain, including the thalamus and hypothalamus (Gantz *et al.*, 1993; Cerda-Reverter *et al.*, 2003). In the limbic system (hippocampus and amygdala), MC₄ was thought to have functions in memory and feeding behaviour (Wikberg *et al.*, 2000). Based upon evidence that selective and non-selective MC₄ antagonists (HS014 and SHU9119) reversed the inhibitory effect of leptin on food intake and that leptin treatment stimulated rat POMC expression, a role for MC₄ in food intake and body weight was demonstrated (Schiöth and Watanobe, 2002). HS014 and SHU9119 intra-cerebroventricular administration also lowered LH and prolactin concentrations compared to leptin alone (Watanobe *et al.*, 1999). These effects, however, were only noticed in female rodents as treatment of leptin-deficient male mice with the melanocortin peptides, agouti-related peptide (AgRP) or SHU9119 (non-selective MC₃ and MC₄ antagonists), showed no effects on LH, FSH or testosterone release which could suggest a role for the ovarian steroids in the leptin stimulatory pathway (Schiöth and Watanobe, 2002). Although these findings suggest a role for melanocortin in mediating the release of the gonadotropins from the pituitary; this may not be a reciprocal action, Sandrock and colleagues have shown that MC₄ knockout obese mice had ovarian failure despite a regular estrous cycle and the group attributed this finding to possibly abnormal gonadotropin release (Sandrock *et al.*, 2009).

2. 1. 3. 5 Melanocortin 5 receptor (MC₅)

The last member of the melanocortin receptor family to be cloned was MC₅ and it was found in skeletal muscles, spleen and the brain (Gantz *et al.*, 1994; Cerdá-Reverter *et al.*, 2003). It is also found in the lacrimal and sebaceous glands where it is suggested to have an excretory function; MC₅ is also postulated to have a role in lipolysis and in mediating an anti-inflammatory response (Abdel-Malek, 2001). The expression of MC₅ protein was detected during the proliferative and secretory phases of the menstrual

cycle; it is found in the stromal cells and glandular epithelium of the uterus, where, in addition to stimulating the release of the uterine secretions, it may also affect vascular stability and hence menstrual flow (Lantang *et al.*, 2015).

2. 1. 4 Endogenous antagonists

These include agouti, which is also known as agouti signalling protein (ASP), and agouti-related protein (AgRP). ASP antagonises the actions of both MC₁ and MC₄ whereas AgRP competitively binds to MC₃ and, again, MC₄ (as reviewed by Yang, 2011). AgRP is mainly found in the hypothalamus, but a shorter variant of AgRP is also found in the adrenals, the testis and the dorsal root ganglia (Illytska and Argyropoulos, 2008). The AgRP neurons, together with the neuropeptide Y, have an orexigenic role, initiating food intake, in the neuroendocrine circuit located in the arcuate nucleus of the hypothalamus (Bagnol *et al.*, 1999). This role was thought to be mediated by suppressing the melanocortin peptides binding to the receptors that inhibit food intake.

Humans with the Ala67Thr SNP in AgRP have a reduced risk of type 2 diabetes and obesity later in life. AgRP^{-/-} mice fed a high-fat diet when older were found to live longer than wild-type animals (Redmann and Argyropoulos, 2006).

2. 1. 5 Melanocortin receptors accessory proteins (MRAPs)

Two accessory proteins have been recognised: MC₂ accessory protein 1 (MRAP1) and MRAP2 (Asai *et al.*, 2013). They are required by MC₂, and maybe the other MCs, to facilitate receptor trafficking, expression and intracellular signalling. The MRAP1 is predominantly expressed in the adrenal cortex transporting MC₂ to the cell membrane thereby facilitating MC₂'s response to ACTH (Asai *et al.*, 2013). Deficiency of MRAP1 causes familial glucocorticoid deficiency (FGD) type 2, and FGD type 2 is associated with mutations in a gene locus mapping to chromosome 21q22.1, which encodes for MRAP1: previously known as fat tissue-specific low molecular weight protein (Jackson *et al.*, 2015). MRAP2, which is encoded by a gene located at chromosome 6q14.2, is expressed in the adrenal gland and in the brain, where it has a similar pattern of expression to MC₄. MRAP2 may be involved in regulating metabolism: in contrast to wild-type mice, MRAP2 knock out mice were found to be obese, and this was not related to food intake (Asai *et al.*, 2013). Unlike MRAP1 effects on MC₂, reduced

signalling was noticed when both MRAP1 and MRAP2 were found co-expressed with the other MCs, and the two appear to inhibit dimer formation of the MCs (Webb and Clark, 2010).

2. 1. 6 The melanocortin system and reproduction

Most research characterising the roles of the melanocortin system in reproduction has focused on the central melanocortins (MC₃ and MC₄), although all MCs have been described in the reproductive axis (Amweg *et al.*, 2011; Simamura *et al.*, 2011; Dowejko, 2014; Lantang *et al.*, 2015). The expression of MC₁, MC₂ and MC₃ was detected in different compartments of the bovine ovaries and the melanocortin peptide, ACTH, is thought to be involved in the function of the ovaries (Amweg *et al.*, 2011). Despite suggesting that the melanocortin system affects fertility, there has been little research into the effects of age or physiological condition on the expression of the MCs in females.

The influence of age was investigated in the male reproductive axis of mice and, while all five melanocortin receptors were found to be expressed, the pattern varied. In the hypothalamus and pituitary gland, the expression of all MCs was found to be greater in 14 weeks old mice, but MC₅ expression was more significant in the pituitary gland of younger age groups (8 weeks old). In the testes of mice MC₃, MC₄ and MC₅ expression were greatest in young adult mice (8 weeks) compared to an MC₂ expression which was doubled at 14 weeks. Preliminary findings indicate that all melanocortin receptors are expressed throughout the female reproductive system, but the expression levels vary and are influenced by age and physiological status (Dowejko, 2014).

3 Materials and Methods

3. 2 Materials

Ethics approval for all the work described herein was granted by the University of Westminster (Ethics Approval VRE1415-0209). The animal tissues were provided by Dr Paul Le Tissier and Dr Joanne Murray from the University of Edinburgh. The animals were killed by a Schedule 1 method in accordance with the Home Office's Animal Scientific Procedures Act (1986). The tissues were used in the reverse transcription quantitative polymerase chain reaction (RT-qPCR) and the chromogenic RNA *in situ* hybridisation (RNAscope®) studies.

RNA extraction and cDNA synthesis: *RNAlater*® (ThermoScientific, UK) was purchased from Life Technologies, UK. RNA isolation reagents included TRI reagent® and molecular chloroform from Sigma Aldrich, UK, RNeasy micro kits and RNase-free DNase sets from Qiagen, UK, and SuperScript™ II reverse transcriptase cDNA synthesis kits from Invitrogen, ThermoScientific, UK.

RT-qPCR expression analyses: Both the GeNorm kits with SYBRgreen and the PrecisionPLUS qPCR master mixes were obtained from Primer Design, UK. Primers for the gene expression studies were purchased from Qiagen, Primer Design and Eurofins. RNAscope® reagents used in the RNA *in situ* hybridisation included: RNAscope® 2.5 HD reagent kit-Brown; RNAscope® 2.5HD duplex reagent kit; RNAscope® 2-plex negative control probe; RNAscope® duplex positive control probe; RNAscope® probe- *Mm-MC3r-C1* and *C2* (Catalogue number 412541,412541-2 respectively); RNAscope® Probe *Mm-Mrap2-C1* and *C2* Catalogue number 474411 and 474411-2); RNAscope® probe *Mm-MC5r-C1* (Catalogue number 3000031); RNAscope® probe *Mm-Gh-C2* (Catalogue number 320269-C2); and RNAscope® probe *Mm-Lhb- C2* (Catalogue number 321584). All RNAscope® reagents were purchased from ACD Diagnostics. Tissue sections were mounted on Superfrost® PLUS slides from FisherScientific, UK.

The HTLA cells were kindly provided by Prof Wesley K Kroeze, (Kroeze *et al.* (2015), University of North Carolina, USA). The cell culture reagents included Dulbecco's modified eagle's medium (DMEM) (Catalogue number 41965-039 supplemented with 10% foetal bovine serum (Catalogue number A9576), 100 IU/ml penicillin-streptomycin 100 IU/ml and 2.5 µg/ml amphotericin B, (all reagents were from Gibco®, ThermoScientific, UK). Hygromycin B 100 µg/ml (Catalogue number ant-hg-1,

Invivogen, UK) and puromycin dihydrochloride 2 µg/ml (Catalogue number 4089, Tocris, UK) were used for cell selection. For bacterial transformation, DH5 α and SOC media were purchased from Invitrogen™ (Catalogue number 18265017, UK); LB agar and broth were from Sigma Aldrich (Catalogue number L3147-1KG and L3522-1KG respectively, UK). Plasmid Qiaprep spin miniprep extraction kit was purchased from Qiagen (Catalogue number 27104, UK). The transfection reagent polyJet™ was purchased from SignaGen Laboratories (Catalogue number SL100688, USA). The cell transfection reagents included DMEM without phenol red (Catalogue number 21063-029, Gibco®, UK); fluorescent plasmids [pCDNA3- enhanced- green fluorescent protein (pCDNA3.1-E-GFP) and/or pCHERRY10 (Addgene, catalogue numbers: 13031 and 24664 respectively, USA)]. The pmCHERRY-N1 plasmid was a kind gift from Dr Sarah Coleman, University of Westminster. The PRESTO-TANGO assay plasmids *MC₃-TANGO* and *MRAP1-pCDNA3.1* were a generous gift from Dr Paul Le Tissier and Dr Joanne Murray, University of Edinburgh. *MRAP2-pCDNA3.1-myc* was a kind gift from Dr Li Chan, The William Harvey Research Institute, UK. Viability tests reagents included the MTT reagent A [MTT reagent (3-(4,5-dimethyl-2-thiazolyl)-2,5-diphenyl -2H-tetrazolium bromide), Catalogue number M5655, Sigma Aldrich, UK].

3. 2 Methods

3. 2. 1 Tissue Collection

The hypothalamus, pituitary gland, ovaries and uterus were removed from C57BL/6 virgin mice aged 2, 6,10 and 14 weeks as well as pregnant mice (9 weeks at mating and tissue taken at approximately day 13 day of gestation which is equivalent to mid-pregnancy) and placed in RNALater® to stabilise and protect the RNA (Table 3.1).

Table 3-1: Mouse ages and their physiological status.

Mouse Age (in weeks)	Physiological state
Two weeks old	Neonatal
Six weeks old	Peri-pubertal
9-10 weeks old	Sexually mature: young adult
14 weeks old	Mature adult
Nine weeks old (13 days pregnant \pm 1 day)	Pregnant: mid-gestation

3. 2. 2 RNA Extraction

The tissues (no more than 3-5 mg) were disrupted in 800 μ l of TRIreagent and homogenised for 5 minutes at 22°C. Chloroform (160 μ l) was then added to the homogenate before being mixed using a vortex for 10 seconds and incubated on ice for 3 minutes. The homogenates were then centrifuged at 8,000 g at 4°C for 30 minutes. Approximately 500-700 μ l of the colourless aqueous phase of the supernatant were transferred to a new tube; an equal volume of 70% ethanol prepared in RNase-free water was added, and the samples were vortexed for 5 seconds. The sample: ethanol mixture (700 μ l) was then transferred into spin column tubes (RNAeasy kit) placed in collecting tubes. Samples were centrifuged at \geq 8,000 g for 30 seconds and the flow-through discarded. RW1 (350 μ l) buffer (RNeasy kit) was added to the spin columns; the samples were spun at \geq 8,000 g for 30 seconds and the flow-through discarded. The samples were then incubated with DNase I (1500 Kunitz units, 10 μ l of the DNase stock to 70 μ l of the DNase I Buffer RDD as described in the RNase-free DNase I protocol from Qiagen, UK) at 22°C for 15 minutes to remove any remaining genomic DNA (a necessary step when using the samples in the sensitive real-time PCR assays). Buffer RW1 was added to the spin column to stop the DNase treatment and to wash the sample. Washing and precipitating the DNA was done by adding 500 μ l of Buffer RPE (RNeasy kit) to the spin columns, the samples were centrifuged and the flow-through discarded. To continue RNA precipitation, 500 μ l of 80% ethanol were added to the spin columns before the samples were centrifuged at \geq 8,000 g for 2 minutes. To remove any carryover of ethanol, the lid of each tube with the sample was left open and the tubes re-centrifuged at maximum speed for 5 minutes. To elute the RNA, 14 μ l of RNase-free water were added to each

sample, left on the bench for 1 minute and then the tubes were centrifuged at maximum speed for 2 minutes. The concentration of the purified total RNA was measured with a spectrophotometer at wavelengths of 260 and 280 nm (Nanodrop 2000, ThermoScientific®). An acceptable RNA yield was about 150-300 ng and accepted 260:280 and 260:230 ratios were approximately 2.00 and 2.0-2.2, respectively. The samples were either used directly to make complementary DNA (cDNA) or stored at -80°C.

3. 2. 3 Complementary DNA (cDNA) synthesis

The SuperScript II reverse transcriptase protocol for cDNA synthesis was followed (Invitrogen™, UK). A 20 µl reaction volume contained: ~300 ng of RNA; 150 ng of random hexamer primers; dNTPs (10 µM each) (both from Sigma-Aldrich, UK). This reaction mixture was incubated at 65°C for 5 minutes to allow the primers to anneal. First strand buffer (1.0 M Tris-HCl, pH 8.3, 1.5 M KCl and 60 mM MgCl₂), 0.2 M of dithiothreitol (DTT) and RNase-free water were added and left at room temperature for 2 minutes. The addition of 200 U/µl SuperScript II reverse transcriptase (RT) enzyme was followed by incubating the mixture at room temperature (22°C) for 10 minutes to activate the enzyme. This was followed by incubating the reaction mixture at 42°C for 50 minutes for cDNA synthesis. Finally, the reaction was inactivated by incubating the mixture at 70°C for 15 minutes. Negative controls (NO-RT) were also included by adding RNase-free water instead of the RT enzyme. The cDNA was then stored at -80°C until used for RT-qPCR.

3. 2. 4 Reverse transcription - quantitative polymerase chain reaction (RT-qPCR)

3. 2. 4. 1 Reference gene stability analysis

To determine the stability of reference genes for each tissue, the expression stabilities of twelve reference genes (GeNorm kit, Primer design, UK) were identified. Table 3.2 lists the reference genes from the GeNorm kit with accession numbers and product length. The reference genes' expression stabilities were examined in the cDNA samples (25 ng) of two biological replicates of the hypothalamus, the pituitary gland, the ovaries and the uterus of all age groups and nine weeks old pregnant (13 ± 1 day post coitus, dpc). Each tissue was analysed separately. The samples were run in duplicates with RT-qPCR (total number was 24 samples). The threshold cycle (CT) values, (the number of cycles needed for the fluorescence to cross the threshold that was set above the background noise) were exported into Excel worksheets and analysed using GeNorm. To validate the results of GeNorm, three other different software packages (detailed below) were also used to analyse the same data to select the most stable reference genes for each tissue.

Table 3-2: Reference genes names, function, accession numbers and product length.

Primer	Full name of the gene	Function	Accession number	Product Tm (°C)	Amplicon size (bp)
18S	18S ribosomal RNA	RNA constituent	NR_003278.3	82.9	93
ACTB	β-actin	Nucleosome binding –cytoskeleton component	NM_007393.3	90.2	84
ATP5B	ATP synthase	ATP biosynthesis	NM_016774.3	89.8	112
B2M	β-2-microglobulin	Glycoprotein binding	NM_009735.3	84.7	120
CANX	Calnexin	Ca ⁺ binding activity	NM_007597.3	86.3	105
CYC1	Cytochrome c isoform 1	Electron activity	NM_025567.2	92.1	141
EIF4A2	eukaryotic translation initiation factor 4A2	ATPase and helicase activity	NM_013506.2	84.4	152
GAPDH	glyceraldehyde-3-phosphate dehydrogenase	Different metabolic processes	NM_008084.2	90.8	127
RPL13A	ribosomal protein L13a	RNA constituent	NM_009438.5	91.0	130
SDHA	succinate dehydrogenase complex flavoprotein subunit A	Mitochondrial electron transport	NM_023281.1	87.1	133
UBC	ubiquitin C	Protease binding	NM_019639.4	96.8	129
YWHAZ	Tyrosine 3-Monooxygenase/Tryptophan 5-Monooxygenase Activation Protein Zeta	Involved in the signalling pathway	NM_011740.3	87.8	141

The reference genes used include 18S, β-actin, ATP5B, B2M, CANX, CYC1, EIF4A2, GAPDH, RPL13A, SDHA, UBC, YWHAZ (GeNorm kit, Primerdesign, UK). The reference genes' stabilities were examined using RT-qPCR in technical duplicates of two hypothalami, two pituitary glands, two ovaries and two uteri (each tissue separately) of mice aged 2, 6, 10 and 14 weeks and nine weeks old pregnant (13 +1 DPC). Analyses were done using GeNorm (qBase+, Biogazelle, Belgium) and three other reference genes stability analyses software: BestKeeper, Normfinder and Delta CT. Available from <http://150.216.56.64/referencegene.php>.

3. 3. 4. 2 Reference gene selection software analyses

a. GeNorm

This software relies on calculating a normalisation factor based on multiple reference genes; GeNorm software hypothesises that two or more normalisers (reference genes) should have the same expression ratio across all samples and experimental conditions. A measure, “M”, which reflects the reference gene stability is established through the standard deviation of the logarithmically transformed expression CT ratios. The most stable genes will have the lowest “M” values. The normalisation factor is then calculated using the geometric mean from expression levels of the most stable reference genes. This software recommends the use of at least 2-3 of the most stable reference genes to calculate the normalisation factor; adding a fourth gene does not significantly contribute to the expression stability analysis (Vandesompele *et al.*, 2002).

b. BestKeeper

Pfaffl and colleagues developed a BestKeeper tool on the basis that the most stable reference genes show the least variability in their CT values across the samples examined. The software algorithm utilises the reference gene’s CT data calculating the geometric mean, the arithmetic mean, and standard deviation (St. Dev); represented as minimum CT, maximum CT and CT St. Dev. Reference genes with a St. Dev more than one are considered unstable. To be able to choose more than one stable gene, a pair-wise correlation analysis is done to estimate the inter-gene relations of all possible pairs: a BestKeeper index combines the most stably expressed reference genes. Then, the Pearson correlation coefficient, the coefficient of determination and the p-value statistically describe the correlation between this index and the reference genes (Pfaffl *et al.*, 2004; Palombella *et al.*, 2017).

c. NormFinder

NormFinder is a mathematical model describing the RT-qPCR log CT values, estimation of inter- and intra-group variations, sub-group analyses and, finally, the calculation of stability values of the reference genes examined. The reference genes are then ranked according to their stability value with the most stable gene having the lowest stability value (Andersen *et al.*, 2004; Palombella *et al.*, 2017).

d. Delta CT

The process of exclusion is the basis of this method. The relative expression of a pair of genes is compared in different samples using the delta CT and St.Dev: stable genes would not show any variability in the different samples. This procedure is used with more than one pair and various conditions and pairs that show variable expression among samples, and hence have fluctuating expression stability, are excluded.

In addition to these four software packages, a comprehensive ranking tool considers the data collected by the four software packages and provides a ranking order for the reference genes' expression stabilities.

3. 2. 4. 3 Primers for each of the genes of the MC system

The primers for *MC₁*, *MC₃₋₅*, *POMC*- full-length gene and *AgRP* were purchased from Qiagen, UK. Primers for *MC₂* were purchased from Primer Design, UK. *MRAP 2* primers, as described by Asai and colleagues (2013), were obtained from Eurofins. Primers for the *POMC*-truncated gene were designed by the researcher and purchased from Eurofins, for sequences see table 3. 3.

3. 2. 4. 3. A Determining primer pair amplification efficiency

Before conducting the RT-qPCR expression analyses, the amplification efficiencies for all the primers were validated by generating RT-qPCR - standard curves. For each primer pair, cDNA from the most appropriate positive control tissue was used to prepare the standard curve. A 1:10 or 1:2 serial dilution [(100, 10, 1, 0.1 and 0.01 ng/μl) or (100, 50, 25, 12.5 and 6.25 ng/μl)] was prepared from cDNA made from mouse testis (for *MC₁*), adrenal gland (for *MC₂* and *MRAP1*), pituitary gland (for *MC₃* and *POMC*), hypothalamus (for *MC₄* and *MRAP2*), preputial gland (for *MC₅*) and skin (for *AgRP*). The serial diluted cDNA samples were used in a total reaction volume of 20 μl: 12.5 μl of 2X Rotor-Gene SYBRgreen® master mix [HotStart *Taq Plus* DNA polymerase; Rotor-Gene SYBR Green RT-qPCR buffer (TrisCl, KCl, (NH₄)₂SO₄ and MgCl₂) plus the 10 μM dNTPs mix (dATP, dCTP, dGTP, and dTTP: Qiagen, UK); 300 nM primers (primers were from Primer Design, Qiagen or Eurofins; the relevant

accession numbers, sequences and product size for each primer are listed in Table 3.3); and RNase-free water.

In addition to the reactions described above, each run contained a non-template control (cDNA volume replaced by RNase-free water, NTC) and a no reverse transcriptase control, NO-RT. The NTC control demonstrates that the reaction is not contaminated by a previously amplified product.

Each RT-qPCR was carried out with an initial activation step at 95°C for 15 minutes, and this was then followed by 40 cycles of denaturation at 95°C for 15 seconds; annealing at 60°C for 30 seconds; and extension at 72°C for 30 seconds. A melt curve was also produced at the end of each run to check the specificity of the reaction. The wells were labelled as instructed by the thermal cycler software (Rotor-gene Q thermal cycler, Qiagen, UK). A standard curve, which includes information on the slope and efficiency, was generated by the cycler software (the graph in Figure 3.1 was produced using the log values of the concentration, X-axis, against the threshold crossing point "CT" values, Y-axis).

Table 3-3: Primers used for determining primer pair amplification efficiency.

Primer	Positive control tissue (mouse)	Catalogue No	Accession no.	Sequence (if given)	Product size (BP)
MC₁	Testis	QG*- QT00305011	NM_008559	-	127
MC₂	Adrenal gland	PD*	NM_001271 716	F:5'-ACAGGGAGCGGCATCAC-3' R:5'-ACCAGCATCAAAGGGAACAG-3'	86
MC₃	Pituitary gland	QG*- QT00264404	NM_008561	-	108
MC₄	Hypothalamus	QG*- QT00280861	NM_016977	-	106
MC₅	Preputial gland	QG*- QT01166494	NM_013596	-	90
POMC (full gene)	Pituitary gland	QG*- QT00162218	NM_008895	-	99
POMC (truncated gene)	Pituitary	‡	NM_008895	F: CATGACCTCCGAGAAGAGCC R: GTGCGCGTTCTTGATGATGG	70
MRAP 1	Adrenal gland	Self - designed	NM_029844	F:5'-GCATTCCATTGTTTCATCGCCC-3' R:5'-CCGACCAGGACATGTAGAGC-3'	86
MRAP 2	Hypothalamus	‡	NM_001101 482.2	F:5'TGCTGACTTTGCTGACGAAGACAGGTG -3' R: 5'-TGGACTCCTCGTTGCCCTGACG-3'	150
AgRP	Skin	QG*- QT00291424	NM_0012 71806	-	63

Column 2 indicates which mouse tissue was used as a positive control, here duplicates of the serial dilution cDNA were prepared from the positive control of different ages and used to determine primer efficiency starting with 100 ng/μl. QG*: Qiagen (UK; primer pair sequences are unpublished); PD*: Primer Design (UK); ‡: obtained from (Asai *et al.*, 2013) and purchased from Eurofin (UK).

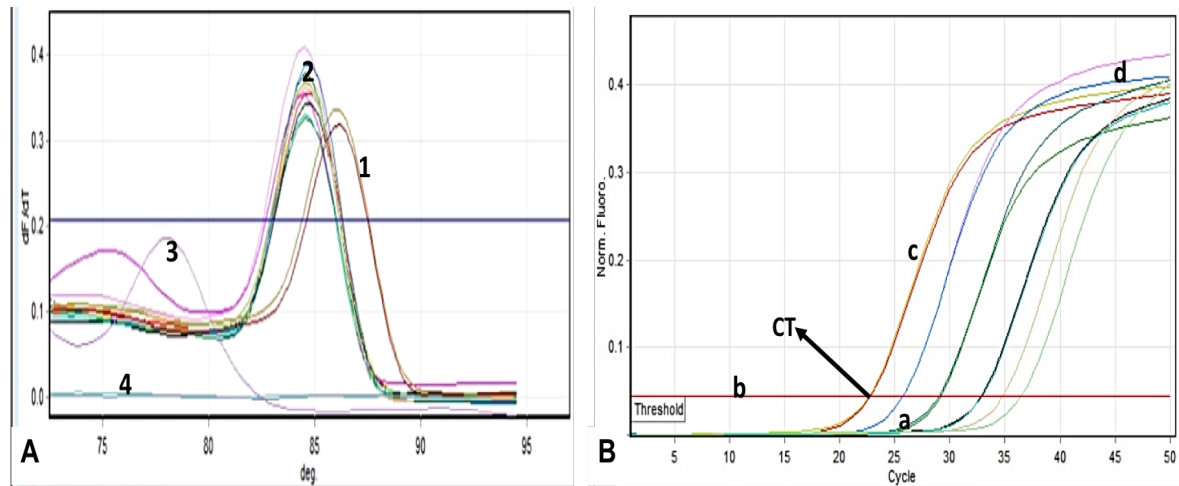


Figure 3.1: RT-qPCR melt curve and amplification curves. A: the RT-qPCR melt curve is a temperature dissociation curve to check for amplification specificity. The dissociation temperature is pre-set to 65°-90°C by the Rotor-Gene Q thermal cycler. After the end of the amplification reaction, the sample temperature starts to increase while the cycler measures the fluorescence produced by SYBRgreen [the double strand (dsDNA) intercalating dye] until a peak is reached. The increased temperature denatures the amplified dsDNA into a single strand DNA leading to the fall in fluorescence. The fluorescence course is then plotted. 1: the reference gene; 2: the target gene; 3: primer dimer (non-specific binding of the primers) from the reverse transcription negative control (NO-RT); 4: non-template control (NTC). B: Amplification curve. a: low levels of amplification; b: a threshold that is set above the noise; c: exponential phase from the specific amplification reaction; d: plateau which is the end of the reaction due to the limitation of the RT-qPCR reaction.

3. 2. 4. 3. B Determination of MC expression in female reproductive axis

Duplicate reactions of 4-6 biological replicates (25 ng) of hypothalamus, pituitary gland, ovary and uterus from mice aged 2, 6, 9, 10 and 14 weeks and 9 weeks old pregnant (13 +1 dpc) samples were carried out using the correct pairs of primers for *MC* (1-5), *POMC*, *MRAP1* and 2 and *AgRP* (see Table 3.4 for primers' details) in RTqPCR assays to examine the expression of the melanocortin system in these tissues. Each tissue used different reference genes determined from the GeNorm assays (section 3. 2. 4. 1) to normalise the tissue expression data: CANX and YWHAZ (hypothalamus); CANX, YWHAZ and EIF4A2 (pituitary gland); EIF4A2, YWHAZ and GAPDH (ovary); and ATP5B, ACTB and YWHAZ (uterus).

The 20 µl final volume RT-qPCR for each reaction consisted of 10 µl of 2x reaction buffer (0.025 U/µl *Taq* Polymerase, 5 mM MgCl₂ and dNTP Mix [200 µM of dATP, dCTP, dGTP, and dTTP], Primer Design, UK), 300 nM primers and RNase-free water.

NTC and NO-RT controls were also included in the assays. The reaction conditions included activation of *Taq* polymerase for 2 minutes at 95°C. This was followed by 40 cycles of cDNA denaturation at 95°C for 15 seconds; combined annealing and extension at 60°C for 30 seconds and a melt curve was set at dissociation temperature 65°-90°C.

3. 2. 3. 4. 3. C Determination of MC system expression workflow

The relative expressions of members of the MC system in the female reproductive axis were calculated using the $\Delta\Delta CT$ method developed by Livak and Schmittgen (2001). The amplification threshold was set to 0.05. CT data were generated by the Rotor-Gene Q software and imported into an Excel analysis worksheet. Appendix 1 shows an example of the analysis for one of the genes in the MC system.

Calculating ΔCT (normalised raw data) by subtracting the geometric mean of the CT values of the reference genes:

$$\Delta CT = CT_{\text{gene of interest}} - CT_{\text{reference genes geometric mean}}$$

As there are no control samples used, two-week samples were used as a reference sample or a calibrator; this was used to calculate $\Delta\Delta CT$ by subtracting ΔCT of the gene of interest from the calibrator:

$$\Delta\Delta CT = \Delta CT_{\text{gene of interest}} - \Delta CT_{\text{calibrator}}$$

Converting the $\log^{-2} \Delta\Delta CT$ to a linear scale was used to calculate the fold change which is the measure of the relative expression used to compare between the examined age groups and the pregnant samples.

$$\text{Fold change} = 2^{-(\Delta\Delta CT)}$$

To carry out statistical analyses for expression significance assessment, the $\log^2 \Delta CT$ of the replicates were converted to the linear scale; that is, equal to $2^{-\Delta CT}$.

One-way ANOVA (analysis of variance) was then conducted using GraphPad (Prism, USA) to determine the P-value. Post Tukey's multiple comparison tests were also included to compare between the age groups and pregnant samples.

3. 2. 4. 3. D Gel electrophoresis of the RT-qPCR products

The RT-qPCR amplification products were separated on 2% (W/V) agarose gel electrophoresis prepared in 1X 0.089 M *Tris*/ 0.089 M *Borate*/ 0.002 M *EDTA* (TBE) buffer. SYBR[®]safe (1 µl/ 50 ml agarose), a DNA intercalating dye (ThermoFisher Scientific, UK), was then added to the melted gel and the gel was poured in the gel trays and left to set. The RT-qPCR products (including NTC samples) and 100 bp DNA ladder or Low range DNA ladder (0.5 µg/ µl) (ThermoFisher Scientific, UK) were run at 110 volts for 40 minutes and visualised at 300 nm using UVIPRO Silver transilluminator (Uvitec, UK).

3. 2. 5 Chromogenic RNA *in situ* hybridisation, RNAscope[®]

3. 2. 5. 1 Sample collection and paraffin embedding

RNAscope[®] assays were performed in the laboratory of Dr Cynthia Andoniadou, King's College London. The tissues (hypothalami, pituitaries, ovaries and uteri) of mice aged 2 and 10 weeks old and (14 ± 1 dpc) pregnant mice (10 weeks old) were kindly collected, fixed and embedded by Dr Joanne Murray at the University of Edinburgh. All the solutions used in the tissue preparation were RNase- free to prevent background noise from contaminants.

On the first day, the tissues were dissected, washed in phosphate buffered saline (PBS) and placed in 25 ml of 10% neutral buffered formalin (NBF). The tissues and formalin were placed on a roller and rotated at 4°C for 24 hours (samples from two weeks old) and 48 hours (samples from adult mice).

After formalin fixation, the tissues were washed in PBS three times, one hour each, with rotation and at room temperature. The tissues were then dehydrated in 25%, 50% and 70% ethanol for two hours in each ethanol concentration. The tissues were stored in a fresh change of 70% ethanol at 4°C overnight. On the following day, tissue dehydration continued with 80%, 90%, 95% and 100% ethanol the tissues were left in fresh 100% ethanol rotating at 4°C overnight.

On the final day, the tissues were immersed in fresh 100% ethanol and left at room temperature rotating for 30 minutes. The tissues were immersed in histoclear (pre-

warmed at 60°C) for 10 minutes at room temperature. The tissues were then placed in watch glasses in pre-warmed histoclear and the oven at 60 °C for 10 minutes. The histoclear was replaced then with pre-warmed 50:50 histoclear: wax solution and incubated for 15 minutes at 60°C. This was then replaced with 100% wax solution, and the tissues were incubated at 60°C for one hour. The last step was repeated two times with fresh 100% wax solution. The wax solution was replaced a third time, and the tissue samples were oriented for the tissues to be cut in frontal sectioning and ensuring that the labels of the tissue sample are visible. The tissues samples were then left to set overnight at room temperature. The tissue blocks (3-4 tissues per block) trimmed and cut into 5 µm thick sections using a microtome. The cut ribbons were floated on water heated to 40-45°C and then mounted onto Superfrost® PLUS slides (FisherScientific, UK) 2-4 sections per slide. The sections were dried in the oven at 40°C overnight.

3. 2. 5. 2 Pre-treatment of formalin-fixed paraffin-embedded (FFPE) tissue for RNAscope® 2.5 HD assay

Slides were baked in the oven for 1 hour at 60°C. To remove the paraffin wax from the tissue sections, the slides were placed in two consecutive immersions of 100 % xylene (5 minutes each). The tissue sections were then dehydrated by placing the slides in two successive immersions of 100 % ethanol (3 minutes each). During these steps, the slides were occasionally agitated.

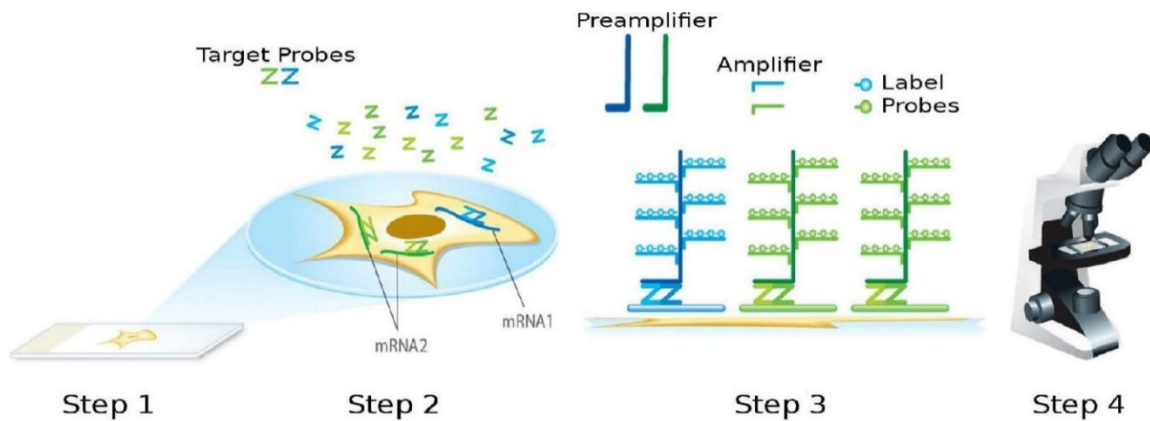


Figure 3.2: The RNAscope® in situ hybridisation workflow. The sections were treated with H₂O₂, RNAscope® target retrieval and protease PLUS (step 1 and 2) to enhance probe hybridisation and block the background noise. The sections were incubated with the RNA probes for 2 hours (step 2). The signal was then amplified through hybridising the sections with a series of amplification and label probe steps (step 3). Signal detection included the use of either 3-3' diaminobenzidine (DAB) detection or the two-channel (green/red) detection system. The samples were then dried, mounted and visualised under a bright-field microscope (permission to use image was granted by ACD diagnostics).

To prepare the tissue sections for the RNA probes hybridisation, the slides were treated with three reagents. To block the endogenous peroxidase activity, the slides were incubated with 1-2 drops of RNAscope® hydrogen peroxide® at room temperature for 10 minutes. The slides were then washed twice in dH₂O and excess fluid tapped off. To improve probe detection in the fixed tissue sections, the slides were placed in a staining rack and a staining dish. They were then carefully placed in a beaker filled with boiling 1X RNAscope® target retrieval reagent for 15 minutes at 72°C (this was prepared by diluting 70 ml RNAscope® 10X target retrieval with 630 ml distilled water in a beaker, covered with foil and left to boil 15 minutes before use) except for the hypothalami sections which were left in the boiling 1X RNAscope® target retrieval reagent for 17 minutes (see optimisation experiments in appendix 2). The staining dish containing the slides was then immediately placed in distilled water to wash the slides. The slides were then placed in the HybEZ slide rack in a humidity control tray, and a drop of RNAscope® Protease PLUS was added (one drop per slide) to permeabilize the cell membrane for better probe penetration. The tray was then covered with the lid and placed in the HybEZ oven, which was set to 40°C, for 30 minutes. The slide rack was removed from the oven: each slide was then tapped to remove excess fluid and washed once with distilled water.

After being warmed for 10 minutes before use, the target probes (*MC₃*, *MC₅* and *MRAP2*, see table 3.5 for probes details) were applied to the sections, one drop per section. The slides were then placed in the covered HybEZ tray and the tray incubated in the HybEZ oven at 40°C for 2 hours: this incubation allowed hybridisation between the probes and the complementary RNA sequence in the tissue sections. In each run, two control slides were included: sections on one slide were exposed to a positive control probe, a housekeeping gene peptidylprolyl isomerase B (*PPIB*), to ensure the treatment conditions are optimised for each tissue. The sections on a second slide were exposed to a negative control probe, a bacterial protein called dihydrodipicolinate reductase B (*DAPB*), to check for background staining. The next part of the assay involved amplification and detection of the expression signals using either RNAscope® 2.5HD Brown or RNAscope® 2.5HD Duplex assays.

Table 3-4: RNAscope® probes used in the RNAscope® Brown assays.

Gene	Entrez Gene ID	Accession No.	Target region	No. of Pairs	Channel	Catalogue no.
<i>PPIB</i> (peptidylprolyl isomerase B)	19035	NM_011149.2	98 - 856	15	C1*	313911
<i>DAPB</i> (dihydrodipicolinate reductase)	#	EF191515	414 - 862	10	C1	310043
<i>Mm-MC₃-C1</i>	17201	NM_008561.3	1627 - 2621	20	C1	412541
<i>Mm-MC₅-C1</i>	17203	NM_013596.2	2 - 1154	20	C1	478381
<i>Mm-MRAP2-C1</i>	244958	NM_001177731.1	183 - 1387	20	C1	474411

C1*: refers to the probes used for the RNAscope® Brown and channel 1 Duplex assays. N/A: not applicable as *DAPB* is a bacterial gene. #: gene unique to bacteria hence should not be expressed in mammalian tissue. Sequence unknown because manufacturer has not disclosed details.

3. 2. 5. 2. 1 RNAscope® 2.5 HD Brown detection assay

After probe hybridisation, a series of amplifiers (that binds to the preamplifier attached to the target probes) were added to the tissue sections to amplify the target-specific signals. This is followed by detecting the signal using the DAB detection system which produces brown pigments due to oxidation by the RNAscope® hydrogen peroxide®.

After probe hybridisation (see section 3. 2. 5. 2), the slide rack was then removed from the oven, excess fluid tapped off and washed with 1X RNAscope® wash buffer (200 ml) twice (this was prepared by diluting 60 ml of 50X RNAscope® wash buffer with 2.94 L distilled water). With the slide rack, still, in the HybEZ rack and tray, a series of six signal amplification steps were carried out for signal enhancement (see step 3, Figure 5). RNAscope® 2.5 AMP1® (one drop per section) was hybridised for 30 minutes at 40°C in the HybEZ oven, this was followed by washing the slides with 200 ml of 1X RNAscope® wash buffer twice for 2 min and tapping excess fluid off. The samples were washed twice for 2 minutes with 200 ml of 1X RNAscope® wash buffer after each subsequent amplification step. AMP2® was added, and the sections were incubated at 40°C for 15 minutes followed by washing the samples with 200 ml of 1X RNAscope® wash buffer twice for 2 min and tapping off excess fluid. AMP3® and AMP4® were also hybridised with the tissue sections using same incubation time, temperature and washes as AMP1® and AMP2® respectively. The next two amplification steps were conducted at 22°C with the slide rack still in the HybEZ tray; AMP 5® was incubated for 30 minutes and AMP6® for 15 min.

Signal detection and counter-staining

The 3, 3'-diaminobenzidine (DAB) reagent (which is oxidised to a brown product in the presence of hydrogen ions produced from the reaction of hydrogen peroxide with the horseradish peroxidase) was used to detect the signal produced by the probe hybridisation with the RNA in the tissues. Equal volumes of the two-component liquid substrate system (DAB-A and DAB-B) were mixed in a 1.5 ml microcentrifuge tube. A total volume of 40 µl of substrate system DAB-A: DAB-B were added per section; the tray containing the slides with DAB was covered and incubated for 10 min at 22°C. In the hood, the DAB from each slide was carefully disposed of (according to regulations) and then all the slides were washed three times with fresh distilled water. The tissue sections were counterstained with 50% haematoxylin (a basic dye that stains the

negatively charged structures of the cells such as the nucleic acids and the ribosomes) for 30 seconds and then immediately washed with distilled water until the sections were stained purple and the rest of the slide was clear.

Slides dehydration and mounting the samples

After washing in distilled water, the slides were then placed into a staining dish and, in the hood, the tissue sections were passed through a dehydration two 100% ethanol incubations (each for 2 minutes). This was followed by two immersion in xylene (each for 5 minutes) to remove lipid residues. From the xylene, one slide at a time, the excess fluid was tapped off the slides, and then three drops of Eco-mount (Biocare Medical, USA) were added on each coverslip which was then mounted on the slide. The slides were left to air-dry for 5 minutes.

3. 2. 5. 2. 2 RNAscope® 2.5 HD Duplex detection assay

The same FFPE pre-treatment (section 3. 2. 5. 2) was followed for both the brown and the duplex assays. The probes used were designed for 2 channels (C1 and C2) with the higher expressed probe in C1 which produces a green signal and the lower expressed probe at C2 which gives the red signal. Table 3.6 lists the probe names, accession and catalogue numbers, target region and channels designed and purchased from ACD Diagnostics®.

Table 3-5: RNAscope® probes used in the RNAscope® Duplex assays.

Gene	Entrez Gene ID	Accession No.	Target region	No. of Pairs	Channel	Catalogue no.
<i>PPIB</i> (peptidylprolyl isomerase B)-Mm-PPIB	19035	NM_011149.2	98 - 856	15	C1*	313911
POLR2A (DNA-directed RNA polymerase II subunit RPB1)-Mm-Polr2a	20020	NM_009089.2	2802 - 3678	20	C2**	312471
<i>DAPB</i> (dihydrodipicolinate reductase)	#	EF191515	414 - 862	10	C1	310043
<i>Mm-Mc_{3r}-C1</i>	17201	NM_008561.3	1627 - 2621	20	C1	412541
<i>Mm-Mc_{3r}-C2</i>	17201	NM_008561.3	1627 - 2621	20	C2**	412541-C2
<i>Mm-Mc_{5r}-C1</i>	17203	NM_013596.2	2 - 1154	20	C1	478381
<i>Mm-MRAP2-C1</i>	244958	NM_001177731.1	183 - 1387	20	C1	474411
<i>Mm-MRAP2-C2</i>	244958	NM_001177731.1	183 - 1387	20	C2	474411-C2
<i>GH-C2</i> (growth hormone)	14599	NM_008117.3	9 - 630	14	C2	445361-C2
<i>LHβ-C2</i> (Luteinising hormone –subunit beta)	16866	NM_008497.2	26 - 503	12	C2	478401-C2

C1*: refers to the probes used for the RNAscope® Brown and channel 1 Duplex assays. C2**: relates to probes used for channel 2 RNAscope® Duplex assay. #: gene unique to bacteria hence should not be expressed in mammalian tissue. Sequence unknown because manufacturer has not disclosed details.

After probe hybridisation for two hours, the slides were washed twice in 1X RNAscope® wash buffer, and then transferred and kept at room temperature overnight in 200 ml of X5 Saline-Sodium-Citrate (SSC) buffer (0.15M NaCl, 0.015M sodium citrate). The X5 SSC was made by diluting 50 ml of X20 SSC buffer (0.75M NaCl, 0.075M sodium citrate) (pH 7.0) in 150 ml of dH₂O.

Amplification steps 1-6

The slides were removed from 5XSSC and washed twice with the 1X RNAscope® wash buffer for 2 min. Excess liquid was tapped off, and the first 6 amplification steps were followed exactly as mentioned with the brown detection assay (section 3. 2. 5. 2. 1).

After brief spinning of the RED-B tube. The RED working solution was made by mixing RED-B to RED-A with a ratio of 1:60 and covered with aluminium foil until used. This was made 5 minutes before use as instructed in the protocol, 40 µl of the RED solution were added per section and then incubated covered in the HybEZ humidity control tray at 22°C for 10 min. The slides were then washed twice in 1X RNAscope® wash buffer: each wash was for 2 minutes.

Amplification steps 7-10

After washing, excess liquid was tapped off, and one drop per slide of AMP7® was added and incubated in the HybEZ humidity control tray at 40°C for 15 min. The slides were then washed twice with 1X RNAscope® wash buffer each for 2 min. Excess liquid was removed and a drop of AMP8® was added to each section before being incubated in the HybEZ humidity control tray at 40°C for 30 min. AMP9® was added after washing the slides with 1X RNAscope® wash buffer as mentioned before (section 3. 2. 5. 2. 1) and the slides were then incubated at RT in the HybEZ humidity control tray for one hour. AMP10® was added after washing the slides twice in the 1X RNAscope® wash buffer each for 2 minutes. The slides were incubated in the HybEZ humidity control tray at RT for 15 min then the slides were washed twice with the 1X RNAscope® wash buffer each for 2 minutes.

Green signal detection and counterstaining

The GREEN working solution was prepared by mixing GREEN-B with GREEN-A with a ratio of 1:50. The GREEN solution (40 µl) was added to each section; the slides were then incubated covered in the HybEZ humidity control tray for 15 minutes at room temperature. The slides were immediately washed (less than 30 seconds) with dH₂O. Haematoxylin (50%) was then used to counterstain the slides and left for no more than 30 seconds. The slides were then rewashed with tap water for no more than 30 seconds.

Section mounting

The slide rack was put in the oven (60°C) to dry for 30 minutes and then left at room temperature to cool down. Three drops of Vectamount mounting medium were added to coverslips, and those were then placed carefully over the sections avoiding air bubbles. The slides were left to dry for 5 minutes at 22°C before visualisation.

3. 2. 5. 2. 3 Pituitary gland RNAscope® 2.5 HD Duplex detection assay with channel swap

For the pituitary gland sections, an additional method was used to detect the double expression of *GH* or *LHβ* at C1 and *MRAP2* at C2 channels. The *GH* probe was used as a marker for the somatotrophs, and *LHβ* probe was used as a marker for gonadotrophs. Initially, the method above was followed. However, the expression signal intensity of *GH* and *LHβ* in the pituitary gland was masking the expression signal of the other channel probe. Therefore the signal detection was modified accordingly. Although the channels are as mentioned; the signal detection will be reversed. The signal detected for C1 will be red (instead of green) and for C2 will be green (instead of red). This is done by using the same protocol as in 3. 2. 5. 2. 2 but with swapping AMP4 and AMP8. With AMP8 (instead of AMP4) incubated for 40°C for 15 min and AMP4 (instead of AMP8) incubated at 40°C for 30 min. The RNAscope® C1 channels were found to generate expression signal intensity (GREEN) that is lower than that of C2 (RED). Therefore, the swap allows the cost-effective detection of the C2 designed

probes (in this case *GH* or *LHβ*) at C1 channel and *vice versa* without the need to design new probes for either *GH* or *LHβ*.

Visualization of the RNAscope® probes (Brown or Duplex)

The slides were visualised using a bright-field microscope. For a clear image resolution, the slides were also, visualised using the NanoZoomer-XR Digital slide scanner (Hamamatsu Photonics, Japan). Positive control slides (using the housekeeping gene peptidylprolyl isomerase B (*PPIB*) probe) were inspected for the signal strength. The negative control slides (bacterial gene *DAPB* probe) were checked for background staining (see Figure 3.3).

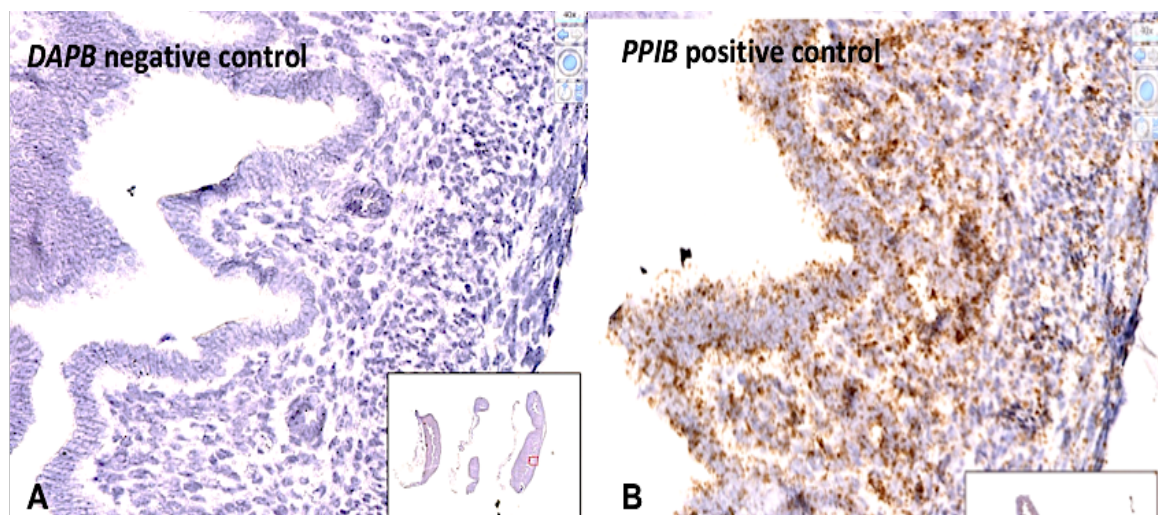
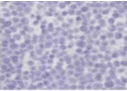
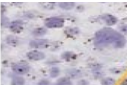
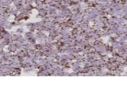


Figure 3.3: RNAscope® HD 2.5 Brown assay in the uterus of 2 weeks old mouse. A: negative control probe (*DAPB*: dihydrodipicolinate reductase) was used to check for background staining. B: Positive brown punctate staining for the positive control probe, *PPIB*: peptidylprolyl isomerase, used to validate the treatment conditions for each tissue.

3. 2. 5. 3 Interpretation of the RNAscope® assay

The mRNA is detected as dots, and each dot represents one copy of mRNA. The intensity of the signal signifies the presence of more than one mRNA copy per one cell. The mRNA expression levels were determined using the scoring guideline provided by ACD Diagnostics (see Table 3.7 for interpretation of the expression signals).

Table 3-6: Scoring guidelines for RNAscope® staining by ACD Diagnostics.

Image	Score	Microscopic appearance or visualisation
	0	0-1 dots/10 cells (40X magnification)
	1	1-3 dots/cell (20X-40X magnification)
	2	4-10 dots/ cell (20X-40X magnification) + few clusters
	3	>10 dots/ cell. Less than 10% positive cells are with clusters
	4	>10 dots/ cell. More 10% positive cells are with clusters

This scoring guideline enables manual semi-quantitative analysis of mRNA transcripts of the target gene. The staining is classified into five grades: 0, 1+, 2+, 3+, and 4+. Dots are representative of mRNA copies with the cells. Cluster refers to overlapping signals due to merged dots). The signal on positive signal sections should be detected as punctate dots all over the tissue section (permission to use table was granted by ACD Diagnostics, USA).

3. 2. 5. 4 Quantification analysis of the RNAscope® 2.5HD brown and duplex assay

In chapter 4, a single hypothalamic section of each target region was analysed to examine areas expression the target genes. To carry out quantitative analyses, consecutive sections of each of the target region would have been required to cover the whole region thickness of each region (rPOA, mPOA and the arcuate nucleus).

In the current study, quantification analysis was conducted on pituitary sections to determine the expression level of *MC₃*, *MC₅* and *MRAP2*. The quantitative studies were also conducted to compare between 2 and 10 weeks old mice and pregnant (14 ± 1 dpc) mice in each of the pituitary gland, the ovary and the uterus. The workflow protocol was as described below.

At the magnification power of about 90X, a rectangle of about 6050 µm² was randomly selected on each section of the anterior pituitary gland where the outline of the cells was visible on each slide from each age group. Artefacts such as air bubbles or black precipitates were identified and excluded from the selection.

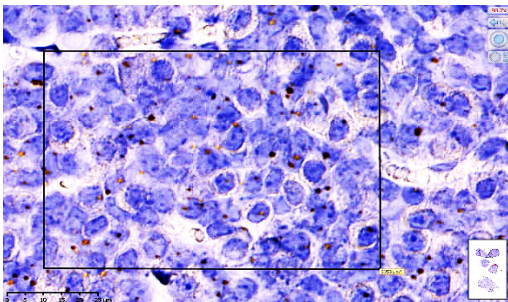


Figure 3.4: Selecting an area for quantification analysis in female mouse pituitary gland. The black rectangle represented an area of about 6050 µm².

The rectangle is then divided into smaller squares to enable counting cells within each square and the expression within each cell.

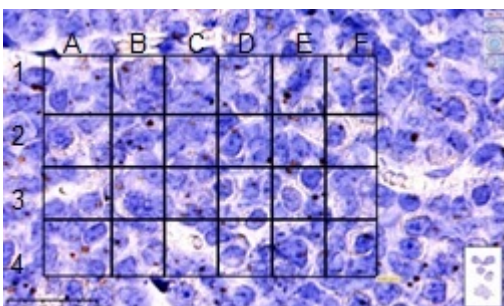


Figure 3.5: Dividing the area to be quantified for expression into small squares for cells expression counting.

The percentage of the expression in each section is measured using the following equation:

$$\text{Expression Percentage} = (\text{expression dots} \div \text{total cell count}) \times 100$$

The last step was calculating the mean of all sections on one slide to measure the overall expression level within one age/pregnant group.

$$\text{Expression (Exp) mean} = (\text{Exp (section 1)} + \text{Exp(section 2)} + \text{Exp(section 3)}) \div 3$$

The Percentage values were then plotted in GraphPad worksheets and analysed using One-way ANOVA to determine for statistical significance (p value) of the differential expression.

4 Molecular and cellular characterisation of the MC system in the female mouse hypothalamus

4. 1 Background

The hypothalamus is the first component of the HPO axis. It contributes to the regulation of the HPO axis through the release of gonadotropin-releasing hormone (*GnRH*) which stimulates the secretion of the gonadotropins (FSH and LH) from the anterior lobe of the pituitary glands. This chapter describes the characterization of both molecular and cellular expression of components of the melanocortin system within areas of the hypothalamus associated with regulation of the reproductive axis.

4. 1. 1 GnRH neurons distribution and axonal projections

The GnRH neurons develop outside the hypothalamus in the olfactory placode and then migrate to their final location within the hypothalamus. In all mammals, the GnRH course is represented as an inverted Y shape starting from the medial septum and diverging at the third ventricle then meeting again at the anterior hypothalamic area (see Figure 4.1). However, there are differences as to where GnRH neurons predominate within that course in different species (Herbison, 2014). The soma of mouse and rat GnRH neurons are mainly found in the preoptic area; they are also found alongside the ventral aspect of the anterior hypothalamic area (AHA). The axons of these neurons project to the arcuate nucleus and median eminence (the latter two are collectively known as the mediobasal hypothalamus, MBH). These terminals release their GnRH content into the hypothalamic-hypophyseal circulation to be transferred to the gonadotropes in the anterior pituitary gland. Some GnRH neurons are found outside the hypothalamus in the periaqueductal area. In humans, in addition to the preoptic GnRH population, some neurons are also found in the arcuate nucleus (Herbison, 2014).

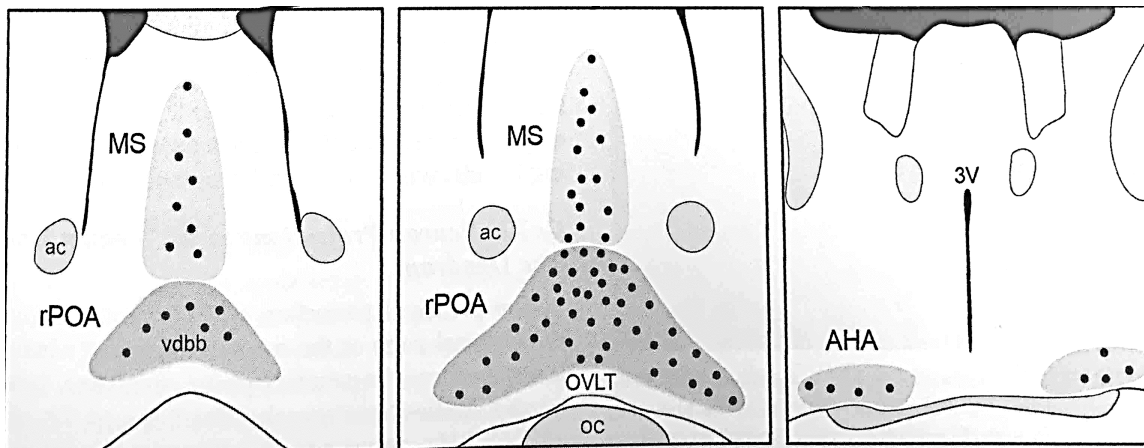


Figure 4.1: GnRH neurons locations within the mouse hypothalamus. The drawings represent the coronal section of the GnRH neurons distribution within the hypothalamus. The neuron distribution takes an inverted Y shape pattern in mice and rats with the predominance within the medial septum (MS), rostral preoptic area (rPOA) and the more caudally anterior hypothalamic area (AHA). (Permission to reproduce this schematic drawing has been granted by Elsevier. (Taken from Herbison, 2014).

4. 1. 2 Postnatal GnRH

After reaching their final location, the unique GnRH soma starts forming the endocrine network by sending their long dendritic axons to the median eminence which connects it with the hypophyseal-portal circulation found in that area (Herbison, 2016). The formation of this dendritic network occurs during the first 2- 3 weeks after birth and is thought to be regulated through glutamatergic and γ -aminobutyric acid (GABA) interactions with those maturing dendrites (Cottrell *et al.*, 2006). The biocytin cell-filling studies conducted in brain slices of postnatal (2 weeks old) and adult (about 8 weeks old) mice by Cottrell and colleagues revealed the extensive branching of the rostral preoptic GnRH neuronal dendrites in postnatal mice compared to adult animals; while the dendritic spines responsible for receiving synaptic input were duplicated near the GnRH neuronal body and proximal dendrites in adult animals compared to postnatal animals (Cottrell *et al.*, 2006). The postnatal development of the synaptic innervation and its interaction with different neuroendocrine input is thought to trigger the GnRH release that is responsible for the mechanism initiating puberty in mice (Cottrell *et al.*, 2006). However, the neuroendocrine factors that are thought to be interact with the GnRH dendritic network during the prepubertal period are yet to be identified. These factors were suggested to include kisspeptin and gonadal steroids.

Estradiol secreted by the growing ovarian follicles exert negative feedback on the release of GnRH. Recent kisspeptin cell specific estradiol receptor alpha mouse knockout (*KERαKO*) studies showed that the effect of estradiol during the juvenile period is exerted on the arcuate kisspeptin neurons (Dubois *et al.*, 2016). Once the ovarian follicles gain full maturity, a final GnRH is activated through the positive feedback mechanism exerted on the kisspeptin neurons located in the anteroventral periventricular area (AVPV); the release of GnRH leads finally to commencement of puberty through the first ovulation (Prevot, 2014; Dubois *et al.*, 2015).

4. 1. 3 GnRH and puberty

The onset of puberty in the female mouse is defined as the vaginal opening; this occurs as a culmination of a series of neuroendocrine and morphological events that occur at each level of the HPO axis leading to ovulation. At the hormonal level, the onset of puberty in girls preceded by a rise in the amplitude of LH pulsatile release during sleep in the hours between 2:00 am to 8:00 in the morning (from about 5 mIU/ml to 12 mIU/ml) (Griffin and Ojeda, 2004). Until now, the pathway that controls this event was not clearly defined, but it has been agreed that the rise in LH rise occurs as a result of an increase in the frequency and amplitude of GnRH pulsatile release (Herbison, 2016). Some of the hypothalamic pathways were found to influence the timing of puberty. These include pathways controlling sexual receptivity and behaviour, energy homeostasis and food intake regulation. AgRP, neuropeptide Y (NPY) and leptin are good examples of peptides involved in the control of food intake. AgRP/NPY neurons are localised in the arcuate nucleus, near to GnRH projections. These peptide hormones are thought to be involved in the timing of puberty (Cardoso *et al.*, 2014; Egan *et al.*, 2017). Leptin, which is an adipocyte-derived peptide, regulates food intake through both NYP/AgRP and POMC neurons (Elias *et al.*, 1999). Furthermore, synaptic communications between GnRH neurons and POMC neurons (through β -endorphin) in mice (Ward *et al.*, 2009) and rats (Chen *et al.*, 1989) support theories regarding the participation of POMC and the MCs in the timing of the onset of puberty (Manfredi-Lozano *et al.*, 2016).

4. 1. 4 GnRH pulsatile release

In rodents, tip-tail blood sampling enabled the measurement of the LH secretions in different phases of the estrous cycle and this was suggested was to reflect the secretion of GnRH (Czieselsky *et al.*, 2016). During metestrus and diestrus and proestrus, LH was released about every hour, and this pulse frequency was reduced to less than half the time during estrus. Ovariectomy was found to increase the LH pulsatile release to about six pulses in 2 hours and also caused increased basal LH release (Czieselsky *et al.*, 2016). The use of the mutant GNR23, that is characterised by an allele-dependent ephrin signalling mutation, with a resultant GnRH migratory failure had been shown to affect the LH pulsatile release, even though the frequency is retained at normal levels. These findings implicate the regulation of the LH pulsatile release by GnRH. The generation of the pulsatile pattern of GnRH release is thought to be regulated by both anteroventral periventricular nucleus (AVPV) and arcuate nucleus kisspeptin (Kiss^{AVPV} and Kiss^{ARC} respectively) neurons (Herbison, 2016), as recently demonstrated using optogenetics (Han *et al.*, 2015). As with the timing of puberty, pulsatile GnRH secretion is also affected by different pathophysiological conditions, such as starvation, which might lead to infertility. Infertility caused by starvation is thought to be mediated by AgRP. The AgRP neurons project directly to and make inhibitory synapses with both Kiss^{AVPV} and Kiss^{ARC} neurons while activation of the AgRP using clozapine has led to decreased fertility through delayed estrous cycles (Padilla *et al.*, 2017).

4. 1. 5 GnRH surge and the estrous cycle of mice

The estrous/menstrual cycle is controlled by the feedback mechanism on the hypothalamus (GnRH) and pituitary gland (LH); this mechanism is mediated by estradiol (E₂) and progesterone. Different studies in rhesus monkeys have shown that E₂ keeps the concentrations of gonadotropins, as well as GnRH, low during the entire ovulatory cycle except for the pre-ovulatory phase (Karsch *et al.*, 1973, Spies and Norman, 1975). The increase in circulating concentrations of E₂ (up to 360 pg/ml compared to of about 20 pg/m in other phases of the cycle) from growing ovarian follicles, evokes a surge in GnRH followed by a LH surge (Xia *et al.*, 1992). The same cycle of events also occurs in rats. Hypothalamic preparations collected from rats

showed constant frequency of GnRH pulses (with inter-pulse intervals of 40 minutes) throughout the estrous cycle. However, the amplitude was seen to rise in the afternoon of proestrus (Parent *et al.*, 2000).

Unlike GnRH pulse generating neurons, the GnRH neurons involved in producing the GnRH surge are localised and found in areas that express *c-fos*, which is a marker of neuronal activity. The *c-fos* expression is found to be upregulated by the time of the LH surge during proestrus (Vastagh *et al.*, 2016). In rodents, the GnRH surge generating neurons are located close to the organum vasculosum of lamina terminalis (OVLT) of the preoptic area (POA) (Herbison, 2016). The hypothalamic regions surrounding the OVLT are also reported to contain melanin-concentrating hormone (MCH) fibres (Murray *et al.*, 2006). MCH is suggested to have a role in the regulation of the generation of GnRH release in female rats through the MCH receptor 1 (MCH1-R) as well as MC₅ (Murray *et al.*, 2006). This might indicate that MC₅ has an indirect role in inducing ovulation.

Other melanocortin receptors are also thought to participate in controlling estrous cyclicity. This is supported by studies using MC₄-knockout mice (MC₄^{-/-}). MC₄^{-/-} adult female mice are obese but appeared to have regular estrous cycles. Their ovaries, however, contain many cystic large follicles and decreased numbers of the corpora lutea which might indicate previous anovulatory cycles (Sandrock *et al.*, 2009). This had led the team to the assumption that these MC₄-deficient mice would have inevitable ovarian failure due to abnormal gonadotropin stimulation or a failure at the hypothalamic-pituitary level (Sandrock *et al.*, 2009). These observations were only made on adult females and did not include animals from different stages of the reproductive cycle.

4. 1. 6 Hypothalamic control of pregnancy

Pregnancy is one of the most extensively researched fields, yet due to the complexity of the interaction between the different molecular, cellular and hormonal cues, it still needs further investigation to understand the maternal adaptation to metabolic, hormonal and other demands of pregnancy. Therefore, this section focuses on some of the hypothalamic inputs and adjustments involved in maintaining pregnancy.

During pregnancy, there is a decreased concentration of GnRH due to the feedback inhibition exerted by the sex steroids produced by the corpus luteum. In pregnant mare serum gonadotropin (PMSG) primed rats, the intra-arcuate and AVPV treatment with progesterone treatment was found to suppress the LH surge compared to vehicle-treated rats (He *et al.*, 2017). The inhibition of GnRH was found to persist after parturition but the inhibitory mechanism(s) at this stage were not well understood. Prolactin was thought to be responsible for suppressing GnRH during lactation. In 2007, Grattan and colleagues suggested that prolactin inhibits LH secretion through regulation of GnRH secretion in the mouse arcuate nucleus. This study had also shown the prolactin receptor to be expressed in a subpopulation of GnRH neurons in the murine arcuate nucleus (Grattan *et al.*, 2007).

As a physiological condition, pregnancy causes an increased metabolic demand to meet the requirements of the growing embryo and to prepare the mother for lactation after giving birth. This is achieved by an alteration in the neural circuit controlling appetite and energy homeostasis. Many neuroendocrine peptides are involved in this neural circuit such as leptin, ghrelin and prolactin. All of these peptides interact with two distinct populations of neurons, POMC neurons and NPY/AgRP neurons; both of which reside in the arcuate nucleus (Tong and Pelletier, 1992; Cowley *et al.*, 2001; Cowley *et al.*, 2003). As expected, AgRP is upregulated in pregnancy (Rocha *et al.*, 2003). This might explain the decreased sensitivity to α -MSH during pregnancy that has been recently reported (Ladyman *et al.*, 2016). There are no reports on whether hypothalamic POMC or its derived products (and hence α -MSH) are differentially expressed and accordingly differentially regulated during pregnancy. However, one of the end products of POMC is β -endorphin, which was found to stimulate food intake in rats is also found to be upregulated in pregnancy (Grandison and Guidotti, 1977). Therefore, examining the manner of POMC processing during pregnancy could reveal whether POMC processing changes to meet the metabolic demands of pregnancy.

4. 1. 7 The different approaches on hypothalamic organisation

There are different theories describing how the hypothalamus is organised. This is attributed to various reasons; first, the exact course of the hypothalamic remodelling during its development is still a perplexing argument to most neurobiologists (Puelles and Rubenstein, 2015). Second, different fundamental survival functions are controlled by this small region of the forebrain; this was proved by finding neurons of various physiological functions overlapped in the same hypothalamic area (Loes *et al.*, 1991). The third reason was the method or the technique that was used to define the different regions of the hypothalamus such, MR imaging (Loes *et al.*, 1991); histochemical studies (Pilgrim, 1974) and using the immunofluorescence techniques (Moga *et al.*, 1990). In this research, we have adopted the following functional organisation of the mouse hypothalamus: the hypothalamus is divided into the preoptic region, the tuberal region (which is made of the arcuate nucleus, ventromedial and dorsomedial nuclei as well as the median eminence) and the posterior region. The areas of interest in this research are the preoptic and the tuberal hypothalamus, as both regions contain GnRH nuclei and projections that are involved in mouse reproduction, as explained earlier.

The account of the hypothalamic role in reproduction highlighted above implies a role for the MC system at all stages of the reproductive cycle. Several research studies have focused on the indirect interaction of the central MC system with different components of the hypothalamus (Humphreys, 2004; Murray *et al.*, 2006; Sandrock *et al.*, 2009). This chapter aims to:

1. Determine suitable reference genes in the mouse hypothalamus for normalisation using GeNorm expression stability analysis.
2. Characterise *MC*₍₁₋₅₎, *MRAP1* and *MRAP2*, *POMC* and *AgRP* expression in the hypothalamus of different aged mice (2, 6, 10 and 14 weeks old).
3. Compare the expression of the melanocortin system members listed above in pregnant and non-pregnant mice.
4. Determine cellular expression of *MC*₃, *MC*₅ and *MRAP2* using chromogenic *in situ* hybridisation (RNAscope®).

4. 2 Methods

For a detailed account of the materials and techniques used see chapter 3.

4. 2. 1 Determining suitable reference genes in the hypothalamus

The most stable reference genes in the hypothalamus were selected using the GeNorm analysis described in detail in section 3. 2. 3. 4. 1. Duplicates of cDNA samples from each age group were used in these analyses.

4. 2. 2 Characterising the gene expression of the MC system

The identified reference genes were used to normalise data obtained from the RT-qPCR assays of the reverse transcribed RNA extracted from whole hypothalamic of female C57BL/6 mice aged 2, 6, 9, 10, 14 weeks and pregnant mice (14 ±1 day post coitus, dpc) (n=5; n=3 for 9 weeks and n=4 for 10 weeks). The efficiencies of the primers used in these assays were examined using standard curves with positive controls for each primer pair (see section 3. 2. 3. 4. 3 for details). The RT-qPCR amplification products were then separated on 2% agarose gel to check the size of the band and verify they were of the predicted size and to check for non-specific bands. The RT-qPCR data were analysed using the delta-delta CT method mentioned in section 3. 2. 3. 4. 3. C.

4. 2. 3 RNAscope® 2.5HD protocol

The hypothalamus sections were collected from female C57BL/6 mice aged 2 weeks, 10 weeks and pregnant (14 ± 1 dpc). Slides were selected for the RNAscope® studies with sections observed with the regions of interest: rostral and medial preoptic (rPOA; mPOA) and arcuate nucleus of the hypothalamus (as in Figure 4.1).

First studies included using RNAscope® 2.5HD single-plex (brown) staining kit with *MC₃*, *MC₅* and *MRAP2* as well as positive and negative controls.

The second group of studies included using RNAscope® 2.5HD duplex (C1-green/C2-red) staining kit with *MRAP2* at C1 and *MC₃* at C2 channels as well as 2-plex positive and 2-plex negative controls. See section 3. 2. 5 for full details.

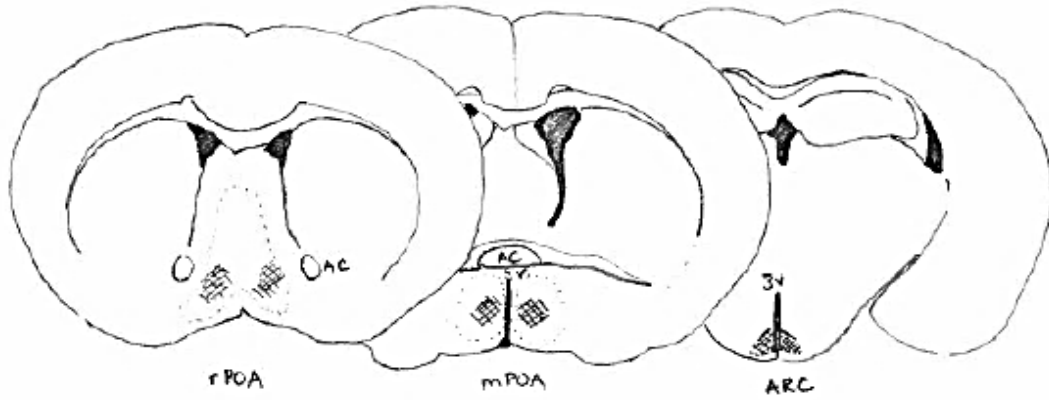


Figure 4.2: Hypothalamic sections showing the regions of interest studied with RNAscope®. rPOA: rostral preoptic area; mPOA: medial preoptic area and ARC: the arcuate nucleus of the hypothalamus. Drawings made by JF Murray using Franklin and Paxinos (2008).

4. 3 Results

4. 3. 1. A. Reference gene stability in the hypothalamus

In the female C57BL/6 mouse hypothalamus, tyrosine 3-monooxygenase/tryptophan 5-monooxygenase activation protein zeta (*YWHAZ*), calnexin (*CANX*) and glyceraldehyde-3-phosphate dehydrogenase (*GAPDH*) were the most stable genes whereas Ubiquitin C (*UBC*), actin beta (*ACTB*) and *18S* were the least stable genes (Figure 4. 3).

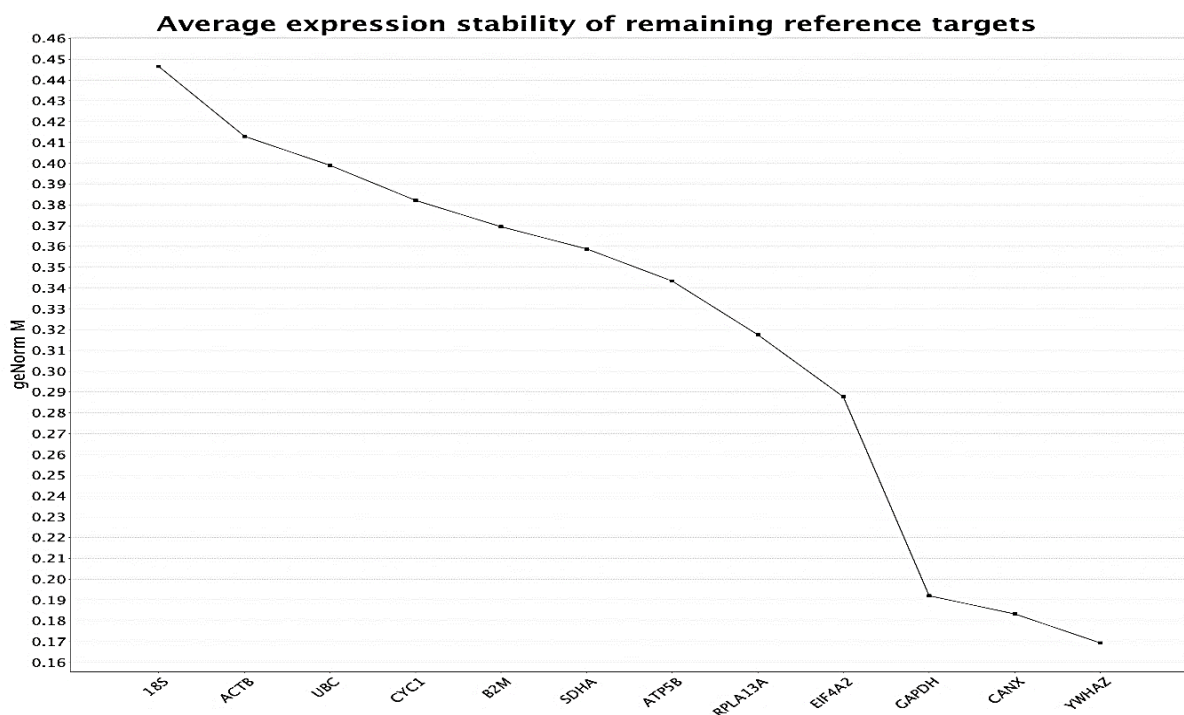


Figure 4.3: GeNorm ranking order of reference genes' stability in the female mouse hypothalamus. The ranking is based on calculating the geometric mean of the ranking values from Delta CT, BestKeeper, Normfinder and GeNorm reference gene analyses tools. The stability of 12 reference genes was examined using hypothalami of female mice aged 2, 6, 9, 10, 14 weeks and pregnant mice (14+1 dpc). The samples were run in duplicates. The reference genes are 18S, ACTB, ATP5B, B2M, CANX, CYC1, EIF4A2, GAPDH, RPL13A, SDHA, UBC and YWHAZ. CT values were imported to the qBase+ software and analysed using GeNorm (Biogazelle, Belgium).

The Optimal number of housekeeping genes to be used in normalising the RT-qPCR data was two for the hypothalamus. This was obtained by calculating the pairwise variation (V-score) with the sequential addition of each reference gene one at a time. A V-score above 0.15 indicates the optimal number of most stable reference genes to be used (Figure 4. 4). The V-score was calculated using GeNorm analysis by qBase+ software (Biogazelle, Belgium). See Appendix 3. A for graphs of the BestKeeper, Normfinder, Delta CT and comprehensive reference genes stability analyses.

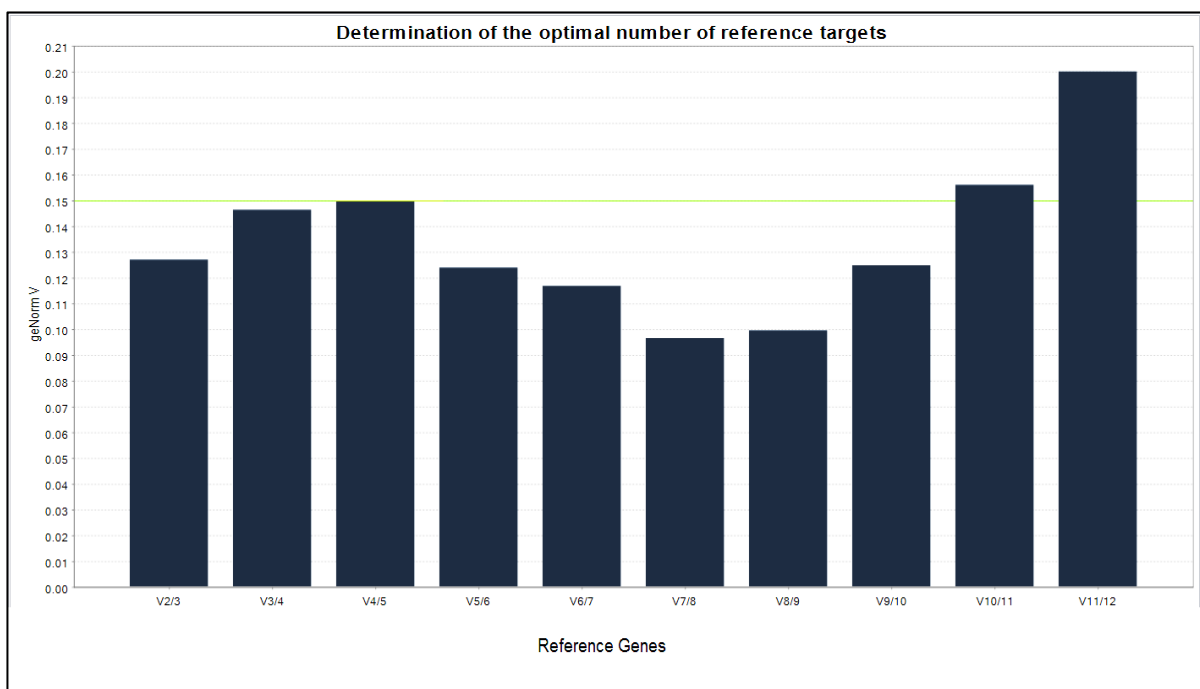


Figure 4.4: Variation score (V- score) by GeNorm. An optimal number of stable genes used normalisation was calculated by pairwise variation with the addition of each reference gene one at a time. A V-score equal or below 0.15 indicated the insignificance of using more reference genes. In this graph, 10 reference genes V-score results indicates the optimal number of most stable housekeeping genes (HKG) to be used in the hypothalamus are two (GeNorm by qBase+, Biogazelle, Belgium).

4. 3. 1. B. Amplification efficiencies of CANX and YWHAZ

The amplification efficiency is defined as the doubling of the cDNA template for each RT-qPCR cycle. Table 4.1 lists the standard curve slope (M), the coefficient of determination (R^2) and amplification efficiency (E) of CANX (80%) and YWHAZ (98%). These observations reflect the order of the stability of both reference genes as YWHAZ was most stable followed by CANX. See Figure 4. 5.

Table 4-1: Amplification efficiency of CANX and YWHAZ in the hypothalamus.

Gene	R^2 (Coefficient of Determination)	M (Measurement of Efficiency)	E (Efficiency)
CANX	0.99	-3.90	80%
YWHAZ	0.99	-3.62	98%

Pooled cDNA from all samples used in MC system expression in the hypothalamus were used in generating 1:2 standard curves. The efficiency was calculated automatically using the Rotor-Gene Q software (Qiagen, UK).

4. 3. 2 MC system expression

4. 3. 2. 1 Primers amplification efficiency

Different optimisation steps were needed to validate the RT-qPCR assay used in examining *MC* (₁₋₅), *MRAP1*, *MRAP2*, *POMC* and *AgRP* expression in the female reproductive axis. These included choosing the right annealing temperature for primer specific binding and evaluating the RT-qPCR efficiency. A 100% efficient RT-qPCR assay means that the cDNA amplification doubles each cycle.

A low primer efficiency (<90%) could be due to poor optimisation, poorly designed primers or the presence of *Taq* polymerase inhibitors. Nonspecific products, such as primer dimers, could cause an efficiency higher than 110%. Determining the efficiencies is typically done by serial dilutions of the tissue of interest, as explained in chapter 3.

In Figure 4. 5. A, amplification curve 1 represents the most concentrated sample. The the curves shift to the right as the samples are more diluted as seen with amplification curve 5. Table 4. 2 lists the primer pair amplification efficiencies for the *MC* (1-5), *MRAP1*, *MRAP2*, *POMC* and *AgRP*.

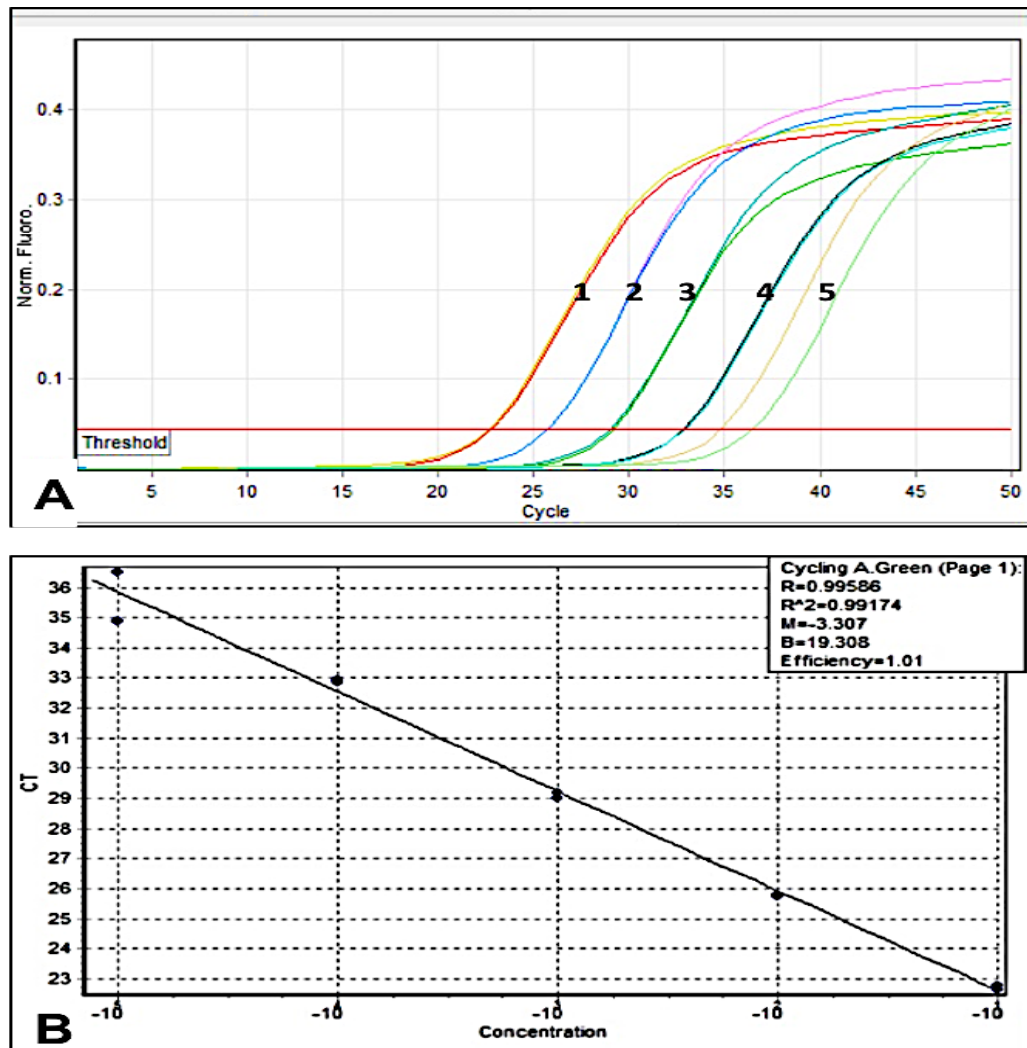


Figure 4.5: A representative example of the data acquired for the calculation of primer pair efficiency (MC_5 standard curve). A: an amplification curve produced by plotting the number of amplification cycle for a five-point serial dilution of cDNA against the normalised fluorescence units. The efficiency of the primer pair for MC_5 was tested using cDNA from a preputial gland from a male mouse. The cDNA input range is from 30.61 ng to 0.0031 ng (10X fold dilutions). B: semi-log regression line plot of CT value vs log of nucleic acid concentration. CT: threshold crossing point, M: is the line of best fit. Efficiency is calculated automatically using the Rotor-Gene Q software (Qiagen, UK).

Table 4-2: Primer pair amplification efficiencies for the MC₍₁₋₅₎, MRAP1, MRAP2, POMC and AgRP.

Primer	R² (Coefficient of Determination)	M (Measurement of Efficiency)	E (Efficiency)
<i>MC₁</i>	0.96	-3.33	100%
<i>MC₂</i>	0.99	-2.68	136.20%
<i>MC₃</i>	0.98	-3.03	113.81%
<i>MC₄</i>	0.95	-3.28	101.78%
<i>MC₅</i>	0.99	-3.31	100.50%
<i>POMC</i>	0.99	-3.27	102.21%
<i>MRAP 1</i>	0.97	-3.11	109.67%
<i>MRAP 2</i>	0.99	-3.16	107.04%
<i>AgRP</i>	0.99	-3.31	100.00%

Different female mouse tissues were used for testing the each of the primer pairs' efficiencies (whole mouse brain for MC₁, adrenal gland for MC₂ and MRAP1, pituitary gland for MC₃ and POMC, hypothalamus for MC₄ and MRAP2, preputial gland (male) for MC₅ and skin for AgRP). R²: coefficient of determination, M: The graph slope and E: efficiency. The efficiency was automatically calculated using ThermoScientific qPCR Efficiency Calculator (ThermoScientific, 2015). See Table 1 for primer sequences and expected products sizes.

4. 3. 2. 2 MC system expression

All the MC system members (*MC₍₁₋₅₎*, *MRAP1*, *MRAP2*, *POMC* and *AgRP*) are expressed in the hypothalamus. The expression of the mRNA for these targets is not the same. At 2, 6, 9, 10 and 14 weeks old and pregnant (14 ±1 dpc), the hypothalamic expression of both MC₁ and MC₂ was very low (Figure 4. 6 A and B, respectively).

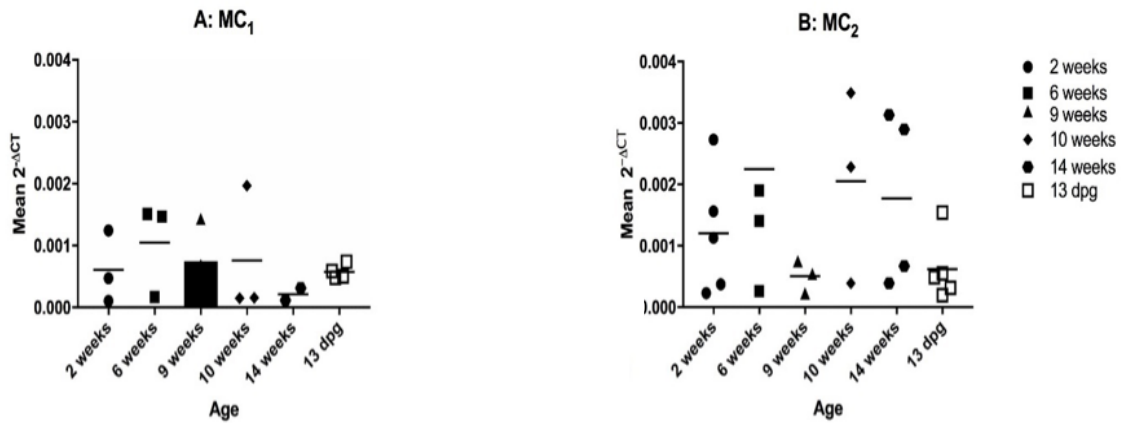


Figure 4.6: MC_1 and MC_2 expression in the female mouse hypothalamus. Hypothalamic cDNA duplicates from female C57BL/6 mice aged 2, 6, 9, 10 and 14 weeks and pregnant mice (14 +1 DPC) (No. of animals =3-5) were used in the RT-qPCR studies. A: MC_1 ; B: MC_2 . CT values of each assay were exported to an Excel worksheet, analysed using the delta CT Method developed by Pfaffl (2001). The skewed data seen in the graphs are due to animal sample variations (old vs. newly obtained samples). The $2^{-\Delta CT}$ values were imported to GraphPad and analyses using one-way analysis of variance (ANOVA). (Prism 7, USA).

In Figure 4. 7. A, there appeared to be a decrease in hypothalamic MC_3 expression between 2 and 6 weeks of age, however, as the animals got older the expression increased so that at 10 and 14 weeks of age the amount of MC_3 expressed was similar to that at 2 weeks of age. Pregnancy appeared to not affect expression compared to 9 weeks old non-pregnant mice. There were no significant differences in expression between any of the age groups or pregnant animals.

The expression of MC_4 appeared to be of a similar pattern of expression to MC_3 in the 2, 6, 9, 10 and 14 weeks old hypothalami. In the pregnant animal, MC_4 expression was decreased compared to 14 weeks old animals. Age and pregnancy did not affect the pattern of MC_4 expression in the mouse hypothalamus as seen in Figure 4. 7. B.

Age had an effect on the expression of MC_5 in the mouse hypothalamus. Neonatal animals had an increased MC_5 ($P = 0.0011$) compared to 6, 9, 10 and 14 weeks old and pregnant (14 ± 1 dpc) animals which appeared to have the same level of MC_5 expression as shown in Figure 4. 7. C.

$MRAP1$ expression appears to higher in older animals (10 and 14 weeks old mice) compared to the younger animals (2, 6 and 9 weeks old mice: Figure 4. 7. D). Pregnant animals showed a similar level of $MRAP1$ expression to a non-pregnant animal of the same age (9 weeks old mice). However, there were no significant changes in the

expression in relation to both age and pregnancy. *MRAP2* expression appeared to be increased between 2 weeks and 6 weeks old mice and then the expression dropped to lower levels in 9 weeks old animals (Figure 4. 7. E). However, older mice (10 and 14 weeks old mice) appeared to have higher *MRAP2* expression than both 2 weeks and 6 weeks old mice. Pregnant animals appeared to have higher *MRAP2* expression compared to non-pregnant animals of the same age (9 weeks old mice) but still lower than the expression seen in 10 and 14 weeks old mice. Nonetheless, both age and pregnancy did not affect *MRAP2* expression significantly.

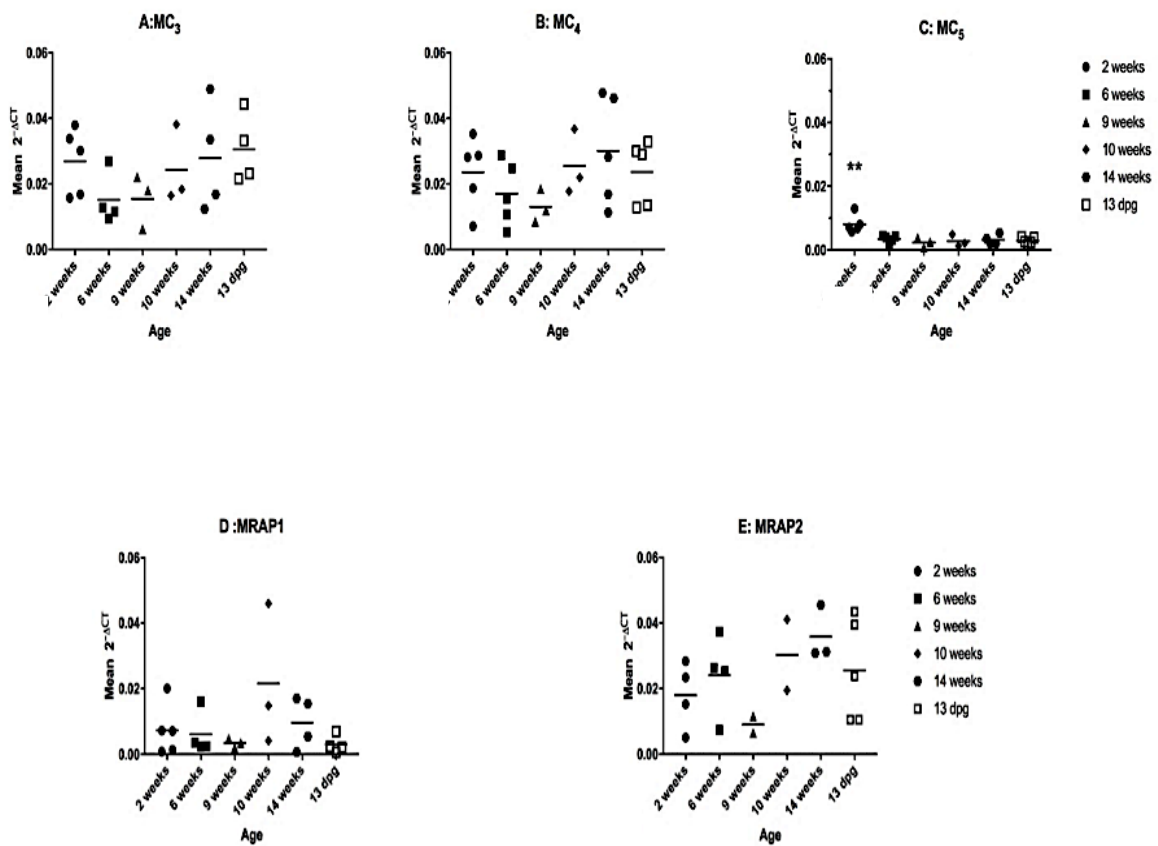


Figure 4.7: MC₃₋₅, MRAP1 and MRAP2 expression in the female mouse hypothalamus. Hypothalamic cDNA duplicates from female C57BL/6 mice aged 2, 6, 9, 10 and 14 weeks and pregnant mice (13 +1 DPC) (No. of animals =3-5) were used in the RT-qPCR studies. A: MC₃; B: MC₄; C: MC₅; D: MRAP1; E: MRAP2. **: P value= 0.0011. CT values of each assay were exported to an Excel worksheet, analysed using the delta CT Method developed by Pfaffl (2001). The skewed data seen in the graphs are due to animal sample variations (old vs. newly obtained samples). The $2^{-\Delta CT}$ values were imported to GraphPad and analyses using one-way analysis of variance (ANOVA). (Prism 7, USA).

Both POMC and AgRP showed higher expression levels than other members of the MC system (*MC₁₋₅*, *MRAP1* and *MRAP2*). POMC expression increased between 2 weeks old and 6 weeks old mice then showed a small decrease in expression in 9 weeks old mice. The expression of POMC increased dramatically in older animals (14 weeks old mice) ($P = <0.0001$) compared to 2 weeks old mice. Pregnant animals showed a small increase in expression compared to non-pregnant animals of the same age (9 weeks old mice: Figure 4. 8. A).

AgRP expression appeared to be decreased between 2 weeks and 6 weeks old mice and got higher in 9 weeks old mice (Figure 4. 8. B). Older mice (10 and 14 weeks old mice) had a similar expression that was lower than that seen in 9 weeks old mice. Pregnancy did not change the expression of AgRP as seen when compared to non-pregnant animals of similar age (9 weeks old mice). A summary of the *MC₍₁₋₅₎*, *MRAP1*, *MRAP2*, *POMC* and *AgRP* expression in the female mouse hypothalamus is presented in Table 4.3.

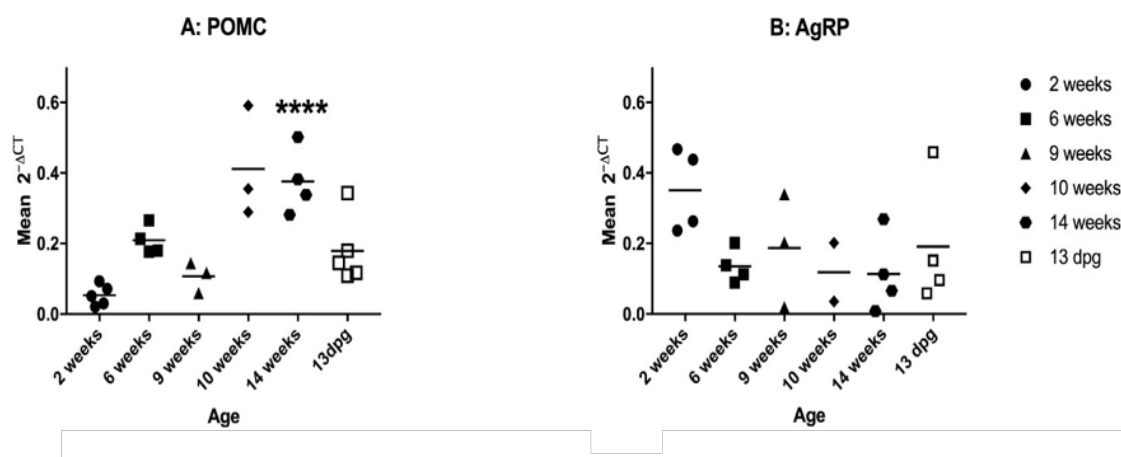


Figure 4.8: POMC and AgRP expression in the female mouse hypothalamus. Hypothalamic cDNA duplicates from female C57BL/6 mice aged 2, 6, 9, 10 and 14 weeks and pregnant mice (14 +1 DPC) (No. of animals =3-5) were used in the RT-qPCR studies. A: POMC; B: AgRP. CT values of each assay were exported to an Excel worksheet, analysed using the delta CT Method developed by Pfaffl (2001). The skewed data seen in the graphs are due to animal sample variations (old vs. newly obtained samples). The $2^{-\Delta CT}$ values were imported to GraphPad and analyses using one-way analysis of variance (ANOVA). (Prism 7, USA).

Table 4-3: MC system expression in the female hypothalamus.

HYPOTHALAMUS (n= 3-5)				
Gene	Expression	P value	Effect of Age	Effect of Pregnancy
<i>MC₁</i>	+	0.80	-	-
<i>MC₂</i>	+	0.35	-	-
<i>MC₃</i>	+	0.33	-	-
<i>MC₄</i>	+	0.36	-	-
<i>MC₅</i>	+	0.0011	++	-
<i>POMC</i>	+	<0.0001	++++	-
<i>AgRP</i>	+	0.18	-	-
<i>MRAP1</i>	+	0.20	-	-
<i>MRAP2</i>	+	0.27	-	-

The table represents each gene examined in hypothalamic cDNA from 3-5 female C57BL/6 mice. Age and pregnancy effects were examined by using animals aged 2, 6, 9, 10 and 14 weeks and pregnant mice (14 +1dpc). *MC₍₁₋₅₎*, *MRAP1*, *MRAP2*, *POMC* and *AgRP* were found in the hypothalamus. Age had an impact on the expression of *MC₅* (p-value 0.0011) and *POMC* (p-value <0.0001). There appeared to be no effect of pregnancy on the expression of any of the genes of interest when compared to non-pregnant mice of similar age (9 weeks old). (+) Indicate the presence of a gene or significant effect by age or pregnancy; (++) indicate moderate significance; (++++): indicate high significant were p <0.0001; (-): indicates the absence of a gene or insignificant effect by age or pregnancy. N/A: not applicable.

4. 3. 2. 3 Validation of the MC system expression

The products of the RT-qPCR of *MC₍₁₋₅₎*, *POMC*, *MRAP1*, *MRAP 2* and *AgRP*, as well as *CANX* and *YWHAZ*, were examined by electrophoresis on a 2% agarose gel (composition and method described in section 3. 2. 4. 3. 3: Figure 4. 9). Included were non-template controls for each of the target genes and the reference genes to check for genomic contamination.

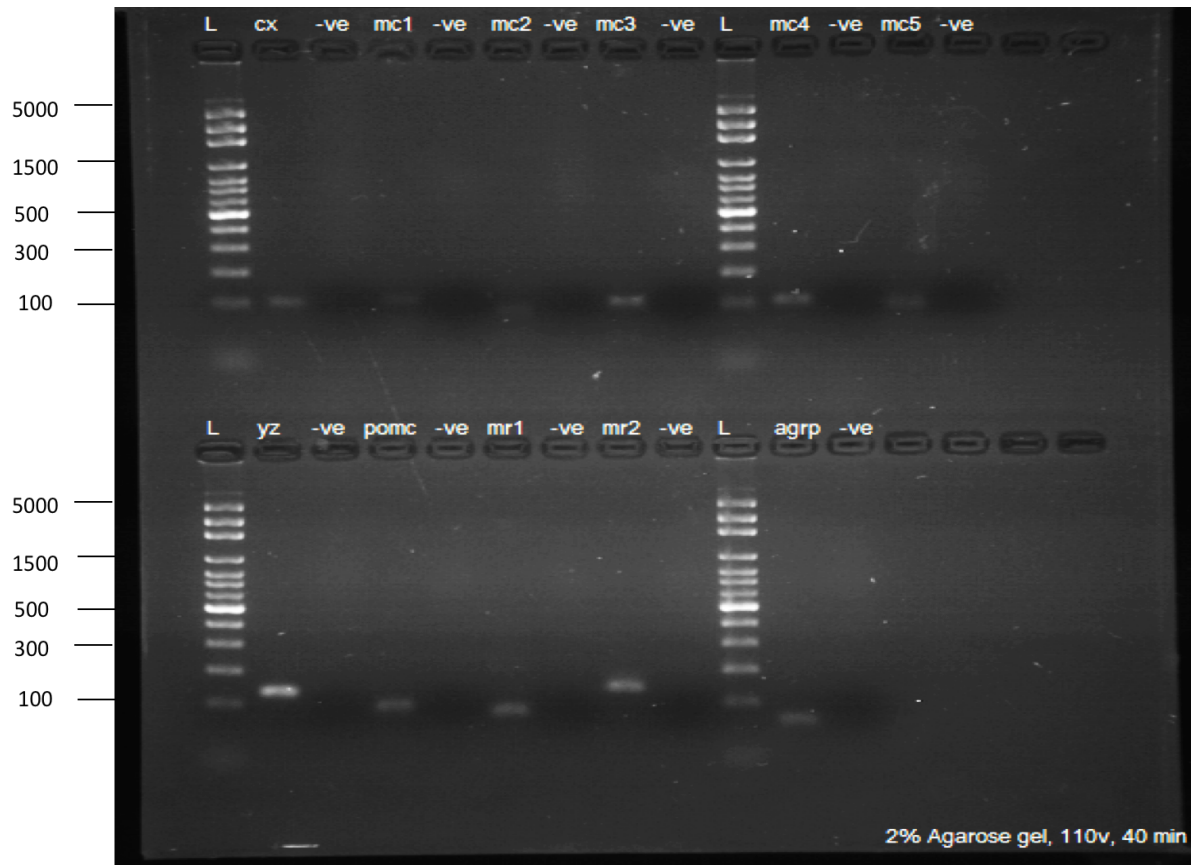


Figure 4.9: Gel electrophoresis of RT-qPCR of MC system in the hypothalamus. The RT-qPCR products were separated on 2% agarose gel at 110 volts for 40 minutes. Where L = ladder 100 bp to 5000 bp; (ThermoScientific, UK); CX = CANX, 105 bp; MC₁ = 127 bp et cetera, MC₂ = 86 bp, MC₃ = 108 bp, MC₄ = 106 bp, MC₅ = 90 bp, yz = YWHAZ (141 bp), POMC = 99 bp, MRAP1 = 86 bp, MRAP2 = 150 bp, AgRP = 63 bp, -ve: non-template control for gene of interest in previous lane. Gel image was taken using UVIPRO (Uvitec, UK).

4. 3. 3 Localisation of MC₃, MC₅ and MRAP2 mRNA transcripts in the female mouse hypothalamus

In the RNAscope[®] 2.5HD single-plex (brown) assays, a single gene of interest was studied on each hypothalamic section. Positive target probe signal is visible as punctate brown dots within cells.

Before studying each of the genes of interest, it was necessary to optimise the RNAscope[®] pre-treatment conditions with the female mouse hypothalamic tissues. An incubation in the RNAscope[®] target retrieval reagent of 15 minutes produced a very weak signal in the hypothalamic sections (data not shown). Therefore, the incubation time was increased to 17 minutes. This period was enough to produce a strong expression signal (Figure 4. 10. A) and did not show any background staining in the

negative control (Figure 4. 10. B). The negative control is a probe designed to hybridise with mRNA copies of bacterial protein 4-hydroxy-tetrahydrodipicolinate reductase, *DAPB* that should not be expressed in other species. No staining with the negative control indicates optimal treatment conditions that aimed to block non-specific binding of the mRNA probes. The intense staining signal seen with the positive control, Peptidylprolyl Isomerase B, *PPIB* mRNA probe indicates section treatment conditions enabled effective tissue permeability facilitating the hybridisation of the target probes with their target sequence within the tissue sections (Figure 4. 10. A).

The difference of expression between 2, 10 weeks old and the pregnant could not be determined due to lack of time and resources as calculating the expression levels should be done in serial hypothalamic sections to cover the whole thickness of the of each area. Therefore, the assay is considered a qualitative assay instead of quantitative one.

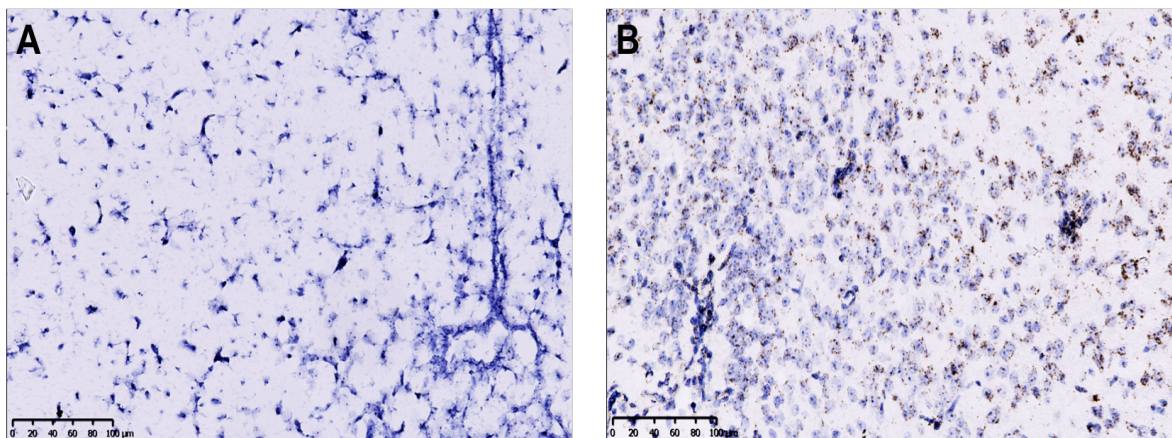


Figure 4.10: The RNAscope® 2.5HD Brown assay in the female mouse hypothalamus. A: RNAscope® 2.5HD Brown assay of negative probe (DAPB). This was included to ensure there is no background staining indicating optimum treatment conditions. B: RNAscope® 2.5HD Brown using positive probe (PPIB). The expression signal represented with brown dots of mRNA copies with the tissue. 3V: third ventricle. Images were taken using a NanoZoomer slide scanner (Hamamatsu Photonics) at King's College London.

In the RNAscope® 2.5HD duplex assays, two different target probes were hybridised as two channels, channels 1 (C1) and channel 2 (C2). The signal detection of the RNAscope® duplex assay represented as green (C1) and/or red (C2) dots. The horseradish peroxidase detects the green signal while the red signal is detected through the activity of alkaline phosphatase as demonstrated in Figure 4. 11. A. The probes used in Figure 4. 11. A were *PPIB* at C1 (green) and RNA polymerase II subunit (*POLR2A*) at C2 (red).

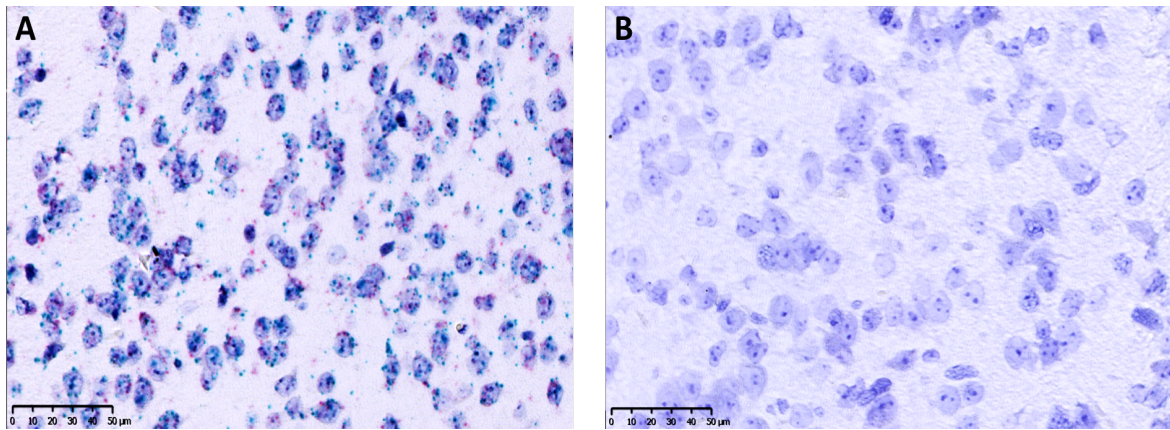


Figure 4.11: The RNAscope® 2.5HD Duplex assay in the female mouse hypothalamus. A: The RNAscope® 2.5HD Duplex 2-plex assay using positive probes. The double expression is seen as green dots for the expression of the *PPIB* at (C1) and the red dots for the expression of *POLR2A* (C2). B: The RNAscope® 2.5HD Duplex 2-plex negative probes (DAPB) which was included to ensure the absence of background staining and optimum conditions. Images were taken using a NanoZoomer slide scanner (Hamamatsu Photonics) at King's College London.

4. 3. 3. 1. B RNAscope® 2.5HD detection of *MC₃*, *MC₅* and *MRAP2* in the rPOA

1. RNAscope® 2.5HD-singleplex (Brown) assay

Based on the RNAscope® results, *MC₃* expression was detected in the mouse rPOA of 2 weeks, 10 weeks and pregnant (14 ± 1 dpc) mice. The expression appeared to increase between 2 and 10 weeks old mice. Pregnant mice appeared to have a lower level of expression than both 2 weeks and 10 weeks old animals (Figure 4.12, A-F).

MC₅ was detected at lower levels than *MC₃* in the rPOA. The *MC₅* expression levels did not change between 2 weeks, 10 weeks old mice and in pregnant (14 ± 1 dpc) mice hypothalamic section (Figure 4.13, A-F).

MRAP2 was detected in the rPOA of 2 weeks, 10 weeks and pregnant (14 ± 1 dpc) mice hypothalami at higher levels than *MC₃* and *MC₅*. Pregnant animals appeared to have the highest level of expression compared to 2 weeks and 10 weeks old mice while the latter two ages seemed to have the same level of expression (Figure 4.14, A-F)

The assay included both positive (*PPIB*) and negative (*DAPB*) probes to make sure that optimal hybridization conditions were maintained and that there was no background staining, respectively. Results of those sections were similar to those in Figure 4. 10. B and C, respectively.

2. RNAscope® 2.5HD-duplex assay in rPOA of female mouse hypothalamus

Double expression of *MRAP2* (C1-green) and *MC₃* (C2-red) was observed in hypothalamic sections of 2 weeks, 10 weeks and pregnant (14 ± 1 dpc) (Figure 4. 15). In the current findings, there appeared to be more co-expression in 10 weeks old mice and the hypothalamic section of pregnant mice compared to 2 weeks old mouse hypothalamus (Figure 4.15, A - F). In addition to the double expression there were cells expressing either *MC₃* or *MRAP2* alone.

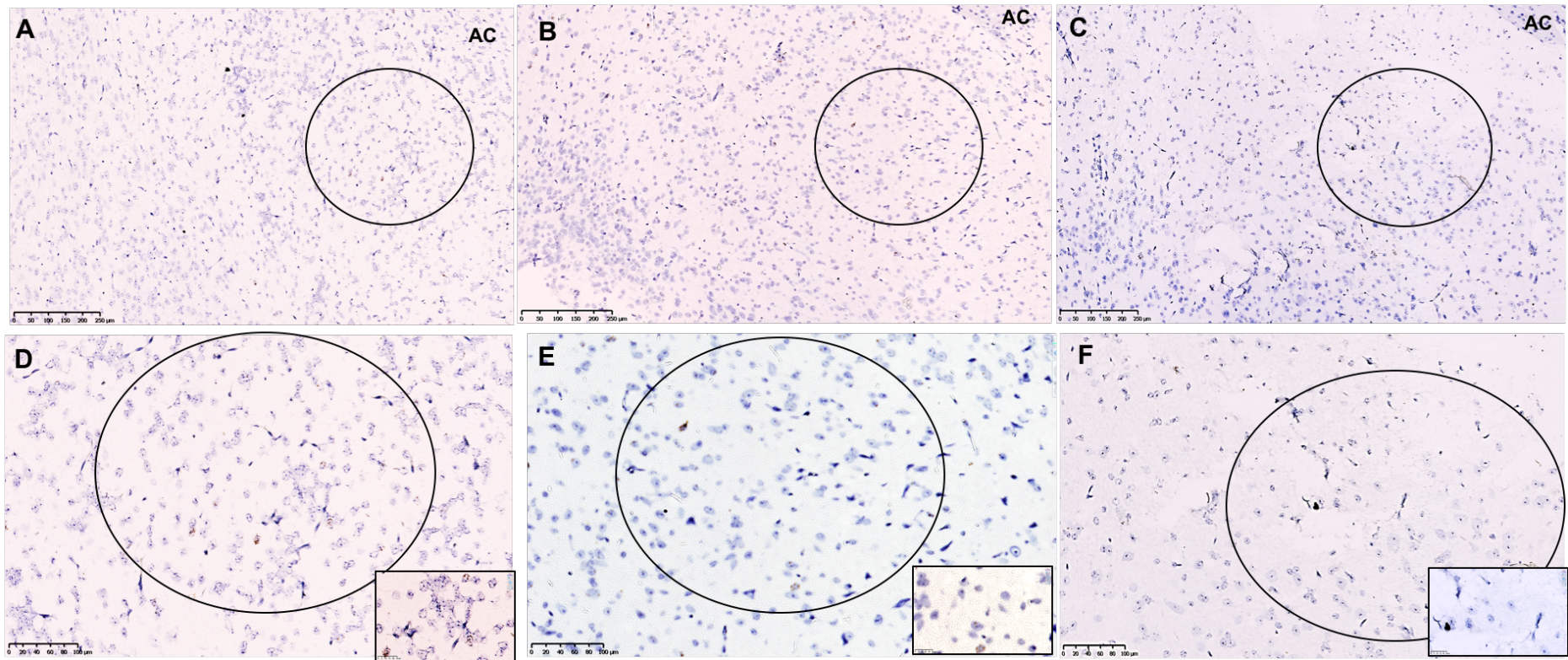


Figure 4.12: RNAscope® 2.5HD Brown assay of MC₃ in rPOA of female mouse hypothalamus. The assay was carried in hypothalami of mice aged 2 weeks, 10 weeks and pregnant (14 ± 1) mice. A: MC₃ expression in 2 weeks hypothalamus; B: MC₃ expression in 10 weeks hypothalamus; C: MC₃ expression in pregnant (14 ± 1 dpc) hypothalamus; D: Higher magnification of MC₃ expression in 2 weeks hypothalamus E: Higher magnification MC₃ expression in 10 weeks hypothalamus and F: Higher magnification MC₃ expression in pregnant (14 ± 1 dpc). The black circles represent the rPOA which is medial to the anterior commissure (AC). Each age group was conducted as two slides with two sections per slide. Images were taken using a NanoZoomer slide scanner (Hamamatsu Photonics) at King's College London.

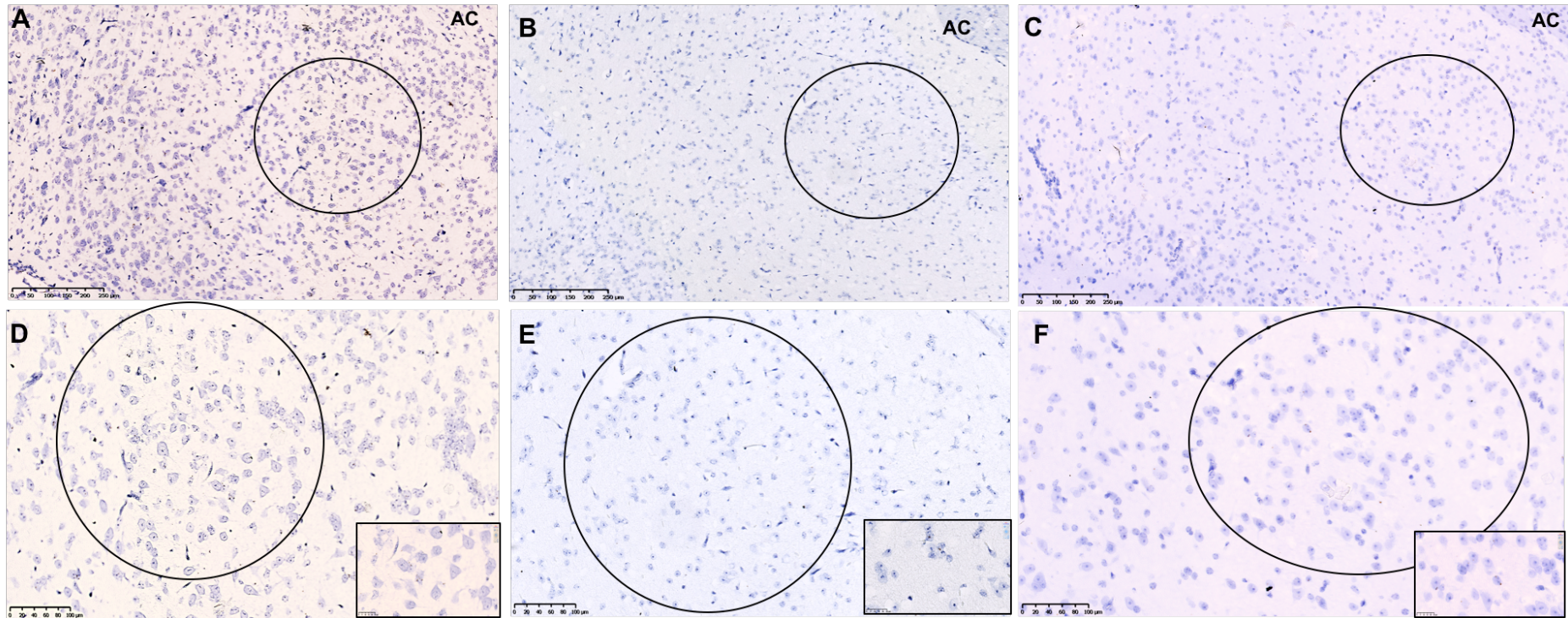


Figure 4.13: RNAscope® 2.5HD Brown assay of MC₅ in rPOA of female mouse hypothalamus. The assay was carried in hypothalami of mice aged 2 weeks, 10 weeks and pregnant (14 ±1) mice. A: MC₅ expression in 2 weeks hypothalamus; B: MC₅ expression in 10 weeks hypothalamus; C: MC₅ expression in pregnant (14 ±1 dpc) hypothalamus; D: Higher magnification of MC₅ expression in 2 weeks hypothalamus E: Higher magnification MC₅ expression in 10 weeks hypothalamus and F: Higher magnification MC₅ expression in pregnant (14 ±1 dpc). The black circles represent the rPOA which is medial to the anterior commissure (AC). Each age group was conducted as two slides with two sections per slide. Images were taken using a NanoZoomer slide scanner (Hamamatsu Photonics) at King's College London.

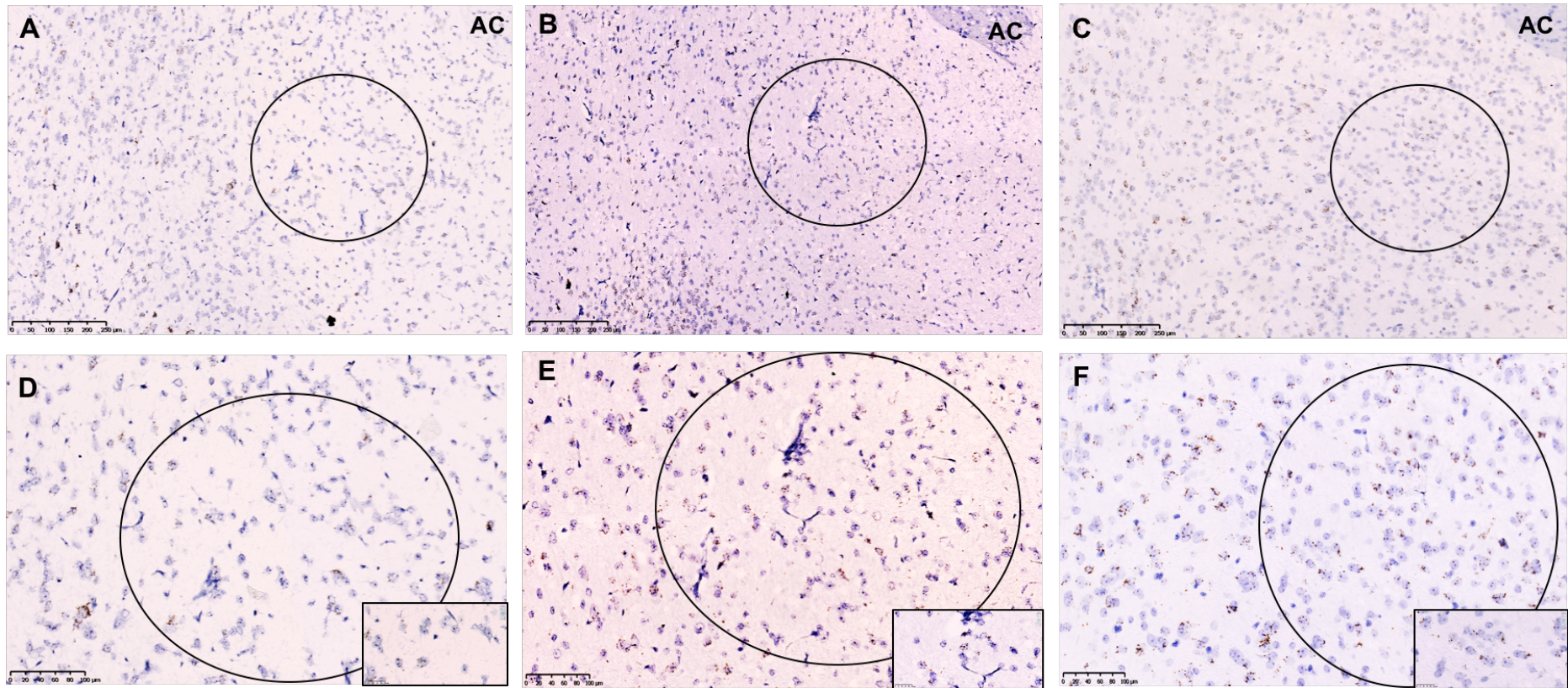


Figure 4.14: RNAscope® 2.5HD Brown assay of MRAP2 in rPOA of female mouse hypothalamus. The assay was carried in hypothalami of mice aged 2 weeks, 10 weeks and pregnant (14 ± 1) mice. A: MRAP2 expression in 2 weeks hypothalamus; B: MRAP2 expression in 10 weeks hypothalamus; C: MRAP2 expression in pregnant (14 ± 1 dpc) hypothalamus; D: Higher magnification of MRAP2 expression in 2 weeks hypothalamus E: Higher magnification MRAP2 expression in 10 weeks hypothalamus and F: Higher magnification MRAP2 expression in pregnant (14 ± 1 dpc). The black circles represent the rPOA which is medial to the anterior commissure (AC). Each age group was conducted as two slides with two sections per slide. Images were taken using a NanoZoomer slide scanner (Hamamatsu Photonics) at King's College London.

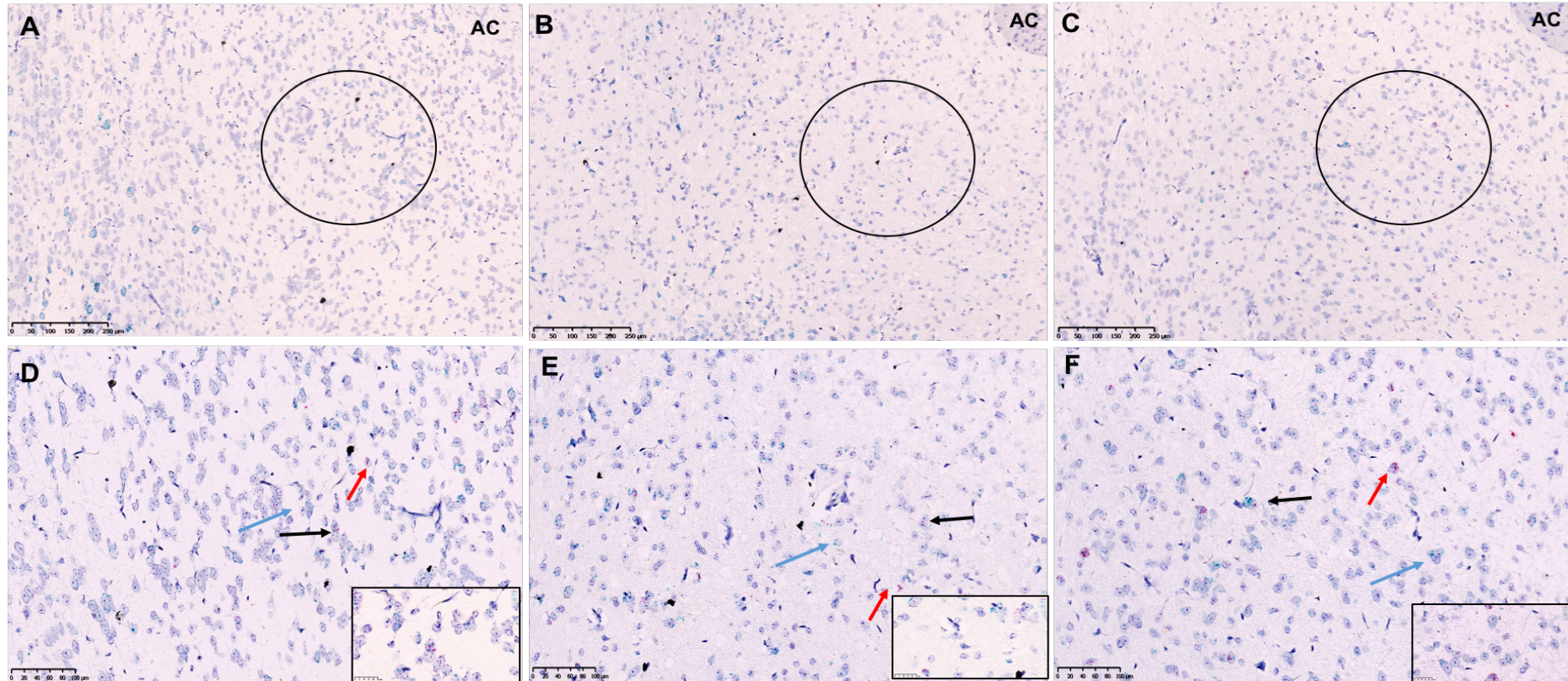


Figure 4.15: RNAscope® 2.5HD Duplex assay showing MRAP2 (C1-green)-MC₃ (C2-red) expression in rPOA of female mouse hypothalamus. The assay was carried in hypothalami of mice aged 2 weeks, 10 weeks and pregnant (14 ± 1) mice. The hypothalamic sections show expression and co-expression of MC₃ (red arrow) or MRAP2 (blue arrow) or both (black arrow). A: 2 weeks hypothalamus; B: 10 weeks hypothalamus; C: pregnant (14 ± 1 dpc) hypothalamus; D: Higher magnification of MRAP2-MC₃ expression in 2 weeks hypothalamus, E: Higher magnification of MRAP2-MC₃ expression in 10 weeks hypothalamus and F: Higher magnification of MRAP2-MC₃ expression in pregnant (14 ± 1 dpc). The black circles represent the rPOA which is medial to the anterior commissure (AC). The black rectangular demonstrate a zoomed in area of each section (80X). Each age group was conducted as two sections per slide and n=2. Images were taken by NanoZoomer slide scanner (Hamamatsu Photonics) at King's College London.

4. 3. 3. 1. A. RNAscope® 2.5HD detection of *MC₃*, *MC₅* and *MRAP2* in the mPOA

1. RNAscope® 2.5HD-singleplex (Brown) assay

MC₃ was detected in the mPOA area of 2 weeks, 10 weeks and pregnant (14 ± 1 dpc) mice. The expression appeared to be higher in 10 weeks old mice and pregnant mice compared to 2 weeks old mice (Figure 4. 16, A-F).

By contrast, although *MC₅* was detectable in the mPOA, the level of expression was lower in 2 weeks, 10 weeks old mice and pregnant (14 ± 1 dpc) mice hypothalami than that of *MC₃*. *MC₅* expression appeared to be increased in the 10 weeks old mice compared to both 2 weeks old and pregnant animals (Figure 4. 17, A-F).

MRAP2 was highly expressed in the mPOA of 2, 10 weeks old mice and pregnant (14 ± 1 dpc) animals. Importantly, there was high *MRAP2* expression throughout the hypothalamus at the level of the mPOA (Figure 4. 18, A-F).

2. RNAscope® 2.5HD-duplex assay in mPOA of female mouse hypothalamus

In the mPOA hypothalamic sections, the signal of *MC₃* (red) and *MRAP2* (green) was detected in 2 weeks, 10 weeks old and pregnant (14 ± 1 dpc) mice. The double expression levels were higher in 2 weeks old mice and pregnant animals compared to the 10 weeks old mice (Figure 4. 19, A-F). In addition to the double expression, there were cells expressing either *MC₃* or *MRAP2* with the latter been found more than that of cells expressing *MC₃* alone.

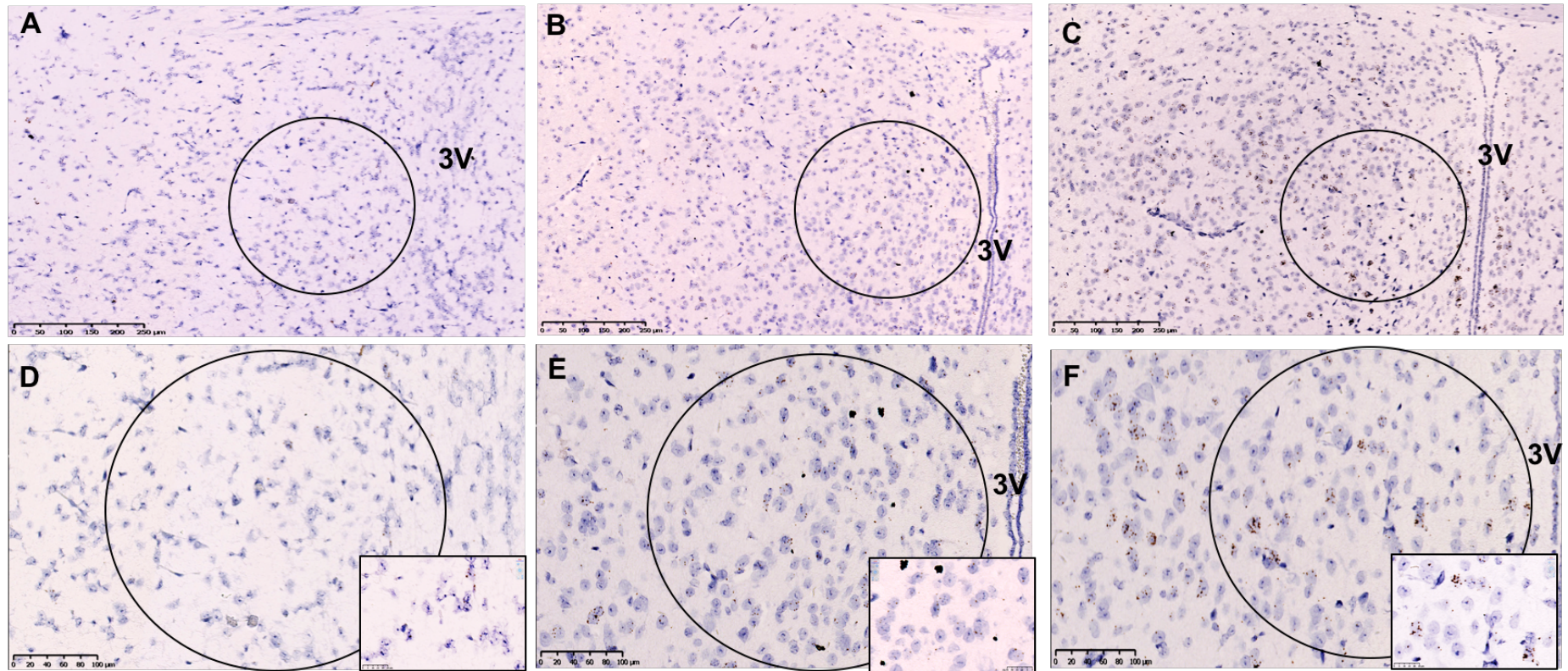


Figure 4.16: RNAscope[®] 2.5HD Brown assay of MC₃ in mPOA of female mouse hypothalamus. The assay was carried in hypothalami of mice aged 2 weeks, 10 weeks and pregnant (14 ± 1) mice. A: MC₃ expression in 2 weeks hypothalamus; B: MC₃ expression in 10 weeks hypothalamus; C: MC₃ expression in pregnant (14 ± 1 dpc) hypothalamus; D: Higher magnification of MC₃ expression in 2 weeks hypothalamus E: Higher magnification MC₃ expression in 10 weeks hypothalamus and F: Higher magnification MC₃ expression in pregnant (14 ± 1 dpc). The black circles represent the mPOA which is lateral to the third ventricle (3V). The black rectangular demonstrate a zoomed in area of each section (80X). Each age group was conducted as two slides with two sections per slide. Images were taken using a NanoZoomer slide scanner (Hamamatsu Photonics) at King's College London.

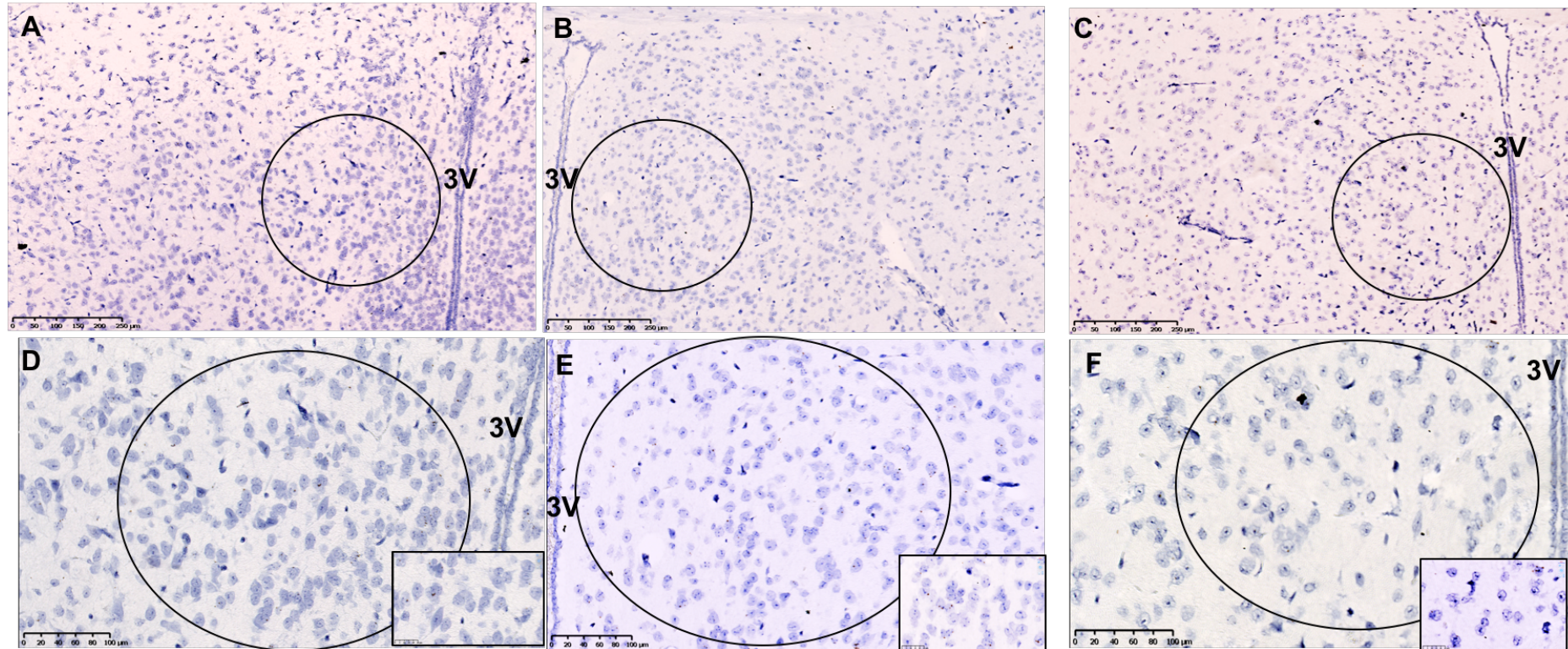


Figure 4.17: RNAscope® 2.5HD Brown assay of MC₅ in mPOA of female mouse hypothalamus. The assay was carried in hypothalami of mice aged 2 weeks, 10 weeks and pregnant (14 ± 1) mice. A: MC₅ expression in 2 weeks hypothalamus; B: MC₅ expression in 10 weeks hypothalamus; C: MC₅ expression in pregnant (14 ± 1 dpc) hypothalamus; D: Higher magnification of MC₅ expression in 2 weeks hypothalamus E: Higher magnification MC₅ expression in 10 weeks hypothalamus and F: Higher magnification MC₅ expression in pregnant (14 ± 1 dpc). The black circles represent the mPOA which is lateral to the third ventricle (3V). The black rectangular demonstrate a zoomed in area of each section (80X). Each age group was conducted as two slides with two sections per slide. Images were taken using a NanoZoomer slide scanner (Hamamatsu Photonics) at King's College London.

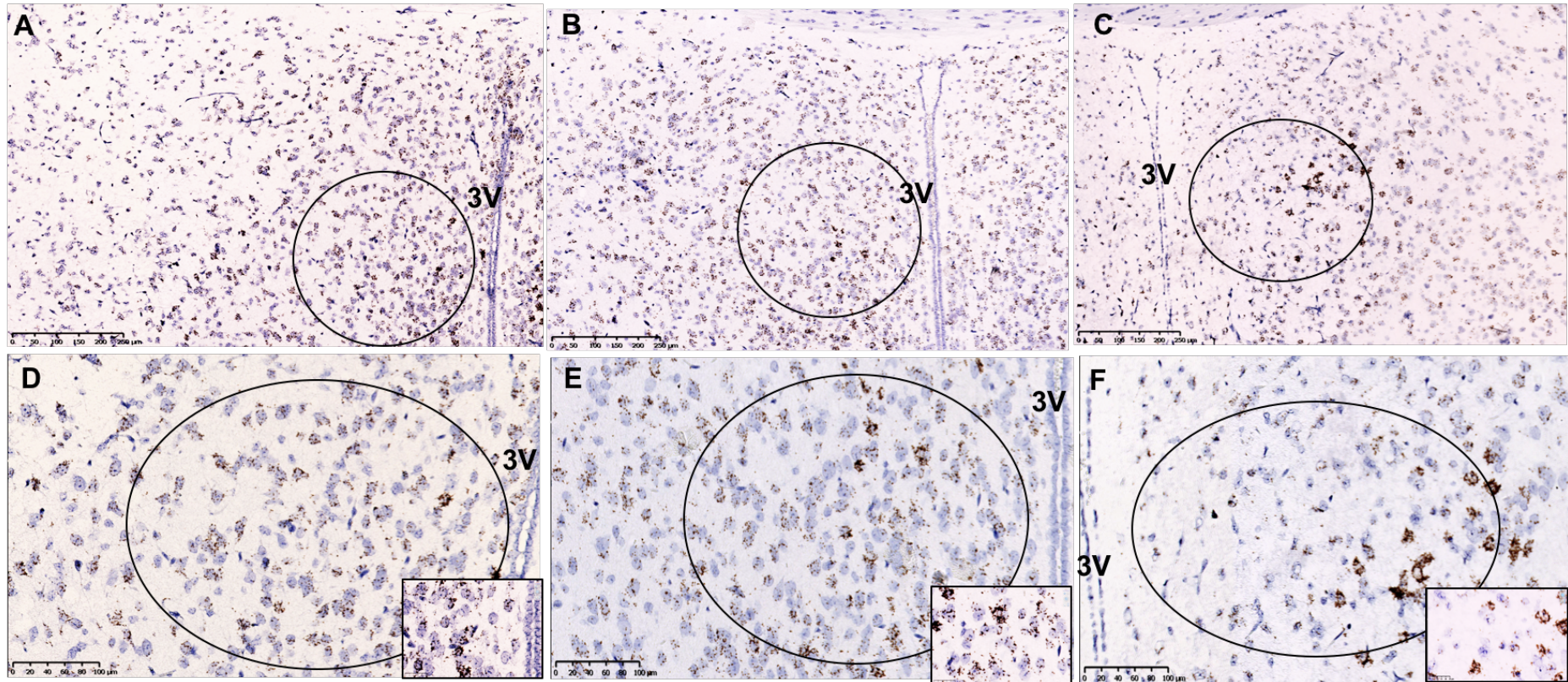


Figure 4.18: RNAscope® 2.5HD Brown assay of MRAP2 in mPOA of female mouse hypothalamus. The assay was carried in hypothalami of mice aged 2 weeks, 10 weeks and pregnant (14 ± 1) mice. A: MRAP2 expression in 2 weeks hypothalamus; B: MRAP2 expression in 10 weeks hypothalamus; C: MRAP2 expression in pregnant (14 ± 1 dpc) hypothalamus; D: Higher magnification of MRAP2 expression in 2 weeks hypothalamus E: Higher magnification MRAP2 expression in 10 weeks hypothalamus and F: Higher magnification MRAP2 expression in pregnant (14 ± 1 dpc). The black circles represent the mPOA which is lateral to the third ventricle (3V). The black rectangular demonstrate a zoomed in area of each section (80X). Each age group was conducted as two slides with two sections per slide. Images were taken using a NanoZoomer slide scanner (Hamamatsu Photonics) at King's College London.

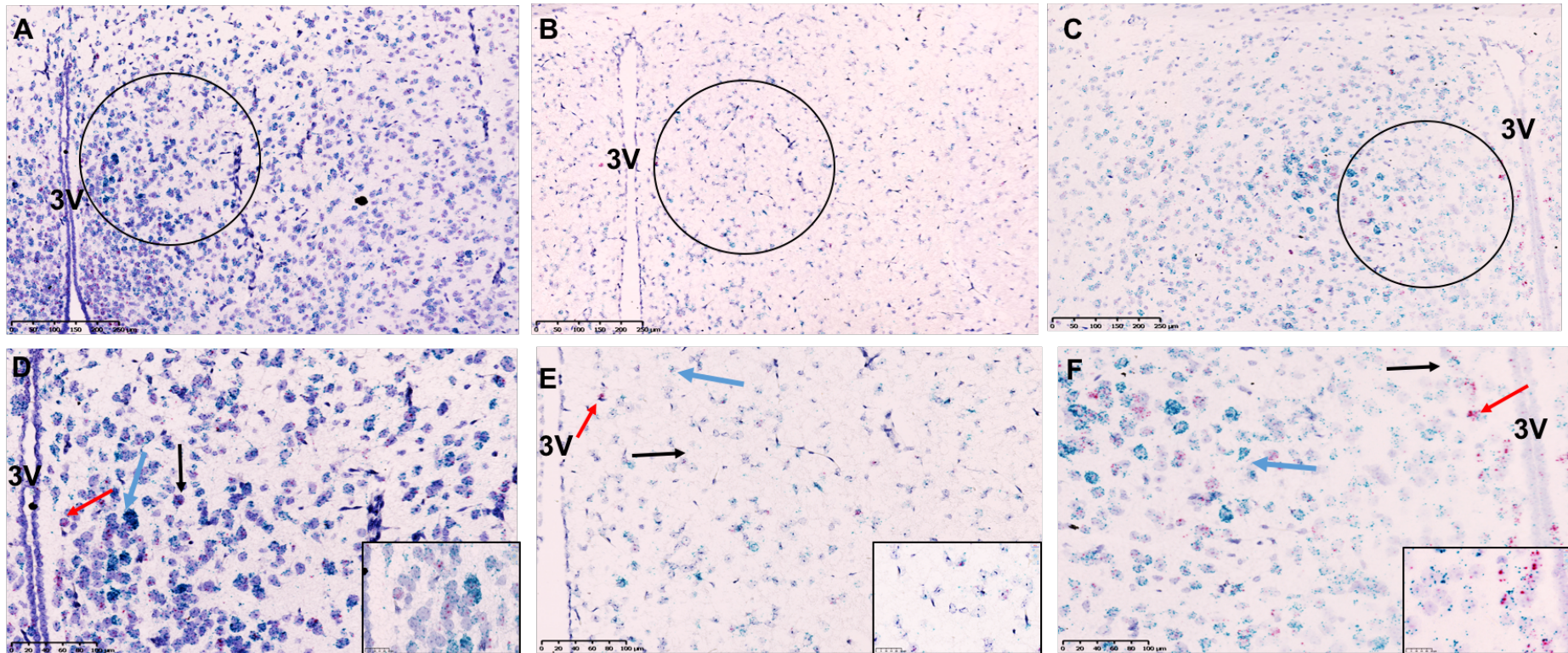


Figure 4.19: RNAscope® 2.5HD Duplex assay showing MRAP2 (C1-green)-MC₃ (C2-red) expression in mPOA of female mouse hypothalamus. The assay was carried in hypothalami of mice aged 2 weeks, 10 weeks and pregnant (14 ± 1) mice. The hypothalamic sections show expression and co-expression of MC₃ (red arrow) or MRAP2 (blue arrow) or both (black arrow). A: 2 weeks hypothalamus; B: 10 weeks hypothalamus; C: pregnant (14 ± 1 dpc) hypothalamus; D: Higher magnification of MRAP2-MC₃ expression in 2 weeks hypothalamus, E: Higher magnification of MRAP2-MC₃ expression in 10 weeks hypothalamus and F: Higher magnification of MRAP2-MC₃ expression in pregnant (14 ± 1 dpc). The black circles represent the mPOA which lateral to the third ventricle (3V). Each age group was conducted as two sections per slide and n=2. Images were taken by NanoZoomer slide scanner (Hamamatsu Photonics) at King's College London.

4. 3. 3. 1. C RNAscope® 2.5HD detection of MC₃, MC₅ and MRAP2 in the Arcuate nucleus

1. RNAscope® 2.5HD-singleplex (Brown) assay

Expression of *MC₃* was detected in the arcuate nucleus of 2 and 10 weeks old mice as well as in the pregnant (14 ± 1 dpc) animals. The expression was higher in the arcuate nucleus of 10 weeks female mice and pregnant animals compared to 2 weeks old mice (Figure 4. 20, A-F).

There were only low levels *MC₅* expressed in the arcuate nucleus of pregnant (14 ± 1) mice compared to *MC₃*. The arcuate nucleus of 2 and 10 weeks old mice did not express *MC₅*. (Figure 4. 21, A-F).

The expression of *MRAP2* in the arcuate nucleus was detected at 2 and 10 weeks old mice and pregnant (14 ± 1) mice hypothalamic sections. The expression levels were higher 2 week and 10 weeks old mice compared to pregnant animals (Figure 4. 22, A-F). However, the expression of *MRAP2* in 2 and 10 weeks old mice and pregnant animals was higher than that seen with *MC₃* and *MC₅*.

2. RNAscope® 2.5HD-duplex assay in the arcuate nucleus of the female mouse hypothalamus

MRAP2-C1 (green)/*MC₃*-C2 (red) expression was detected in the arcuate nucleus of 2 weeks and 10 weeks old and pregnant (14 ± 1) mice (Figure 4. 23 A-F). In the current findings, *MC₃* was higher in both 10 weeks and pregnant mice compared to 2 weeks old mice (Figures 4. 23 A/D and B/E) and that of *MRAP2* in the same hypothalamic sections. Also, there were less cells expressing both *MC₃* and *MRAP2* in pregnant animals compared to 2 weeks and 10 weeks old mice (Figure 4. 23 A-F).

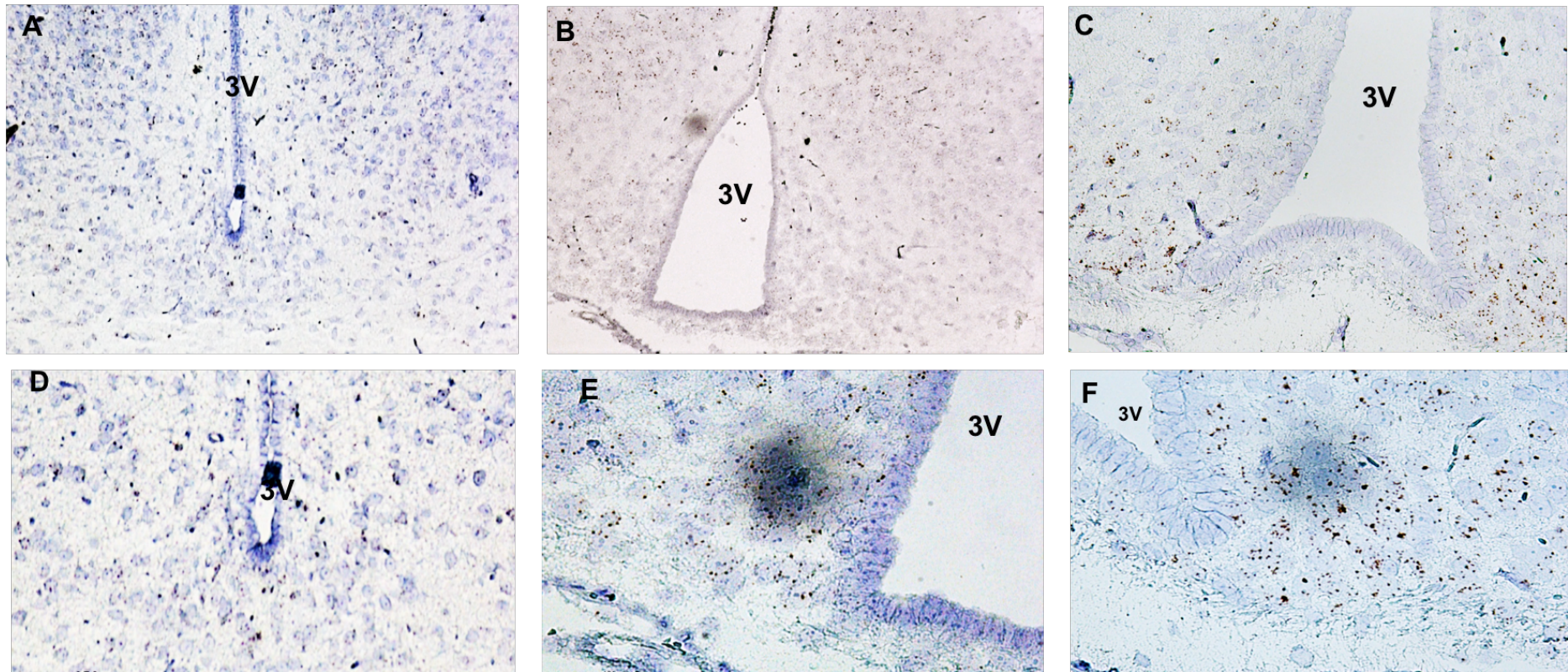


Figure 4.20: RNAscope® 2.5HD single-plex (brown) assay showing MC₃ expression in the arcuate nucleus of female mouse hypothalamus. The assay was carried in hypothalami of mice aged 2 weeks, 10 weeks and pregnant (14 ± 1) mice. The hypothalamic sections show expression of MC₃. A: 2 weeks hypothalamus (20X); B: 10 weeks hypothalamus (20X); C: pregnant (14 ± 1 dpc) hypothalamus (20X); D: Higher magnification of MC₃ expression in 2 weeks hypothalamus (40X); E: Higher magnification of MC₃ expression in 10 weeks hypothalamus (40X) and F: Higher magnification of MC₃ expression in pregnant (14 ± 1 dpc) (40X). The arcuate nucleus is found lateral to and the base of the third ventricle (3V). Each age group was conducted as two sections per slide and n=2. Images were taken using Leica bright-field DM, University of Westminster, London.

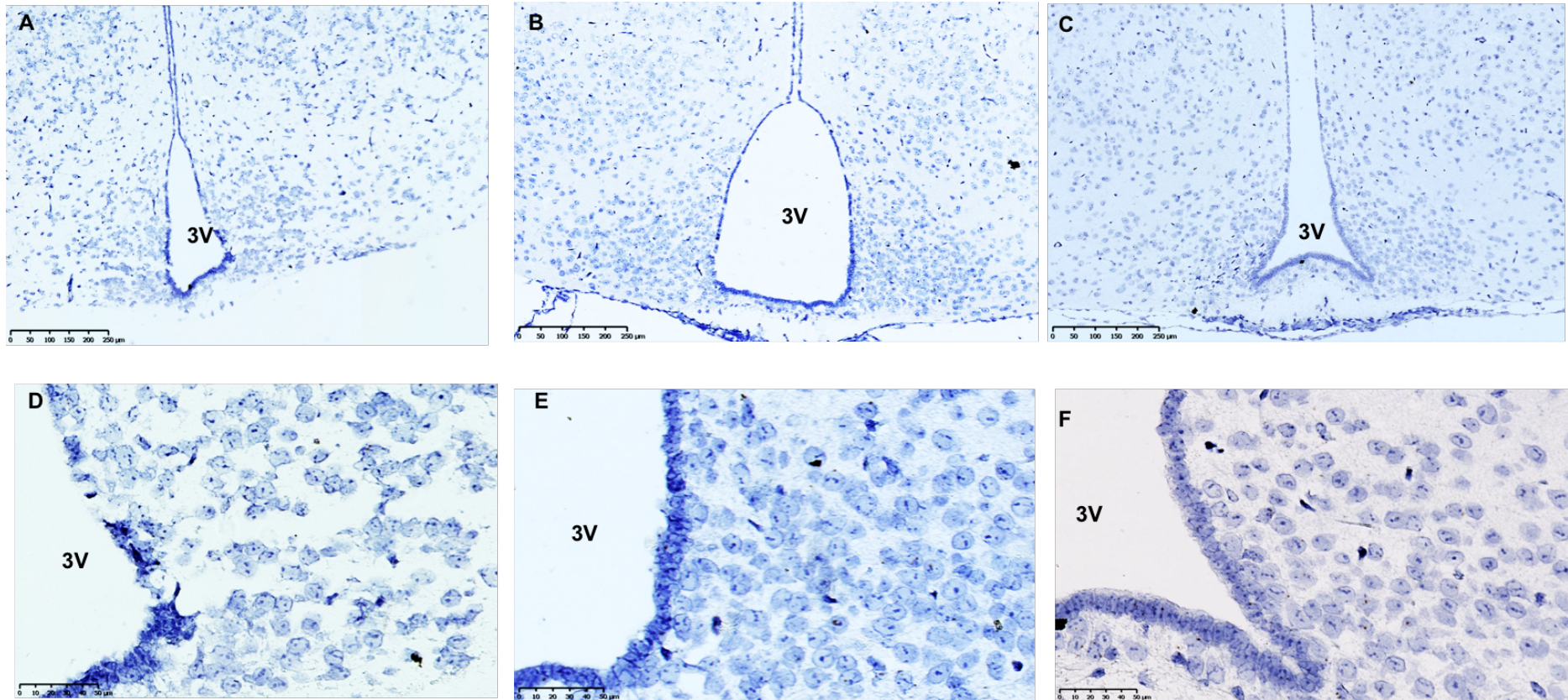


Figure 4.21: RNAscope® 2.5HD single-plex (brown) assay showing MC₅ expression in the arcuate nucleus of female mouse hypothalamus. The assay was carried in hypothalami of mice aged 2 weeks, 10 weeks and pregnant (14 ± 1) mice. The hypothalamic sections show expression of MC₅. A: 2 weeks hypothalamus; B: 10 weeks hypothalamus; C: pregnant (14 ± 1 dpc) hypothalamus; D: Higher magnification of MC₅ expression in 2 weeks hypothalamus; E: Higher magnification of MC₅ expression in 10 weeks hypothalamus and F: Higher magnification of MC₅ expression in pregnant (14 ± 1 dpc). The arcuate nucleus is found lateral to and the base of the third ventricle (3V). Each age group was conducted as two sections per slide and n=2. Images were taken by NanoZoomer slide scanner (Hamamatsu Photonics) at King's College London.

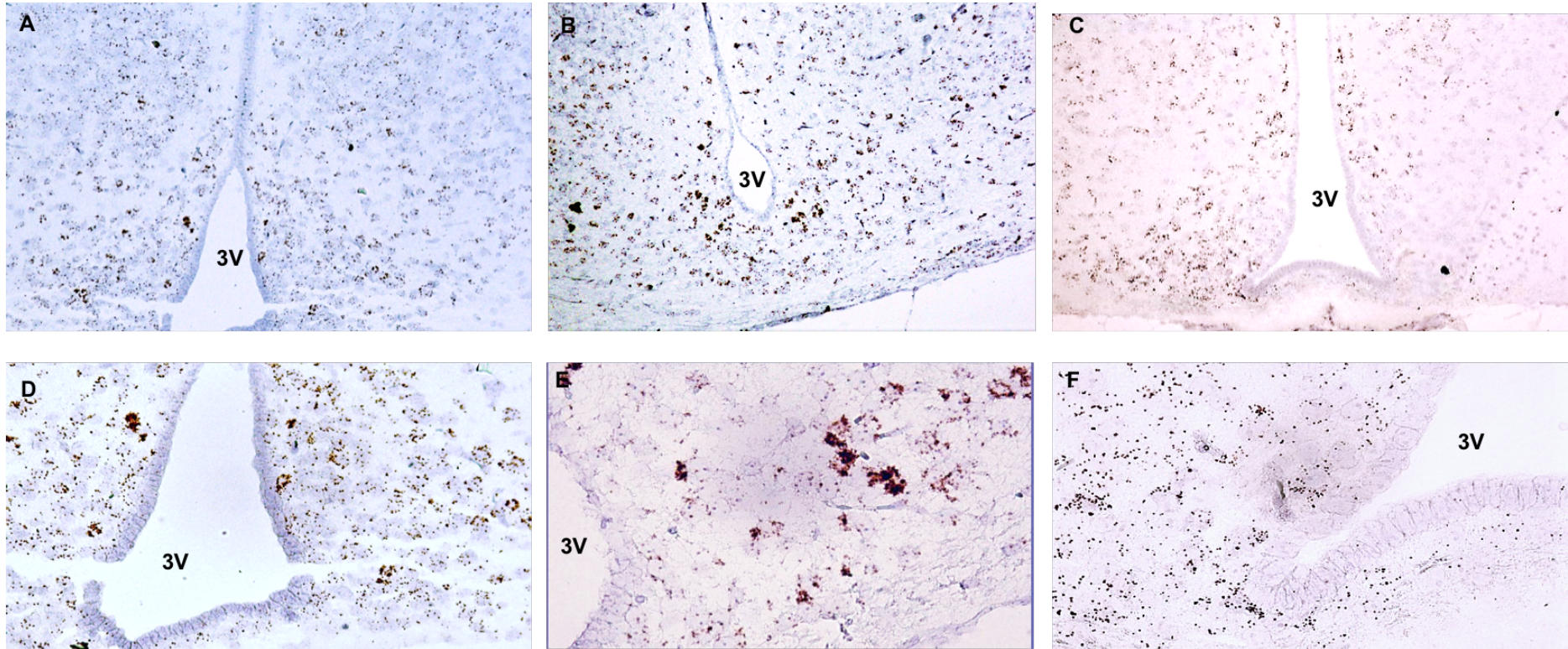


Figure 4.22: RNAscope® 2.5HD single-plex (brown) assay showing MRAP2 expression in the arcuate nucleus of female mouse hypothalamus. The assay was carried in hypothalami of mice aged 2 weeks, 10 weeks and pregnant (14 ± 1) mice. The hypothalamic sections show expression of MRAP2 (black arrow). A: 2 weeks hypothalamus (10X); B: 10 weeks hypothalamus (10X); C: pregnant (14 ± 1 dpc) hypothalamus (10X); D: Higher magnification of MRAP2 expression in 2 weeks hypothalamus (20X); E: Higher magnification of MRAP2 expression in 10 weeks hypothalamus (20X) and F: Higher magnification of MRAP2 expression in pregnant (14 ± 1 dpc) (20X). The arcuate nucleus is found lateral to and at the base of the third ventricle (3V). Each age group was conducted as two sections per slide and $n=2$. Images were taken by Leica-Bright-Field microscope DM, University of Westminster, London.

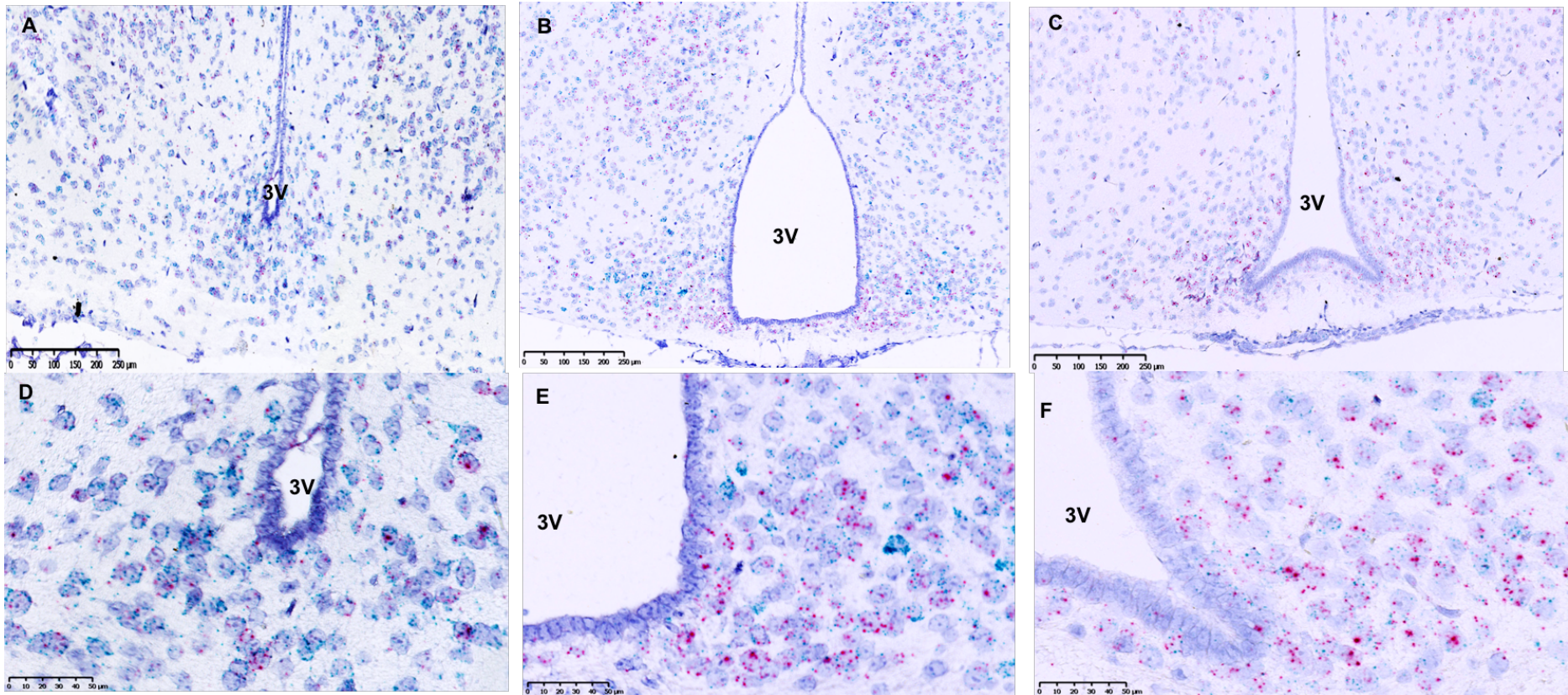


Figure 4.23: RNAscope® 2.5HD Duplex assay showing MRAP2 (C1)-MC₃ (C2) expression in the arcuate nucleus of female mouse hypothalamus. The assay was carried in hypothalami of mice aged 2 weeks, 10 weeks and pregnant (14 ± 1) mice. The hypothalamic sections show expression and co-expression of MC₃ (red arrow) or MRAP2 (blue arrow) or both (black arrow). A: MRAP2- MC₃ expression in 2 weeks hypothalamus; B: MRAP2- MC₃ expression in 10 weeks hypothalamus; C: MRAP2- MC₃ expression in pregnant (14 ± 1 dpc) hypothalamus; D: Higher magnification of MRAP2- MC₃ expression in 2 weeks hypothalamus; E: Higher magnification of MRAP2- MC₃ expression in 10 weeks hypothalamus and F: Higher magnification of MRAP2- MC₃ expression in pregnant (14 ± 1 dpc). The arcuate nucleus is found lateral to and at the base of the third ventricle (3V). Each age group was conducted as two sections per slide and n=2. Images were taken by NanoZoomer slide scanner (Hamamatsu Photonics) at King's College London.

4.4 Discussion:

All of the findings in the current research study revealed the expression of *MC₃*, *MC₅* and *MRAP2* in areas of the hypothalamus known to be involved in regulating the reproductive function. The RNAscope® *in situ* chromogenic study had revealed the cellular expression of *MC₃*, *MC₅* and *MRAP2* in rPOA at the level of OVLT and in the mPOA as well as the arcuate nucleus. The RNAscope® double expression had confirmed the singleplex findings and also showed the presence of cells expressing both *MC₃* and *MRAP2* in the same areas of the singleplex expression studies. By RT-qPCR it has been demonstrated that all of the MC system members (*MC₍₁₋₅₎*, *MRAP1* and *2*, *POMC* and *AgRP*) are expressed in the female C57BL/6 mouse hypothalamus. Both *POMC* and *AgRP* were more highly expressed than *MC₃*, *MC₄*, *MC₅*, *MRAP1* and *MRAP2*. Both *MC₁* and *MC₂* were expressed at very low levels. Age was found to influence the expression of *MC₅* and *POMC* with the former being higher in 2 weeks old female mice and the latter being higher in the older mice compare to all other age groups examined in this research. Pregnancy did not have any impact on the expression level of the MC system members in the female mouse hypothalamus in the RT-qPCR analyses. Nonetheless, the current chromogenic mRNA *in situ* hybridisation study findings had revealed more expression of *MC₃* and *MRAP2* in pregnant animals in the mPOA area of the hypothalamus. This is the first report of *MRAP1* expression in the hypothalamus of the female mouse.

In the hypothalamus, all the members of the melanocortin system were detected. The central melanocortin members: *MC₃*, *MC₄* and *POMC* are well characterised in the hypothalamus (Roselli-Reh fuss *et al.*, 1993; Gantz *et al.*, 1993; Iqbal *et al.*, 2001). The central *MC₃*, *MC₄* and *POMC* are involved in the neuroendocrine circuit that controls appetite and energy homeostasis (Cone, 2005). Through RT-PCR and Southern blot analyses, *MC₄* was found in different areas of the goldfish hypothalamus including the preoptic area (Cerdá-Reverter *et al.*, 2003). The preoptic area is known to contain a large population of the GnRH neurones (Jennes *et al.*, 1985). Dowejko (2014) managed to detect the rest of the receptors (*MC₁*, *MC₂*, *MC₅*) and *POMC* in both the male and female hypothalamus and the data presented in this research study confirms Dowejko's findings.

Expression of MC_1 in the central nervous system, in particularly in the periaqueductal grey matter, was previously reported by Chhajlani (1996). The present study detected MC_1 at a low level in the female hypothalamus confirming preliminary observation by our research group in 2014 (Dowejko, 2014). Age and pregnancy did not alter the expression pattern of MC_1 expression. The anti-inflammatory role of MC_1 might explain its presence in the hypothalamus as MC_1 detected in the glial cells (Catania *et al.*, 2004) which are found in different parts of the brain including the hypothalamus. There was a very low expression signal detected for MC_2 in the hypothalamus. Dowejko's findings also showed that the expression of MC_2 is higher in male compared to female (Dowejko, 2014). Little is known about the role of MC_2 in extra-adrenal tissues although it was thought to have a mediating role in organogenesis in different tissues, including the brain, in mouse embryos (Nimura *et al.*, 2006). However, further research is necessary to delineate the specific function of MC_2 in the brain.

The effect of age was also found to effect *POMC* RT-qPCR expression as *POMC* was found to be higher in adult mice (14 weeks old mice) compared to 2, 6, 9 and 10 weeks old mice. These findings contradict reports in rats which indicated a decline in *POMC* population in older female rats (Lloyd *et al.*, 1991; Gruenewald and Matsumoto, 1991), Lloyd and colleagues used middle-aged and older rats, since both of these studies were conducted on rat brain it might indicate a species difference in the pattern of *POMC* expression. Nelson and colleagues also reported reduced hypothalamic *POMC* mRNA in about 30 months (2.5 years) old mice compared to younger (7-month-old) mice (Nelson *et al.*, 1988); however, Nelson's group had tested much older mice than those used in this research.

As mentioned earlier, this is the first report of *MRAP1* expression in the hypothalamus of the female mouse. The presence of *MRAP1* in the brain could be to do with its role in assisting MC_2 trafficking and signalling activity as in adrenal gland (Chan *et al.*, 2009; Asai *et al.*, 2013) or could be regulating the expression of the other melanocortin receptors as reported by (Chan *et al.*, 2009; Sebag and Hinkle, 2009).

In the RT-qPCR in the current research, a mid-gestational stage of pregnancy (14 ± 1 dpc) did not seem to affect the expression pattern of the MC system in the hypothalamus. This was an unanticipated finding as in pregnancy, a down-regulation of the anorexigenic central melanocortin receptors would be expected to facilitate food intake and thus providing for foetal growth and maintain maternal health. However, the dilutional effect of RT-qPCR which might have masked *MRAP2* differential expression in pregnancy, suggested in the RNAscope® assays and could explain the reason for the unchanged expression of the MC system during mid-pregnancy in mice. AgRP was detected in the hypothalamus as expected: the AgRP-expressing neurones of the arcuate nucleus of the hypothalamus are well characterized and have an important role in appetite and food intake regulation (Bagnol *et al.*, 1999). However, although insignificant, there was fluctuation in expression in relation to age and pregnancy.

The first series of studies aimed to select the most stable reference genes for normalising the RT-qPCR data in C57BL/6 female mouse hypothalamus using GeNorm expression stability analysis. The most suitable reference genes were *CANX* and *YWHAZ*. Both *CANX* and *YWHAZ* showed stable expression when examined in the 2, 6, 9, 10 and 14 weeks old mice and pregnant (14 ± 1 dpc) mice compared to more commonly used reference genes such as *GAPDH*. *CANX* is part of the endoplasmic reticulum membrane proteins and is known to be constantly expressed in high amount (Denzel *et al.*, 2002). On the other hand, *YWHAZ*, is involved in signal transduction and is expressed at high levels in the brain. *YWHAZ* was a reference gene of choice in a study conducted on rat hypothalami (Li *et al.*, 2014).

In this research, two aspects were considered to choose the method by which *MC₃*, *MC₅* and *MRAP2* could be characterised at a cellular level. Firstly, the physiological organisation of the hypothalamic areas; this approach was adopted to characterise the mentioned genes and the functions of specific regions of the hypothalamus. Secondly, the method used to localise the target genes was considered. The chromogenic *in situ* hybridisation using RNA probes or in fewer words, “RNAscope®”, was decided as the method of choice because it would preserve the structural organisation of the hypothalamus using the haematoxylin counterstaining. The RNAscope® was used to characterise the target genes in the hypothalamic rPOA, mPOA and the arcuate

nucleus regions. GnRH neurons soma are known to be in the preoptic areas whilst their fibers reside in the arcuate nucleus (Herbison, 2014). Antibodies have been shown to be unreliable for detecting the melanocortin receptors due to their non-specificity (Kathpalia *et al.*, 2011), therefore, using the RNA probes would provide specificity. The RNAscope[®] was chosen to allow observations of subtle changes in specific cell types which are masked in the RT-qPCR, conducted using RNA from the entire hypothalamus. The changes seen here with *MC₅* from the RT-qPCR analysis, the literature about *MC₃* (Roselli-Rehfuss *et al.*, 1993; Nocetto *et al.*, 2004; Rowland *et al.*, 2010; Manfredi-Lozano *et al.*, 2016) and evidence from knockout studies and the emerging role of the *MRAP2* prompted the decision to investigate these targets at a cellular level using the RNAscope[®].

The expression of *MC₃* in the rostral preoptic area of the C57BL/6 female mouse could suggest a contribution in modulating the activity of LH surge through *GnRH* found in the rPOA. Herbison and colleagues located populations of GnRH neurons in the rPOA in GNR23 female mice (Herbison *et al.*, 2008). The rPOA is found to be one of the main areas controlling ovulation in rodents (Wang *et al.*, 2016). The melanocortin receptor contribution in ovulation might be through activating kisspeptin expression (Backholer *et al.*, 2009). Kisspeptin was suggested to have a role in the generation of GnRH surge in POA (Wang *et al.*, 2016). This study has found that the expression of *MC₃* was lowest in the pregnant animals (14 ± 1 dpc) compared to pre-weaned female animals (2 weeks old) and 10 weeks old mice. That both 2 weeks old mice and pregnant mice had higher expression of *MRAP2* compared to 10 weeks old mice; the double *MC₃ / MRAP2* expression confirms these findings, as there was more double expression in the 2 weeks old mice and pregnant. This suggests that *MRAP2* might be modulating *MC₃* surface expression, as well as the *MC₃* intracellular cascade.

The RNAscope[®] expression of *MC₃* was detected in the mPOA and although the pattern of expression of *MC₃* was similar to the rPOA, higher levels of *MC₃* were detected in mPOA compared to the rPOA. The localisation of *MC₃* in the mPOA emphasises its proposed role in mediating ovulation. The mPOA includes a population of GnRH neurons that are involved in generating the GnRH surge (Herbison, 2014).

This is augmented by surgical lesion studies conducted on rat mPOA hypothalamic regions which led to constant estrus (Freeman, 2006). The suggested role for the preoptic MC₃ is also supported by reports of restored fertility and puberty in leptin knockout mice and stimulated GnRH neuron activity after MTII treatment, an MC₃ and MC₄ agonist (Israel *et al.*, 2012). Israel *et al.* characterised the expression of MC₄ in the mPOA area through single-cell RT-qPCR (scRT-qPCR) of green fluorescent plasmid (GFP) positive *GnRH* male and female mice brain slices (Israel *et al.*, 2012). This study did not include a selective MC₄ agonist and/or antagonist to confirm that the actions mediated by MTII were through activation of MC₄. Therefore, MTII, as an agonist to both MC₃ and MC₄, might also have activated MC₃ instead of MC₄ or both, there is a possibility that this might be by forming heterodimers (Mandrika *et al.*, 2005), restoring fertility in the leptin receptor-deficient mice. The RNAscope[®] expression of *MRAP2* was also, significantly higher than that observed in the rPOA. The RNAscope[®] *MRAP2* expression in the mPOA was also relatively higher than that of MC₃. Furthermore, there was higher level of MC₃/*MRAP2* double expression in the mPOA in contrast to the rPOA, which could be due to higher level of expression of both genes in the mPOA.

The detection of MC₃ in the arcuate nucleus using RNAscope[®] 2.5HD assay adds evidence to previous studies reporting MC₃ expression in the arcuate nucleus. The highest level of MC₃ expression was detected in arcuate nucleus of pregnant mice followed by the 10 weeks old mice and the lowest expression was observed in the 2 weeks old mice. Compared to the other two areas, the expression of *MRAP2* appeared to be higher in the 2 weeks and 10 weeks old mice compared to the pregnant animals. The MC₃ role through the arcuate nucleus circuit controlling appetite has been extensively investigated (Cone, 1999; Hohmann *et al.*, 2000; Cowley *et al.*, 2001; Lee *et al.*, 2006; Xu *et al.*, 2011). The arcuate nucleus is known to contain GnRH axonal projections that are controlling GnRH pulsatile release (Yeo and Herbison, 2014). Gene profiling in the arcuate nucleus of C57BL/6 male and female mice revealed the expression of *GHSR-1a*, *MCH* receptors, *ERs*, dopamine receptors, prolactin releasing peptide receptor, kisspeptin receptors and γ -Aminobutyric acid (*GABA*) receptors (Rønnekleiv *et al.*, 2014); all of these receptors were found to be linked to the GnRH neural network (Kokay *et al.*, 2011; Farkas *et al.*, 2013). The gene profiling studies had also identified MC₁, MC₃, MC₄ and MC₅ within the arcuate nucleus

(Rønnekleiv *et al.*, 2014). The receptors GHSR1-a, MCH receptors, ERs, kisspeptin receptors and GABA were also reported to interact with the MCs (Schiöth and Watanobe, 2002; Murray *et al.*, 2006; Schellekens *et al.*, 2013; Bond and Smith, 2014). Roa and Herbison, 2012 have reported that α -MSH (Pan MCs agonist) as well as D(Trp⁸) - γ MSH (MC₃ agonist) and other arcuate nucleus peptides such as AgRP and β -endorphin affect GnRH firing (with the melanocortins stimulating GnRH activity) using electrophysiological studies on female *GnRH – GFP* mice brain slices. A combination of these findings implies a role of MC₃ in the neural reproductive circuit. The pattern of MC₃ expression in the mPOA and rPOA in the RNAscope[®] singleplex and duplex expression studies are consistent with RT-qPCR findings.

Extremely low levels of MC₅ were found in the entire hypothalamic sections of all ages and pregnant animals. However, there was high expression of MC₅ in the pia mater (the single layer of cells that is enveloping the brain). The expression of the MC₅ in the two preoptic areas was very low. However, this could be further characterised by a greater quantification in all hypothalamic areas. The expression within both preoptic areas confirms reports by Murray *et al.* of an MC₅ antagonist (FFMI-60) inhibiting LH release (via stimulating GnRH) through MCH in female rats (Murray *et al.*, 2006). However, further studies are needed to investigate if the MC₅ effect on MCH is imitated by the other central MCs such as MC₃, that was also found expressed in the same areas as MC₅. Other explanations of MC₅ hypothalamic expression might be heterodimerisation or dimerization with either MC₃ or MC₅ detected in areas similar to those of MC₃ in this research. Reports of MCs (MC₁ and MC₃) forming heterodimers (Mandrika *et al.*, 2005) support this implication.

The expression of MC₅ in the arcuate nucleus was scarce, but a couple of reports of MC₅ expression in the arcuate nucleus confirm this finding (Cerdá-Reverter *et al.*, 2003; Ronnekleiv *et al.*, 2014). More studies are needed to determine MC₅ function within this region of the hypothalamus. Surprisingly, the age difference reported here was not observed in data from the RNAscope[®]. However, the RNAscope[®] is detecting expression in specific regions (rPOA, mPOA and the arcuate nucleus) within the hypothalamus, unlike the RT-qPCR that is conducted on RNA from all cell types such as endothelial, epithelial and glial cells found in the hypothalamus.

High expression of *MRAP2* was observed through most of the hypothalamic areas including ventromedial and dorsomedial nuclei and paraventricular nucleus not only the areas of interest to this research. This is consistent with the results from the RT-qPCR as compared to the *MCs*. *MRAP2* was found expressed in the hypothalamus (Chan *et al.*, 2009) and the loss of its function was associated with lowered *MC₄* expression, indicating a role in *MC₄* trafficking (Asai *et al.*, 2013). In chicken, increased responsiveness to *ACTH* was recorded when either *MC₃* or *MC₄* was co-expressed with *MRAP2* (Zhang *et al.*, 2017). *In vitro* studies conducted in this and further discussed in chapter 8 recorded increased *MC₃* responses to *ACTH* (1-39) when co-expressed with *MRAP2* (see chapter 8 for data Figures). Based on the RNAscope® results, *MRAP2* expression in the preoptic areas was higher in pregnancy than age-matched virgin mice; *in vitro* studies conducted in this research had also showing decreased responsiveness to α -MSH when *MC₃* was co-expressed with *MRAP2* (see chapter 8 for PRESTO-Tango cell study data Figures). These findings could explain reports of attenuated α -MSH response observed during rat pregnancy (Ladyman *et al.*, 2016). In addition to the *MC₃* / *MRAP2* double expression seen in the RNAscope® duplex assays, there were cells expressing *MRAP2* alone in all of the three areas investigated. These findings indicate that *MC₃* could either be mediating its hypothalamic function without the *MRAP* co-expression or that it could be regulated by *MRAP1* (not included in the current RNAscope® study). In addition to a possible role in regulating *MC₃* signalling and responsiveness, *MRAP2* may also have a role interacting with other melanocortin receptors as described by (Chan *et al.*, 2009) or with non-melanocortin receptors such as prokineticin receptor 1, orexin receptor and GHSR1-a (Chaly *et al.*, 2016; Srisai *et al.*, 2017; Rouault *et al.*, 2017 respectively).

To summarise, the characterisation of *MC* (1-5), *POMC*, *MRAP1*, *MRAP2* and *AgRP* using RT-qPCR confirmed expression within the hypothalamus. The expression did not seem to be affected by age except for *MC₅* and *POMC*. Even though previous reports documented decreased anorexic effects exerted by the melanocortin receptors during pregnancy, the *MC* system expression was unchanged within the hypothalamus of pregnant mice. However, as there are changes in the hormonal profile during the different stages of pregnancy, other stages of pregnancy may need to be examined to explore if there would be any changes in the *MC* system expression

during early or later stages of pregnancy. The *MC₃*, *MC₅* and *MRAP2* cellular localisation displayed specific hypothalamic regions of expression; these included the preoptic area (both medial and rostral areas) and the arcuate nucleus. The areas of the hypothalamus expressing *MC₃*, *MC₅* and *MRAP2* suggest that they are in regions containing GnRH neurons, this could be confirmed in future studies using GnRH probes in RNAscope[®] however, due to high cost of the RNAscope[®] reagents and probe, using a GnRH probe the examined regions could not be carried out within this study. Therefore, a further study RNAscope[®] duplex assay combining GnRH/*MC₃*, GnRH /*MC₅* would enhance the findings from this research. Other consideration for future work includes the addition of more hypothalamic samples from female mice of other physiological conditions such as the early and later stages of pregnancy, lactation, weaning stage of the reproductive cycle. Additionally, studying the RT-qPCR expression of POMC in older animal should also be considered to determine if there is a decline in POMC expression with age as seen in other studies. All of these stages are controlled by different neuroendocrine interactions within the hypothalamus that might be involving the melanocortin system. The current research study was set to characterise the expression and cellular localisation of the MC system members in the first level of the reproductive axis. The following chapters will analyse the MC expression in the pituitary gland, the ovary and the uterus in an attempt to explore the role of this system in female mouse fertility.

5 Molecular and cellular characterisation of the MC system in the female mouse pituitary gland

5.1 Background

Hypothalamic GnRH stimulates gonadotrophs in the anterior pituitary gland to synthesise and release LH and FSH. Both hormones are involved in ovarian steroidogenesis. Additionally, the hormone LH induces ovulation and stimulates the formation of the *corpus luteum* while FSH stimulates folliculogenesis and estrogen secretion. The mouse pituitary gland is divided into three main lobes: anterior, intermediate and posterior lobes, also respectively known as *pars distalis*, *pars intermedia* and *pars nervosa*. This research will focus on the anterior pituitary gland. Reviewing the posterior lobe is beyond the scope of this research. This chapter will mainly discuss the endocrine, autocrine and the paracrine regulation of anterior pituitary gonadotrophs and their function in the female mice.

5. 1. 1 Components of the anterior pituitary gland

The anterior pituitary gland is made of three main components:

- 1) Five types of hormone-secreting cells (ACTH-secreting corticotrophs; gonadotropin-secreting (LH and FSH) gonadotrophs; prolactin-secreting lactotrophs, growth hormone-secreting (GH) somatotrophs; and thyroid stimulating hormone secreting, TSH, thyrotrophs) (Griffin and Ojeda, 2004).
- 2) Support cells known as folliculostellate cells (Le Tissier *et al.*, 2012).
- 3) A fenestrated capillary network in between the cells (Griffin and Ojeda, 2004).

During development the cells of the anterior pituitary originate from Rathke's pouch in a specific fashion of distribution within the gland. The percentage, spatial organisation and function of each of the 5 trophic cell types are summarised in table 5. The anatomical fate of these cells is controlled by specific transcription factors such as the *pit-1* and prophet of *Pit-1* (*PROP1*) for somatotrophs and gonadotrophs differentiation, respectively (Ward *et al.*, 2006). A greater discussion about the different cell lineages and differentiation can be found in the review by Scully and Rosenfeld (2002).

Table 5-1: Anterior pituitary cells and their percentage, distribution, hormones and functions in mouse.

Trophic cell	Percentage	Anatomical distribution	Hormone produced	Principal function
corticotrophs	10-20%	strands of cells in the ventral surface extending to the parenchyma	POMC→ ACTH	glucocorticoid synthesis
gonadotrophs	10%	strands of cells in close association with corticotrophs in medioventral surface	LH and FSH	gametogenesis, folliculogenesis and steroidogenesis
lactotrophs	10-25%	networks within the parenchyma with higher density in the ventral region of anterior pituitary lobe	Prolactin	lactation and corpus luteum formation
somatotrophs	about 50%	clusters of cells throughout the parenchyma	GH	Growth and metabolism
thyrotrophs	10%	Unknown	TSH	thyroid hormone production

POMC: proopiomelanocortin; ACTH; adrenocorticotrophic hormone; LH: luteinising hormone; FSH: follicular stimulating hormone; GH: growth hormone and TSH: thyroid-stimulating hormone. The information in this table are adopted from Yeung *et al.*, (2006); Mollard *et al.*, (2012); Le Tissier *et al.*, (2012).

These hormone-producing cells are primarily controlled by the hypothalamic stimulatory and inhibitory regulators. Additionally, peripheral hormones regulate the release of the anterior pituitary hormones through feedback mechanisms. All of these regulators interact with receptors expressed on each of the anterior pituitary cells. Table 5. 2 summarises the receptors of the hypothalamic regulators and their main functions. From a reproductive point of view, this research will focus on the gonadotrophs and their regulation by different mechanisms including the intra-pituitary interactions.

Table 5-2: Hypothalamic regulators of the anterior pituitary hormone-producing cells in female mice.

Trophic cells	Stimulatory regulator(s)	Receptor	Function	Inhibitory regulator(s)	Receptor	function
Somatotrophs	GHRH	GHRHR	Stimulate GH synthesis and release; somatotroph proliferation	Somatostatin	SST2R	Suppress GH release and inhibit somatotrophs proliferation
Lactotrophs	*TRH / VIP / somatostatin	-	stimulate prolactin release	Dopamine	D1/D2R	Inhibit lactotrophs proliferation and prolactin release
Corticotrophs	CRH	CRF-1/2	stimulate ACTH release	could be CRIH	unknown	N/A
Thyrotrophs	TRH	TRH-R	stimulate TSH production	somatostatin / dopamine	Unknown SSTR and dopamine receptor subtypes	inhibit TSH release
Gonadotrophs	GnRH	GnRHR	stimulate LH, FSH synthesis and release	Lowered GnRH activity	-	suppress gonadotroph responsiveness

ACTH: adrenocorticotrophic hormone; CRH: corticotropin releasing hormone; CRF-R: corticotropin releasing factor receptor; D1/D2R: dopamine receptors 1 and 2; GH: growth hormone; GHRH/ GHRH-R: growth hormone releasing hormone and receptor; GnRH/GnRHR: gonadotropin releasing hormone and receptor; SST2R: somatostatin 2 receptor; TRH/ TRH-R: thyroid releasing hormone and receptor and TSH: thyroid- stimulating hormone. The information in the table are adopted from (Stefaneanu, 2001).

The gonadotropin-secreting gonadotrophs mediate the synthesis and release of LH and FSH primarily through the activation of the GnRH receptor (GnRHR). GnRHR expression is considered one of the critical steps in regulating the estrous cycle in rodents, with three-fold upregulation of *GnRHR* expression on the afternoon of proestrus compared to metestrus (Bauer-Danton *et al.*, 1993). This rise persists until the evening of proestrus then drops to basal levels after 12 hours to reach levels similar to those reported in metestrus (Bauer-Danton *et al.*, 1993). The period between the GnRH incubation and the pituitary cell response in this study correlates with the response observed after the GnRH surge as explained in section 4.1.5. The GnRHR is autoregulated through GnRH as continuous stimulation was found to cause receptor desensitisation and internalisation. This was shown by incubating female rat pituitary cells with GnRH, which resulted in increased *GnRHR* expression 6 hours after incubation followed by a downregulation of the receptor expression in the continuous presence of GnRH (Bjelobaba *et al.*, 2016).

5. 1. 2 Regulation of gonadotroph function

The regulation of the GnRHR responsiveness and *LH* and *FSH* synthesis depends on different pathways. These pathways include endocrine pathways, autocrine autoregulation and paracrine intra-pituitary communication that is modulated by different factors.

5. 1. 2. 1 The endocrine regulation of gonadotrophs

The role of estrogen in exerting feedback on the pituitary, as well as progesterone's role, are well documented (Messinisi, 2006). Gonadectomy with estradiol and/or progesterone treatment has facilitated the understanding of the roles of the gonadal hormones in the regulation of the gonadotropin release and hence the induction of ovulation. Discussing the roles of both gonadotropins is beyond the scope of this research but has been detailed by Levine (1997).

5. 1. 2. 2 Intra-pituitary regulation of gonadotropin synthesis and release

The cells of the anterior pituitary exist in well-defined networks and communicate with each other through autocrine, paracrine and endocrine pathways. Direct communication between the different hormone-producing cells of female rat *pars distalis* was revealed using high-density plating studies (Wilfinger *et al.*, 1984). These findings might indicate a direct paracrine input between the different hormone-producing cells in the gland or cell-cell communication through, for example, gap junction coupling (Tortonese, 2016).

Prolactin secreted by the lactotrophs plays an essential role in the murine estrous cycle. Prolactin concentration has been found to be relatively similar to that of LH, with a basal concentration of about 20 ng/ml during the entire cycle but peaking on the afternoon of proestrus to about 300 ng/ml (Levine, 2014). This high concentration of prolactin is thought to have roles in luteolysis, receptivity to males, embryo implantation and/or mammary development (Grattan and Le Tissier, 2015). Prolactin was also found to stimulate LH production in L β T2 cells when used alone, an effect that was abolished after adding bromocriptine, a dopamine agonist (Henderson *et al.*, 2008). In support of these findings, Henderson and colleagues have also detected prolactin receptors in another gonadotroph cell line, the α T₃-1 cell line, and demonstrated *in vitro* that treatment with prolactin reduced α -GSU expression, in α T₃-1 cells (Henderson *et al.*, 2008).

Although a direct somatotrophic effect on gonadotroph function is still under investigation, research examining the interaction between the two cell types has suggested somatotrophs could be influencing the gonadotropin release through follistatin. This was suggested after co-culturing L β T2 cells with the prolactin-secreting somatotrophic cell line GH3 (Kanasaki *et al.*, 2011). Follistatin produced by the GH3 cells had no effect on prolactin synthesis but when GH3 cells were co-cultured with L β T2, follistatin suppressed *FSH β* promoter activity; this was attributed to its inhibitory effect on activin, which is known to stimulate *FSH β* promoter activity (Kanasaki *et al.*, 2011). Another study has shown a less indirect interaction between gonadotrophs and somatotrophs, which is through the ghrelin receptor, which is expressed on somatotrophs, and was found to inhibit LH and FSH release in women (Kluge *et al.*, 2012). Co-localisation studies using GHSR1-a-eGFP mice have detected the

expression of the *GHSR1-a* in gonadotrophs, in addition to somatotrophs and the other pituitary cells (Reichenbach *et al.*, 2012). These findings might indicate the gonadotroph stimulation could be mediated by either an autocrine or paracrine mechanism.

Gonadotrophs have also been found to be in close association with corticotrophs (Mollard *et al.*, 2012). Mollard and colleagues have described a group of LH-producing gonadotrophs that follow the corticotroph migration across the ventral surface, and later, parts of the anterior lobe, during development. Using tridimensional imaging studies, Budry and colleagues confirmed close anatomical proximity between gonadotropes and corticotropes and the knockout of *Tpit*, a transcriptional factor responsible for corticotroph differentiation, caused an expansion of the gonadotrophs network (Budry *et al.*, 2011). In addition to this anatomical association, corticotrophs also contribute to the regulation of reproductive functions through activation of the hypothalamic-pituitary adrenal (HPA) axis. Pathophysiological conditions, such as stress, are known to activate the HPA axis; this axis suppresses the female reproductive axis at all levels through glucocorticoids that inhibit GnRH and LH release. At the pituitary level, the glucocorticoids that are produced from the adrenal gland in response to stress cause reduced *LH β* expression and responsiveness to GnRH. This was suggested to be a direct effect of the glucocorticoids on the gonadotrophs after detecting the glucocorticoid receptor in mouse gonadotrophs (Breen *et al.*, 2012). CRH, from the hypothalamus, induces the corticotrophs to release ACTH that activate adrenal glucocorticoid synthesis via activating MC₂. Earlier studies revealed that there was an increase in α -MSH content in the intermediate lobe of female rat pituitary gland and this was found to cause a partial inhibition in LH and prolactin plasma concentration (Khorram *et al.*, 1985). Both MC₃ and MC₅ were found expressed in all levels of the HPA axis (Wachira *et al.*, 2004). Based on these findings, the melanocortin system could be involved in the inhibitory effect of the stress axis on the LH and prolactin function.

There is little known about the molecular pathways modulating the interactions between gonadotrophs and other pituitary cell types. Many candidates have been suggested, such as the growth factors (reviewed by Childs and Unabia, 2001;

Denef, 2008; Luckenbach *et al.*, 2010). Other factors that may mediate paracrine pituitary interactions are ligands that activate melanocortin receptors. Recent unpublished findings by our group suggest that MC₃ may be a target for these ligands. Ablating MC₃ resulted in a significant reduction in the pituitary content of LH, FSH, GH and prolactin in adult male mice (see Figure 5. 1. A) compared to wild-type. In the adult female, ablating MC₃ resulted in decreased pituitary content for GH only (see Figure 5.1.B) whilst LH, FSH and prolactin content tended to be lower but not significantly so (Dowejko *et al.*, 2014). It should be noted that the study was conducted in female mice without determining the stage of the estrous cycle.

Other anterior pituitary cell types have been found to be regulated by the melanocortins. Langouche and colleagues (2001) reported the increase of calcium influx in GH3 cells (a prolactin and growth hormone-producing cell line) after treatment with γ_3 -MSH. Even though γ_3 -MSH mediates its functions mainly through MC₃, the RT-PCR analysis of these cells detected only MC₅. These findings might indicate the involvement of MC₅ in stimulating GH3 cells despite treatment with SHU9119, a known MC₅ partial agonist, did not have any effect in this study. The same research group conducted similar experiments on primary pituitary cells prepared from neonatal rats, showing that γ_3 -MSH and surprisingly an AgRP analogue (AgRP⁸³⁻¹³²), stimulated prolactin release and concluded, again, that the effect was not mediated by MC₃ even though it was detected in those rat pituitary preparations, and the receptor involved is yet to be identified (Langouche *et al.*, 2004). These studies show the involvement of the melanocortins in the function of different cells but there are different mechanisms that could underlie these effects. Given the interaction between the anterior pituitary cells described above, the melanocortins could be interacting with cells through either autocrine or paracrine pathways which have yet to be identified.

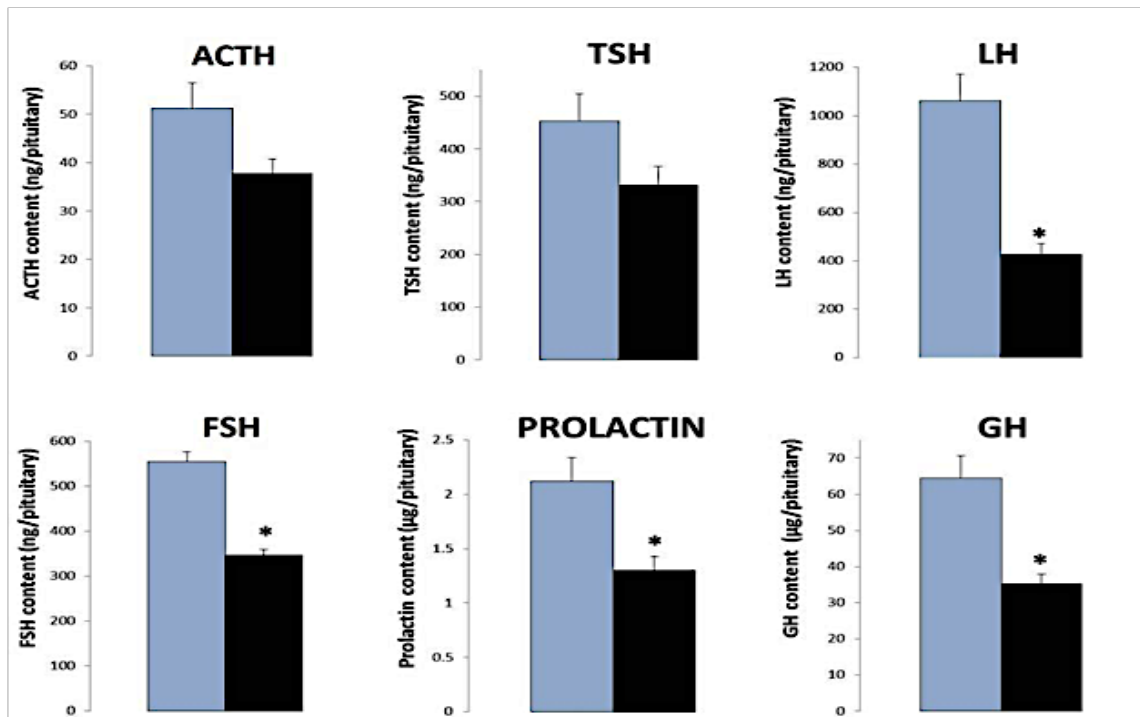
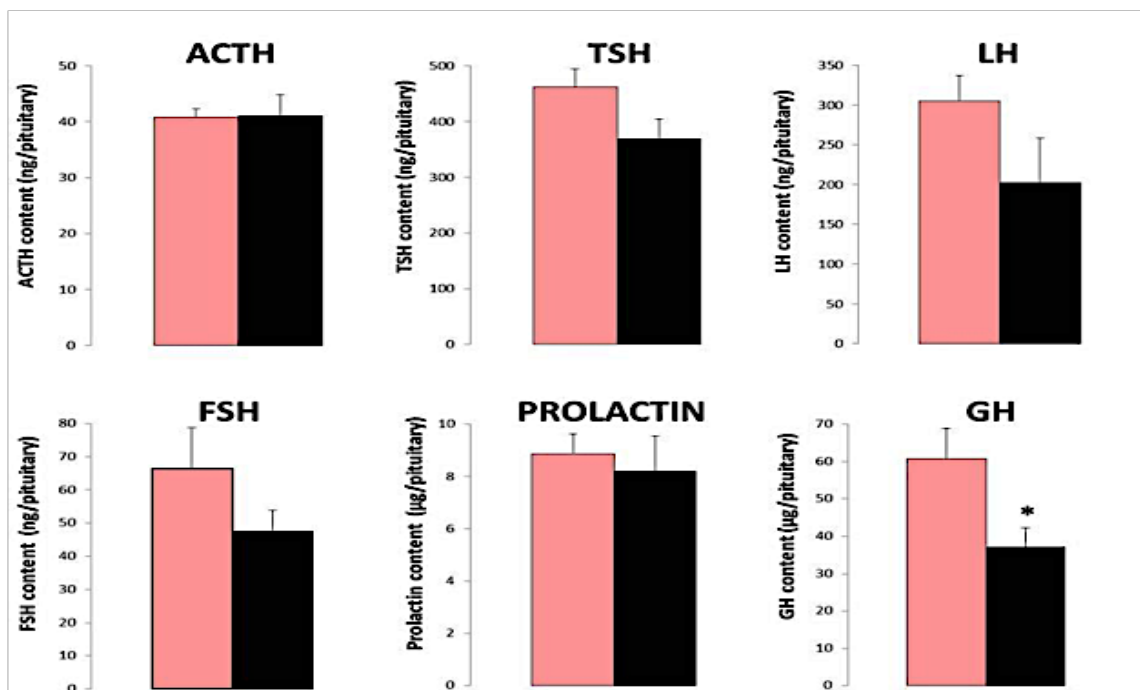
A**B**

Figure 5.1: Hormonal pituitary content of MC₃^{-/-} and wild type male (A) and female (B) adult mice. Radioimmunoassay was used to measure the pituitary content of adrenocorticotrophic hormone (ACTH), thyroid stimulating hormone (TSH), luteinising hormone (LH), follicular stimulating hormone (FSH), prolactin and growth hormone (GH). The data is presented as mean ± SEM. * p<0.05 vs. WT (t-test). Figures are taken from (Dowejko, 2014).

Thus, published studies have revealed different mechanisms regulating gonadotrophs; these included indirect effects of the melanocortin system in the regulation of the LH and FSH synthesis and release. The MC receptors have been detected in some of the pituitary cells such as the lactotrophs and corticotrophs. However, further characterisation might detect these receptors in other cell types including the gonadotrophs which would provide more evidence for a direct association of the MC system with reproduction via the pituitary gland. Therefore, the aims of the series of studies to be described in this chapter are to:

1. Determine suitable reference genes in the mouse pituitary gland for normalisation using GeNorm expression stability analysis.
2. Characterise *MC₍₁₋₅₎*, *MRAP1* and *MRAP2*, *POMC* and *AgRP* in the pituitary gland of mice at different ages (2, 6, 10 and 14 weeks old).
3. Determine the expression of the same melanocortin family members listed above in pregnant and non-pregnant mice.
4. Determine, at the cellular level, *MC₃*, *MC₅* and *MRAP2* expression using chromogenic *in situ* hybridisation (RNAscope®).
5. Determine if either *MC₃* or *MRAP2* are specifically expressed in colocalising somatotrophs and/or gonadotrophs using *GH* and *LH* probes, respectively.

5. 2 Methods

For a detailed account of the materials and techniques used see chapter 3.

5. 2. 1 Determining suitable reference genes for RT-qPCR analysis of the pituitary gland of C57BL/6 female mice

The most stable reference genes in the pituitary gland were selected using the GeNorm analysis described in detail in section 3. 2. 3. 4. 1. Technical duplicates of cDNA samples from 2, 6, 9, 10 and 14 weeks old mice and pregnant (14 ± 1) mice were used in this analysis.

5. 2. 2 Characterising the gene expression of the MC system

These reference genes were used to normalise data obtained from the RT-qPCR assays of the reverse transcribed RNA extracted from whole pituitary glands of female C57BL/6 mice aged 2, 6, 9, 10 and 14 weeks and pregnant mice (14 ± 1 dpc) (n=5 for each group except n=3 for 9 weeks and n=4 for 10 weeks). The RT-qPCR amplification products were separated on a 2% agarose gel to check the size of the band and verify they were of the predicted size as well as to confirm that there were no non-specific bands.

The RT-qPCR data collected were analysed using the delta-delta CT method described in section 3.2.3.4.3.C.

5. 2. 3 RNAscope® 2.5HD protocol

The pituitary gland sections were collected from female C57BL/6 mice aged 2 weeks, 10 weeks and pregnant (14± 1 dpc) mice.

First studies included using RNAscope® 2.5HD single-plex (brown) staining kit with *MC₃*, *MC₅* and *MRAP2* as well as positive and negative controls.

The second group of studies included using RNAscope® 2.5HD duplex (C1-green/C2-red) staining kit with *MRAP2* at C1 and *MC₃* at C2 channels; *GH* (somatotrophs markers) at C1 and *MC₃* at C2 channels; *LHβ* (gonadotrophs marker) at C1 and *MC₃* at C2 channels. Also, the RNAscope® 2.5HD duplex assays included the *GH* or *LHβ* at C1 and *MRAP2* at C2; that is, a signal channel detection swap (see section 3.2.5.2.3 for the protocol of channel swap) and 2-plex positive and 2-plex negative controls. See section 3.2.5 on methods for full details.

The RNAscope® expression signals were quantified using the workflow described in section 3.2.4.5 and statistically analysed using one-way ANOVA in GraphPad (Prism, USA).

5. 3 Results

5. 3. 1. A. Reference gene stability in the Pituitary gland

Using the range of genes listed in Figure 5.2, we found that in the female C57BL/6 mouse pituitary gland, calnexin (*CANX*) and Eukaryotic Translation Initiation Factor 4 A 2 (*EIF4A2*) were the most stable genes, whereas Beta-2-Microglobulin (*B2M*) and Ribosomal Protein L13A (*RPL13A*) were the least stable genes (Figure 5. 2). As *YWHAZ* expression in the pituitary is within the first five most stable genes, it was also included in the normalisation of the pituitary RT-qPCR data to have a consistency of using the same reference genes with that of the hypothalamus.

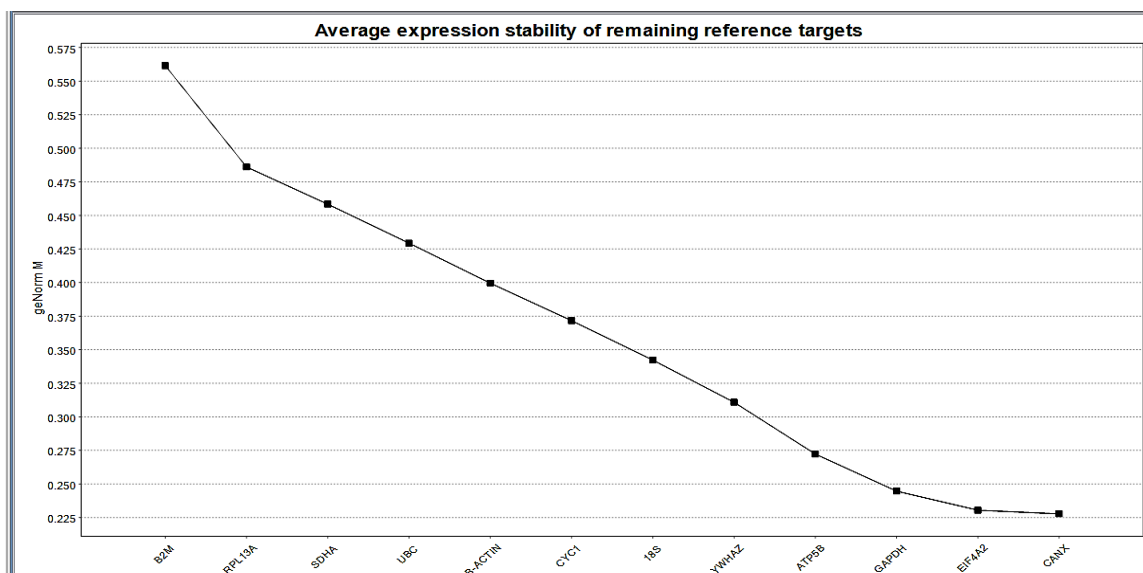


Figure 5.2: GeNorm ranking order of reference genes stability in the female mouse pituitary gland. The ranking is based on calculating the geometric mean of the ranking values from Delta CT, BestKeeper, Normfinder and GeNorm reference gene analyses tools. The stability of 12 reference genes was examined using the pituitary gland of female mice aged 2, 6, 9, 10, 14 weeks, and pregnant mice (14+1 dpc). The samples were run in duplicate. The reference genes are 18S, ACTB, ATP5B, B2M, CANX, CYC1, EIF4A2, GAPDH, RPL13A, SDHA, UBC and *YWHAZ*. CT values were imported to the qBase+ software and analysed using GeNorm (Biogazelle, Belgium).

GeNorm analysis suggested the optimal number of housekeeping genes to be used in normalising the RT-qPCR data was two for the pituitary gland. This was obtained by calculating the pairwise variation (V-score) with the sequential addition of each reference gene one at a time. A V-score above 0.15 indicates the optimal number of most stable reference genes to be used (Figure 5. 3). The V-score was calculated using GeNorm analysis by qBase+ software (Biogazelle, Belgium). See appendix 3. B

for graphs of the BestKeeper, Normfinder, Delta CT and comprehensive reference genes stability analyses.

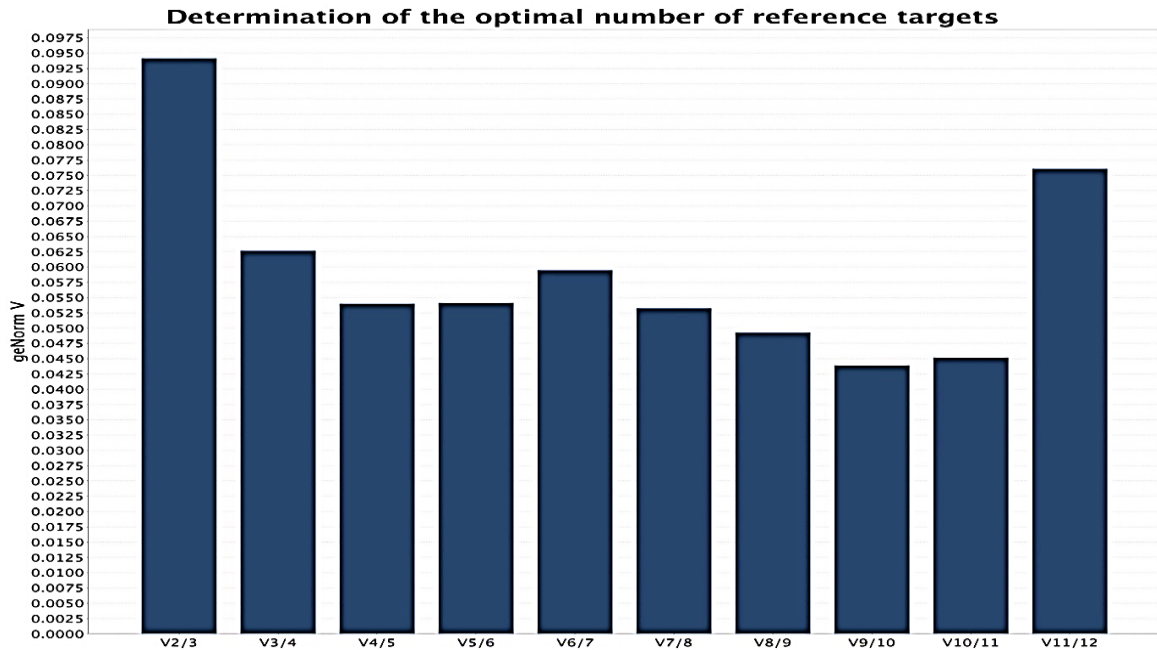


Figure 5.3: Variation score (V- score) by GeNorm. An optimal number of stable genes used normalisation was calculated by pairwise variation with the addition of each reference gene one at a time. A V-score equal or below 0.15 indicated the insignificance of using more reference genes. In this graph, 10 reference genes V-score results means the optimal number of most stable HKG to be used in the pituitary gland are two (GeNorm by qBase+, Biogazelle, Belgium).

5. 3. 1. B. Amplification efficiencies of *CANX* and *EIF4A2*

The amplification efficiency is defined as 100% if the signal from amplification of the cDNA template doubles for each RT-qPCR cycle. Table 4.1 lists the standard curve slope (M), the coefficient of determination (R^2) and amplification efficiency (E) of *CANX* (100%) and *YWHAZ* (103%). *EIF4A2* was expressed in a lower amount than that seen with the GeNorm analysis or when used in parallel with MC expression analyses which might indicate lower stability than that of *CANX* and *YWHAZ*. Therefore, it was excluded from the normalisation.

Table 5-3: Amplification efficiency of CANX and YWHAZ in the pituitary gland.

Gene	R ² (Coefficient of Determination)	M (Measurement of Efficiency)	E (Efficiency)
CANX	0.99	-3.31	100%
YWHAZ	0.99	-3.26	103%
EIF4A2	0.52	-2.61	142%

Pooled cDNA from all samples used in MC system expression in the pituitary gland were used in generating 1:2 standard curves. The efficiency was calculated automatically using the Rotor-Gene Q software (Qiagen, UK).

5. 3. 2 MC system expression

*MC*₁ and *MC*₂ were not detected in the pituitary of the C57BL/6 female mouse while *MC*₍₃₋₅₎, *MRAP1*, *MRAP2*, *POMC* and *AgRP*) expression could be detected. The expression of the mRNA for these targets is not the same. At 2, 6, 9, 10 and 14 weeks old and pregnant (14 ±1 dpc) mice, the pituitary expression of *POMC* was dramatically higher than all the other expressed MCs members (Figure 5. 4). This high level of expression remains relatively constant across 2, 6, 9, 10 and 14 weeks old mice and in pregnant mice. However, age and pregnancy did not cause any variation in *POMC* expression levels.

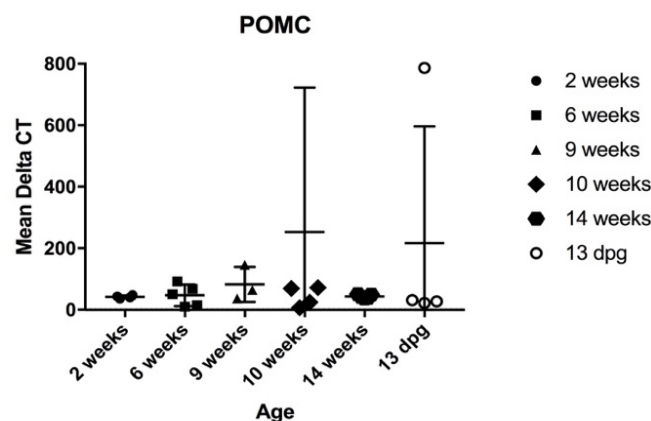


Figure 5.4: POMC expression in the female mouse pituitary gland. Pituitary cDNA duplicates from female C57BL/6 mice aged 2, 6, 9, 10 and 14 weeks and pregnant mice (14 +1 DPC) (n=3-5) were used in the RT-qPCR studies. CT values of each assay were exported to excel worksheet, analysed using the delta CT Method developed by Pfaffl (2001). The skewed data seen in the graphs are due to animal sample variations (old vs. newly obtained samples). The 2^{-ΔCT} values were imported to GraphPad and analyses using one-way analysis of variance (ANOVA). (Prism 7, USA).

The expression of both *MC₃* and *AgRP* was detected in the 2, 6, 10 and 14 weeks old mice and pregnant mice. There was a gradual increase in *MC₃* expression between 2 weeks and 6 weeks and between 10 weeks and 14 weeks old mice and pregnant mice. Age and pregnancy did not have any significant effect on *MC₃* expression (Figure 5.5.A). *AgRP* expression, on the other hand, remained constant across 2, 6, 9, 10 and 14 weeks old mice and only appeared to increase in pregnant animals compared to non-pregnant 9 weeks old mice. There was however no significant *AgRP* expression variation in relation to age and pregnancy (Figure 5.5.B).

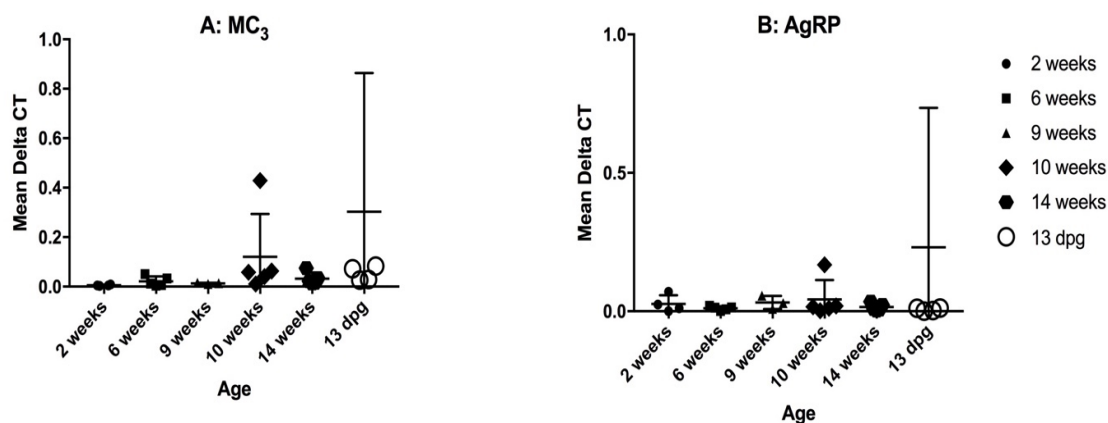


Figure 5.5: *MC₃* and *AgRP* expression in the female mouse pituitary gland. Pituitary cDNA duplicates from female C57BL/6 mice aged 2, 6, 9, 10 and 14 weeks and pregnant mice (14 +1 DPC) (n=3-5) were used in the RT-qPCR studies. A: *MC₃* expression in female mouse pituitary gland. B: *AgRP* expression in female mouse pituitary gland. CT values of each assay were exported to excel worksheet, analysed using the delta CT Method developed by Pfaffl (2001). The skewed data seen in the graphs are due to animal sample variations (old vs. newly obtained samples). The $2^{-\Delta CT}$ values were imported to GraphPad and analyses using one-way analysis of variance (ANOVA). (Prism 7, USA).

Age did not have any effect on the expression of *MRAP1*. However, *MRAP1* expression appeared to be slightly higher in 2 weeks compared to 6 and 9 weeks old mice and then it appeared to increase between 10 weeks and 14 weeks. Pregnant animals, although insignificant, appeared to have higher *MRAP1* expression compared to non-pregnant 9 weeks old mice (Figure 5.6.A). *MRAP2* expression appeared to increase gradually from 2 weeks old to 10 weeks old mice. *MRAP2* expression then was found to drop in 14 weeks old mice. This pattern of *MRAP2* expression was not significantly affected by age. Pregnant mice had lower expression than non-pregnant mice of the same age (9 weeks old mice). However, the pregnancy effect was also not significant (Figure 5. 6. B).

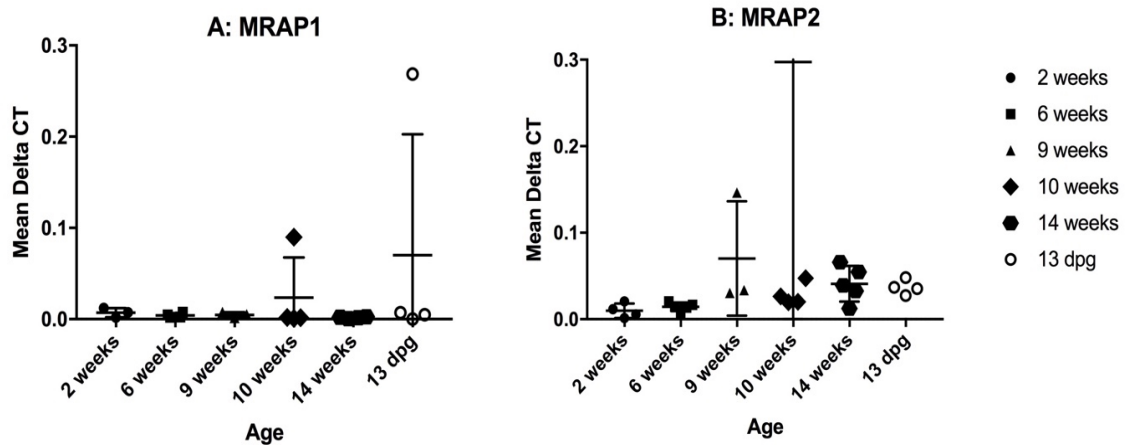


Figure 5.6: MRAP1 and MRAP2 expression in the female mouse pituitary gland. Pituitary cDNA duplicates from female C57BL/6 mice aged 2, 6, 9, 10 and 14 weeks and pregnant mice (14 +1 DPC) (n=3-5) were used in the RT-qPCR studies. **A:** MRAP1 expression in female mouse pituitary gland. **B:** MRAP2 expression in female mouse pituitary gland. CT values of each assay were exported to excel worksheet, analysed using the delta CT Method developed by Pfaffl (2001). The skewed data seen in the graphs are due to animal sample variations (old vs. newly obtained samples). The $2^{-\Delta CT}$ values were imported to GraphPad and analyses using one-way analysis of variance (ANOVA). (Prism 7, USA).

MC_4 and MC_5 had the lowest expression levels compared to the other MC system members in the female mouse pituitary gland. There were no significant variations due to either age or pregnancy. In 2 weeks old mice pituitary MC_4 expression was higher than 6 weeks old mice. This expression rose again in the 9 weeks old mice. The 10 weeks and the 14 weeks old mice, as well as the pregnant animals, had lower MC_4 expression than the younger animals (Figure 5.7.A). MC_5 expression was higher in younger animals (2, 6 and 9 weeks old mice) compared to the older animals (10 and 14 weeks old mice) and pregnant animals (Figure 5.7.B). It is worth mentioning that MC_4 was undetectable in 1 out of 4 animals in most age groups and MC_5 undetectable in 2 out of 5 of most age groups. A summary of $MC_{(1-5)}$, $MRAP1$, $MRAP2$, $POMC$ and $AgRP$ expression in the female mouse pituitary gland is presented in Table 5.2.

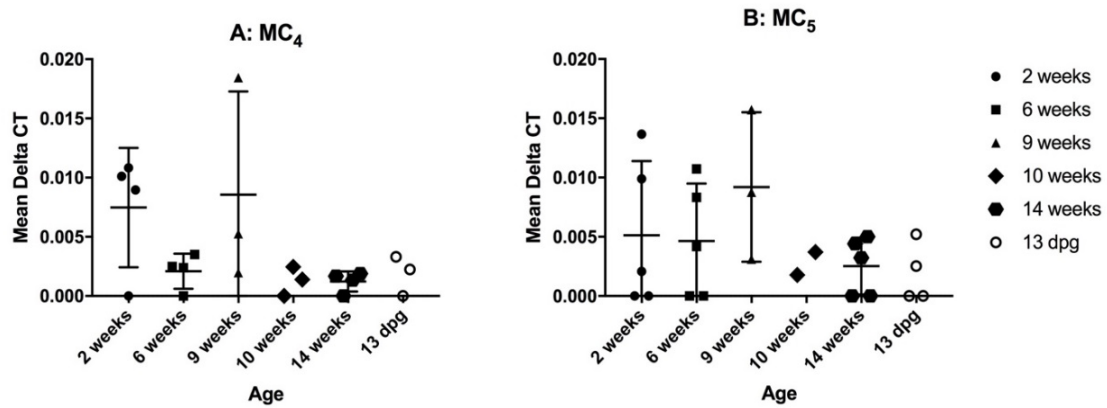


Figure 5.7: MC₄ and MC₅ expression in the female mouse pituitary gland. Pituitary cDNA duplicates from female C57BL/6 mice aged 2, 6, 9, 10 and 14 weeks and pregnant mice (14 +1 DPC) (n=3-5) were used in the RT-qPCR studies. **A:** MC₄ expression in female mouse pituitary gland. **B:** MC₅ expression in female mouse pituitary gland. CT values of each assay were exported to excel worksheet, analysed using the delta CT Method developed by Pfaffl (2001). The skewed data seen in the graphs are due to animal sample variations (old vs. newly obtained samples). The $2^{-\Delta CT}$ values were imported to GraphPad and analyses using one-way analysis of variance (ANOVA). (Prism 7, USA).

Table 5-4: MC system expression in the female pituitary gland.

PITUITARY (n= 3-5)				
Gene	Expression	P value	Significance of Age	Significance of Pregnancy
MC ₁	-	N/A	N/A	N/A
MC ₂	-	N/A	N/A	N/A
MC ₃	+	0.46	-	-
MC ₄	+	0.67	-	-
MC ₅	+	0.67	-	-
POMC	+	0.68	-	-
AgRP	+	0.15	-	-
MRAP1	+	0.60	-	-
MRAP2	+	0.64	-	-

The table represents each gene examined in hypothalamic cDNA replicates of 3-5 female C57BL/6 mice. Age and pregnancy effects were studied by using animals aged 2, 6, 9, 10 and 14 weeks and pregnant mice (14 +1dpc). MC₍₃₋₅₎, MRAP1, MRAP2, POMC and AgRP were found in the pituitary gland. There appeared to be no effect of pregnancy or age on the expression of any of the genes of interest. (-): indicates the absence of a gene or insignificant impact by age or pregnancy. N/A: not applicable.

5. 3. 3 Validation of the MC system expression

The products of the RT-qPCRs for *MC* (₁₋₅), *POMC*, *MRAP1*, *MRAP2* and *AgRP*, as well as *CANX* and *YWHAZ*, were separated by electrophoresis on a 2% agarose gel (composition and method described in section 3. 2. 4. 3. 3). The products also contained non-template control for each of the target and reference genes to check for genomic contamination (Figure 5. 8).

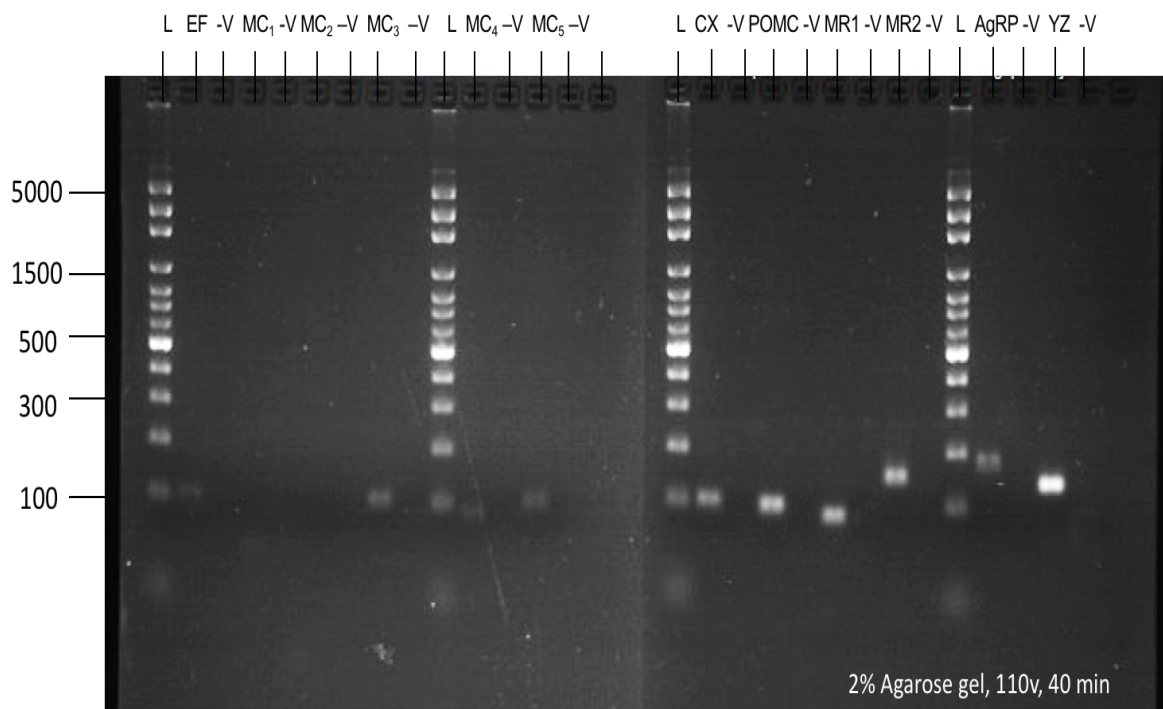


Figure 5.8: Gel electrophoresis of RT-qPCR of MC system in the pituitary gland. The RT-qPCR products were separated on 2% agarose gel at 110 volts for 40 minutes. Where L = ladder 100 bp to 5000 bp; (ThermoScientific, UK); EF: EIF4A2 = 152; MC₁, MC₂ MC₃ = 108 bp, MC₄ = 106 bp, MC₅ = 90 bp, CX: CANX = 105 bp, POMC = 99 bp, MR1: MRAP1 = 86 bp, MRAP2 = 150 bp, AgRP = 63 bp, yz = YWHAZ = 141 bp, -ve: non-template control for gene of interest in previous lane. Gel image was taken using UVIPRO (Uvitec, UK).

5. 3. 4 Localization of *MC₃*, *MC₅* and *MRAP2* mRNA transcripts in the female mouse Pituitary gland

The RNAscope[®] expression signals of *MC₃*, *MC₅* and *MRAP2* were identified as brown dots. Figure 5. 9 included positive (*PPIB*) controls to ensure optimised conditions were achieved and negative (*DAPB*) control to ensure there are no background noise in the anterior pituitary cells. The expression in the pituitary gland sections was quantified and the data was presented in as a percentage. A 100% expression indicated the detected number of expression signals (in dots) of the target gene(s) is equivalent to the number of the cells. A percentage higher than 100% is due to more than one mRNA copy of target gene within the cells.

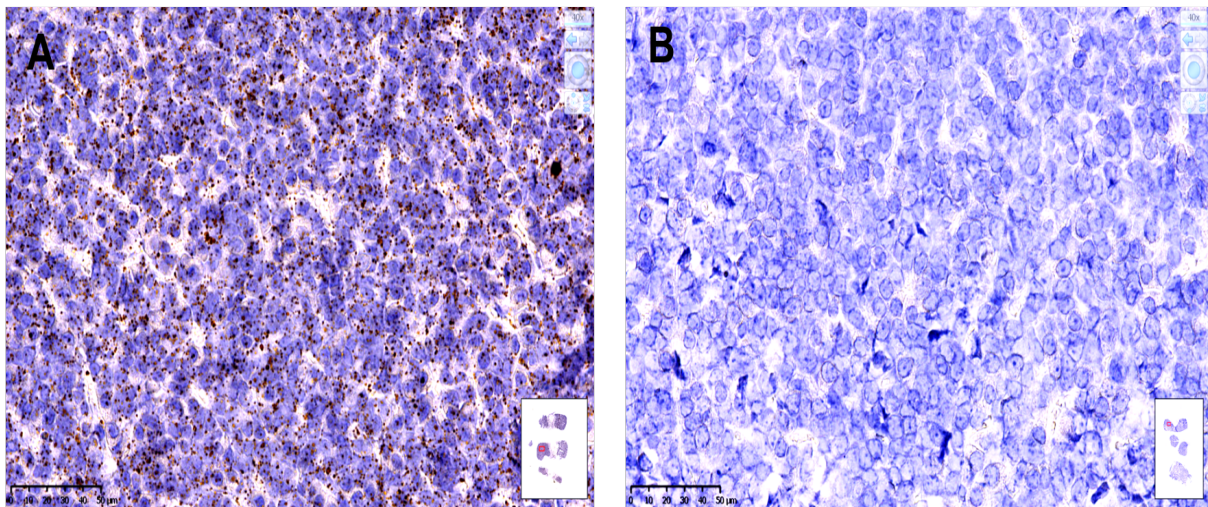


Figure 5.9: RNAscope[®] 2.5HD single-plex (brown) assay in the female mouse pituitary gland. The assay was show expression of positive (*PPIB*) control to illustrate how the expression signal as brown dots in cells, counterstained with Haematoxylin (Hx). B: negative (*DAPB*) control in the pituitary showing no background staining. Each group was conducted as 3 sections per slide (2 weeks were 4 sections per slide) and assay was carried out twice. Images were taken by NanoZoomer slide scanner (Hamamatsu Photonics) at King's College London.

5. 3. 4. A. RNAscope® 2.5HD brown detection of *MC₃*, *MC₅* and *MRAP2* in the pituitary gland

The expression of *MC₃* was detected in the pituitary gland of 2 and 10 weeks old C57BL/6 female mice and pregnant (14 ± 1 dpc) mice. The pregnant mice appeared to have higher expression (100.26%) than the 2 weeks and the 10 weeks old mice with expression percentages of 71.18% and 69.74% respectively (Figure 5. 10 A-C). However, neither age nor pregnancy had a significant impact on *MC₃* expression. Table 5. 5 shows *MC₃* mRNA expression levels in pituitary gland of 2 and 10 weeks and pregnant (14 ± 1 dpc) mice.

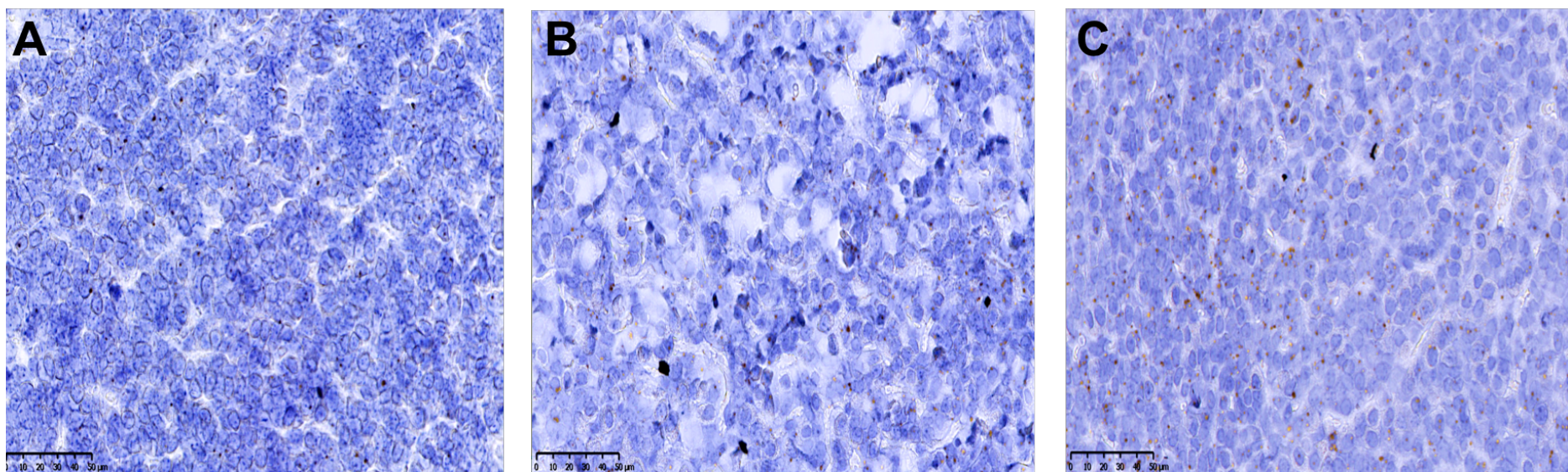


Figure 5.10: RNAscope® 2.5HD Brown assay of MC₃ in female mouse anterior pituitary gland. The assay was carried in pituitaries of mice aged 2, 10 weeks old mice and pregnant (14 ± 1 dpc) mice. A: MC₃ expression in 2 weeks old mice; B: MC₃ expression in 10 weeks old mice. C: MC₃ expression in pregnant (14 ± 1 dpc) mice. The expression of MC₃ was quantified manually within each section (within the black square) was calculated. The mean expression of all section on one slide representing an age group was measured. See quantification analyses workflow in methods section 3. 2. 5. 4. Each age group was conducted as two slides with two sections per slide. Images were taken using a NanoZoomer slide scanner (Hamamatsu Photonics) at King's College London.

Table 5-5: The percentage of MC₃ expression in the RNAscope® brown assay in the mouse anterior pituitary gland.

Age	Section 1 (%)	Section 2 (%)	Section 3 (%)	Section 4 (%)	Mean (%)±SEM	Number of animals
2 weeks	60.18	57.26	61.72	105.5	71.18±11.5	4
10 weeks	62.5	86.54	60.19	N/A	69.74± 8.4	3
(14 ± 1 dpc)	113.9	86.89	100	N/A	100.26± 7.8	3

The RNAscope® brown expression in 2 and 10 weeks old C57BL/6 female mice and pregnant (14 ± 1 dpc) mice were quantified manually, and the percentage of expression within each section was calculated. The mean expression ± SEM of all sections on one slide representing an age group (4 sections per slide for 2 weeks old; 2 sections per slide for 10 weeks old and 3 sections per slide for 14 ± 1 dpc pregnant) was measured. See quantification analyses workflow in methods section 3. 2. 5. 4.

The expression of MC₅ was detected in the pituitary gland of 2 and 10 weeks old mice and pregnant (14 ± 1 dpc) mice. The MC₅ expression level (68.31%) in the 2 weeks animal is relatively similar to levels seen with MC₃ in 2 and 10 weeks old mice. However, the expression was significantly higher in 2 weeks mice old (68.31%; p value= 0.0434) compared to 10 weeks old mice (43.92%). MC₅ expression was greater in pregnant animals compared to similarly aged virgin mice reaching levels (60.13%), which is similar to that seen in 2 weeks old mice (Figures 5. 11 A-C). Table 5.4 shows MC₅ expression levels in pituitary glands of 2 and 10 weeks and pregnant (14 ± 1 dpc) mice.

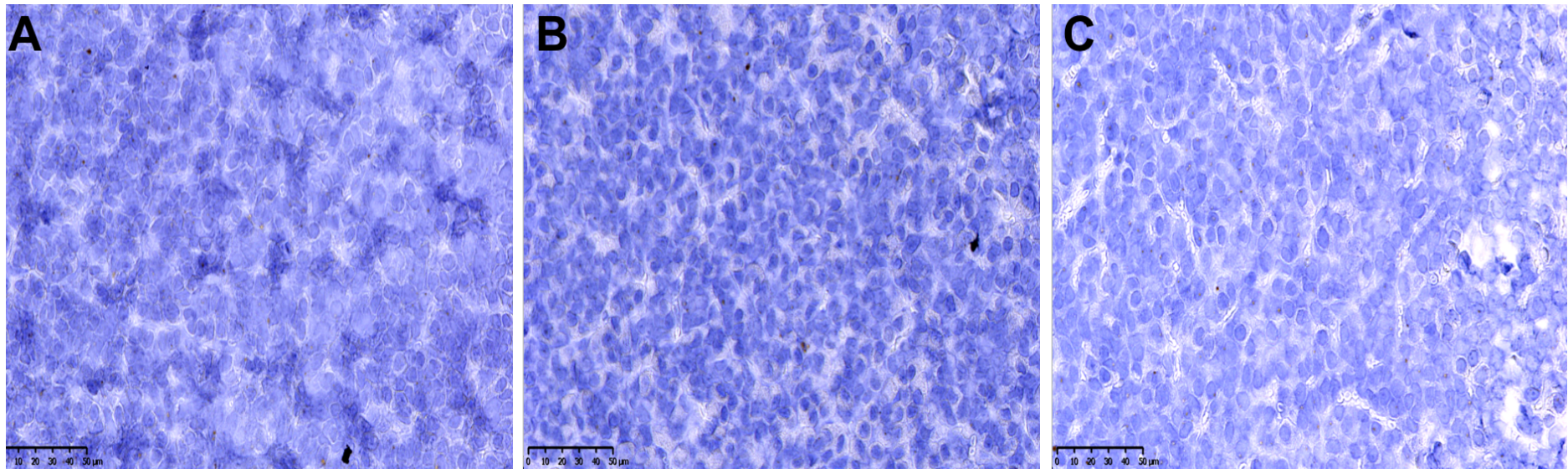


Figure 5.11: RNAscope® 2.5HD Brown assay of MC₅ in female mouse anterior pituitary gland. The assay was carried in pituitaries of mice aged 2, 10 weeks old mice and pregnant (14 ± 1 dpc) mice. A: MC₅ expression in 2 weeks old mice; B: MC₅ expression in 10 weeks old mice; C: MC₅ expression in pregnant (14 ± 1 dpc) mice. The expression of MC₅ was quantified manually within each section (within the black squares) was calculated. The mean expression of all section on one slide representing an age group was measured. See quantification analyses workflow in methods section 3. 2. 5. 4. Each age group was conducted as two slides with two sections per slide. Images were taken using a NanoZoomer slide scanner (Hamamatsu Photonics) at King's College London.

Table 5-6: The percentage of MC₅ expression in the RNAscope® brown assay in the mouse anterior pituitary gland.

Age	Section 1 (%)	Section 2 (%)	Section 3 (%)	Section 4 (%)	Mean (%)±SEM	Number of animals
2 weeks	87.8	61.83	60.53	63.06	68.31± 6.5	4
10 weeks	49.06	42.7	40	N/A	43.92± 2.7	3
(14 ± 1 dpc)	50.55	68.04	61.8	N/A	60.13±5.1	3

The RNAscope® brown expression in 2 and 10 weeks old C57BL/6 female mice and pregnant (14 ± 1 dpc) mice were quantified manually, and the percentage of expression within each section was calculated. The mean expression ± SEM of all sections on one slide representing an age group (4 sections per slide for 2 weeks old; 2 sections per slide for 10 weeks old and 3 sections per slide for 14 ± 1 dpc pregnant) was measured. See quantification analyses workflow in methods section 3. 2. 5. 4.

Similar to *MC₅*, *MRAP2* expression increased significantly between 2 weeks (p value= 0.024) and 10 weeks old female mice and between 10 weeks old mice and pregnant animals (92.72%, 159.4% and 172.8% respectively) (Figure 5. 12 A-C). Table 5. 7 shows *MRAP2* expression levels in the pituitary gland of 2 and 10 weeks old mice and pregnant (14 ± 1 dpc) mice.

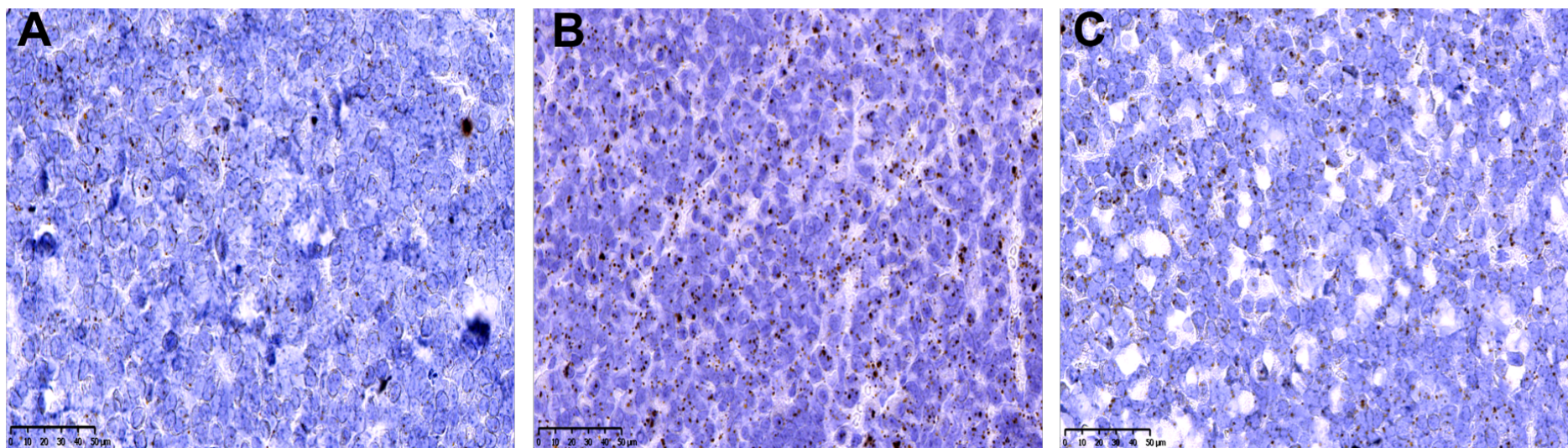


Figure 5.12: RNAscope[®] 2.5HD Brown assay of MRAP2 in female mouse anterior pituitary gland. The assay was carried in pituitaries of mice aged 2 and 10 weeks old and pregnant (14 ± 1 dpc) mice. A: MRAP2 expression in 2 weeks old mice ; B: MRAP2 expression in 10 weeks old mice; C: MRAP2 expression in pregnant (14 ± 1 dpc) mice. The expression of MRAP2 was quantified manually within each section was calculated. The mean expression of all section (within black squares) on one slide representing an age group was measured. See quantification analyses workflow in methods section 3. 2. 5.4. Each age group was conducted as two slides with two sections per slide. Images were taken using a NanoZoomer slide scanner (Hamamatsu Photonics) at King's College London.

Table 5-7: The percentage of MRAP2 expression in the RNAscope® brown assay in the mouse anterior pituitary gland.

Age	Section 1 (%)	Section 2 (%)	Section 3 (%)	Section 4 (%)	Mean (%)±SEM	Number of animals
2 weeks	77.5	80.88	122.5	90	92.72± 10.2	4
10 weeks	135.9	215.1	127.3	N/A	159.43±28	3
(14 ± 1 dpc)	148.2	180.8	189.4	N/A	172.82±12.5	3

The RNAscope® brown expression in 2 and 10 weeks old C57BL/6 female mice and pregnant (14 ± 1 dpc) mice were quantified manually, and the percentage of expression within each section was calculated. The mean expression ± SEM of all sections on one slide representing an age group (4 sections per slide for 2 weeks old; 2 sections per slide for 10 weeks old and 3 sections per slide for 14 ± 1 dpc pregnant) was measured. See quantification analyses workflow in methods section 3. 2. 5. 4.

Differences between pituitary gland *MC₃*, *MC₅* and *MRAP2* expression were detected in the 10 weeks old mice and the pregnant animals. In the 10 weeks old mice, *MRAP2* expression was significantly higher than both *MC₃* and *MC₅*. Pregnant animals had significantly lower *MC₅* expression compared to both *MC₃* and *MRAP2*. The younger animals did not show a difference in the expression between *MC₃*, *MC₅* nor *MRAP2*. Figure 5. 13 A-C shows *MC₃*, *MC₅* and *MRAP2* expression comparison in 2 weeks, 10 weeks old and pregnant (14 ± 1 dpc) mice bar charts.

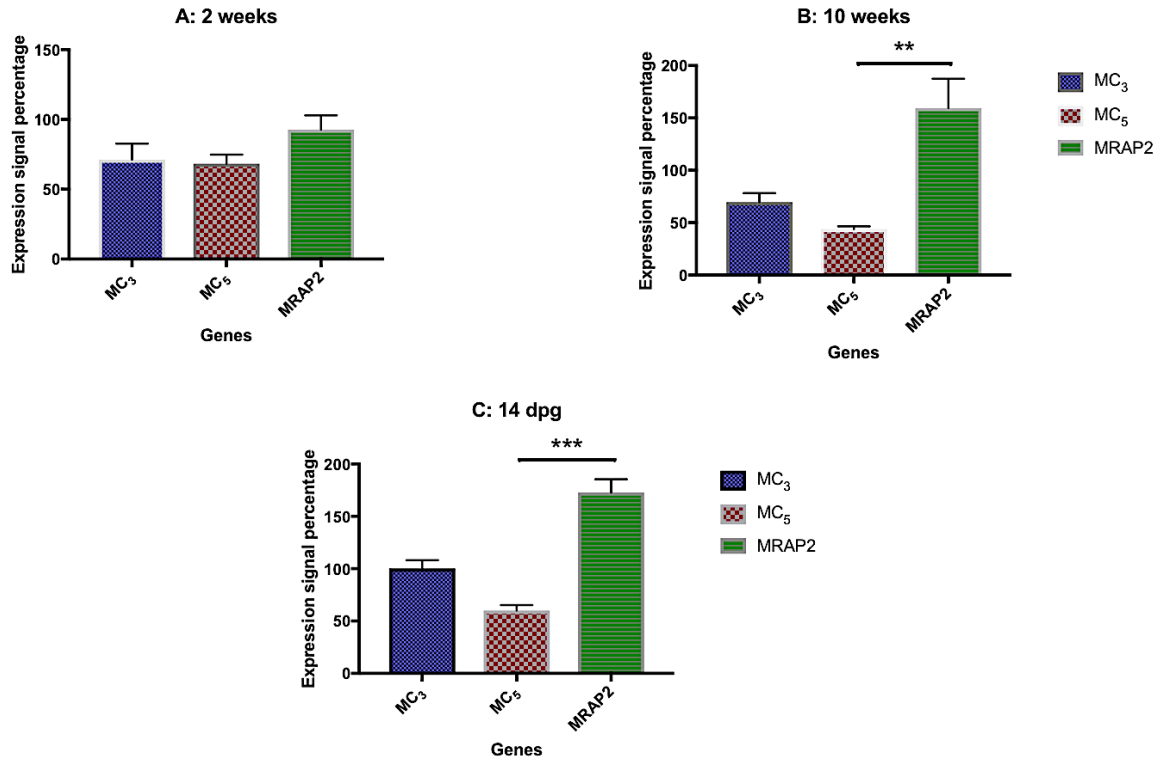


Figure 5.13: Comparison between MC₃, MC₅ and MRAP2 expression in RNAscope® 2.5HD brown of the female mouse pituitary gland. The percentage values of each gene for each of the sections of 2 weeks, 10 weeks old or pregnant (14 ± 1 dpc) mice were plotted in GraphPad and analysed using non-parametric tests (Kruskal-Wallis test; Prism 7.04). A: MC₃, MC₅ and MRAP2 expression in 2 weeks old mice (p value= 0.16). B: MC₃, MC₅ and MRAP2 expression in 10 weeks old mice (p value= 0.002). C: MC₃, MC₅ and MRAP2 expression in pregnant (14 ± 1 dpc) mice (p value= 0.002).

5. 3. 4 RNAscope® 2.5HD Duplex detection in the pituitary gland

The RNAscope® duplex assay was conducted with five different sets of target probes in the pituitary gland:

MC₃ (C1) / MRAP2 (C2).

MC₃ (C1) / GH (C2).

MC₃ (C1) / LHβ (C2).

MRAP2 (C1) / GH (C2) with channel swap.

MRAP2 (C1) / LHβ (C2) with channel swap.

The signal detection of the first three sets is green for C1 and red for C2. The channel swap conducted with latter two sets caused an exchange of C1 signal detection to red instead of green, and C2 was detected as green instead of red.

1. Co-expression of *MC₃* and *MRAP2*

The green / red double expression of *MC₃* / *MRAP2* was detected in 2 and 10 weeks old mice and pregnant (14 ± 1 dpc) mice pituitary glands. The dual expression (represented in as a percentage) appeared to increase between 2 and 10 weeks old animals (69.32% and 75.53% respectively). The expression in pregnant animals than was found to decrease lower than the double expression seen in 2 weeks old animals (58.41%) (Figure 5. 15 A-C). However, there was no significant change observed in *MC₃* / *MRAP2* co-expression in relation to age or pregnancy. In addition to the double expression, some cells had either *MC₃* or *MRAP2* expressed alone. Table 5. 8 lists the percentages of *MC₃* / *MRAP2* double expression, *MC₃*, *MRAP2* expression and cell that had no expression detected. Positive (*PPIB* / *POL2A*) and negative (*DAPB* 2plex) duplex assay were included to ensure optimum conditions (see Figure 5. 14).

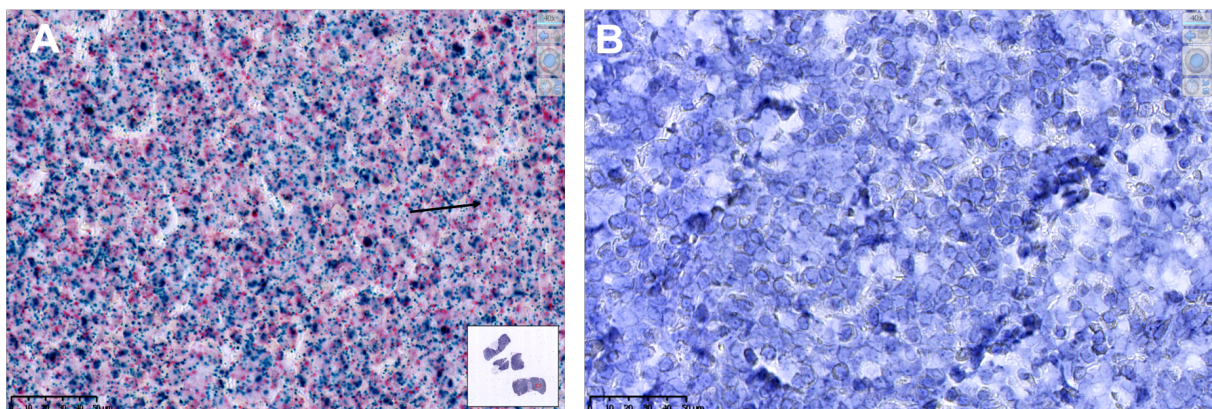


Figure 5.14: RNAscope[®] 2.5HD duplex assay in female mouse pituitary gland. A: A pituitary gland section showing signal detection of the 2-plex positive control (*PPIB*-C1-green -blue arrow) and (*POLR2A*-C2-red-red arrow) (40X). There is also co-expression of both genes in the same cells (black arrow). B: A magnification power of 40 pituitary gland section with a 2-plex negative (*DAPB*) control to ensure there is now background staining. Images were taken by NanoZoomer slide scanner (Hamamatsu Photonics) at King's College London.

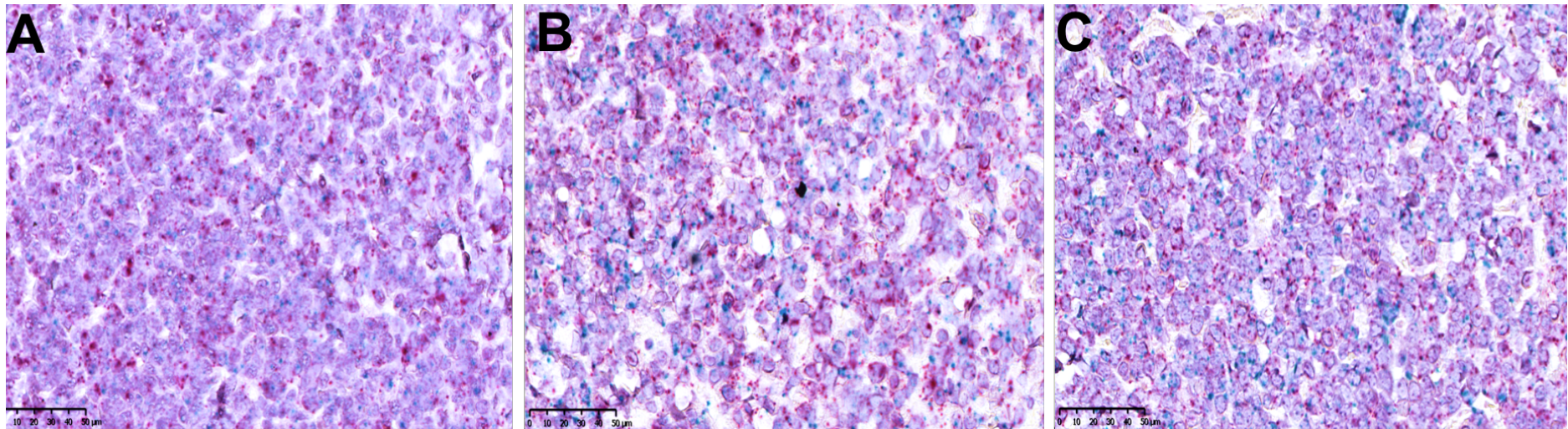


Figure 5.15: RNAscope® 2.5HD Duplex assay showing MC₃ (C1)-MRAP2 (C2) expression in the female mouse pituitary gland. The assay was carried in pituitaries of mice aged 2 and 10 weeks old mice and pregnant (14 ± 1 dpc) mice. The pituitary sections show expression and co-expression of MC₃ (green arrow) or MRAP2 (red arrow) or both (black arrow). A: MC₃ - MRAP2 expression in 2 weeks old mice; B: MC₃ - MRAP2 expression in 10 weeks old mice; C: MC₃ - MRAP2 expression in pregnant (14 ± 1 dpc) mice. The expression was quantified manually of each gene within each cell in each section (within the black squares) was calculated. The mean expression of all section on one slide representing an age group was measured. See quantification analyses workflow in methods section 3. 2. 5. 4. Each age group was conducted as two sections per slide and n=2. Images were taken by NanoZoomer slide scanner (Hamamatsu Photonics) at King's College London.

Table 5-8: The percentage of MC_3 / MRAP2 expression in the RNAscope® Duplex assay in the mouse anterior pituitary gland.

Age	Mean of MC_3 / MRAP2 (%)	Mean of MC_3 (%)±SEM	Mean of MRAP2 (%)±SEM	Mean of Cells with no expression (%)±SEM	Number of animals
2 weeks	69.32±5.9	10.96±3.7	13.11±3.3	6.74±1.8	4
10 weeks	75.53±0.4	8.88±3.7	9.98±5.5	5.6±2.5	3
(14 ± 1 dpc)	58.41±5.7	11.84±2.2	21.15±5.2	8.63±1.5	3

The RNAscope® duplex expression in 2 and 10 weeks old C57BL/6 female mice and pregnant (14 ± 1 dpc) mice were quantified manually, and the percentage of expression of each within each section was calculated in cells showing co-expression and single expression. The mean expression ± SEM of all section on one slide representing an age group was measured. See quantification analyses workflow in methods section 3. 2. 5. 4.

2. Co-expression of MC_3 and GH and $LH\beta$

The RNAscope® duplex assays with MC_3 / GH and MC_3 / $LH\beta$ were qualitative assays to determine if MC_3 expression is in the somatotrophs and/or gonadotrophs of the C57BL/6 female mouse.

The intensity of the expression signal of GH was extremely high in most of the cells, which led to the masking of the MC_3 expression signal within the same cells. GH signal was visible in these sections with the naked eye. Some MC_3 expression could be detected in somatotrophs that had a lower GH expression signal (Figure 5.16 A-C). The double expression was detected in the anterior pituitary of 2 and 10 weeks old mice and pregnant (14 ± 1 dpc). The MC_3 expression signal was also detected in some of the anterior pituitary cells that did not express GH (Figures 5. 16 A-C).

The expression signal of *LH β* , although lower than that of *GH*, was also of such a high intensity such that it masked the expression of *MC₃*. Nonetheless, *MC₃* appeared to be expressed in the same cells expressing *LH β* , the gonadotrophs. The *MC₃ / LH β* expression was seen in anterior pituitary of 2 and 10 weeks old mice and pregnant (14 \pm 1 dpc) (Figure 5.17 A-C). Some of the other pituitary cells that do not express *LH β* were found to express *MC₃* (Figures 5.17 A-C).

The current findings also reveal a reduction in the number of both *GH* and *LH β* expressing cells during pregnancy (see Figures 5. 16, C and 5. 17, C respectively) compared to 2 weeks and 10 weeks old mice.

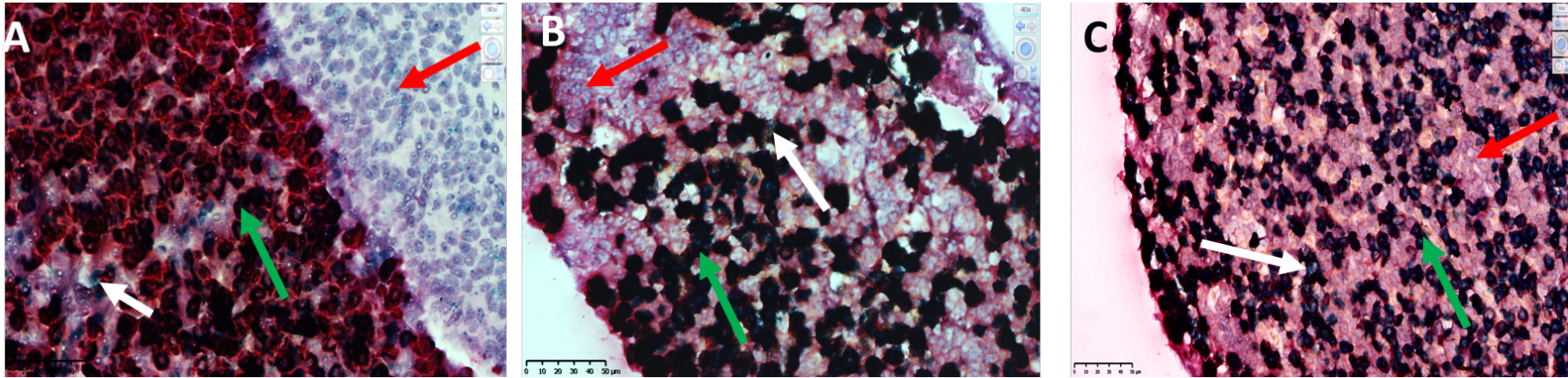


Figure 5.16: RNAscope® 2.5HD Duplex assay showing MC₃ (C1)-GH (C2) expression in the female mouse pituitary gland. The assay was carried in pituitaries of 2 and 10 weeks old mice and pregnant (14 ± 1 dpc) mice. The pituitary sections show expression and co-expression of MC₃ (red arrow) or GH (green arrow) or both (black or white arrow). A: MC₃- GH expression in 2 weeks old mice; B: MC₃- GH expression in 10 weeks old mice; C: MC₃- GH expression in pregnant (14 ± 1 dpc) mice; The GH expression was of high intensity that masked the MC₃ expression in most cells making quantification analyses difficult to achieve. Images were taken by NanoZoomer slide scanner (Hamamatsu Photonics) at King's College London.

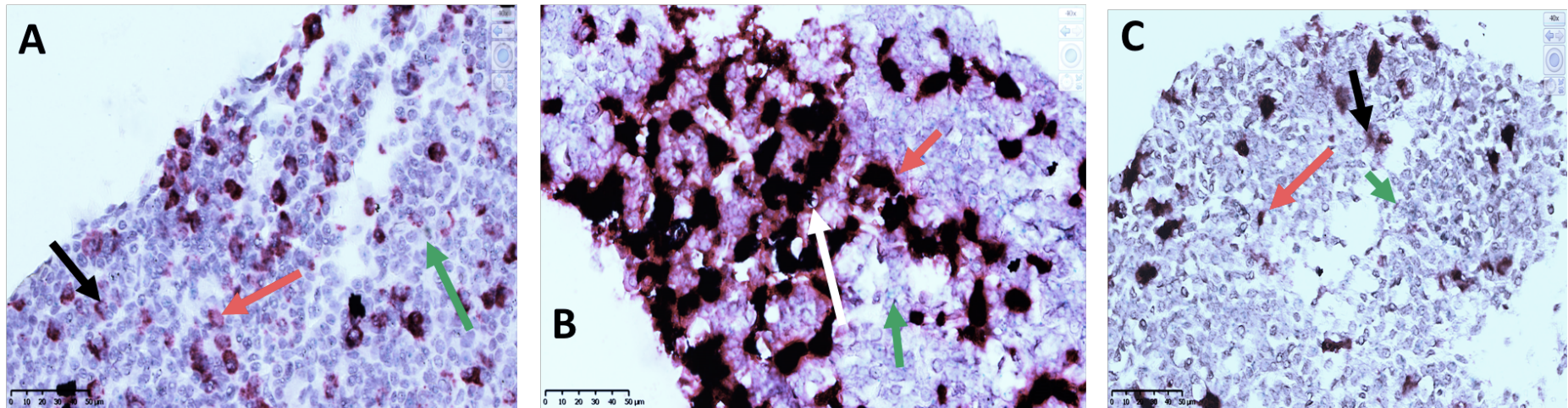


Figure 5.17: RNAscope® 2.5HD Duplex assay showing MC_3 (C1)- $LH\beta$ (C2) expression in the female mouse pituitary gland. The assay was carried in pituitaries of mice aged 2 and 10 weeks and pregnant (14 ± 1 dpc) mice. The pituitary sections show expression and co-expression of MC_3 (red arrow) or $LH\beta$ (green arrow) or both (black or white arrow). A: MC_3 - $LH\beta$ expression in 2 weeks old mice; B: MC_3 - $LH\beta$ expression in 10 weeks old mice; C: MC_3 - $LH\beta$ expression in pregnant (14 ± 1 dpc) mice. The GH expression was of high intensity that masked the MC_3 expression in most cells making quantification analyses difficult to achieve. Images were taken by NanoZoomer slide scanner (Hamamatsu Photonics) at King's College London.

3. Co-expression of *MRAP2* and *GH* or *LHβ* with a channel swap

The RNAscope® duplex assays were conducted to reduce the signal intensity of *GH* and *LHβ* to enable better detection of *MRAP2* expression. Although lowering the expression signal intensity was achieved, the signal was still masking *MRAP2* co-expression with of *GH* or *LHβ*.

MRAP2 expression was detected in the somatotrophs of 2 and 10 weeks old mice and pregnant (14 ± 1 dpc) (Figure 5.18 A-C). *MRAP2* expression could also be found in cells that do not express *GH* (Figures 5.18 A-C).

The gonadotrophs were also found to express *MRAP2*. Co-expression *MRAP2* and *LHβ* was detected in gonadotrophs of 2 and 10 weeks old mice and pregnant (14 ± 1 dpc) (Figure 5. 19 A-C).

Figure 5. 18, C and 5. 19, C reveals a reduction in the number of *GH* and *LHβ* expressing cells during pregnancy compared to 2 weeks and 10 weeks old mice.

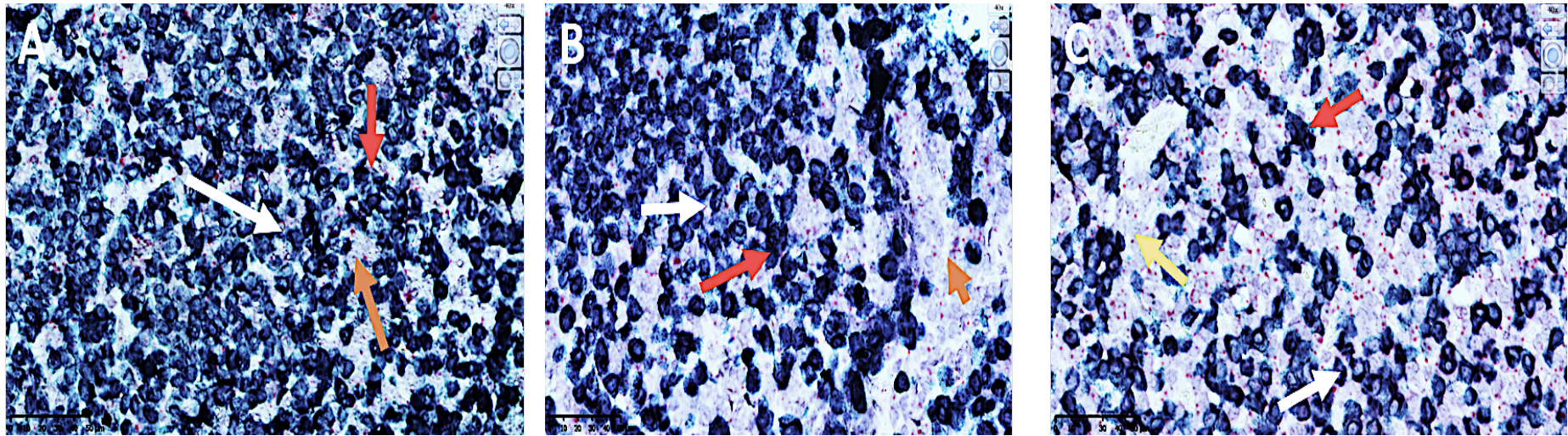


Figure 5.18: RNAscope® 2.5HD Duplex assay showing MRAP2 (C1)-GH (C2) expression after channel swap in the female mouse pituitary gland. The assay was carried in pituitaries of mice aged 2 and 10 weeks and pregnant (14 ± 1 dpc) mice. The pituitary sections show expression and co-expression of MRAP2 (red arrow) or GH (orange arrow) or both (white arrow). A: MRAP2 – GH expression in 2 weeks old mice; B: MRAP2 – GH expression in 10 weeks old mice; C: MRAP2 – GH expression in pregnant (14 ± 1 dpc) mice. The GH expression was of high intensity that masked the MRAP2 expression in most cells making quantification analyses difficult to achieve. Images were taken by NanoZoomer slide scanner (Hamamatsu Photonics) at King's College London.

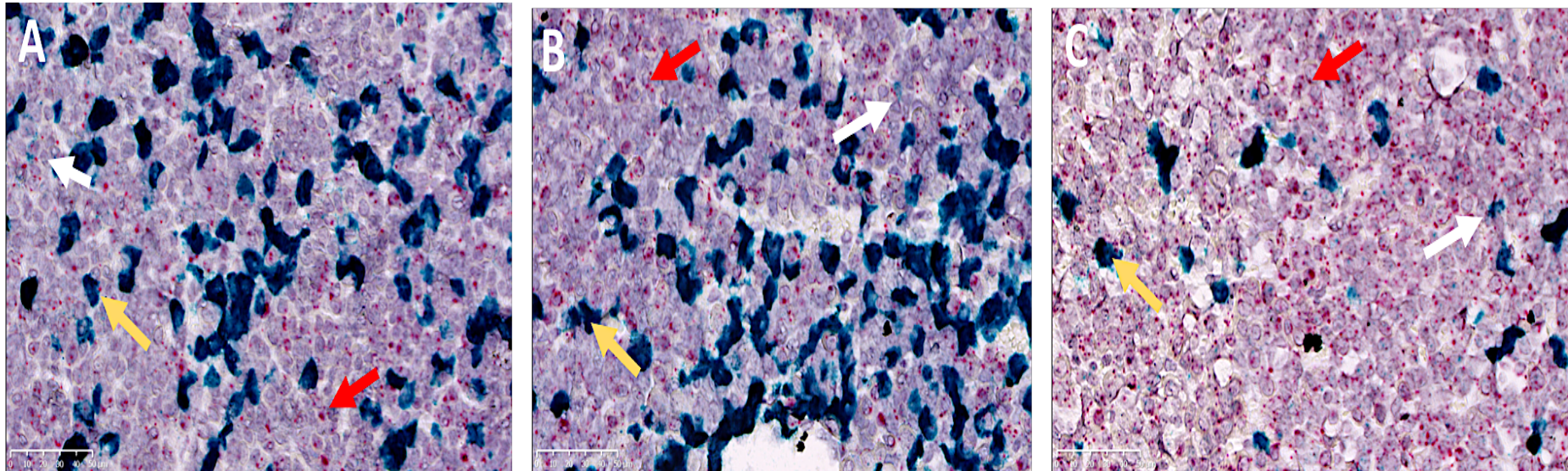


Figure 5.19: RNAscope® 2.5HD Duplex assay showing MRAP2 (C1)- LHβ (C2) expression after channel swap in the female mouse pituitary gland. The assay was carried in pituitaries of mice aged 2 and 10 weeks and pregnant (14 ± 1 dpc) mice. The pituitary sections show expression and co-expression of MRAP2 (red arrow) or LHβ (orange arrow) or both (white arrow). A: MRAP2 – LHβ expression in 2 weeks old mice; B: MRAP2 – LHβ expression in 10 weeks old mice; C: MRAP2 – LHβ expression in pregnant (14 ± 1 dpc) mice. The LHβ expression was of high intensity that masked the MRAP2 expression in most cells making quantification analyses difficult to achieve. Images were taken by NanoZoomer slide scanner (Hamamatsu Photonics) at King's College London.

5. 3 Discussion

The current research study characterised the expression of *MC₃* and *MRAP2* in gonadotrophs and somatotrophs of the anterior pituitary gland using RNAscope®. This RNA *in situ* technique had also shown, for the first time, *MC₅* to expressed in the pituitary gland of C57BL/6 female mouse. Both *MC₅* and *MRAP2* were significantly upregulated with age. Pregnancy resulted in a dramatic rise in *MRAP2* expression level. *MRAP2* expression was also significantly higher than that of *MC₃* and *MC₅* in the anterior pituitary gland. The RT-qPCR data confirmed the expression of *MC₃*, *MC₅* and *MRAP2* in the anterior pituitary, as well as *MC₄*, *MRAP1*, *POMC* and *AgRP*, while *MC₁* and *MC₂* were not detected in the pituitary gland. *POMC* expression was substantially higher the other MC system members followed by *AgRP* and *MC₃*, *MRAP1* and then *MRAP2*, while *MC₄* and surprisingly *MC₅* had the lowest expression. Age and pregnancy did not influence the RT-qPCR expression levels of the MC system in the pituitary gland, which is contradicting the data obtained using the RNAscope®. However, it is worth mentioning that the RT-qPCR data was conducted on RNA obtained from whole pituitaries including all three lobes of the pituitary gland.

The first study of this chapter included selecting the most suitable reference genes for normalising the RT-qPCR data in the pituitary gland using GeNorm expression stability analysis. Those genes were *CANX* and *EIF4A2*. *EIF4A2* is a eukaryotic translation initiation factor 4A2 and is needed in mRNA binding to ribosomes. *CANX* showed stable expression when examined in the 2, 6, 9, 10 and 14 weeks old mice and pregnant (14 ± 1 dpc) mice compared to other reference genes that are commonly used in research. When the same group of samples were examined with *EIF4A2* and *YWHAZ*, *YWHAZ* was found to be stable; whereas *EIF4A2* CT values were varied across the different age groups by 2- 3 cycles. *YWHAZ* was ranked first in the GeNorm expression stability for the hypothalamus and was fifth for the pituitary samples. Normalisation using *CANX* and *YWHAZ* showed similar data to that when normalisation was conducted with *CANX*, *YWHAZ* and *EIF4A2*. However, using the *CANX* and *YWHAZ* provided more reliable data regarding using stable reference genes as when compared to using *EIF4A2*. Therefore, *EIF4A2* was excluded from normalising the pituitary gland RT-qPCR data.

The second series of studies conducted with the RT-qPCR data revealed the absence of MC_1 and MC_2 from the pituitary gland. Little is known about the expression (if any) of both genes in the pituitary gland.

The current series of studies detected MC_3 expression in the pituitary gland, by both RT-qPCR and RNAscope[®]. Although insignificant, the MC_3 expression was gradually increased with age. The RNAscope[®] had also detected the expression of MC_3 in the intermediate lobe of the pituitary gland. In the RNAscope[®], MC_3 expression was not substantially affected by age. In pregnancy there was a 45% increase in expression of MC_3 , although this was not statistically significant. The RNAscope[®] duplex assays using either GH or $LH\beta$ with MC_3 indicated that MC_3 was localised in somatotrophs and gonadotrophs. However, observations on the effect of age and pregnancy on MC_3 in somatotrophs and gonadotrophs could not be made because the high intensity of GH and $LH\beta$ expression masked much of the MC_3 signal, making quantifying the expression within each cell difficult. Finding MC_3 in the somatotrophs and the gonadotrophs indicates that MC_3 could be involved in mediating developmental and reproductive roles, respectively.

These findings strengthen the proposed role of MC_3 in regulating $LH\beta$ and $FSH\beta$ gene expression in the pituitary suggested by (Jiang *et al.*, 2017). The present findings are also consistent with previous rat and mouse studies: in young rats (14 day old), it has been shown that MC_3 were detected in anterior and intermediate lobes of the pituitary gland (Lorsignol *et al.*, 1999) and that *in vitro* stimulation of dissociated rat pituitary cells with γ_3 -MSH causes an increase Ca^{+2} influx. After the addition of SHU9119, Ca^{+2} influx was seen only in half of the cell population (Lorsignol *et al.*, 1999). Additionally, Regard and colleagues detected the expression of MC_3 in the anterior pituitary gland of 12 weeks C57BL/6 male and female mice through GPCR anatomical profiling in different tissues (Regard *et al.*, 2008).

The expression of MC_3 in somatotrophs could influence the response of these cells to ghrelin (which stimulates growth hormone release (Bouzo-Lorenzo *et al.*, 2016)), since it has been shown that GHSR1-a and MC_3 can heterodimerise and that this alters the responses of these GPCRs (Rediger *et al.*, 2011); with a reduction in GHSR1-a response to stimulation, that may be due to receptor internalization (Schellekens *et al.*, 2013). Based on these findings, MC_3 detected on the somatotrophs could be

involved in the regulation of somatotrophs sensitivity to ghrelin and thus regulating GH secretion from the somatotrophs.

The expression of MC_3 in the gonadotrophs also supports the hypothesis of a direct effect of MC_3 on gonadotropins synthesis and release from the gonadotrophs. This could also occur through the heterodimerisation of MC_3 with MC_4 . As mentioned earlier, MC_4 was reported to stimulate $LH\beta$ and $FSH\beta$ synthesis after *in vitro* treatment with THIQ (MC_4 selective agonist) and NDP- α -MSH respectively (Jiang *et al.*, 2017).

Previous studies had reported the expression of MC_3 in lactotrophs of mice (Matsumura *et al.*, 2003) and in another study, the same research group had observed upregulation of MC_3 in the anterior pituitary gland after estradiol treatment in ovariectomized mice (Matsumura *et al.*, 2004). Although lactotrophs are known to express $ER\alpha$ (Mitchner *et al.*, 1998), the estradiol effect could have been mediated through MC_3 expression in either gonadotrophs or somatotrophs [which is also known to express $ER\alpha$ (Avtanski *et al.*, 2014)] As the RT-qPCR studies by Matsumura *et al.*, 2004 were carried out on RNA from the entire anterior pituitary gland, it was unclear which specific pituitary cell types expressed the gene. Matsumura and colleagues also reported that after 20 days of age female mouse had an increase in the levels of MC_3 expression, which is unlike the stable levels that were observed in male mice (Matsumura *et al.*, 2004). These RT-qPCR data were consistent with the current research data. Despite the insignificant change in MC_3 expression in relation to age, there was a moderate rise in the level of MC_3 expression seen in our studies between prepubertal mice and adult mice, consistent with a rise observed between pre-pubertal and 45-day old female mice made by Matsumura and colleagues findings (see Figure 5.5. A) (Matsumura *et al.*, 2004).

The detection of MC_3 in both somatotrophs and gonadotrophs could indicate another indirect role in both cells which is through forming heterodimers with other GPCRs. Previous reports had revealed the heterodimerisation of MC_3 with $GHSR1-a$ in the hypothalamus (Rediger *et al.*, 2011). The $GHSR1-a$ receptor was found expressed in adenomas of all pituitary cell types including both those of somatotroph and the gonadotroph origin (Korbonits *et al.*, 2001). Furthermore, the use of double staining studies in $GHSR1-a$ - (eGFP) reporter mouse had confirmed the $GHSR1-a$ expression in all in each cell type with highest expression in the male and female mouse

somatotrophs (77%) followed by 21% and 9% of lactotrophs; 18% and 19% of gonadotrophs; 19% and 12.6% of corticotrophs and the least was detected in thyrotrophs with 3% and 9% in males and females, respectively (Reichenbach *et al.*, 2012). Considering these findings, MC₃ and the GHSR1-a could be regulating gonadotrophic and somatotrophic functions by forming heterodimers in both cell types. The same could also be investigated for MC₃ and the Kisspeptin receptor. Kisspeptin receptors were also found expressed in the pituitary gland and were found to stimulate LH release (Gutiérrez-pascual *et al.*, 2007) and this might indicate that MC₃ is indirectly influencing LH release through interacting with kisspeptin in the gonadotrophs.

The expression of MC₃ in both gonadotrophs and somatotrophs adds further evidence to the interactions between the two cell types since it may act to coordinate the activity of these two cell types. A feedback circuit has been reported in fish by (Zhou *et al.*, 2004). In addition to being stimulated in an autocrine fashion, GH synthesis was found to be also mediated by LH or (HCG) in fish pituitary cells preparations; and the effect was dose-dependent. Growth hormone, in turn, was found to reduce the basal concentrations of LH even though GH was found to stimulate the β-subunit expression (Zhou *et al.*, 2004). The feedback loop between the two cell types could be mediated by MC₃ expressed in either or both cells. This is suggested because MC₃ regulates gonadotropin release from the gonadotrophs and, through GHSR1-a dimerisation, is likely to moderate GH secretion.

The RNAscope® duplex results indicated the co-expression of MC₃ and MRAP2 (the latter was also detected by RT-qPCR studies conducted in this research) in some cells of the anterior pituitary, and to a lower level in the intermediate lobe. The double expression was higher in older mice (10 weeks old) by about 6% compared to the pre-weaned 2 weeks old mice. Even though the single RNAscope® studies indicated the upregulation of both genes in pregnancy, the co-expression of the MC₃ and MRAP2 was reduced in pregnancy by about 17% compared to 10 weeks old mice. However this reduction was not significant. The downregulation of the double expression during pregnancy could be attributed to the fact that MRAP2 is associated with regulating other melanocortin receptors, as well as, non-melanocortin receptors such as GHSR1-a and prokineticin receptor-1 (Sebag and Hinkle, 2009; Srisai *et al.*, 2017; Chaly *et al.*,

2016 respectively). These findings might indicate MRAP2 role during pregnancy is in favour of other GPCR in the pituitary gland.

The wide expression of *MRAP2* seen in the pituitary is similar to that seen in the female mouse hypothalamus data from the previous chapter. These findings also agree with the emerging evidence of *MRAP2* expression in the pituitary and the hypothalamus (Novoselova *et al.*, 2016). *MRAP2* was found to regulate *MC₃* and *MC₄* responsiveness to the melanocortin peptides as reported in the *in vitro* studies with *MC₃* in the current research (see chapter 8 for data Figures) and also, in recent studies (Sebag *et al.*, 2013; Zhang *et al.*, 2017).

MRAP2 expression increased with age as the 10 weeks old mice had significantly higher expression (p value= 0.024) than the pre-weaned 2 weeks old mice by about 65%. Pregnancy caused only a 10% upregulation of *MRAP2* compared to the 10 weeks old virgin mice. The expression of *MRAP2* was the highest in adult and pregnant animals when compared to both *MC₃*. Similar to *MC₃* co-expression studies, the RNAscope® duplex assays using the *GH* and *LHβ* were also conducted with *MRAP2*, and had shown *MRAP2* to be localised in somatotrophs and gonadotrophs.

Although quantifying *MC₃* or *MRAP2* co-expression with either *LHβ* or *GH* was not possible, it was apparent that the number of both *LHβ* and *GH* expressing cells in the RNAscope® data were reduced during pregnancy. These findings are consistent with previous studies which have reported a decrease of both gonadotrophs and somatotrophs in pregnancy (Molitch, 2000). The decrease in the somatotrophs could be attributed to their transdifferentiation to assist in producing prolactin which is significantly increased during pregnancy (Stefaneanu *et al.*, 1992). The RNAscope® studies of the single gene expression of *MC₃* and *MRAP2* had shown increased expression of both during pregnancy. Considering the RNAscope® single and duplex assays finding and findings by (Stefaneanu *et al.*, 1992), *MC₃* and *MRAP2* increased expression could be attributed to the increased lactotrophs in the pituitary during pregnancy. Using a prolactin marker for the *in situ* studies together with *MC₃* and *MRAP2* would confirm this hypothesis.

In the present research, we confirm characterisation of *MC₄* in the pituitary gland; although there was no difference in differential expression in relation to age or pregnancy. Previous studies have included a phenotypic examination of *MC₄^{-/-}* mice,

which have concluded that MC₄, which was detected in the pituitary gland, could be affecting the LH release and pulse frequency. However, the underlying mechanism was unclear but could involve a direct action on the HPG axis (Chen *et al.*, 2017). There are several different mechanisms which would lead to alteration of LH release and pulsatility by MC₄, either at the level of the hypothalamus or the pituitary. Stimulation of LH release by activated MC₄ could occur through the postsynaptic stimulation of GnRH, which in turn stimulates LH release, by α -MSH-activation MC₄ in the hypothalamus. In the pituitary, MC₄ could be modulating LH release through a paracrine mechanism, this is supported by the evidence of α -MSH production by the intermediate lobe of the pituitary gland (Bicknell, 2008) which might be activating MC₄ expressed on the cell surface of anterior pituitary cells (Chen *et al.*, 2017).

Our finding that MC₅ is expressed in the pituitary gland confirms the widespread expression of MC₅ in the central and peripheral tissues (Labbé *et al.*, 1994; Boston and Cone, 1996; Chhajlani, 1996). The RNAscope[®] single gene detection assays had shown that MC₅ also to be expressed in C57BL/6 female mouse pituitary gland. The expression of MC₅ was found significantly higher (p value= 0.0434) in pre-weaned animals (2 weeks old mice) compared to 10 weeks old mice and pregnancy was shown to upregulate MC₅ expressions to levels similar to that seen in the pre-weaned animals. Our identification of MC₅ expression in the pituitary gland increases the possibility of heterodimerization between the melanocortin receptors (Kobayashi *et al.*, 2016). MC₅ were thought to be involved in stimulating the GH3 cells as it was detected expressed in these cells (Langouche *et al.*, 2001). However, this role could not be confirmed as using MC₅ agonist (SHU9119) did not have any effect on the cells. Therefore, MC₅ exact role in the pituitary gland is yet to be investigated. MC₃, MC₅ and MRAP2 were also detected in lower levels in the intermediate lobe of the female mouse pituitary gland (see appendix 4 for Figures).

POMC showed the highest expression of all the members of the melanocortin system in the pituitary gland and was found to have constant expression unaffected by age or pregnancy. Since both anterior and intermediate lobes of the pituitary were included in the samples used for RNA preparation, it is unclear whether reciprocal changes in corticotrophs and melanotrophs may mask any changes in these cell types. In their study, Nelson *et al.* (1988) had shown a fluctuation in the expression of POMC in the mouse pituitary gland. There was a two-fold increase in the concentration of POMC

RNA in old mice (31 months old) compared to young (7 month) and middle aged (15 month) mice. However, Nelson *et al* had attributed this increase as proportionate loss of prolactin and GH mRNA which was found to be reduced significantly in older animals (as reviewed by (Nelson *et al.*, 1988).

Also, the high expression of POMC in the current research study is expected due to a high demand for ACTH release from the pituitary, as well as the other peptides deriving from POMC with varying physiological functions such as modulating pain, stress, appetite and memory (Millington *et al.*, 2001).

We also found AgRP expression in the pituitary gland. Takeuchi *et al.*, 2000 found AgRP was widely distributed in chicken's peripheral tissues (Takeuchi *et al.*, 2000) and our studies extend these findings to the pituitary gland of the mouse. This suggests that AgRP may have a role in the regulation of the peripheral melanocortin receptors as previously suggested by (Takeuchi *et al.*, 2000). However, AgRP analogue (AgRP⁸³⁻¹³²) was found to stimulate prolactin production by the GH3 cells (Langouche *et al.*, 2004). AgRP⁸³⁻¹³² was found to act as an inverse agonist on hMC₃ and hMC₄ (Nijenhuis, 2001). Based on these findings, AgRP might be mediating a role in the pituitary gland through MC₃.

MRAP 1 was also detected in the pituitary suggesting that that they may have a role as accessory proteins to the melanocortin receptors, similar to that described in the adrenal gland (Novoselova *et al.*, 2013). Even though MC₂ was not detected in the pituitary gland, MRAP1 is thought to have an inhibitory role on the other melanocortin receptors as shown by the studies of (Chan *et al.*, 2009).

The expression of MC₅ in the pituitary gland was found to be higher in pre-weaned mice which might indicate a developmental role for MC₅ in these animals as suggested by (Nimura *et al.*, 2006). MC₅, is expressed in the pituitary gland of goldfish and it, was found to be responsive to MTII (pan MCs agonist) and HS014 (a selective MC₄ antagonist) (Cerdeira-Reverter *et al.*, 2003). These findings might indicate that the MC₃ and MC₄ roles in regulating *LHβ* and *FSHβ* gene expression could also be mediated by MC₅.

MC₅ expression decreased from neonatal animals through to adults but was found to be high again in pregnancy, this pattern was also observed with MC₃ and MRAP2.

This might indicate increased demand of the pituitary function(s) mediated by the melanocortin system during pregnancy that have yet to be identified.

As mentioned in section 5.1, a range of paracrine activities have been described in the different pituitary cell types which may have important regulatory functions. Paracrine factors from gonadotrophs have been shown to stimulate prolactin release from lactotrophs following GnRH stimulation of male rat pituitary cells aggregates; whilst GnRH treatment in preparation from adult animals that did not have an effect on prolactin release (Denef and Andries, 1983). The GnRH by itself was not able to stimulate prolactin release, which indicates that other gonadotroph regulatory components are needed for the GnRH to stimulate the lactotrophs. The expression of MC_3 in both lactotrophs and gonadotrophs may mediate coordinated cell activity.

Therefore, MC_3 activity on prolactin release might be mediated through different mechanisms: 1) The autocrine mechanism as MC_3 was detected on lactotrophs (Matsumura *et al.*, 2004). 2) The paracrine mechanism through the activation of gonadotrophs and these cells, in turn, stimulate prolactin release by the lactotrophs (based on the current RNAscope[®] findings). 3) The heterodimerisation of MC_3 with other GPCR such as kisspeptin which was found to stimulate prolactin release in cows pituitary cells (Kadokawa *et al.*, 2008). Other possible GPCR candidates for heterodimerisation with MC_3 that need to be investigated are dopamine receptors. Dopamine is a known regulator of prolactin production and secretion (Shin *et al.*, 2010) and dopamine 2 receptor (D2) was found expressed in the pituitary corticotrophs (Pivonello *et al.*, 2004) and prolactin-secreting adenomas (De Camilli *et al.*, 1979).

The current research findings in the pituitary gland add more elements to the complexity of the intra- communications that are associated with the regulation of the anterior pituitary gland hormonal function. The involvement of the melanocortin system in regulation of the anterior pituitary gland has just started to be revealed. The current research managed to detect MC_3 and $MRAP2$ in the gonadotrophs and the somatotrophs. Due to lack of resources, MC_5 could not be included in the RNAscope[®] duplex assays although it might have provided insight into a potential role of MC_5 in pituitary gland function.

Additionally, members of the melanocortin system detected in the RT-qPCR studies of this research confirm previous reports of MC_4 expression in the pituitary and might

have identified new roles for MC members in the pituitary gland. Furthermore, examining other anterior pituitary cell types for the expression of *MC₃* and *MRAP2* with the RNAscope[®] duplex assays could have identified possible regulatory mechanisms through which both candidates might be mediating their anterior pituitary role. However, because of the time and financial limitations, these targets could not be included in the current research.

The following chapters will analyse the MC expression in the ovary and the uterus in an attempt to explore the role of this system in female mouse fertility.

6 Molecular and cellular characterisation of the MC system in the female mouse ovary

6.1 Background

The pituitary gland secretes the gonadotropins (LH and FSH) which are then transported via the circulation to their primary target in the female, the ovary. The main functions of the ovary are 1) oogenesis (oocyte growth and development), 2) folliculogenesis (follicular growth and development) and 3) steroidogenesis (steroid hormone synthesis). The development of mouse ovaries occurs at embryonic stages but is completed after birth. The developing ovary is made of female germ cells surrounded by somatic cells, both of which have different origins. The mouse ovariogenesis is composed of oogenesis accompanied by the growth of the somatic cells into follicular cells. This chapter will briefly describe the processes of mouse oogenesis and folliculogenesis. It will also briefly discuss the ovarian cycle and some of the regulatory - endocrine, paracrine and autocrine pathways of the ovarian cycle. Finally, a description of what is known to date about the roles of the melanocortin system in the mouse ovary will be given.

6. 1. 1 Murine Oogenesis

Oogenesis is the process of development and maturation of female germ cells (aka gametes). The primordial germ cells are first detected on embryonic day 7 and they migrate to the developing urogenital ridge by embryonic day 10. The oogonia undergo mitotic activity to make the primordial germ cells that last the entire reproductive life of the animal, and this mitotic activity is completed by embryonic day 15 (Peters, 1969). The primordial germ cells (primary oocytes) all enter meiosis I (starting on embryonic day 13.5) but become arrested in late prophase I until ovulation (Amleh and Dean, 2002). The oocytes (diameter is about 20 μm) are found in clusters (forming germ cells nests) in the cortical tissue of the ovary with some oocytes surrounded by a single layer of epithelial cells called the pre-granulosa cells (primordial follicle), whereas other oocytes are freely touching. By the end of the 7th day after birth, all oocytes are surrounded by pre-granulosa cells (Peters, 1969). By the end of the postnatal period, the ovary is full of primordial follicles and growing follicles. Shortly before ovulation, which is also before the differentiation of the follicles to the mature antral (Graafian) follicles, the oocytes undergo maturation growing to mature morphology (reaching 70 μm in diameter). The LH surge triggers meiosis in oocytes destined for ovulation. Meiosis is again arrested in the metaphase of meiosis II and will only be completed

when a spermatozoon enters the oocyte. Similar to the meiotic events, folliculogenesis is all but complete by ovulation (Wassarman and Josefowicz, 1978).

The process of oogenesis is controlled by different molecular, hormonal autocrine and paracrine elements. Describing each element regulating the different stages of oogenesis is beyond the focus of the research; so for a detailed description see the review by Sánchez and Smitz, (2012). Oocyte maturation from oogonia to primary oocytes ready for ovulation is accompanied by differentiation of the follicular cell layers in a process called folliculogenesis.

6. 1. 2 Folliculogenesis

Folliculogenesis is the name of the process involving the growth and development of the ovarian follicle. There are different types of ovarian follicles based on their stage of development (Barnett *et al.*, 2006):

Primordial follicles: the oocyte is surrounded by 3 to 4 squamous epithelial pre-granulosa cells. The oocyte is about 20 µm in diameter. These follicles are considered quiescent.

Primary follicles: when a primordial follicle starts to grow, the pre-granulosa cells become cuboidal in shape and increase in number to form a single layer surrounding the oocyte. The oocyte also starts to increase in diameter. Primary follicles start to appear by postnatal day (PND) 3.

Pre-antral follicles: these are made of multiple layers of granulosa cells and the surrounding stromal cells differentiate to form the theca interna and theca externa cell layers. The oocyte reaches maximum growth (70 µm in diameter) with the surrounding cells producing interstitial follicular (antral) fluid.

Antral follicles: at this stage, the follicles attain its greatest increase in diameter due to the accumulation of antral fluid. Once the follicle reaches maximal growth, it becomes responsive to FSH. These follicles can synthesise and release androgens, as a result of the action of LH on thecal cells, and estrogen, aromatisation of androgen to estrogen in granulosa cells influenced by FSH.

The increased production of estrogen stimulates the hypothalamic-pituitary LH surge leading to ovulation of 10- 20 oocytes, whilst most of the other antral follicles

degenerate (Rajkovic *et al.*, 2006). Although ovarian folliculogenesis is mainly mediated by FSH, there are other regulators of the different stages of folliculogenesis. One of these mechanisms includes the paracrine interaction between the growing oocytes and the follicular granulosa cells. This interaction was found to involve different elements such as the tyrosine kinase receptor, Kit and its ligand (KitL) which have been shown to be essential for follicular growth and oocyte maturation (Thomas and Vanderhyden, 2006). Other factors controlling follicular and oocyte maturation include regulatory genes, such as the factor in the germline alpha (FIGLA) and the newborn ovary Homeobox gene (Nobox). Both factors are oocyte-specific factors; hormones such anti-Mullerian hormone (which is thought to regulate primordial follicles numbers postnatally: (Durlinger *et al.*, 1999); growth factors including insulin-like growth factor-I (IGF-I) and transforming growth factor beta 1 (TGF- β 1); and hormones such as estrogen and progesterone. The details of the functions of these elements are further reviewed by (Rajkovic *et al.*, 2006; Sánchez and Smitz, 2012).

6. 1. 3 Ovulation

Ovulation is the process by which the mature oocyte is released from the ovary into the oviduct. Ovulation occurs approximately 10 hours after the beginning of estrus in rodents. This is preceded by an increased FSH concentration in the circulation during proestrus. The high FSH concentration stimulates the recruitment of some of the antral follicles which continue to undergo final maturation. The LH surge enables the oocytes to recommence meiosis whilst other antral follicles undergo atresia.

The growing follicles secrete more estrogen, that influences the pituitary positively, leading to an LH surge (McGee and Hsueh, 2000). However, under an unknown mechanism, about 10- 20 follicles are selected for ovulation in mice, but one selected follicle produces a variety of factors which have an autocrine effect leading to increased sensitivity to FSH. This dominant follicle is also thought to produce degenerative factors acting in a paracrine fashion on the unselected follicles (McGee and Hsueh, 2000). The mural, granulosa and theca cells also contribute to the ovulatory process. This was proposed based on data reporting the expression of LH-receptors in the mural granulosa cells of the preovulatory follicles while the cumulus granulosa cells require FSH to increase their sensitivity to LH (Russell and Robker, 2007). Activation of the LH mediated signalling pathways in both groups of cells leads

to a reduction in the gap junctions between the two layers causing the separation of the cumulus-oocyte complex (COC) from the follicular mural layer making them float in the antral fluid, in addition there is upregulation of transcriptional genes regulating the oocyte meiosis, thus, enabling oocyte maturation (Russell and Robker, 2007).

The ovulatory process includes mediating an acute local inflammatory response that consists of increased vascular permeability leading to follicular protein efflux and infiltration of leukocytes, mainly macrophages. The leukocytes secrete different cytokines, interleukins, proteolytic enzymes all of which are downstream of progesterone receptors (PR) and LH. These inflammatory elements contribute to the local disintegration of the ovarian surface epithelium through which the destined follicle will rupture (Kim *et al.*, 2009). Some of these cytokine receptors were found expressed in the granulosa and theca cells of rat and mouse ovarian follicles. These include TNF- α , interferons (INFs) and IL-1 β which were thought to participate in the remodelling of the follicle before ovulation through the production of proteolytic enzymes that assist in the follicular wall disintegration (Machelon and Emilie, 1997).

6. 1. 4 Ovarian luteinisation and luteolysis

After the release of the oocyte, luteinisation of the residual follicular tissues occurs through the differentiation of follicular cells, tissue remodelling and changes in the composition of the extracellular matrix: all these changes lead to the formation of the corpus luteum (Stocco *et al.*, 2007). Vascular remodelling was also found to be part of the luteinisation process, and this is established through the production of angiogenic cytokines, such as vascular endothelial growth factor (VEGF) and TGF- β 1 (Machelon and Emilie, 1997). The luteinisation process is regulated by different molecular factors which are involved also in the regulation of the expression of LH, FSH, P₄ and prolactin receptors and the signalling pathways downstream of these receptors (Stocco *et al.*, 2007). Rodents have different types of corpora lutea (CL), these are:

1. CL of the cycle: these are formed as a result of luteinisation of the ovulating follicles under the effect of the preovulatory LH surge. This type of corpora lutea lasts for about 14 days with the maximum size reached at estrus of the following cycle. Within an ovary the CLs are therefore of 3 different ages reflecting the ovulations of the previous 3 estrous cycles (Greenwald and Rothchild, 1968).

2. CL of pseudopregnancy: if cervical stimulation occurs at estrus, biphasic release of prolactin from the pituitary gland results and the prolactin acts on the CL to induce progesterone synthesis for up to 12 days.
3. CL of pregnancy: this type of CL is a continuation of the CL of pseudopregnancy which increases in size reaching maximal growth on day 13 and progesterone production by this type of CL continues until day 16 (Greenwald and Rothchild, 1968).
4. CL of lactation: in other species the corpus luteum regresses after parturition. However, in rodents, prolactin, which increases as a result of pup suckling, is thought to regulate the maintenance of the corpus luteum which is now called the corpus luteum of lactation and it lasts up to 4 weeks in rodents.

Granulosa and theca cells differentiate into large lutein and small lutein cells respectively; this is accompanied by the upregulation of enzymes involved in the synthesis of progesterone, such as cytochrome *P-450* and 3β -hydroxysteroid hydrogenase (*3\beta-HSD*), and downregulation of enzymes associated with estrogen and androgen release (Niswender *et al.*, 2000). The mechanisms involved in the formation of the corpora lutea, their maintenance and luteal steroidogenic activity are further reviewed by (Bachelot and Binart, 2005).

At the end of the lifespan of the corpus luteum, the regression of the corpus luteum, luteolysis, occurs in two stages: functional luteolysis and structural luteolysis. Functional luteolysis occurs before structural luteolysis and is characterised by a decline in progesterone concentration. The lowered progesterone concentration is thought to be mediated mainly by prostaglandin $F2\alpha$ ($PGF2\alpha$) and the activation of the protein kinase C cascade (Bachelot and Binart, 2005). Apoptosis was found to be the main cause of structural luteolysis as reported by (Morales, 2000) in the human corpus luteum. Luteal apoptosis is mediated by different cytokines such as $INF\gamma$ and $TNF-\alpha$, Fas and Fas-ligand and caspase-3; this was found to be mediated by the prolactin surge that occurs concomitantly with LH surge (Sugino and Okuda, 2007).

6. 1. 5 Implication of the MC system in the functions of the mouse ovary

Although the melanocortin system is mediating different functions in different organs, little is known about its expression or function in the mouse ovary. The expression of melanocortin receptors in the ovaries of species other than mice have been reported (Amweg *et al.*, 2011; Guelfi *et al.*, 2011). The expression of the melanocortin receptors was thought to mediate the estradiol and testosterone concentrations via ACTH in follicles of different stages and also the corpora lutea and therefore suggested an ovarian steroidogenic and luteal role by melanocortin receptors. The melanocortin system could also be contributing to the different immunomodulatory events that are part of the follicular tissue remodelling during folliculogenesis, luteinisation and luteolysis. There are data, albeit in non-reproductive tissues, reporting a modulating action of the melanocortin peptides and receptors on different cytokines; such as, TNF- α and IL-1 β by (Catania *et al.*, 2004; Getting, 2006; Kaneva *et al.*, 2012). Therefore, the aims of studies described in this chapter are to:

1. Determine suitable reference genes in the mouse ovary for normalisation using GeNorm expression stability analysis.
2. Characterise *MC*₍₁₋₅₎, *MRAP1* and *MRAP2*, *POMC* (full-length gene and the truncated gene) and *AgRP* in the ovary of different aged mice (2, 6, 10 and 14 weeks old).
3. Compare the expression of the genes listed above in pregnant and non-pregnant mice.
4. To evaluate the cellular expression of *MC*₃, *MC*₅ and *MRAP2* expression using chromogenic *in situ* hybridisation (RNAscope[®]).

6. 2 Methods

For a detailed account of the materials and techniques used see chapter 3.

6. 2. 1 Determining suitable reference genes in the uterus

The most stable reference genes in the ovary were selected using the GeNorm analysis described in detail in section 3. 2. 3. 4. 1. Duplicates of cDNA samples from each age group were used in this analysis.

6. 2. 2 Characterising the gene expression of the MC system

These reference genes were used to normalise data obtained from the RT-qPCR assays of the reverse transcribed RNA extracted from whole ovaries of female C57BL/6 mice aged 2, 6, 9, 10, 14 weeks and pregnant mice (14 ± 1 day *post-coitus*, dpc) (all n=5; except n=3 for 9 weeks and n=4 for 10 weeks). The efficiencies of the primers used in these assays were examined using standard curves with positive controls for each primer pair (see section 3. 2. 3. 4. 3 in methods for details). The RT-qPCR amplification products were then separated on 2% agarose gel to check the size of the band and verify they were of the predicted size, and to check for non-specific bands.

The RT-qPCR data collected were analysed using the delta-delta CT method mentioned in section 3. 2. 3. 4. 3. C in methods.

6. 2. 3 RNAscope® 2.5HD protocol

The ovarian sections were collected from female C57BL/6 mice aged 2 weeks, 10 weeks and pregnant (14 ± 1 dpc). The tissues were prepared and cut in cross-sections. The studies included using RNAscope® 2.5HD single-plex (brown) staining kit with *MC₃*, *MC₅* and *MRAP2* as well as positive and negative controls. Based on the results from the single-plex studies, the duplex studies were not included for the ovary.

6. 3 Results

6. 3. 1 Reference gene stability in the female mouse ovary

In the female C57BL/6 mouse ovary, ATP synthase subunit beta (*ATP5B*) and Glyceraldehyde 3-phosphate dehydrogenase (*GAPDH*) were the most stable genes whereas Beta-2-Microglobulin (*B2M*) and Eukaryotic Translation Initiation Factor 4A2 (*EIF4A2*) were the least stable genes (Figure 6.1).

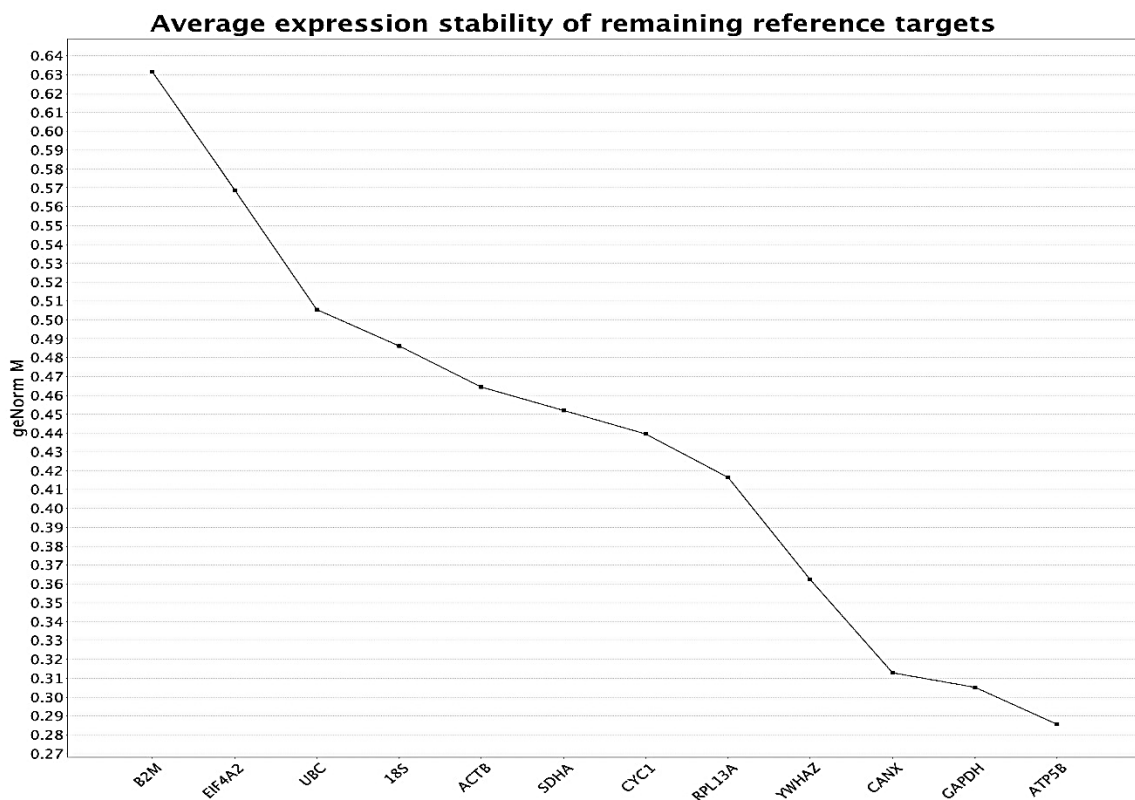


Figure 6.1: GeNorm ranking order of reference genes stability in the female mouse ovary. The ranking is based on calculating the geometric mean of the ranking values from Delta CT, BestKeeper, Normfinder and GeNorm reference gene analyses tools. The stability of 12 reference genes was examined using the ovaries of female mice aged 2, 6, 9, 10, 14 weeks, and pregnant mice (14+1 dpc). The samples were run in duplicates. The reference genes are 18S, ACTB, ATP5B, B2M, CANX, CYC1, EIF4A2, GAPDH, RPL13A, SDHA, UBC and YWHAZ. CT values were imported to the qBase+ software and analysed using GeNorm (Biogazelle, Belgium).

The Optimal number of housekeeping genes to be used in normalising the RT-qPCR data was two for the female mouse ovary. This was obtained by calculating the pairwise variation (V-score) with the sequential addition of each reference gene one at a time. A V-score above 0.15 indicates the optimal number of most stable reference

genes to be used (Figure 6.2). The V-score was calculated using GeNorm analysis by qBase+ software (Biogazelle, Belgium). See appendix 3. C for graphs of the BestKeeper, Normfinder, Delta CT and comprehensive reference genes stability analyses.

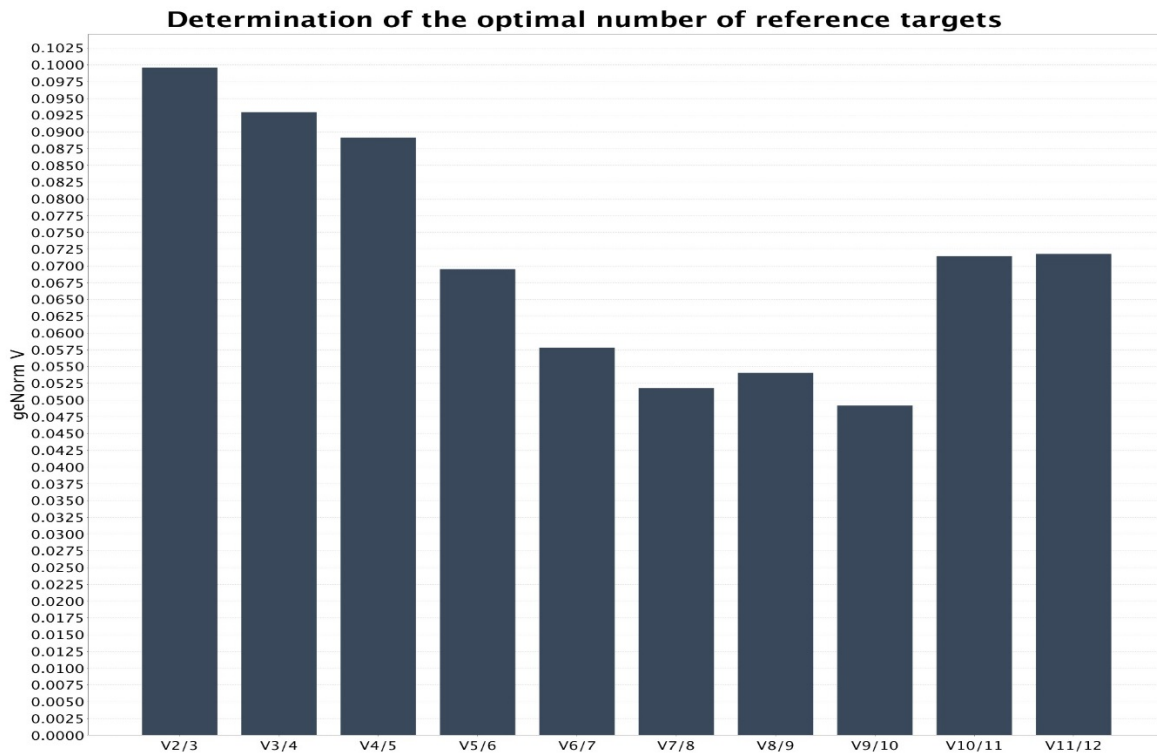


Figure 6.2: Variation score (V- score) by GeNorm. An optimal number of stable genes used normalisation was calculated by pairwise variation with the addition of each reference gene one at a time. A V-score equal or below 0.15 indicated the insignificance of using more reference genes. In this graph, 10 reference genes V-score results indicates the optimal number of most stable HKG to be used in the ovary are three (GeNorm by qBase+, Biogazelle, Belgium).

6. 3. 1. B Amplification efficiencies of *ATP5B*, *GAPDH* and *YWHAZ*

The amplification efficiency is defined as the doubling of the cDNA template for each RT-qPCR cycle. Table 6.1 lists the standard curve slope (M), the coefficient of determination (R^2) and amplification efficiency (E) of *ATP5B* (100%), *GAPDH* (97%) and *YWHAZ* (100%).

Table 6-1: Amplification efficiency of ACTB, ATP5B and YWHAZ in the female ovary.

Gene	R ² (Coefficient of Determination)	M (Measurement of Efficiency)	E (Efficiency)
<i>ATP5B</i>	0.99	-3.32	100%
<i>GAPDH</i>	0.99	-3.38	97%
<i>YWHAZ</i>	0.99	-3.32	100%

Pooled cDNA from all samples used in MC system expression in the ovary was used in generating 1:2 standard curves. The efficiency was calculated automatically using the Rotor-Gene Q software (Qiagen, UK).

6. 3. 2 MC system expression

The RT-qPCR analysis of the C57BL/6 mouse ovary showed *MC₂*, *MC₄*, *MC₅*, *MRAP1*, *MRAP2*, *POMC* (truncated gene) and *AgRP* were all detected. *MC₁*, *MC₃* and full-length *POMC* were not expressed in the female mouse ovary. The expression of the mRNA for these targets is not the same between the MC system members. Compared to the hypothalamus and the pituitary gland, the expression of all detected members was found at low levels.

The expression of *MC₂* (Figure 6. 3. A), although low, appeared to be higher in pre-weaned mice (2 weeks old) compared to 6 weeks old mice. Expression increased again at 9 weeks old before decreasing again in older mice (10 and 14 weeks old). However, age did not have a substantial effect on *MC₂* expression. Pregnancy caused a significant decrease in the expression of *MC₂* compared to the non-pregnant animals (p- value= 0.017) and non-pregnant animals of the same age. The expression of *MC₄* was similar at all ages and there were no significant age influences on expression. Melanocortin 4 receptor was not detected in pregnant animals (Figure 6. 3. B). Apart from being higher in 2 weeks old mice, *MC₅* expression showed no change in 6, 9, 10,

14 weeks old mice and pregnant mice. There were no age or pregnancy effects on ovarian expression of *MC₅* (Figure 6. 3. C).

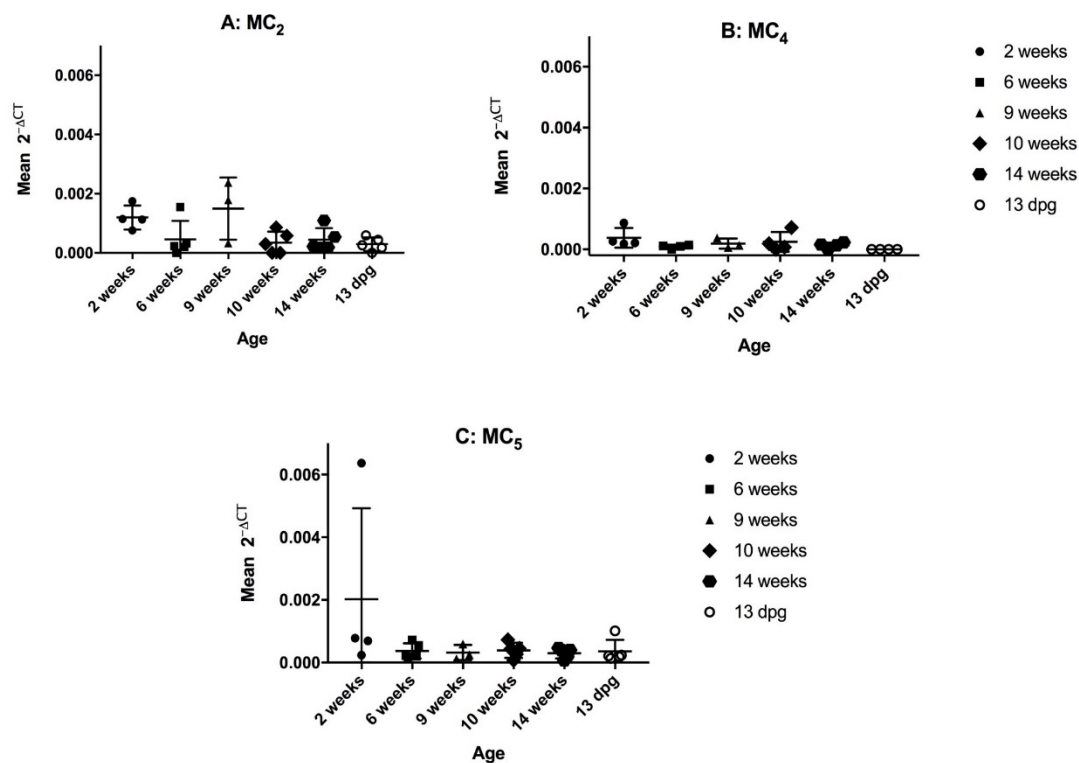


Figure 6.3: *MC₂*, *MC₄* and *MC₅* expression in the female mouse ovary. Ovarian cDNA duplicates from female C57BL/6 mice aged 2, 6, 9, 10 and 14 weeks and pregnant mice (14 +1 DPC) (n=3-5) were used in the RT-qPCR studies. A: *MC₂*; B: *MC₄* and C: *MC₅*. The CT values of each assay were exported to excel worksheet, analysed using the delta CT Method developed by Pfaffl (2001). The skewed data seen in the graphs are due to animal sample variations (old vs. newly obtained samples). The $2^{-\Delta CT}$ values were imported to GraphPad and analyses using one-way analysis of variance (ANOVA). (Prism 7, USA).

Even though age and pregnancy did not alter the expression significantly, *MRAP1* expression appeared to increase between the 6 weeks old mice and the pre-weaned animals (2 weeks old); and was lower in 9 weeks old compared to older animals (10 and 14 weeks old). Pregnant animals had higher *MRAP1* expression compared to the non-pregnant animals of the same age. (Figure 6. 4. A). Interestingly, the expression of *MRAP2* followed a similar pattern of *MC₅* with a low *MRAP2* expression in all ages and pregnant mice compared to 2 weeks old mice. Both age and pregnancy did not have any influence on *MRAP2* expression (Figure 6. 4. B).

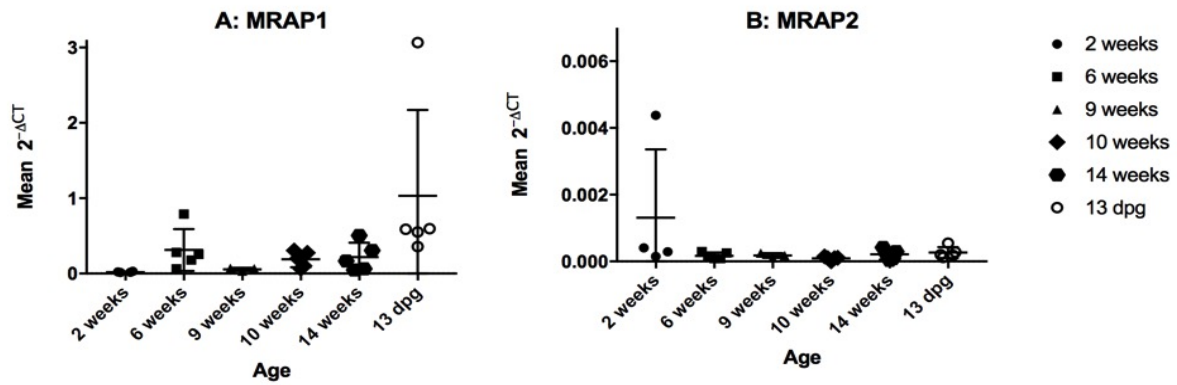


Figure 6.4: MRAP1 and MRAP2 expression in the female mouse ovary. Ovarian cDNA duplicates from female C57BL/6 mice aged 2, 6, 9, 10 and 14 weeks and pregnant mice (14 +1 DPC) (n=3-5) were used in the RT-qPCR studies. A: MRAP1 and B: MRAP2. The CT values of each assay were exported to excel worksheet, analysed using the delta CT Method developed by Pfaffl (2001). The skewed data seen in the graphs are due to animal sample variations (old vs. newly obtained samples). The 2^{-ΔCT} values were imported to GraphPad and analyses using one-way analysis of variance (ANOVA). (Prism 7, USA).

Although full-length *POMC* transcript was absent, 5'-truncated *POMC* gene transcript was detected in the ovary. The expression of *POMC* (5'-truncated gene transcript) appeared to decrease gradually. Younger animals (2 weeks old) mice had higher expression than older animals. Expression of *POMC* was not different between pregnant and non-pregnant animals of the same age (Figure 6. 5. A). *AgRP* expression did not show any alterations between the different ages and pregnant animals (Figure 6. 5. B). A summary of *MC* (1-5), *MRAP1*, *MRAP2*, *POMC* (5'- truncated transcript) and *AgRP* expression in the female mouse ovary is presented in Table 6.2.

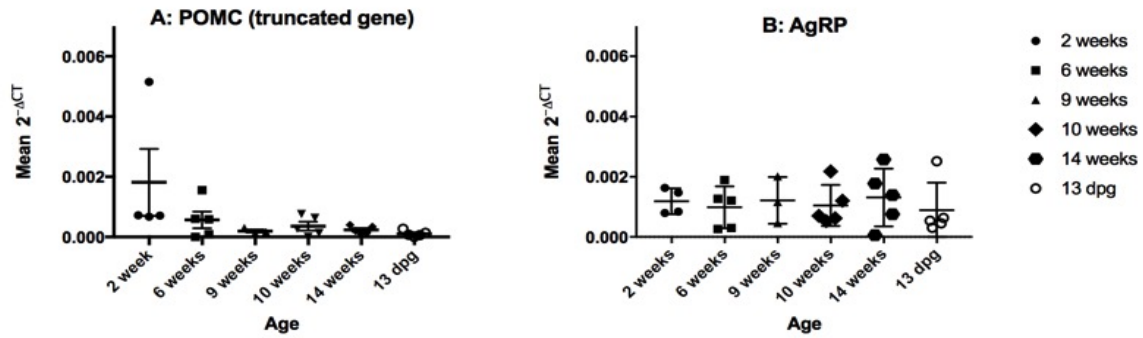


Figure 6.5: POMC (truncated transcript) and AgRP expression in the female mouse ovary. Ovarian cDNA duplicates from female C57BL/6 mice aged 2, 6, 9, 10 and 14 weeks and pregnant mice (14 +1 DPC) (n=3-5) were used in the RT-qPCR studies. A: POMC and B: AgRP. The CT values of each assay were exported to excel worksheet, analysed using the delta CT Method developed by Pfaffli (2001). The skewed data seen in the graphs are due to animal sample variations (old vs. newly obtained samples). The $2^{-\Delta CT}$ values were imported to GraphPad and analyses using one-way analysis of variance (ANOVA). (Prism 7, USA).

Table 6-2: MC system expression in the mouse ovary.

Ovary (n:3-5)				
Gene	Expression	P value	Significance of Age	Significance of Pregnancy
MC ₁	-	N/A	N/A	N/A
MC ₂	+	0.02	-	+
MC ₃	-	N/A	N/A	N/A
MC ₄	+	0.20	-	-
MC ₅	+	0.23	-	-
POMC (FULL)	-	N/A	N/A	NA
POMC (Trunc.)	+	0.11	-	-
AgRP	+	0.96	-	-
MRAP1	+	0.07	-	-
MRAP2	+	0.26	-	-

The table represents each gene examined in ovarian cDNA duplicates of 3-4 C57BL/6 mice. Age and pregnancy effects were examined by using animals aged 2, 6, 9, 10 and 14 weeks old mice and pregnant (14 +1DPC) mice. MC₂, MC₄, MC₅, MRAP1, MRAP2, POMC (truncated transcript) and AgRP were found in the ovary. Pregnancy had a significant impact on the expression of MC₂ (with a p-value of 0.02). Age did not affect the expression. (+) Indicate the presence of a gene or significant effect by age or pregnancy; (-): indicates the absence of a gene or insignificant effect by age or pregnancy. N/A: not applicable.

6. 3. 3. Validation of the MC system expression

The products of the RT-qPCR of *MC*₍₁₋₅₎, *MRAP1*, *MRAP2*, *5'-truncated POMC*, and *AgRP*, as well as *GAPDH*, *ATP5B* and *YWHAZ* were separated on 2% agarose gel (composition and method described in section 3. 2. 4. 3. 3). The products also contained non-template control for each of the target genes and the reference genes to check for genomic contamination (Figure 6.6).

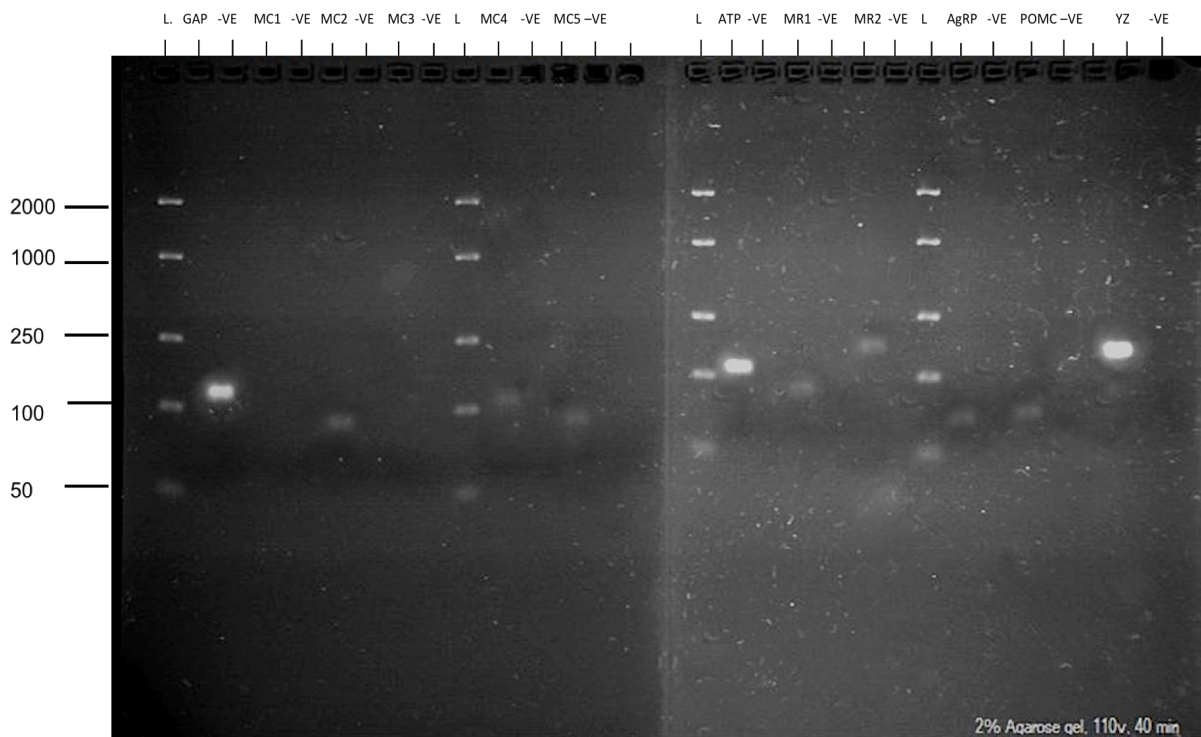


Figure 6.6: Gel electrophoresis of RT-qPCR of MC system in the female mouse ovary. The RT-qPCR products were separated on 2% agarose gel at 110 volts for 40 minutes. Where L = ladder 50 bp to 2000 bp; (ThermoScientific, UK); GD: GAPDH = 127 bp: MC₁, MC₂ = 86 bp, MC₃, MC₄ = 106 bp, MC₅ = 90 bp, ATP: ATP5B = 112 bp; MRAP1 = 86 bp, MRAP2 = 150 bp, AgRP = 63 bp, POMC (truncated gene) = 77 bp, YZ: YWHAZ = 141 bp. -ve: non-template control for gene of interest in previous lane. Gel image was taken using UVIPRO (Uvitec, UK).

6. 3. 3 Localization of *MC₃*, *MC₅* and *MRAP2* mRNA transcripts in the female mouse Ovary

RNAscope® brown expression signal is detected as brown dots which represent mRNA copies of the target gene. These assays included positive (*PPIB*) and negative (*DAPB*) controls to ensure optimised conditions were achieved. Figure 6.7 illustrates the expression and the absence of background staining in sections hybridized with the positive and negative control probes, respectively.

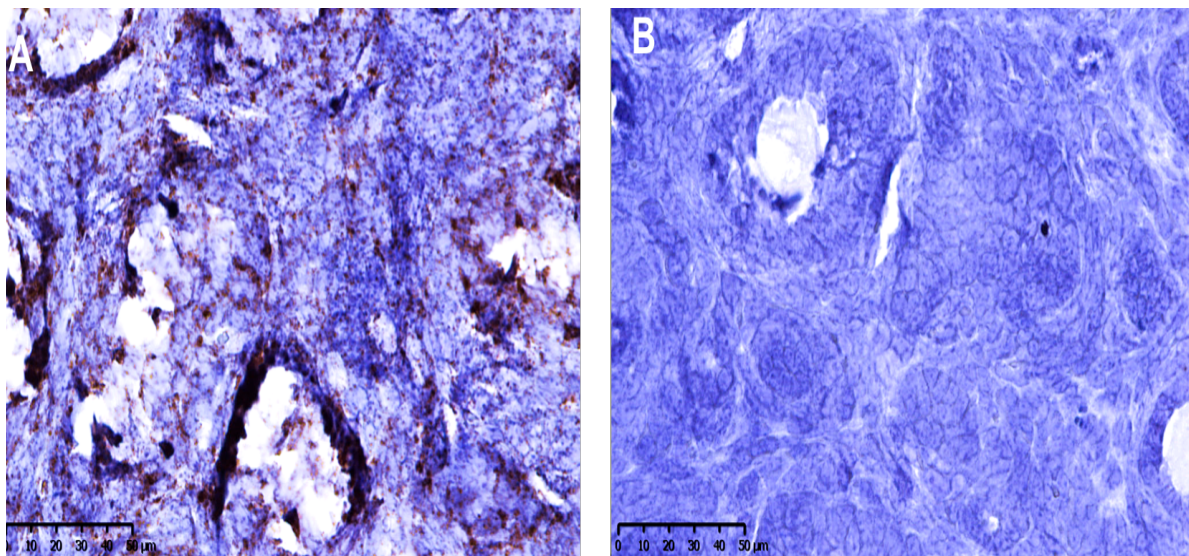


Figure 6.7: RNAscope® 2.5HD single-plex (brown) assay in the female mouse ovary. The assay was carried out in the ovaries of mice aged 2 weeks, 10 weeks and pregnant (14 ± 1) mice. A: The ovarian sections show expression of positive (*PPIB*) control to illustrate how the expression signal as brown dots in cells, counterstained with Haematoxylin (Hx). B: negative (*DAPB*) control in the uterus showing no background staining. Each group was conducted as 4 sections per slide. Images were taken by NanoZoomer slide scanner (Hamamatsu Photonics) at King's College London.

MC₃ is expressed in both ovarian follicles and the interstitial tissues albeit very sparsely (Figure 6. 8. A). These findings contradict the RT-qPCR data. The expression of *MC₅* is very similar to that of *MC₃* (Figure 6. 8. B). Compared to *MC₃* and *MC₅*, *MRAP2* expression was at a lower level but was detected in the same compartments (Figure 6. 8. C).

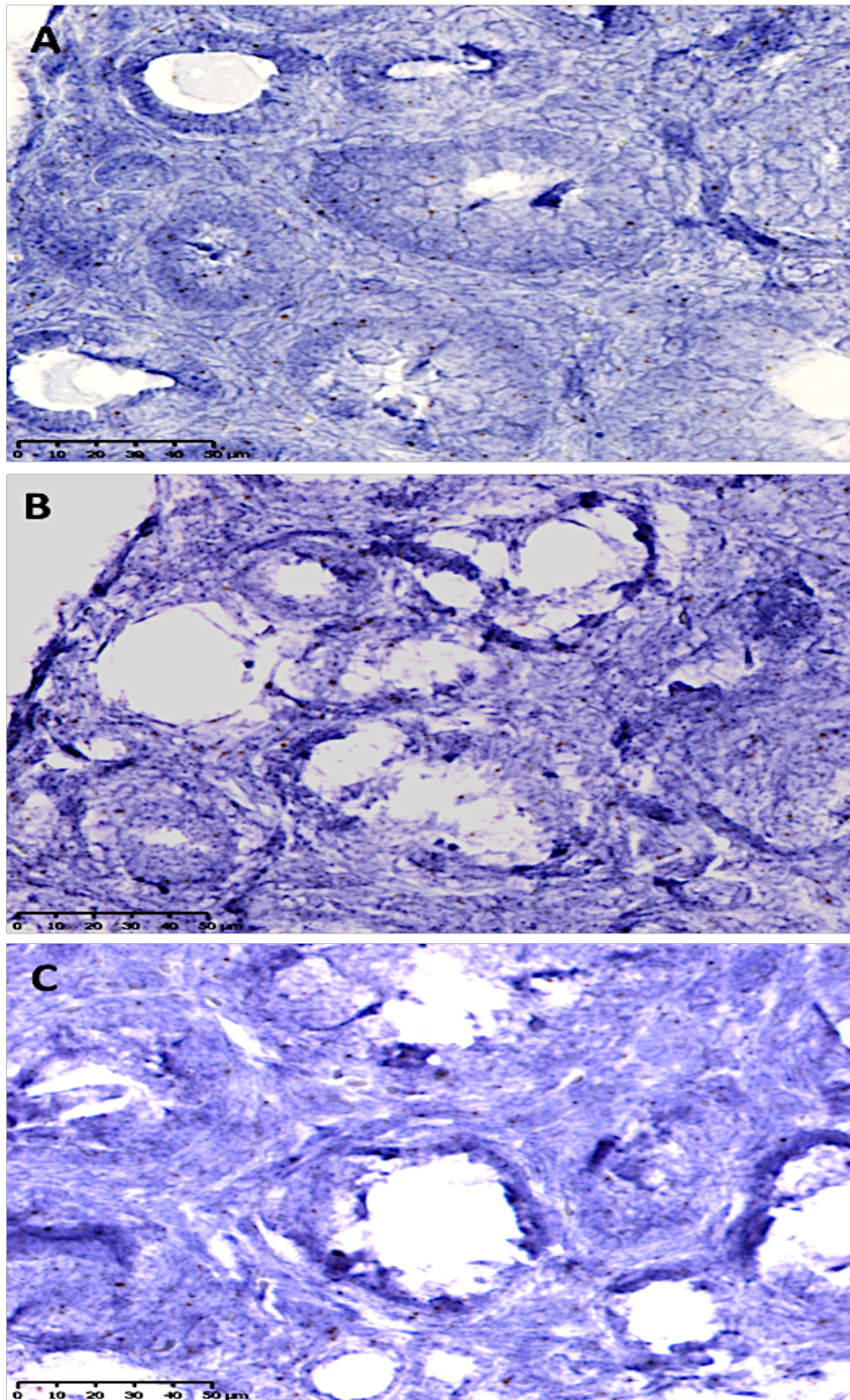


Figure 6.8: RNAscope® 2.5HD single-plex (brown) assay of *MC₃*, *MC₅* and *MRAP2* in the female mouse ovary. The assays were carried out in the ovaries of mice aged 2 weeks, 10 weeks and pregnant (14 ± 1) mice. A: *MC₃* expression in the female mouse ovary. B: *MC₅* expression in the female mouse ovary. C: *MRAP2* expression in the female mouse ovary. Each group was conducted as 4 sections per slide, and the assays were carried out twice. Images were taken by NanoZoomer slide scanner (Hamamatsu Photonics) at King's College London.

6. 4 Discussion

MC₂, *MC₄*, *MC₅*, *MRAP1*, *MRAP2*, *POMC* (5'-truncated gene transcript) and *AgRP* were all detected in the mouse ovary. Even though *MC₃* was not detected in the ovary by RT-qPCR (as well as *MC₁* and full-length *POMC* gene transcript), *MC₃* expression was very sparsely expressed in both the ovarian follicles and the surrounding interstitial tissue as shown by the RNAscope® brown assay. The expression of both *MC₅* and *MRAP2* in the mouse ovary was confirmed by the RNAscope® brown assay and, as for *MC₃*, both *MC₅* and *MRAP2* were expressed sparsely in both the ovarian follicles and the surrounding interstitial tissue. There appeared to be no effect of age on the expression of any of the expressed members of the melanocortin system however, both *MC₂* and *MC₄* ovarian expression were reduced during pregnancy by RT-qPCR.

The GeNorm expression stability analysis found the most suitable reference genes for use in normalising the C57BL/6 female mouse ovary RT-qPCR data were *ATP5B* and *GAPDH*. These two reference genes showed stable expression when examined in the 2, 6, 9, 10 and 14 weeks old mice and pregnant (14 ± 1 dpc) mice. The optimal number needed for normalising RT-qPCR data in the ovary was two. In the ovary, *YWHAZ* was also included in the RT-qPCR data to be consistent with normalisation of the hypothalamus, pituitary gland and uterus RT-qPCR data. The expression stability of *YWHAZ* was ranked fourth in the GeNorm stability analysis of the reference genes in the ovary.

MC₂ was found in the ovary with higher expression in the non-pregnant sexually mature adult mice (9 weeks old) compared to pregnant animals. *MC₂* might directly influence ovarian action through ACTH as the current research findings were comparable with findings reported by (Guelfi *et al.*, 2011) using a rabbit model. Guelfi and colleagues reported a dual action of ACTH on P₄ release from the CL with higher P₄ release in the earlier days of pseudopregnancy (day 4) compared to decreased production at the later stages (day 9). The effect of ACTH was consistent with the pattern of immunostaining for *MC₂* in CL (Guelfi *et al.*, 2011). However, the current research had only examined *MC₂* expression in mid-pregnancy. Examining earlier

stages of pregnancy are, therefore, necessary to determine if MC_2 expression levels during early pregnancy in mice agree with those observed in pseudopregnant rabbits.

The absence of MC_1 and MC_3 from the ovaries contradicts findings by Amweg *et al.*, 2011; this research team had localised both receptors in the bovine corpus luteum of the ovary. However, the use of anti- MC_1 and anti- MC_3 antibodies, as well as anti- MC_5 , were reported to produce non-specific binding in many different studies (Kathpalia *et al.*, 2011; Ahmed, 2014; Dowejko, 2014). The absence of MC_3 could also be due to species differences or due to dilutional effects that resulted from using mRNA extracted from a whole tissue especially since the levels of the other detected receptors are at low levels. The latter explanation is supported by the RNAscope[®] findings in which MC_3 was shown to be expressed in both ovarian follicles and the surrounding interstitial tissues. MC_3 modulates inflammation by regulating the expression of some cytokines, such as IL-1 β and TNF- α , by increasing the expression of the anti-inflammatory cytokine, IL-10 (Patel *et al.*, 2010; Henagan *et al.*, 2011). According to these findings, MC_3 could be contributing to keeping the normal inflammatory process in check and the findings that report the regulation of MC_3 promoter expression by estradiol (Okutsu *et al.*, 2015) support this proposed function.

The ACTH luteal effect mediated by MC_2 could also be mediated by MC_4 which was also found expressed in the ovary in the current research. Although there was no mention of MC_4 expression in the ovary, the study conducted by Sandrock *et al.*, 2009 reported reduced CL numbers in $MC_4^{-/-}$ 6-month old obese mice compared to wild type mice. Although Sandrock and colleagues implied an indirect MC_4 role in the ovary based on the present research findings, the luteal effect could be directly mediated by MC_4 on the CL.

MC_5 was suggested to suppress inflammation in the eye through stimulating the production of different cytokines; an action mediated by α -MSH (Clemson *et al.*, 2017) based on these findings, MC_5 might be involved in regulating the proinflammatory events that are accompanying ovulation, luteinisation and luteolysis. The RNAscope[®] data of the current research study had shown MC_5 to be expressed in the ovarian

follicles and interstitial tissue, a distribution similar to that of MC_3 which might indicate mediating the proposed anti-inflammatory role through forming heterodimers.

Although not significant, *MRAP1* was found to be higher in the pregnant mice compared to the non-pregnant control group. In contrast the pattern of MC_2 expression was found to be higher in non-pregnant animals; MRAP1 is known to regulate MC_2 trafficking and surface expression (Chan *et al.*, 2009). However, a recent study has shown MRAP1 is not required in the trafficking of elephant shark MC_2 (Reinick *et al.*, 2012); also MRAP1 could be regulating the expression and signalling of the other expressed MCs as reported by (Chan *et al.*, 2009; Kay *et al.*, 2013). *MRAP2* detection in the ovary agrees with its role as an accessory protein for MCs, and this is augmented by the RNAscope[®] data that showed a similar distribution of *MRAP2* to that of MC_3 and MC_5 in the ovary. Additionally to MCs, MRAP2 is reported to regulate non-melanocortin GPCRs in the hypothalamus (Chaly *et al.*, 2016; Srisai *et al.*, 2017; Liang *et al.*, 2018) and co-localisation studies of *MRAP2* with GPCRs expressed in the ovary might elucidate more regulatory functions by MRAP2.

The next step after characterising the expression of the melanocortin receptors in the ovary is to examine whether their functions would be mediated by locally derived melanocortin peptides or those peptides that reach the ovary from the circulation. The *AgRP* expression had shown it to be expressed in the ovary. Previous studies reported the expression of the IL-1 receptor in the hypothalamic AgRP neurons and the receptor expression was upregulated during inflammation (Scarlett *et al.*, 2008). According to these findings, AgRP could also be involved in the acute inflammatory status during the different ovarian functions. Examining the expression of *POMC* revealed the absence of the full-length gene transcript from the ovary, but the truncated gene transcript was detected at low levels in the ovary. The 5'-truncated *POMC* gene is a shorter sequence that is devoid of both exon 1 and exon 2 and the latter sequence contains the sequence necessary to transport the *POMC* mRNA transcript to the endoplasmic reticulum (ER) to be translated to protein (Ivell, 1994). Therefore, the expressed truncated *POMC* gene cannot be transported to the ER for protein

synthesis. However, why the shorter transcript of *POMC* is expressed needs further investigation.

This research study has identified the expression of *MC₂*, *MC₄*, *MC₅*, *MRAP1*, *MRAP2*, *POMC* (5'-truncated gene transcript) and *AgRP* in C57BL/6 mouse ovary. It has also shown that *MC₅*, *MRAP2* and *MC₃* are distributed in both ovarian follicles and ovarian interstitial tissue. If the resources and time were sufficient, the RNAscope® assay would have included more ages and other stages of pregnancy to examine the effect of both on the expression and the distribution of the MCs and MRAP2 at a cellular level. Also, RNAscope® duplex assays could have been conducted to determine if there is co-localization of either *MC₃* and *MC₅* or if MRAP2 is co-localised with these receptors. The double expression study could also have been used to detect the specific cells expressing the receptors found expressed in the ovary. This could be achieved using cell markers of granulosa (*B4galt2* encoding type II membrane-bound glycoprotein that synthesises N-acetyllactosamine in glycolipids and glycoproteins); macrophages (CD56⁺⁺) and endothelial cells (CD31 or CD34). This research study had shown that most of the MCs are expressed at all levels of the hypothalamic-pituitary-ovarian axis which further strengthen the proposed reproductive role of the melanocortin system. The following chapter will be aimed at determining whether the proposed MC system role in fertility expands to include the uterus.

7 Molecular and cellular characterisation of the MC system in the female mouse uterus

7. 1 Background

The function of the uterus is to provide support in the establishment of pregnancy, provide nutritional, hormonal and immunological support to the developing fetus and through the actions of its muscular contractions that enable birth.

Unlike humans, the mouse uterus is a Y-shaped duplex organ made of two elongated uterine horns that join caudally at the short uterine corpus (uterine body) and a dual cervix. The uterus is made of three compartments:

1. The endometrial luminal columnar epithelium and the glandular cuboidal epithelium.
2. The endometrial stroma which is a supportive connective tissue that surrounds the endometrial glands and contains the spiral arteries.
3. The myometrium which is made of inner circular and outer longitudinal smooth muscle layers.

7. 1. 1 Postnatal uterine development

The uterus develops from the Mullerian duct (paramesonephric duct) in the absence of the sex determinant factors which include the transcription factor SRY, testosterone and anti-Mullerian hormone (Spencer *et al.*, 2012). At birth, the mouse uterus is made of undifferentiated mesenchyme surrounding the simple epithelial tubules. Around postnatal day (PND) 5, the luminal epithelium invaginates forming the endometrial gland; the mesenchyme differentiates into the endometrial stroma, the inner circular and outer longitudinal smooth muscle layers of the myometrium (Spencer *et al.*, 2012). The extension of the endometrial glands into the surrounding endometrial stroma is completed around postnatal day 10. The development of the adult uterus morphology is completed by PND 15 (Spencer *et al.*, 2012).

Previous studies had reported that the differentiation of endometrial epithelium could be regulated locally through the biochemical alteration in the extracellular matrix and composition of glycosaminoglycans (GAGs). These alterations influence the cell cycle and the pattern of branching of developing cells in both the epithelium and the stroma (Gray *et al.*, 2001). Epithelial cellular proliferation was found to be mediated by fibroblast growth factors (FGF) such as FGF-7, FGF-10 and insulin-like growth factors (IGF- I and II) produced by the endometrial (mesenchymal) stroma (Gray *et al.*, 2001).

FGF receptor (FGFR) deletion resulted in eventual infertility due to impaired postnatal development of the luminal epithelium leading to abnormalities in implantation sites (Filant *et al.*, 2014). Activated FGFR signalling pathways include the activation of the Pi3K/ERK phosphorylation pathway (Winterhoff and Konecny, 2017) that stimulates transcriptional factors mediating expression of genes involved in cellular proliferation and function (Zhang *et al.*, 2007). The same signalling pathway was found to be activated by MC₄ and MC₅ (Ramírez *et al.*, 2015; Rodrigues *et al.*, 2009 respectively) which might indicate a proliferative role mediated by MC₄ and MC₅: both of which have been reported to be expressed in human uterine endometrium using immunohistochemistry (Lantang *et al.*, 2015).

Other uterine growth factors include the transcriptional factors coding the Homeobox, or *Hox*, genes and the wingless-type-MMTV integration site genes, or *Wnts* family (19 genes which are known regulators of cellular proliferation). Out of the 19 known *Wnt* genes, three have been detected in the mouse uterus: *Wnt4*, *Wnt5* and *Wnt7*. The regulatory functions of the *Hox* genes and *Wnts* in the uterus are beyond the scope of this research; however, a full description of their roles in the uterus was reviewed by Hayashi *et al.* (2011) and Du and Taylor (2016).

Estradiol (E₂) was found to be non-essential in postnatal uterine development and estrogen receptor α knockout (*ER α KO*) mice have comparable uterine proliferative patterns to wild type mice (Cooke *et al.*, 2015). Progesterone had a paradoxical effect on uterine development, as it was found to both inhibit the growth of endometrial gland and prompt proliferation of the endometrial stroma in neonatal mice (Filant *et al.*, 2012). The neonatal maturation of the uterus is completed by the end of the third week after birth. The effect of the ovarian steroids on the uterus was found to be essential after puberty in mice to regulate the uterine remodelling that occurs in every estrous cycle.

7. 1. 2 Uterine changes during the estrous cycle

During the different stages of the mouse estrous cycle, there are specific changes observed in the luminal and the glandular epithelia and the endometrial stroma of the uterus.

Many studies have suggested that the fluctuations in E₂ and P₄ concentrations are the leading causes of the uterine changes. Wood *et al.* examined this hypothesis in mice by measuring the circulating concentrations of E₂ and P₄ in relation to each stage of the estrous cycle and the uterine morphological changes (Wood *et al.*, 2007). The changes observed in the mouse uterus during the estrous cycle in relation to the concentrations of both E₂ and P₄ are summarized in Table 7.1.

Table 7-1: Circulating E₂ and P₄ concentrations in relation to morphological changes in the mouse uterus during the estrous cycle.

Stage	E ₂	P ₄	Uterine changes
Estrus	↑↑↑ (≈70 pg/ml)	↓↓↓ (less than 5 ng/ml)	highest rate of stromal proliferation Low luminal cell death rate accompanied by a continued normal luminal proliferation Loss of glandular collagen type-IV and profound increase in collagen type-I Neutrophils infiltrating endometrial stroma Macrophages mainly in myometrium and deep in endometrial stroma
Metestrus	↔ (≈50pg/ml)	↔ (≈7.5 ng/ml)	A significant increase in glandular proliferation A significant increase in luminal and stromal cells death which is more profound in luminal epithelium (LE) A profound increase in collagen type-I Neutrophil infiltrating LE Macrophages mainly in myometrium and deep in endometrial stroma
Diestrus	↔ (≈50 pg/ml)	↑↑↑ (≈18 ng.ml)	highest rate of stromal cell death Loss of luminal collagen type-IV Neutrophils infiltrating endometrial stroma Macrophages mainly in myometrium and deep in endometrial stroma
Proestrus	↓ (≈45 pg/ml)	↔ (≈7 ng/ml)	A significant increase in glandular proliferation Neutrophils infiltrating endometrial stroma Macrophages mainly in myometrium and deep in endometrial stroma and near LE

The information in this table was adapted from (Wood *et al.*, 2007).

The regulation of the mouse uterine remodelling by E₂ and P₄ is mediated through their respective receptors ER α and ER β , and PR-A and PR-B. A detailed account of the regulatory role in the mouse uterus during the estrous cycle by these receptors can be found in the following reviews (Wang *et al.*, 2000; Binder *et al.*, 2014; Wood *et al.*, 2007).

In the absence of copulation and pregnancy, the uterus undergoes remodelling through an immunomodulatory process which is under hormonal control. Estradiol treatment in ovariectomized mice was found to increase the influx of leukocytes (mainly neutrophils) into the endometrial stroma and myometrium. The treatment of 8 weeks old wild-type and progesterone receptor knockout (PRKO) mice with estrogen was found to increase the number of macrophages and neutrophils in the uterine stroma (Tibbetts *et al.*, 1999). These proinflammatory effects by estradiol were significantly lowered by concurrent progesterone treatment in the wild-type animals but had no effect in the PRKO mice (Tibbetts *et al.*, 1999). Therefore, the drop in progesterone concentrations during the follicular phase, or proestrus, leads to the increase of the expression of genes coding proinflammatory cytokines, and the leukocyte infiltration of the endometrial epithelium continues. The inflammatory process causes cell death and vascular necrosis and micro-bleeding (Gellersen *et al.*, 2009). A particular type of natural killer cells (NK) are found in the uterus which were referred to as the uterine natural killer (uNK) cells. The uNK population was found to be greatest during the late secretory phase in human (Gong *et al.*, 2017). Both macrophages and uNK were found to have a unique regulatory role in the mouse, and human, uterus; these uNK cells were the first cells to undergo apoptosis at the end of the luteal phase (before the beginning of the next cycle) in women which might indicate an essential role in the uterine remodelling (Yang *et al.*, 2011).

7. 1. 3 Uterine preparation for implantation, decidualisation and maintenance of pregnancy

7. 1. 3. 1 Early pregnancy

After successful fertilisation, an interaction between the growing blastocyst and the maternal uterus leads to implantation of the blastocyst. There is a specific window between fertilisation and implantation called the receptivity window which lasts up to 4 days in rodents (day of the appearance of the murine vaginal plug is day 1) (Wang

et al., 2017). The attachment of the blastocyst to the uterine epithelium causes uterine changes, or decidualisation at the implantation site of the endometrial stroma and henceforth the implantation of the growing embryo into the decidua (stromal implantation site). The changes required to make the uterus receptive for implantation include increased permeability of the epithelial cells and eventually dissolution, the proliferation of the endometrial stroma into decidual secretory cells and uterine vascular angiogenesis. The implantation process involves a variety of molecular, hormonal and cellular regulators such as growth factors (VEGF, EGF and transforming growth factor, TGF- α), ovarian steroids, prolactin and immunomodulatory factors.

Estrogen and progesterone have different roles during the implantation process; while E₂ was found to be essential in determining the receptivity window, progesterone was reported to be required in the process of implantation itself. This is supported by detecting the *ER α* in the endometrial epithelium on the first and second days of conception (Tan *et al.*, 1999). Progesterone was also found to be essential during implantation as the progesterone receptor (PR) was detected in the endometrial epithelium and subluminal stromal layer on day 3-5 of pregnancy (Tan *et al.*, 1999). Progesterone functions involve the regulation of genes that are essential during implantation. These genes include bone morphogenetic protein 2 (*BMP2*) and *Hoxa10*. Detailed description on the ovarian steroids and the regulatory genes affecting implantation is beyond the scope of this research, but they are thoroughly described in the following reviews (Ramathal *et al.*, 2010; Cha *et al.*, 2014; Bhurke *et al.*, 2016).

Another hormone found to have a role during the implantation period is prolactin. Apart from prolactin's leading role in the formation of the corpus luteum of pregnancy (discussed in section 6. 1. 4), it was also found to be expressed in the decidual cells where it is thought to have an adverse regulatory effect on implantation (Eyal *et al.*, 2007).

The implantation process also involves immunomodulatory components including cytokines such as: macrophage colony-stimulating factor, leukaemia inhibitory factor (LIF) and IL-11. LIF is found in high concentrations in the mammalian uterine glands on the fourth day of pregnancy and falls on day 6-7 of pregnancy, which might indicate its requirement during implantation (Kimber, 2005). This cytokine is suggested to be

regulated by Hoxa3, Hoxa11 and estrogen, as the lack of any of these three was reported to down-regulate LIF protein (Kimber, 2005). LIF mediates its function through activating LIF receptor beta (LIF-R β). This receptor activates different signalling pathways such as JAK/STAT and PI3K/Akt pathways.

7. 1. 3. 2 Mid-pregnancy

After successful implantation of the embryo, formation of the placenta is required for the maintenance of pregnancy. The placenta is an embryonic-maternal vascular unit that is required for physical support, and the exchange of gas, nutrients and waste products between the growing foetus and the maternal circulation. It also behaves as an endocrine organ in providing pregnancy-associated hormones. Unlike human, mouse placentation is completed in mid-pregnancy (around day 13.5 of gestation) (Furukawa *et al.*, 2014). The mouse placenta is discoid in shape and is made by the differentiation of the embryonic trophoderm cells into trophoblast giant cells; two types of diploid cells adjacent to the embryonic cell mass arise from the polar trophoderm. These are the outer extraembryonic ectoderm which is differentiated finally into the labyrinth which is supported inwards by the second type of cells, the ectoplacental cone which differentiates into the spongiotrophoblast (Watson, 2005).

Around mid-pregnancy, the uterus is rapidly increasing in size to accommodate the growing foetus, the foeto-maternal unit and the accumulating amniotic fluid. This growth increment is made possible by the myometrium, which experiences hyperplasia, then hypertrophy and finally remodelling of the smooth muscle cells. The smooth muscle hyperplasia was reported to be under the control of estrogen which activates different signalling pathways including the IGF-I and the PI3K/Akt/mammalian target of rapamycin (mTOR) pathways (Jaffer *et al.*, 2009). Myometrial cell hypertrophy was found to be activated by the acute stretching in rats which causes transient myometrial hypoxia, which in turn activates hypoxia-induced transcription factors (HIF-1 α). The latter stimulates intrinsic apoptotic CASP3 cascade (Shynlova *et al.*, 2010). The activation of the CASP3 pathways was suggested to block further myocyte proliferation by lowering the expression of the mTOR pathways thereby causing a switch from myometrial hyperplasia to hypertrophy (Shynlova *et al.*, 2010).

Contractility of the expanding myometrial wall could end pregnancy abruptly. Therefore, the myometrium is quiescent until labour, this is achieved mainly through the effect of progesterone. In humans, progesterone stimulates myometrial relaxation through maintaining a resting membrane potential through Ca^{++} activated K^{+} -gated channels and regulates the expression of genes coding receptors that either stimulate or inhibit myometrial contractility such as oxytocin and atrial natriuretic peptide, respectively (Soloff *et al.*, 2011).

7. 1. 3. 3 Parturition and uterine involution

At term (which is around day 20-21 of gestation in mice), the uterus undergoes dramatic changes to expel the fully grown foetus in a process called parturition. It is impossible to include all mechanisms involved in parturition in this chapter fully. Therefore a summary of the parturition events is included in this chapter, but the parturition mechanisms and events are best reviewed in (Ratajczak and Muglia, 2008). In summary, murine parturition includes a series of events starting with a fall in progesterone due to the degradation of the corpus luteum of pregnancy initiated by prostaglandins (PGs) (Piekorz *et al.*, 2005). There is also an increase in the concentrations of hormones that are essential for: uterine contractions (oxytocin); cervical ripening (relaxin) and CRH which activates the HPA axis and glucocorticoid release, thus, leading to more PGs production. The HPA axis also activates nitric oxide synthase which leads to the vasodilatation of uterine and foetal blood vessels (Snegovskikh *et al.*, 2006). During pregnancy, progesterone antagonises the pro-inflammatory processes that could have been mediated by estrogen. Lack of progesterone causes localised leukocyte infiltration that digests the extracellular matrix proteins in the cervical stroma leading to remodelling and ripening of the cervix; decidual and myometrial infiltration by neutrophils and macrophages initiate the release of potent cytokines such as $\text{IL-1}\beta$, $\text{TNF-}\alpha$ and also prostaglandins which stimulate myometrial contractility (Shynlova *et al.*, 2013).

Postpartum, the uterus utilises different mechanisms to recover the estrous cyclical properties of each compartment, including the remodelling of the myometrium to reduce to the non-pregnant size and the regeneration of the endometrial luminal and glandular epithelia. The main compartment that is dramatically increased in size during

pregnancy is the myometrium. After birth, uterine remodelling occurs through a process of lysosomal degradation of the cytoplasmic component (autophagy) of the myometrial smooth muscle cells without signs of significant apoptosis (Hsu *et al.*, 2014). The recovery from the profound changes in the endometrium that occurred during pregnancy was suggested to be mediated by the endometrial stroma. The transition of the proliferating stromal mesenchymal cells to the luminal and glandular epithelia was reported to be the mechanism by which the endometrial epithelium regenerates. Huang *et al* (2012) reported that a population of progenitor cells differentiates into glandular epithelial cells and those progenitor cells are localised in the endometrial stroma after parturition (Huang *et al.*, 2012).

7. 1. 4 The possible role of the melanocortin system in the mouse uterus

Uterine remodelling during the estrous cycle, pregnancy, parturition and the postpartum involution is known to involve different pathways and mechanisms regulating these changes. These pathways, regulated by different aspects within the uterus can be summarised as follows: 1) the proliferation and differentiation of the uterus and 2) the modulation of the inflammatory response accompanying different events. A recent study reported the expression of the melanocortin receptors in all compartments of the uterus, but mainly in the endometrium; some of the receptors were located in the uNK cells (MC₃ and MC₅) (Lantang *et al.*, 2015). Identification of these receptors in uNK might indicate the implication of the MCs in the immunomodulation pathways. The uNK cells express a group of cell surface markers including CD65⁺. In rheumatoid arthritis, CD65⁺ expressing NK were also found to express all of the melanocortin receptors and were suggested to regulate the uNK cytokines, including TNF α and INF γ (Andersen *et al.*, 2017), although this has not been confirmed in uNK. Based on Andersen *et al.*'s findings, MCs could be mediating an inflammatory response which is essential during uterine remodelling throughout the estrous cycle, pregnancy, parturition and uterine involution after birth. Little is published about either the expression of the MC system in the uterus or any possible indirect interaction with the different uterine functions and pathways.

Therefore, the aims this chapter are to:

1. Determine suitable reference genes in the mouse uterus for normalisation using GeNorm expression stability analysis.
2. Characterise *MC*₍₁₋₅₎, *MRAP1*, *MRAP2*, *POMC* (full-length gene and truncated gene) and *AgRP* in the uterus of different aged mice (2, 6, 10 and 14 weeks old).
3. Compare the expression of the genes listed above in pregnant and non-pregnant mice.
4. To evaluate the cellular expression of *MC*₃, *MC*₅ and *MRAP2* expression using chromogenic *in situ* hybridisation (RNAscope®).

7. 2 Methods

For a detailed account of the materials and techniques used see chapter 3.

7. 2. 1 Determining suitable reference genes in the uterus

The most stable reference genes in the uterus were selected using the GeNorm analysis described in detail in section 3. 2. 3. 4. 1 in methods. Duplicates of cDNA samples from each age group were used in this analysis.

7. 2. 2 Characterising the gene expression of the MC system

These reference genes were used to normalise data obtained from the RT-qPCR assays of the reverse transcribed RNA extracted from whole uteri of female C57BL/6 mice aged 2, 6, 9, 10, 14 weeks and pregnant mice (14 ± 1 day *post-coitus*, dpc) (all n=5 except n=3 for 9 weeks and n=4 for 10 weeks). The efficiencies of the primers used in these assays were examined using standard curves with positive controls for each primer pair (see section 3. 2. 3. 4. 3 in methods for details). The RT-qPCR amplification products were then separated on 2% agarose gel to check the size of the bands and verify they were of the predicted size, and to check for non-specific bands.

The RT-qPCR data collected were analysed using the delta-delta CT method mentioned in section 3. 2. 3. 4. 3. C in methods.

7. 2. 3 RNAscope® 2.5HD protocol

The uterine sections were collected from female C57BL/6 mice aged 2 weeks and 10 weeks as well as pregnant mice (14± 1 dpc). The tissues were prepared and cut in longitudinal sections. The studies included using RNAscope® 2.5HD single-plex (brown) staining kit with *MC₃*, *MC₅* and *MRAP2* as well as positive and negative controls. Based on the results from the single-plex studies, duplex studies were not included for the uterus.

7. 3 Results

7. 3. 1. A Reference gene stability in the female mouse uterus

In the female C57BL/6 mouse uterus, tyrosine 3-monooxygenase/tryptophan 5-monooxygenase activation protein zeta (*YWHAZ*), actin-beta (*ACTB*) and ATP synthase subunit beta (*ATP5B*) were the most stable genes whereas Beta-2-Microglobulin (*B2M*) and 18S ribosomal RNA (*18S*) were the least stable genes (Figure 7. 1).

The Optimal number of housekeeping genes to be used in normalising the RT-qPCR data was three for the female mouse uterus. This was obtained by calculating the pairwise variation (*V*-score) with the sequential addition of each reference gene one at a time. A *V*-score above 0.15 indicates the optimal number of most stable reference genes to be used (Figure 7. 2). The *V*-score was calculated using GeNorm analysis by qBase+ software (Biogazelle, Belgium). See appendix 3. D for graphs of the BestKeeper, Normfinder, Delta CT and comprehensive reference genes stability analyses.

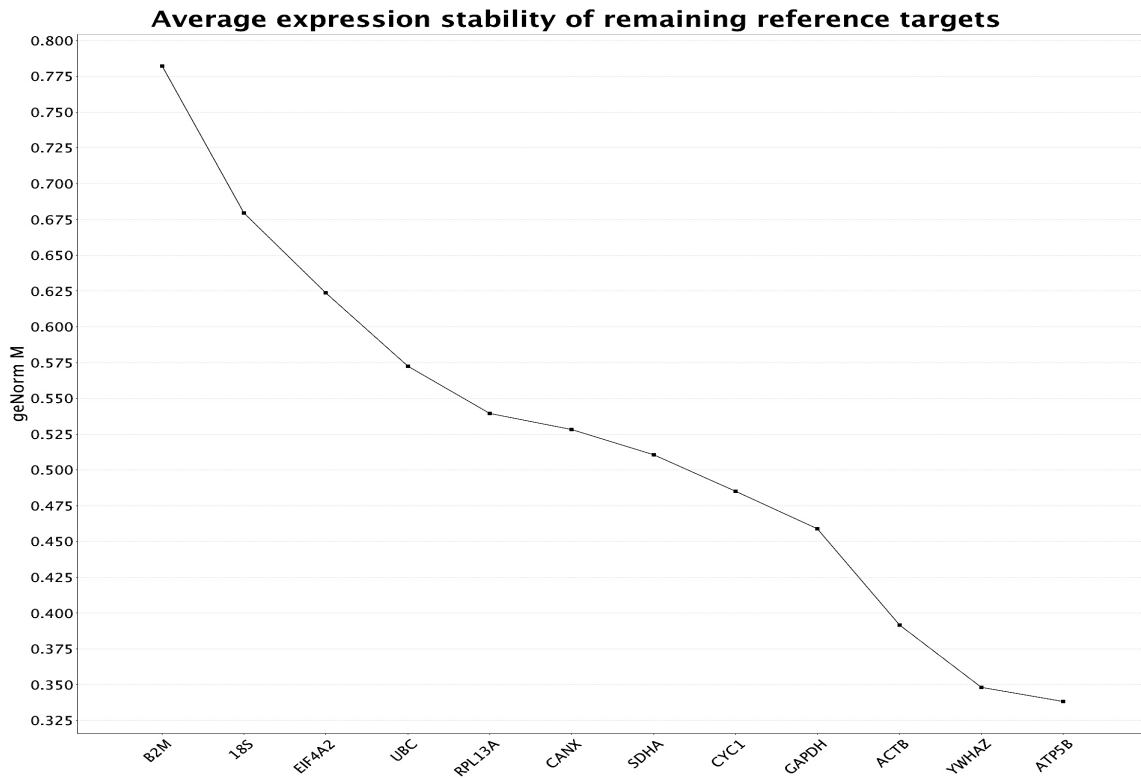


Figure 7.1: *GeNorm ranking order of reference genes stability in the female mouse uterus.* The ranking is based on calculating the geometric mean of the ranking values from Delta CT, BestKeeper, Normfinder and GeNorm reference gene analyses tools. The stability of 12 reference genes was examined using uteri of female mice aged 2, 6, 9, 10, 14 weeks, and pregnant mice (14+1 dpc). The samples were run in duplicates. The reference genes are 18S, ACTB, ATP5B, B2M, CANX, CYC1, EIF4A2, GAPDH, RPL13A, SDHA, UBC and YWHAZ. CT values were imported to the qBase+ software and analysed using GeNorm (Biogazelle, Belgium).

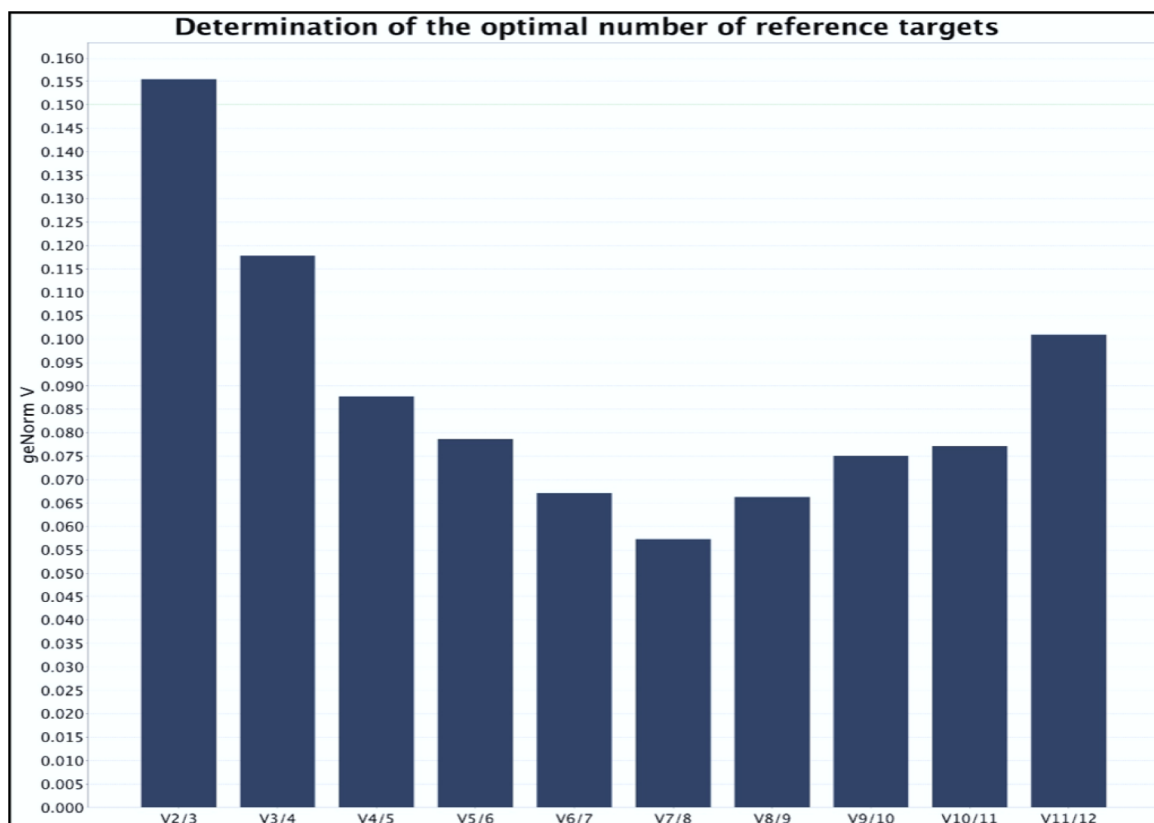


Figure 7.2: Variation score (V- score) by GeNorm. An optimal number of stable genes used normalisation was calculated by pairwise variation with the addition of each reference gene one at a time. A V-score equal or below 0.15 indicated the insignificance of using more reference genes. In this graph, 10 reference genes V-score results indicates the optimal number of most stable HKG to be used in the uterus are three (GeNorm by qBase+, Biogazelle, Belgium).

7. 3. 1. B Amplification efficiencies of *YWHAZ*, *ACTB* and *ATP5B*

The amplification efficiency is defined as the doubling of the cDNA template for each RT-qPCR cycle. Table 7.1 lists the standard curve slope (M), the coefficient of determination (R^2) and amplification efficiency (E) of *ACTB* (79%), *ATP5B* (95%) and *YWHAZ* (94%).

Table 7-2: Amplification efficiency of *ACTB*, *ATP5B* and *YWHAZ* in the female uterus.

Gene	R^2 (Coefficient of Determination)	M (Measurement of Efficiency)	E (Efficiency)
<i>ACTB</i>	0.99	-3.94	79%
<i>ATP5B</i>	0.99	-3.44	95%
<i>YWHAZ</i>	0.97	-3.48	94%

Pooled cDNA from all samples used in MC system expression in the uterus was used in generating 1:2 standard curves. The efficiency was calculated automatically using the Rotor-Gene Q software (Qiagen, UK).

7. 3. 2 MC system expression

The RT-qPCR analysis of the C57BL/6 mouse uterus showed only *MC₂*, *MC₄*, *MC₅*, *POMC* (truncated gene) and *AgRP* were detected in the uterus. *MC₁*, *MC₃*, full-length *POMC*, *MRAP1* and *MRAP2* were not expressed in the female mouse uterus. Compared to the hypothalamus and the pituitary gland, the expression of all detected members was found at low levels.

The expression of *MC₂* appeared to be increased between pre-pubertal (6 weeks old) and pre-weaned female mice (2 weeks old). The expression falls again in older mice (9 and 10 weeks old mice) to be increased mildly again in 14 weeks old mice. Pregnancy showed lower expression than that seen in non-pregnant mice of the same age (9 weeks old mice) (see Figure 7. 3, A for graph). Age and pregnancy did not cause any significant change in expression.

The expression pattern was similar for *MC₄* and *MC₅*. The expression was higher in pre-weaned mice (2 weeks old) compared to 6 and 9 weeks old mice (the expression change was significant for *MC₅*). The expression levels appeared to increase again in 10 weeks old mice and dropped mildly in 14 weeks old mice. Neither *MC₄* nor *MC₅* was expressed in pregnancy (see Figure 7. 3, B and C for graphs).

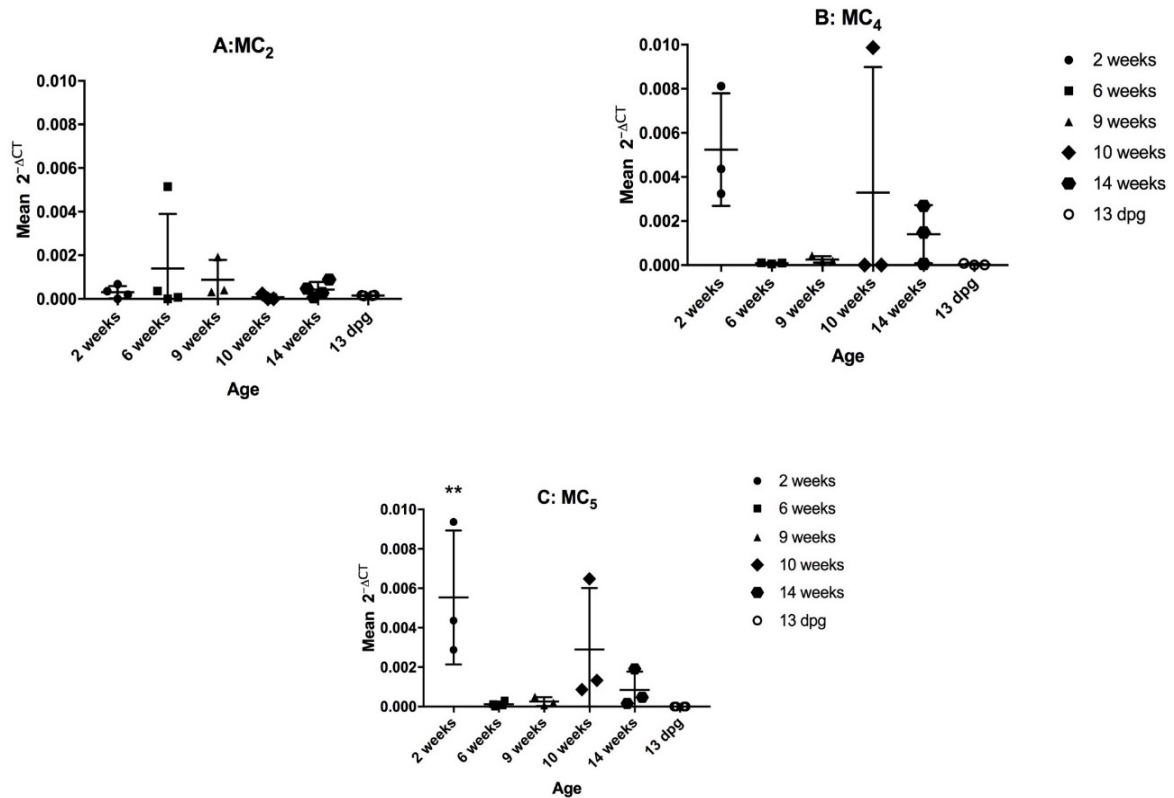


Figure 7.3: MC₂, MC₄ and MC₅ expression in the female mouse uterus. Uterine cDNA duplicates from female C57BL/6 mice aged 2, 6, 9, 10 and 14 weeks and pregnant mice (14 +1 DPC) (n=3-5) were used in the RT-qPCR studies. A: MC₂; B: MC₄ and C: MC₅. (**): Significant MC₅ expression change (p value= 0.0087). CT values of each assay were exported to excel worksheet, analysed using the delta CT Method developed by Pfaffl (2001). The skewed data seen in the graphs are due to animal sample variations (old vs. newly obtained samples). The 2^{-ΔCT} values were imported to GraphPad and analyses using one-way analysis of variance (ANOVA). (Prism 7, USA).

The expression of *POMC* and *AgRP* followed a relatively similar pattern as the expression of both genes appeared to be constant in younger mice (2, 6 and 9 weeks old mice). The expression then increased in 10 weeks old mice and dropped in 14 weeks old mice (*POMC* had lower expression than *AgRP*). Pregnancy had similar expression level seen in non-pregnant mice of the same age (9 weeks old mice) (see Figures 7.4, A and B for graphs). Table 7. 2 summarises the *MC* (1-5), *MRAP1*, *MRAP2*, *POMC* and *AgRP* expression in the female mouse uterus.

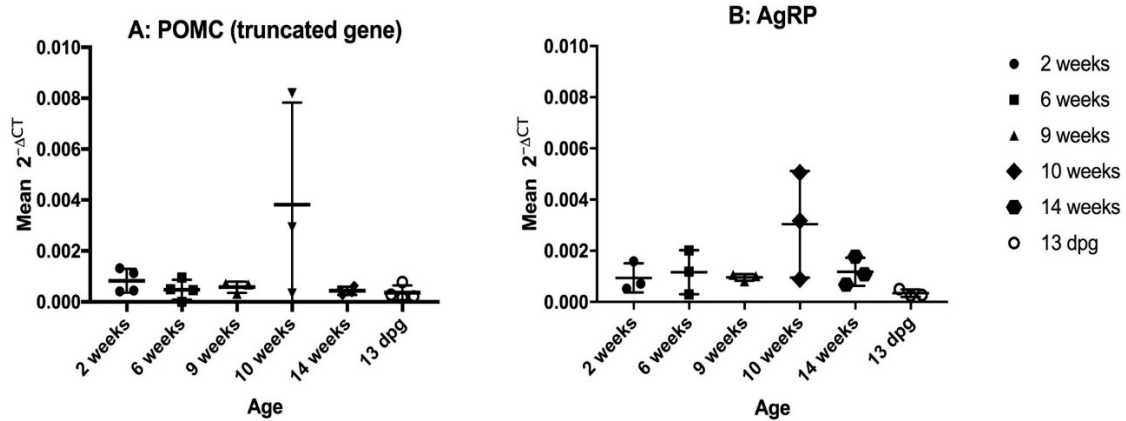


Figure 7.4: POMC (truncated transcript) and AgRP expression in the female mouse uterus. Uterine cDNA duplicates from female C57BL/6 mice aged 2, 6, 9, 10 and 14 weeks and pregnant mice (14 +1 DPC) (n=3-5) were used in the RT-qPCR studies. A: MC₂; B: MC₄ and C: MC₅. CT values of each assay were exported to excel worksheet, analysed using the delta CT Method developed by Pfaffl (2001). The skewed data seen in the graphs are due to animal sample variations (old vs. newly obtained samples). The 2^{-ΔCT} values were imported to GraphPad and analyses using one-way analysis of variance (ANOVA). (Prism 7, USA).

Table 7-3: MC system expression in the uterus.

Uterus (n: 4)				
Gene	Expression	P value	Significance of Age	Significance of Pregnancy
MC ₁	(-)	N/A	N/A	N/A
MC ₂	(+)	0.61	(-)	(-)
MC ₃	(-)	N/A	N/A	N/A
MC ₄	(+)	0.15	(-)	(-)
MC ₅	(+)	0.01	(++)	(-)
POMC (full)	(-)	N/A	N/A	N/A
POMC (trunc.)	(+)	0.06	(-)	(-)
AgRP	(+)	0.08	(-)	(-)
MRAP1	(-)	N/A	N/A	N/A
MRAP2	(-)	N/A	N/A	N/A

The table represents each gene examined in uterine cDNA duplicates of 3-4 C57BL/6 mice. Age and pregnancy effects were examined by using animals aged 2, 6, 9, 10 and 14 weeks old mice and pregnant (14 +1DPC) mice. MC₂, MC₄, MC₅ and AgRP were found in the uterus. Age had a significant impact on the expression of MC₅ (with a p-value of 0.01). Pregnancy did not affect the expression. (+) Indicate the presence of a gene or significant effect by age or pregnancy; (-): indicates the absence of a gene or non-significant effect by age or pregnancy. N/A: not detectable.

7. 3. 3 Validation of the MC system expression

The products of the RT-qPCR of *MC* (1-5), *POMC*, *MRAP1*, *MRAP2* and *AgRP*, as well as β -actin, *ATP5B* and *YWHAZ* were separated on 2% agarose gel (composition and method described in section 3. 2. 4. 3. 3). The products also contained non-template control for each of the target genes and the reference genes to check for genomic contamination (Figure 7. 5).

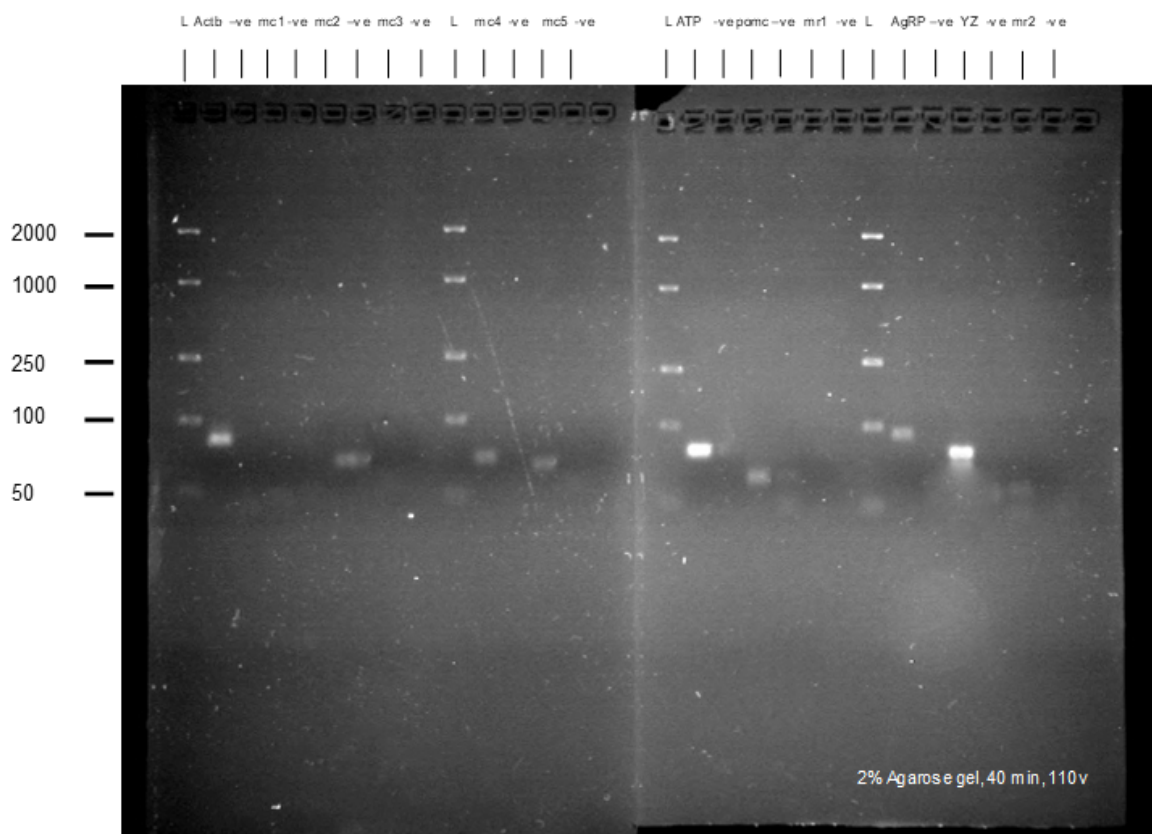


Figure 7.5: Gel electrophoresis of RT-qPCR of MC system in the female mouse uterus. The RT-qPCR products were separated on 2% agarose gel at 110 volts for 40 minutes. Where L = ladder 50 bp to 2000 bp; (ThermoScientific, UK); Actb: β -Actin=84 bp, 105 bp; MC₁ = 127 bp, MC₂ = 86 bp, MC₃ = 108 bp, MC₄ = 106 bp, MC₅ = 90 bp, ATP: ATP5B= 112 bp POMC (truncated)= 70 bp, MRAP1 = 86 bp, MRAP2 = 150 bp, AgRP = 63 bp, yz = YWHAZ (141 bp -ve: non-template control for gene of interest in previous lane. Gel image was taken using UVIPRO (Uvitec, UK).

7. 3. 3 Localization of *MC₃*, *MC₅* and *MRAP2* mRNA transcripts in the female mouse uterus

RNAscope® brown expression signal is detected as brown dots and all sections have been counterstained with haematoxylin (purple) to visualize the tissue architecture. The assays included positive (*PPIB*) and negative (*DAPB*) controls to ensure optimised conditions were achieved (Figure 7.6).

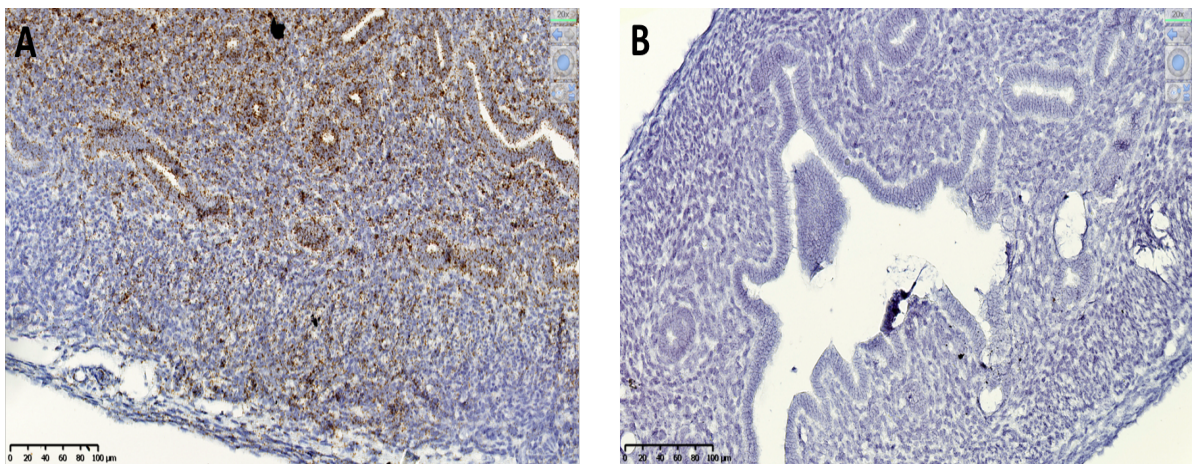


Figure 7.6: RNAscope® 2.5HD single-plex (brown) assay in the female mouse uterus. The assay was carried in uteri of mice aged 2 weeks, 10 weeks and pregnant (14 ± 1) mice. A: The uterine sections show expression of positive (*PPIB*) control to illustrate how the expression signal as brown dots in cells, counterstained with Haematoxylin (Hx). B: negative (*DAPB*) control in the uterus showing no background staining. Each group was conducted as 3 sections per slide and the assays was carried out twice. Images were taken by NanoZoomer slide scanner (Hamamatsu Photonics) at King's College London.

MC₃ was detected at low levels in the uteri of 2 weeks old mice but *MRAP2* was not detected in the uteri of animals of any age or in pregnancy (Figure 7. 7 A and B). Based on the current findings, the expression of *MC₃*, although low, was observed in the luminal and glandular epithelia, endometrial stroma and lower levels in the myometrial layers.

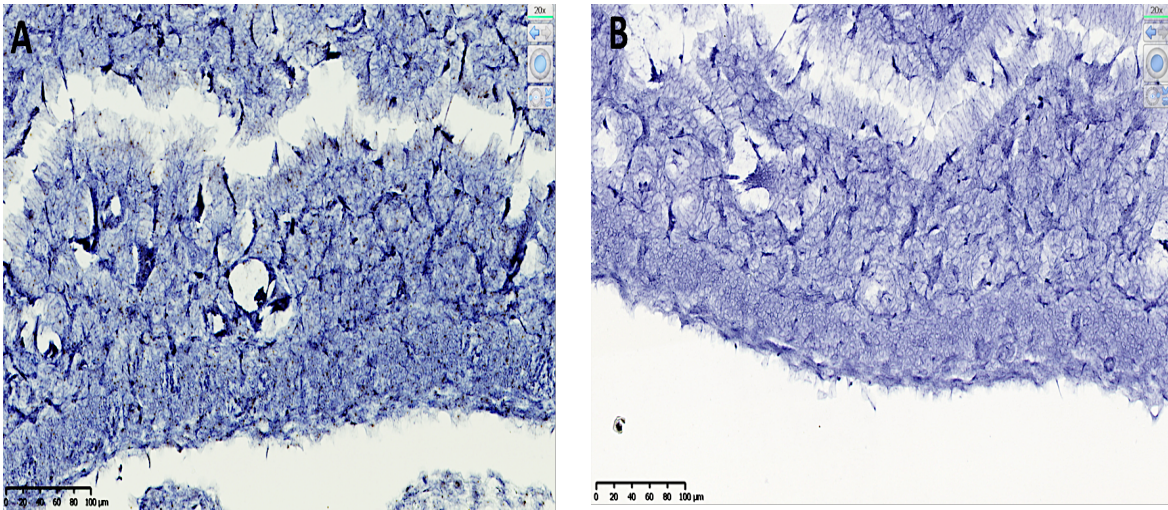


Figure 7.7: RNAscope® 2.5HD single-plex (brown) assay of MC_3 and $MRAP2$ in the female mouse uterus. The assay was carried in uteri of mice aged 2 weeks, 10 weeks and pregnant (14 ± 1) mice. A: MC_3 expression in female mouse uterus (20X). B: $MRAP2$ expression in female mouse uterus (20X). Each group was conducted as 3 sections per slide and the assays was carried out twice. Images were taken by NanoZoomer slide scanner (Hamamatsu Photonics) at King's College London.

Compared to MC_3 and $MRAP2$, MC_5 expression was higher in the female mouse uterus. Based on the current observations, the expression of MC_5 appeared to be higher in the pre-weaned (2 weeks old) and pregnant mice compared 10 weeks old mice. The expression of MC_5 was distributed in all compartments of the mouse uterus (Figures 7. 8 A-F).

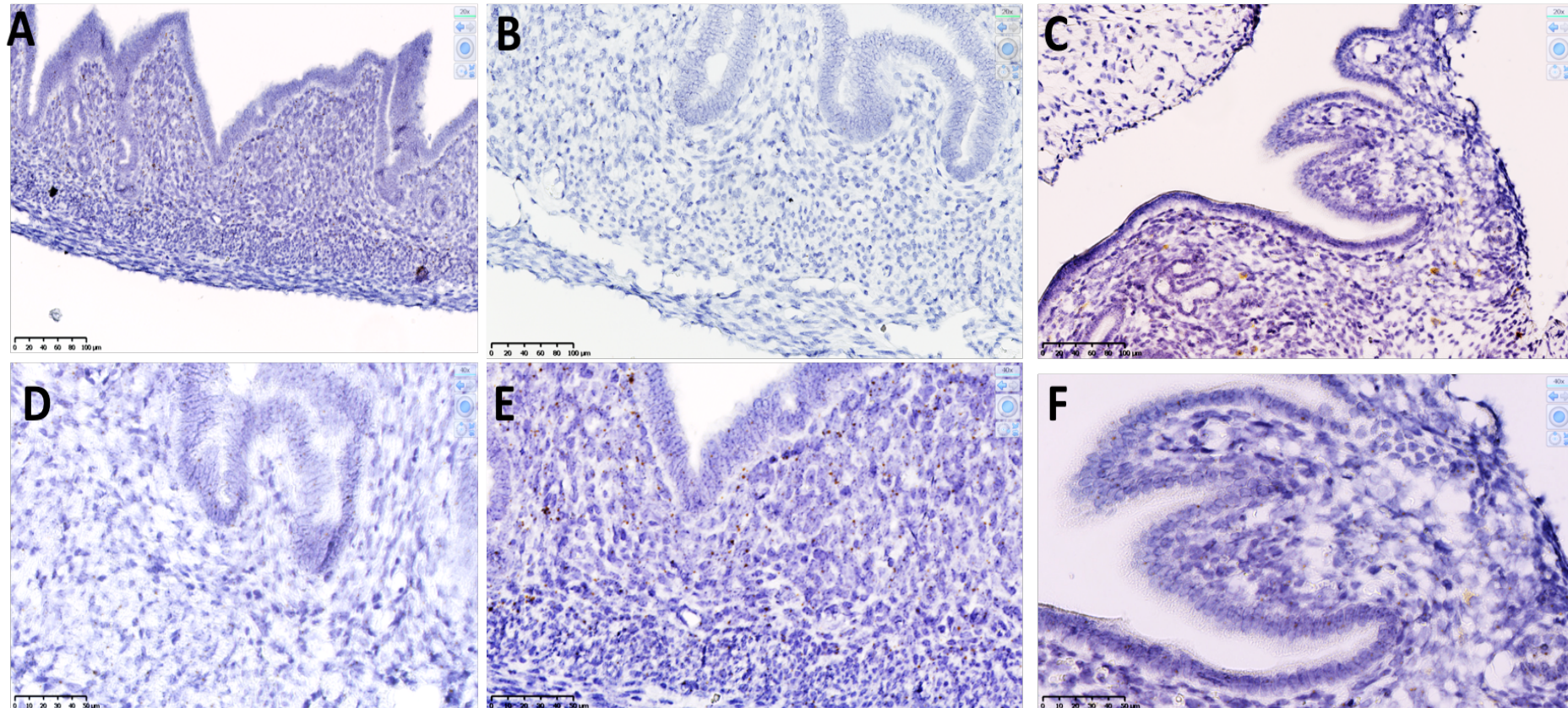


Figure 7.8: RNAscope® 2.5HD single-plex (brown) assay of MC₅ in the female mouse uterus. The assay was carried in uteri of mice aged 2 weeks, 10 weeks and pregnant (14 ± 1) mice. A: MC₅ expression in 2 weeks old female mouse uterus. B: MC₅ expression in 10 weeks old female mouse uterus. C: MC₅ expression in pregnant (14 ± 1) female mouse uterus. D: a higher magnification of MC₅ expression in 2 weeks old female mouse uterus. E: A higher magnification of MC₅ expression in 10 weeks old female mouse uterus. F: A higher magnification of MC₅ expression in pregnant (14 ± 1) mice uterus. Each group was conducted as 3 sections per slide and the assays was carried out twice. Images were taken by NanoZoomer slide scanner (Hamamatsu Photonics) at King's College, London.

7. 4 Discussion

These studies revealed a significant expression of MC_5 in the pre-weaned C57BL/6 mice compared to older age groups. At a cellular level, MC_5 was detected in all three compartments of the uterus (luminal and glandular endometrial epithelia, endometrial stroma and the myometrium) of 2 weeks and 10 weeks old mice. Even though MC_5 could not be detected in the pregnant mouse uterus using the whole tissue RT-qPCR, MC_5 was detected in all compartments of the uterus of pregnant mice at a cellular level with RNAscope[®]. This was also true for MC_3 and $MRAP2$, as both were absent as determined by the RT-qPCR expression studies but detected in pre-weaned mice with a similar localisation to that of MC_5 using the *RNA in situ* chromogenic studies. In addition to MC_5 ; MC_4 , $AgRP$ and truncated $POMC$ gene were also expressed in the C57BL/6 female mouse uterus. All the genes detected in the uterus had lower expression levels compared to those observed in the female mouse hypothalamus and pituitary gland. Other melanocortin system members (MC_1 , $MRAP1$, $MRAP2$ and the full-length $POMC$ gene) were not detected in the female mouse uterus.

GeNorm expression stability analysis found the most suitable reference genes for use in normalising the C57BL/6 female mouse uterus RT-qPCR data were $ATP5B$, $ACTB$ and $YWHAZ$. These three reference genes showed stable expression when examined in the 2, 6, 9, 10 and 14 weeks old mice and pregnant (14 ± 1 dpc) mice. Unlike in the other three tissues examined, the optimal number needed for normalising RT-qPCR data in the uterus was three whereas the optimal number of reference genes in the hypothalamus, the pituitary gland and the ovary was two. This could indicate that using less than three reference genes could cause inaccuracy of the data analysis as explained by (Morley, 2014). The reference gene $ATP5B$ is encoding a mitochondrial ATP synthase subunit beta that catalyses ATP synthesis while $ACTB$ is coding β -actin which is essential for cell motility.

The RT-qPCR data of the uterus is consistent with GPCR anatomical profiling data conducted by (Regard *et al.*, 2008), which included the profiling of MC_3 , MC_4 and MC_5 . The latter two were detected at low levels in the mouse uterus whereas MC_3 was absent. However, the absence of MC_3 in mouse uterus in the current research and the

gene profiling study contradicts findings in the human uterus. Lantang and colleagues found MC_3 expressed in human endometrial glandular and luminal epithelia using immunohistochemistry and most of the MC_3 immune-positive cells were uterine natural killer cells (Lantang *et al.*, 2015). This could be attributed to species differences. Also, it is worth mentioning that the antibodies against the MC_3 were found to produce non-specific interactions as detected by (Kathpalia *et al.*, 2011; Dowejko, 2014).

The study conducted by Lantang and colleagues showed MC_5 immuno-positive cells were extending from the endometrial glandular epithelium to the endometrial stroma; MC_5 was also detected in the endothelial cells and the smooth muscle cells of the endometrial vasculature with less staining in the natural killer cells of the uterus. These MC_5 findings are consistent with the wide distribution of the MC_5 expression using the RNAscope[®] observed in the current research. Uterine natural killer (uNK) cells are thought to be involved in the remodelling of the spiral arteries in both human and mice; uNK were found to secrete angiogenic factors such as vascular endothelial growth factor (VEGF) and placental VEGF making them essential during implantation during early pregnancy (Gaynor and Colucci, 2017). Taking the uNK role and findings by Lantang *et al.* (2015), in this present study MC_5 findings raise the possibility that MC_5 , and possibly MC_3 , might be involved in the vascular remodelling of murine uterine arteries.

MC_5 was found to be expressed in different exocrine glands, such as sebaceous and preputial gland (Zhang *et al.*, 2006; Morgan and Cone, 2006). It was also suggested that MC_5 , together with MC_1 were needed for the differentiation of the sebaceous glands as MC_5 (and MC_1) antagonist, JNJ-10229570 caused a decrease in the sebaceous gland differentiation marker epithelial-membrane antigen when used in primary human sebaceous cells and skin grafts (Eisinger *et al.*, 2011). It is possible to hypothesise that the proliferative effects of MC_5 on the sebaceous glands is more likely to occur in the endometrial glandular epithelium remodelling in the estrous cycle (or menstrual cycle) and in preparing for pregnancy.

Both MC_4 and MC_5 had a relatively similar patterns of expression in the RT-qPCR data (except in pregnancy) indicating that both could be mediating the same role in the mouse uterine tissue either separately or through forming heterodimers. As mentioned for MC_5 , the expression of both was higher in neonatal mice strengthening the association of MC_4 and MC_5 with the endometrial maturation and formation of the gland that occurs postnatally. This is supported by reports of the interaction of phosphatidylinositol 3-kinase (Pi3Ks) signalling pathways with the melanocortin system. The Pi3K signalling pathway was recently suggested to control the endometrial gland proliferation through protein kinase-dependent and independent pathways based on mice Pi3K deficient studies. Mice deficient in Pi3K were found to have reduced uterine gland number around postnatal day 20 indicating impaired postnatal uterine development (Chang *et al.*, 2018). Estradiol and progesterone treatment of the Pi3K deficient mice caused an increased endometrial epithelial mass and decreased endometrial stroma compared to the wild type animals indicating an essential role for Pi3K in regulating the endometrial cell proliferation (Chang *et al.*, 2018). Two independent studies have shown that the treatment of cells transfected with either MC_4 or MC_5 with NDP- α -MSH caused an increased c-AMP production, an effect that was abolished by the Pi3K inhibitors, wortmannin and LY294002 (Vongs *et al.*, 2004; Chang *et al.*, 2018). Based on the findings from these studies, both MC_4 and MC_5 might be associated with endometrial proliferation during development and throughout the estrous cycle. Chang and colleagues had also suggested that the *Pi3K* gene was highly expressed at the time of implantation (Chang *et al.*, 2018). Although the RNAscope[®] studies were conducted on uteri from mid-pregnant animals, MC_5 expression in the uterus could be related to findings by Chang and colleagues. Therefore, an $MC_5 / Pi3K$ *in situ* localisation study in a different stage of mouse pregnancy could provide a direct link between the MC_5 and its function in fertility at the level of the uterus.

As discussed earlier in section 7.1.3, the proliferation of the uterine epithelium is also regulated by the preovulatory ovarian estrogen with estrogen receptors expressed in the glandular epithelium. Both estrogen and progesterone are expressed in the stroma, regulating the stromal proliferation which is necessary for the implantation during early pregnancy (Tan *et al.*, 1999). Estradiol treatment was found to up-regulate

the expression of MC₅ in chicken liver (Ren *et al.*, 2017). In the rat hypothalamus, MC₄ expression was up-regulated by estradiol treatment (Silva *et al.*, 2010). Based on these findings the ovarian steroid mediating the mouse uterine proliferative function through activating MC₄, and possibly MC₅, estradiol, was also found to activate the Pi3K/ERK pathway in the rat uterus (Kazi *et al.*, 2009).

The detection of MC₂, MC₄ and MC₅ in the current research led to the assumption of the expression of either of the MRAPs in the uterus to aid in the expression and signalling of MCs, specifically MC₂, as reported by previous studies (Chan *et al.*, 2009). However, neither of the MRAPs were detected in the uterus.

Although the MC₂, MC₄ and MC₅ could be mediating their function in the uterus through melanocortin peptides which reach the uterus from the circulation, the expression of POMC, the 5'-truncated gene, indicates that the melanocortin peptides might be produced locally. The POMC 5'-truncated was also found expressed in other tissues such as the human skin cells and rat cardiomyocytes (Millington *et al.*, 1999; Zapletal *et al.*, 2013). The 5'-truncated gene is a shorter transcript with exon 1 and 2 missing in this transcript (Ivell, 1994). However, 5'-truncated POMC transcript is missing the signal sequence in exon 2 that enables the POMC polypeptide to be transferred to the ribosomes and endoplasmic reticulum to be translated. Therefore the 5'-truncated POMC transcript is unable to be processed in the uterus, bringing back the suggestion that the MC receptors expressed in the uterus mediate their function through the circulatory melanocortin peptides.

The present studies have detected the expression of MC₂, MC₄, MC₅, 5'-truncated POMC and AgRP in the uterus. Whereas MC₁, MC₃, full-length POMC transcript gene, MRAP1 and MRAP2 were absent. The distribution of MC₅ in the uterus was in the endometrial glandular and luminal epithelia, the stroma and myometrial layers. The expression was more pronounced in the neonatal animals which might indicate a developmental role for MC₅ and maybe MC₄ which had a similar RT-qPCR expression to that of MC₅. It is unfortunate that the RNAscope[®] assays did not include co-

localising MC_5 with uterine markers such as $Pi3K$, $CD56^+$ (for uNK cells), $CD10$ (for the endometrium) and $VEGF$ (for the uterine endothelial cells); these genes would identify the specific cells expressing MC_5 and would help to elucidate the functions mediated by the melanocortin system in the mouse uterus. Further studies should also include the different stages of the mouse estrous cycle, as well as, earlier and later stages of pregnancy to understand the role of the MC system, particularly MC_5 , in the uterine remodelling and the events that occur in preparing the uterus for conception.

The studies in this chapter and the previous three chapters have characterised the expression of the melanocortin system family at each level of the female mouse reproductive system. These included identifying the expression of $MC_{(1-5)}$, $MRAP1$, $MRAP2$, $POMC$ and $AgRP$ in the C57BL/6 mouse hypothalamus, the pituitary gland, the ovary and the uterus. These groups of studies also determined the specific cells or areas that expressed the MC members. The next part of this thesis includes *in vitro* studies that were designed to determine the responsiveness of MC_3 to different agonists using the luminescence reading GPCR platform, PRESTO-Tango (Kroeze *et al.*, 2015).

**8 Melanocortin 3 receptor (MC₃)
regulation by MRAP1 and MRAP2 using the
PRESTO-Tango platform**

8. 1 Background

As previously mentioned, the five melanocortin receptors are part of a GPCR family. The MCs are involved in mediating a variety of biological functions, and this is due to interactions with naturally occurring melanocortin agonists and antagonists distinguishing them from other GPCR. Table 8. 1 lists the MCs and their affinities to different melanocortin peptides and selective analogues.

Table 8-1: The melanocortin receptors and their melanocortin natural and synthetic analogues.

Receptor	Order of MC peptides potency	Selective agonist	selective antagonist	References
MC ₁	α -MSH > β -MSH > ACTH and γ -MSH ¹	MS05 and BMS-470539 ²		1, 2
MC ₂	ACTH ¹	corticotropin zinc hydroxide	ACTH ₍₁₁₋₂₄₎	1
MC ₃	γ -MSH > β -MSH > ACTH > α -MSH ₁	[D-Trp ⁸]- γ -MSH	PG-106	1
MC ₄	β -MSH > α -MSH > ACTH > γ -MSH ₁	THIQ	HS014, MBP10	1
MC ₅	α -MSH > β -MSH > ACTH > γ -MSH ₁	PG-901 ²	PG20N ²	1, 2

The information in this table was collected from 1: Guide to Pharmacology database. 2:(Rossi *et al.*, 2016).

Through their ligands, the MCs activate a variety of G-protein dependent and independent signalling pathways. The expression of the receptors and sensitivity to their ligands were found to be regulated by two accessory proteins, MRAP1 and

MRAP2 (Chan *et al.*, 2009). This introduction will illustrate some of the characterised signalling pathways of the MCs focussing specifically on MC₃, as well as discussing the role of the MRAPs in regulating the expression of MCs and their responses to the melanocortin peptides. Finally, this introduction will include a list of some of the methods by which the GPCR interactions and functions are investigated and describe why the PRESTO-Tango assay was chosen as the method of choice to study MC₃.

8. 1. 1 Melanocortin receptors signalling pathways

Melanocortin receptors mediate different functions in the body, and this is attributed to the receptors' abilities to bind to different melanocortin peptides and activate various signalling pathways. Most of these pathways depend on activating intracellular second messenger signalling cascades. The most commonly adopted signalling pathway consists of the guanine (G) protein complex that is made of three heterotrimeric subunits (α , β and γ). The stimulation of the MCs by their ligands leads to an exchange of GDP (bound to the α -subunit) for GTP which causes a conformational change of the heterotrimeric subunit and initiates dissociation of the α -subunit from the dimeric non-dissociable $\beta\gamma$ -subunit of the G-complex. This in turn leads to the dissociation of the G-complex from the receptor and activation of an intracellular cascade. The specific intracellular cascade that is stimulated depends on the type of the G α -subunit interacting with the receptor. There are four main subtypes of G α : G α_s , G α_q , G α_i , and G α_{12} (Syrovatkina *et al.*, 2016). The most common cascade activated by the MCs is the G α_s -dependent pathway. This pathway activates adenylyl cyclase, leading to an increase in cAMP production which ultimately activates the protein kinase A (PKA) pathway in response to both ACTH and α -MSH (Wikberg *et al.*, 2000).

However, MC₃, and also MC₅, were found to activate other GPCR-dependent pathways such as the G $\alpha_{q/11}$ and PKC-dependent pathway (Konda *et al.*, 1994; Rodrigues *et al.*, 2009). The binding of NDP-MSH (Melanotan I) to MC₃ was found to stimulate cellular proliferation through the G $\alpha_{i/o}$ -phosphoinositide 3-kinase (Pi3K) and extracellular signal-regulated protein kinases 1 and 2 (ERK1/2) pathway (Chai *et al.*, 2007).

In addition to the G-protein dependent pathways, the MCs are also able to activate G-protein independent pathways such as anti-inflammatory cytokine activation by

the JAK/STAT pathway that is mediated by α -MSH activated MC₅ (Buggy, 1998). The aforementioned Pi3K/ERK1/2 is also known to be activated through different mechanisms including growth factors and non-GPCRs. The Pi3K/ERK1/2 was also found to be activated by MC₁ but, through direct activation of the tyrosine kinase dependent pathway (Herraiz *et al.*, 2011).

Another essential G-protein-independent pathway is that of β -arrestin recruitment. Ligand binding to a GPCR activates β -arrestin 1 or 2 which in turn stimulates GPCR kinases, leading to phosphorylation of serine and tyrosine residues on the receptors and causing endocytic internalisation of the receptor into a clathrin-coated vesicle (Lohse and Hoffmann, 2014). The MCs utilise the β -arrestin recruitment mechanism, since AgRP (in addition to antagonising melanocortin binding to the melanocortin receptors) binding causes internalisation of both MC₃ and MC₄ as a result of β -arrestin recruitment (Breit *et al.*, 2006). Other melanocortin peptides are also involved in the recruitment of β -arrestin. The internalisation of MC₁ was reported to occur through GPCR dependent kinase 6 (GRK6) after binding with α -MSH (Wolf Horrell *et al.*, 2016).

8. 1. 2 The regulation of MCs by the MRAPs

The regulatory role of the melanocortin receptors by accessory proteins was first suggested after discovering the role of MRAP1 in the transport of MC₂ to the cell surface which facilitated the activation of the receptor by ACTH (Metherell *et al.*, 2005). The existence of a second MRAP1 related protein was confirmed four years later by (Chan *et al.*, 2009). At first, both of the MRAPs were thought to regulate MC₂ trafficking and signalling in the adrenal gland exclusively. The expression of the MRAPs in extra-adrenal tissues suggested that the MRAPs could be regulating other melanocortin receptors. Expression of MRAP1 was reported in adipose tissue and the gonads while MRAP2 was found to be expressed mainly in the brain (Chan *et al.*, 2009).

Mutational studies suggested MRAP1 was affecting MC₂ expression and signalling as it was found to be acting as a chaperone to MC₂, facilitating its movement from the endoplasmic reticulum to the cell membrane and facilitating the binding of ACTH (Sebag and Hinkle, 2009). Binding to ACTH requires the anti-parallel

homodimerisation of MRAP1 (Malik *et al.*, 2015). The same MRAP1 mechanism of action on the other MCs could not be concluded as different studies suggested an opposite role for the MRAP1 with the other four receptors. Chan *et al.*, 2009 reported a reduced sensitivity of MC₁, MC₃, MC₄ and MC₅ to NDP-MSH in CHO cells in the presence of MRAP1. However, in chicken, Zhang and colleagues reported the presence of MRAP1 increased the constitutive activity of both MC₃ and MC₄ in response to ACTH (Zhang *et al.*, 2017). The contradiction between the two studies could be attributed to either species differences or that the MRAP1 acts differently with the other melanocortin analogues and the same could be extrapolated for the MRAP2 from the same two studies. However, another explanation was provided by Asai *et al.* (2013) regarding the effect of MRAP2. Through their research study, MC₄ responsiveness to α -MSH increases after the co-expression of MC₄ with MRAP2 but this was after the use of higher doses of the MRAP2 plasmid in the transfection procedure.

The role of MRAP2 was found to extend beyond the melanocortin receptors. Within the neuroendocrine circuit that is controlling feeding behaviour, MRAP2 was found to downregulate the prokineticin 1 and 2 receptors, orexin receptor (Rouault *et al.*, 2017) and stimulate GHSR-1 and AgRP signalling (Srisai *et al.*, 2017).

The different characteristics of the melanocortin signalling and regulation discussed above reveals the complexity of the mechanisms by which the melanocortin receptor signalling pathways are affected by different factors. Moreover, a further level of complexity results from the possible dimerisation of the melanocortin receptors with each other and with other GPCRs as reported by (Mandrika *et al.*, 2005; Rediger *et al.*, 2011; Kobayashi *et al.*, 2016) and finally the sequence similarities shared between the melanocortin receptors mentioned in chapter 1. All of these factors complicate identifying the exact mechanism by which each biological activity is mediated by the corresponding MC.

8. 1. 3 The design of the PRESTO-Tango assay

A difficulty in studying all GPCRs is finding an appropriate method to investigate the responsiveness of the GPCRs to their ligand. Recently, a screening platform was developed to investigate different aspects related to the GPCRs, identifying ligands, characterising homo- and heterodimerisation interactions and also investigating their regulatory mechanisms. All of these targets are established by bypassing the different G-protein-dependent signalling pathways activated by the GPCRs. The platform is called PRESTO-Tango which is an abbreviation for Parallel Receptor-some Expression and Screening via Transcriptional Output - transcriptional activation following arrestin translocation. Half of this assay (Tango assay) was developed initially by (Barnea *et al.*, 2008) and its modification allows monitoring of β -arrestin recruitment to a specific GPCR. Briefly, the assay design is based on binding of a ligand to a GPCR this leads to the recruitment of the β -arrestin which is fused to an endoprotease that is in turn activated to cause the cleavage of an activator of luciferase gene expression.

The addition of the reporter substrate (luciferin) leads to the degradation of the luciferin and bioluminescence activity (Barnea *et al.*, 2008). This assay was later adopted by (Kroeze *et al.*, 2015) and was modified into the following design (see Figure 8. 1 for a schematic drawing of the PRESTO-Tango assay design):

The codon optimised Tango construct: which is made of:

1. A signal sequence to facilitate the localisation of the receptor on the cell membrane and a FLAG epitope tag both of which located at the 5'-terminal.
2. A Tobacco Etch Virus (TEV) nuclear inclusion endopeptidase cleavage site sequence and a tetracycline transactivator (*tTA*) fusion protein both located at the 3'-terminal.
3. The carboxyl-terminus sequence of the vasopressin receptor (V_2) that are required for the β -arrestin recruitment. For the possible removal of this V_2 tail, restriction sites are flanking the GPCR and V_2 sequences.

The use of modified HEK293 cells (HTLA cells): the modification of the HEK293 cells included the insertion of a vector comprising a β -arrestin2– TEV fusion gene, a tTA-dependent luciferase reporter and puromycin and hygromycin B resistance genes for the cells' selection.

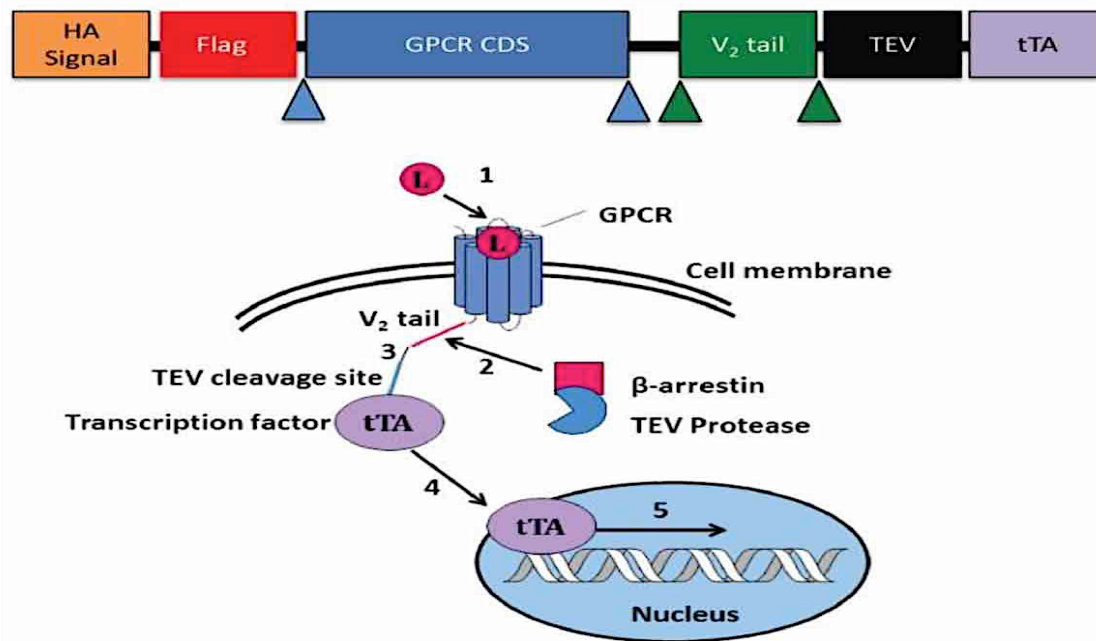


Figure 8.1: The PRESTO-Tango schematic design. The assay consists of the 1) Tango construct which made of the GPCR and V_2 tail sequences; a tetracycline activator (tTA) fusion protein; a Tobacco Etch Virus with endopeptidase cleavage site; a FLAG epitope tag and signal sequence. 2) the HTLA cells which are HEK293 cells with tTA- dependent luciferase reporter gene, β -arrestin 2– TEV fusion gene and puromycin and hygromycin B resistance genes. The permission to use the PRESTO-Tango assay design image (Kroeze *et al.*, 2015) was given by Dr Wesley Kroeze.

The PRESTO-Tango assay was found to overcome challenges of different G-protein-dependent pathways by using the β -arrestin recruitment that is known to be activated by almost all of the GPCRs including the MCs as discussed above. All of the objectives that were planned for this research study were met by this cost-effective platform. Furthermore, the PRESTO-Tango assay overcomes most of the issues raised by the complicated interactions between the melanocortin receptors, the MRAPs and the melanocortin ligands. Therefore, this assay was decided to be the method of choice in achieving the aims of this research study which were to:

1. Determine the dose-response of MC₃ to ACTH after transfecting the HTLA cells with MC₃-Tango.
2. Characterise MC₃ β -arrestin recruitment in response to different melanocortin ligands (ACTH_{(1-39)}}, NDP- α -MSH, (D-Trp⁸)- γ -MSH and SHU9119).
3. Compare the MC₃ response to the melanocortin ligands in the presence or absence of MRAP1 or MRAP2.

8. 2 Methods

8. 2. 1 HTLA cells

Permission for the use of the HTLA cells and transient transfections was granted by the University of Westminster Genetic modification panel (03/07/2017).

HTLA cells were kindly provided by Professor Wesley K Kroeze, HTLA cells are genetically modified human embryonic kidney 293 (HEK 293) cells produced by stably transfecting the tissue transcription activator-dependent reporter, luciferase, and β -arrestin 2-tobacco etch virus fusion genes (Kroeze *et al.*, 2015). HTLA cells were maintained in Dulbecco's Modified Eagle's Medium (DMEM) supplemented with 10% foetal bovine serum, 100 U/ml penicillin, 100 μ g/ml streptomycin, 2.5 μ g/ml amphotericin B (Gibco[®], UK), 2 μ g/ml puromycin dihydrochloride (Tocris, UK) and 100 μ g/ml hygromycin B (Invivogen, UK). The cells were incubated at 37°C and in an atmosphere of >95% humidity and 5% CO₂. They were sub-cultured every three days. The culture growth medium was changed after centrifuging the cells at 100 g for 5 minutes to pellet the cells; the supernatant was then removed and replaced with fresh growth medium.

8. 2. 2 Transforming E. coli (DH5 α) with the different plasmids

a. Preparing Luria-Bertani (LB) agar with ampicillin

LB agar plates were made by dissolving 35 g LB agar (Sigma Aldrich, UK) in 1 L of distilled water and then autoclaving the broth. Under sterile conditions, a final concentration of ampicillin (100 μ g/ μ l) was added to the autoclaved LB agar. The ampicillin is added to select the DH5 α containing the plasmid with an ampicillin resistance gene.

b. Bacterial transformation

To prepare stocks of plasmids, DH5 α cells (Invitrogen, UK) were thawed on ice, 50 μ l of the bacterial cells was mixed with 1 μ l (about 1 μ g/ μ l of each of the plasmids (see Section 3. 2. 6. 3 for details on the plasmids including their respective maps) in separate 1.5 ml tubes. The DH5 α : plasmid mix was incubated on ice for 5 minutes followed by heat shocking the cells with incubation for 45 seconds at 42°C. This was followed by incubating on ice for 5 minutes. Super-optimal broth with catabolite repression (SOC: 250 μ l) was added to the bacterial transformation mix. The resulting mix was then incubated with shaking at 37°C for one hour. Ten microliters of bacteria: plasmid culture was streaked onto the freshly made LB agar plates supplemented with 100 μ g/ μ l of ampicillin and the streaked plates then incubated at 37°C overnight. The following day, single colonies from the LB agar plates were selected, and each was cultured separately in 15 ml Falcon tubes containing 5 ml LB culture media supplemented with 100 μ g/ μ l of ampicillin. The culture tubes were incubated at 37°C for 16-18 hours with shaking at 280 rpm.

c. Plasmid extraction from DH5 α

Plasmid extraction was conducted using Qiagen's Plasmid miniprep kit and following the manufacturer's protocol (Qiagen, UK). The falcon tubes with the bacterial culture containing the plasmids were centrifuged at 8,000 g for 5 minutes to pellet the cells. The culture media were removed and replaced with 250 μ l of pre-chilled suspension buffer P1. The tubes were vortexed until there were no cell clumps visible and the suspended mix was transferred to 1.5 ml micro-centrifuge tubes. To lyse the cells, 250 μ l of the lysis buffer P2 were added and mixed gently by inverting the tube 4-6 times. To alkalinise the mix and precipitate the genomic DNA and the proteins, 350 μ l of the neutralisation buffer N3 were added and mixed gently by inverting the tubes 4-6 times. The tubes were then centrifuged at 13,000 rpm for 10 minutes. The clear supernatant was transferred carefully to spin column tubes placed in 2 ml collecting tubes. The spin columns were centrifuged at 13,000 rpm for 1 minute, and the flow-through was discarded. To wash the plasmids suspended in the spin column membrane, 500 μ l of buffer PB were added to the spin columns and were centrifuged at 13,000 rpm for 1 minute, and the flow-through was discarded. To precipitate the plasmid DNA, 750 μ l of buffer PE were added to the spin columns and centrifuged at 13,000 rpm for 1

minute. The flow-through was discarded. The spin columns were centrifuged at 13,000 rpm for 1 minute to dry the membranes. The collecting tubes were discarded, and the spin columns were placed in 1.5 ml microcentrifuge tubes and 50 µl of the elution buffer TE were added directly to the membranes to elute the plasmid DNA. The tubes were left on the bench for 1 minute and then were centrifuged at 13,000 for 2 minutes. The plasmid DNA was measured using the Nanodrop 2000. The samples were kept at 4°C until used.

8. 2. 3 Co-transfecting HTLA cells with pCherry and Green fluorescent proteins (eGFP) plasmids

In order to check the transfection and co-transfection efficiency of the HTLA cells for the PRESTO-Tango assay the cells were transfected or co-transfected with fluorescent plasmids. A modified SignaGen Laboratories protocol (USA) was followed. A transfection reaction in a well of a 96-well plate consisted of: approximately 25,000 cells; 5 ng of fluorescent plasmid(s) [pDNA3-enhanced green fluorescent protein (pCDNA3-EGFP) and/or pmCHERRY-N1] (see Figure 8. 4 for plasmids maps); 45 or 40 ng of a control plasmid (pCDNA3.1) (Appendix 5 shows pCDNA3.1 full sequence map) to balance the transfection reaction; and 0.8 µl of polyJet™ (catalogue no. SL100688, SignaGen Laboratories, USA) in 10 µl serum-free, phenol-free DMEM (Gibco®, UK).

The plasmid combination in the transfection reactions included was as follows:

- a. 5 ng pCDNA3-EGFP + 45 ng control plasmid
- b. 5 ng pmCherry-N1 + 45 ng control plasmid.
- c. 5 ng pCDNA3-EGFP + 5 ng pmCherry-N1+ 40 ng control plasmid.

On the day of the experiment, the HTLA cells were transferred to 15 ml centrifuge tubes, were counted using a haemocytometer and adjusted to the required volume (25,000-50,000 cells per well in a 96 -well plate). The cells: media mixture was centrifuged; the culture medium was removed. The cells were then kept for 20 minutes at 37°C and 5% CO₂ until used. The transfection reactions were incubated at room temperature for 15 minutes; each transfection reaction was then added to the HTLA cells and mixed gently by pipetting. The cells: transfection mixture was incubated at 37°C and 5% CO₂ for 20 minutes. The HTLA growth medium (100 µl per well) were

then added to the cells and mixed gently by pipetting. Finally, the cells were then seeded in a 6-well plate (1 ml per well). The cells were left in the incubator at 37°C and 5% CO₂ overnight (16-18 hours) for efficient cell transfection. On the next day, the culture medium of transfected cells was replaced with phenol red-free DMEM supplemented with 1% of bovine serum albumin (BSA); and the cells were then incubated overnight (24 hours). On the following day, the transfected cells were visualised using an LSM 510 Axiovert confocal microscope.

The concentration of the fluorescent plasmids (5 ng) was decided after examining the transfection efficiency of different concentrations (0.05-50ng). The concentration 5 ng had the most efficient post-transfection efficiency (See Figure 8. 2 for fluorescent plasmids transfection efficiency in the HTLA cells). Figure 8.3 demonstrate the successful co-expression of pCDNA3-EGFP and pmCherry-N1 plasmids in the HTLA cells.

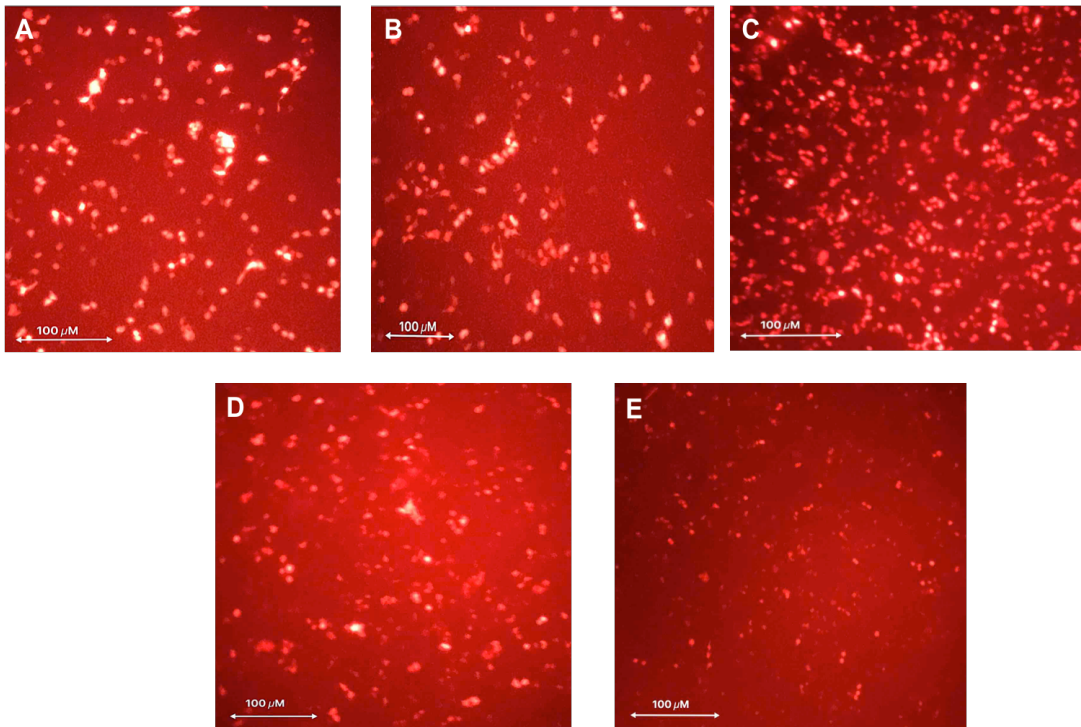


Figure 8.2: Transfection efficiency of the pmCHERRY-N1 plasmid in HTLA cells. The HTLA cells were transfected with different concentrations of pmCHERRY-N1 plasmid (0.5 ng – 1 μg) to test transfection efficiency in the HTLA cells. A: pmCHERRY-N1 plasmid (1 μg); B: pmCHERRY-N1 plasmid (500 ng); C: pmCHERRY-N1 plasmid (50 ng) D: pmCHERRY-N1 plasmid (5 ng) and E: pmCHERRY-N1 plasmid (0.5 ng). Images were taken using an LSM 510 Axiovert confocal microscope.

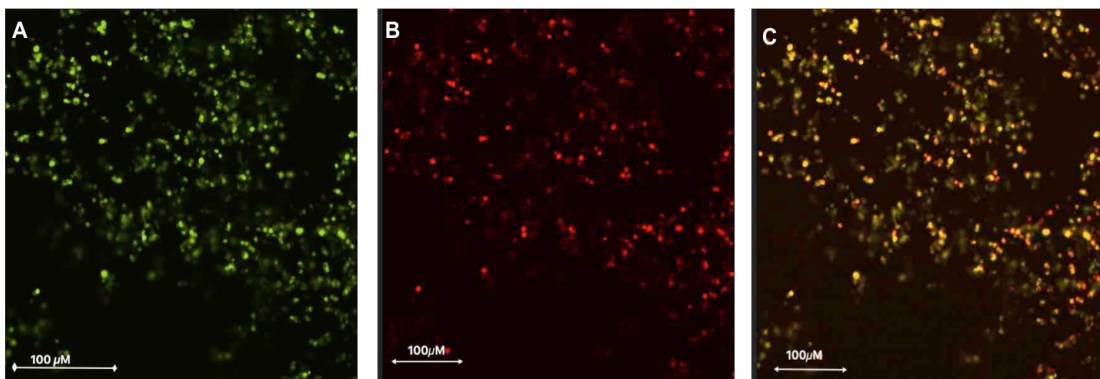


Figure 8.3: Transfection efficiency of the pCDNA3-EGFP and pmCHERRY-N1 plasmids co-transfection in TO test the co-transfection efficiency in the HTLA cells, the HTLA cells were co-transfected with pCDNA3-EGFP (5 ng) and pmCHERRY-N1 (5 ng) and were supplemented with pCDNA3 (control plasmid) for a total reaction concentration of 50 ng. A: pCDNA3-EGFP expression. B: pmCHERRY-N1 expression. C: Co- pCDNA3-EGFP+ pmCHERRY-N1 co-expression. Images were taken using an LSM 510 Axiovert confocal microscope.

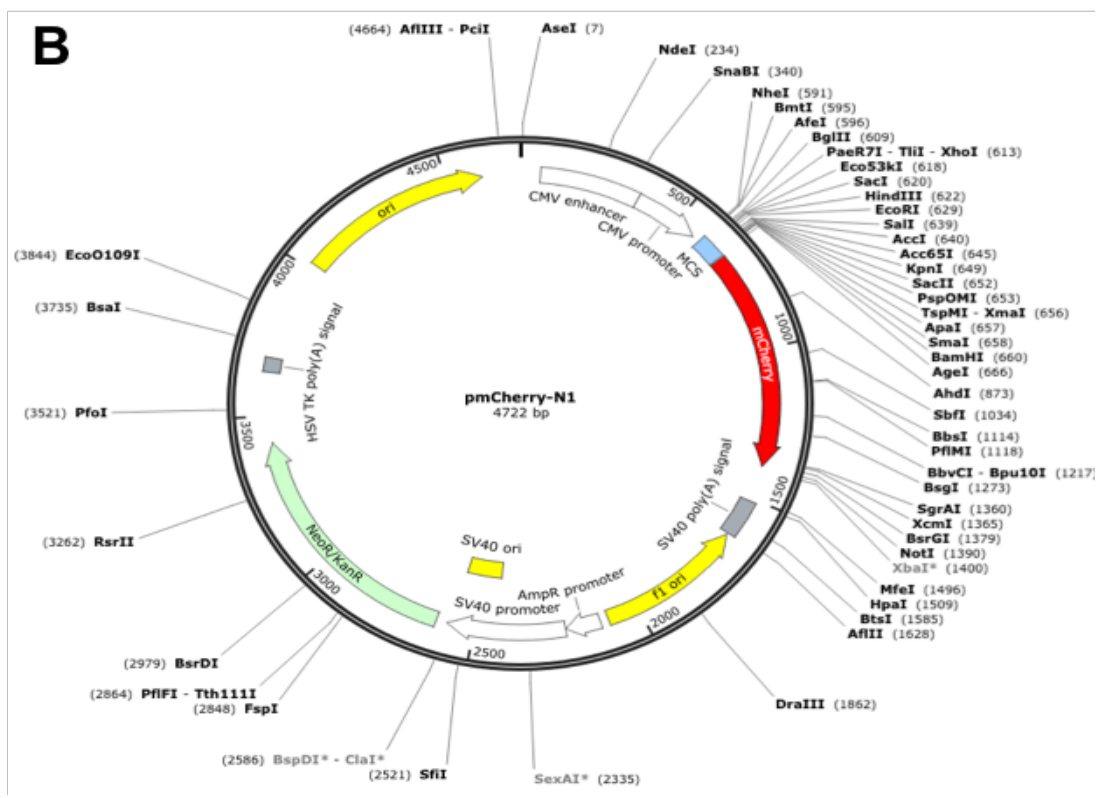
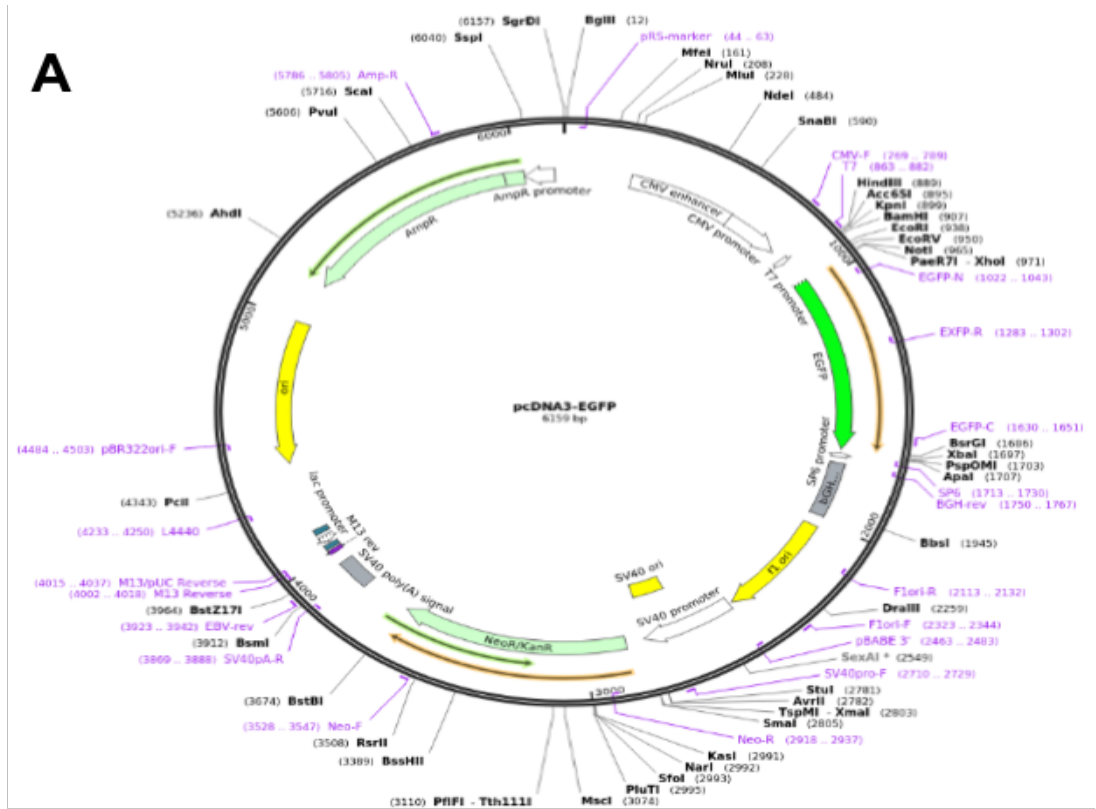


Figure 8.4: Mammalian expression vector. A: pcDNA3-EGFP, the backbone size without the insert is 5446 bp. Insert size is 700 bp (Addgene, USA). B: pmCHERRY-N1. The backbone size without the insert is 5582 bp. Insert size is 1186 bp. Sequence maps obtained from Addgene (USA).

8. 2. 4 The MC₃-Tango transfection

The Tango constructs were developed to be used specifically with the HTLA cells. They were designed by Dr Barnea's group in 2008. The Tango plasmid consists of two fusion proteins; the first fusion protein is made of a receptor (a melanocortin receptor in this research project) joined with a transcription activator (tTA) at its carboxyl end. Both proteins are separated by a cleavage site for a tobacco etch virus (TEV) protease. The second fusion protein is made of the TEV protease attached to human β -arrestin2. After transfection, the fusion genes activate the tTA-dependent reporter gene (Barnea *et al.*, 2008) (see Figure 8. 5 for MC₃-Tango map).

The concentration of the MC₃-Tango plasmid to use (5 ng) was decided after examining the transfection efficiency of different plasmid concentrations (50 ng MC₃-Tango + 0 ng pCDNA3.1 empty vector; 5 ng MC₃-Tango + 45 ng control vector; 0.5 ng MC₃-Tango + 49.5 ng control vector and 0.05 ng MC₃-Tango + 49.95 ng control vector). See appendix 6 for the optimisation graphs.

The transfection protocol is similar to that mentioned in section 3. 2. 6. 2 On the second day, after changing the growth media to phenol red-free DMEM supplemented with 1% BSA, the transfected cells were seeded in 96-well plates (90 μ l per well) and incubated overnight at 37°C and 5% CO₂. On the third day, the cells were treated with a range of concentrations of the ligand (1×10^{-6} - 1×10^{-12} M) indicated in Table 8-2 in order to generate dose-response curves. Each stimulant was made in a total volume of 100 μ l of phenol red-free DMEM supplemented with 1% BSA; 10 μ l was added to each well to give a final volume of 100 μ l. The treated cells were incubated for 18 hours in 37°C and 5% CO₂. On the fourth day, 1 mM of beetle luciferin potassium salt (E1602, Promega[®], UK) prepared in 10 μ l of phenol red-free DMEM supplemented with 1% BSA was added to each well of the treated cells and left at room temperature for 30 minutes; during which time the luciferin reacts with the luciferase resulting following the activation of the MC₃-Tango construct transfected into the HTLA cells. The plate was then read by the GloMax[®] multi-detection system plate reader using the SteadyGlo protocol (Promega[®]). The data were analysed using GraphPad on Prism 7 (See analysis flow work in section 8. 2. 7).

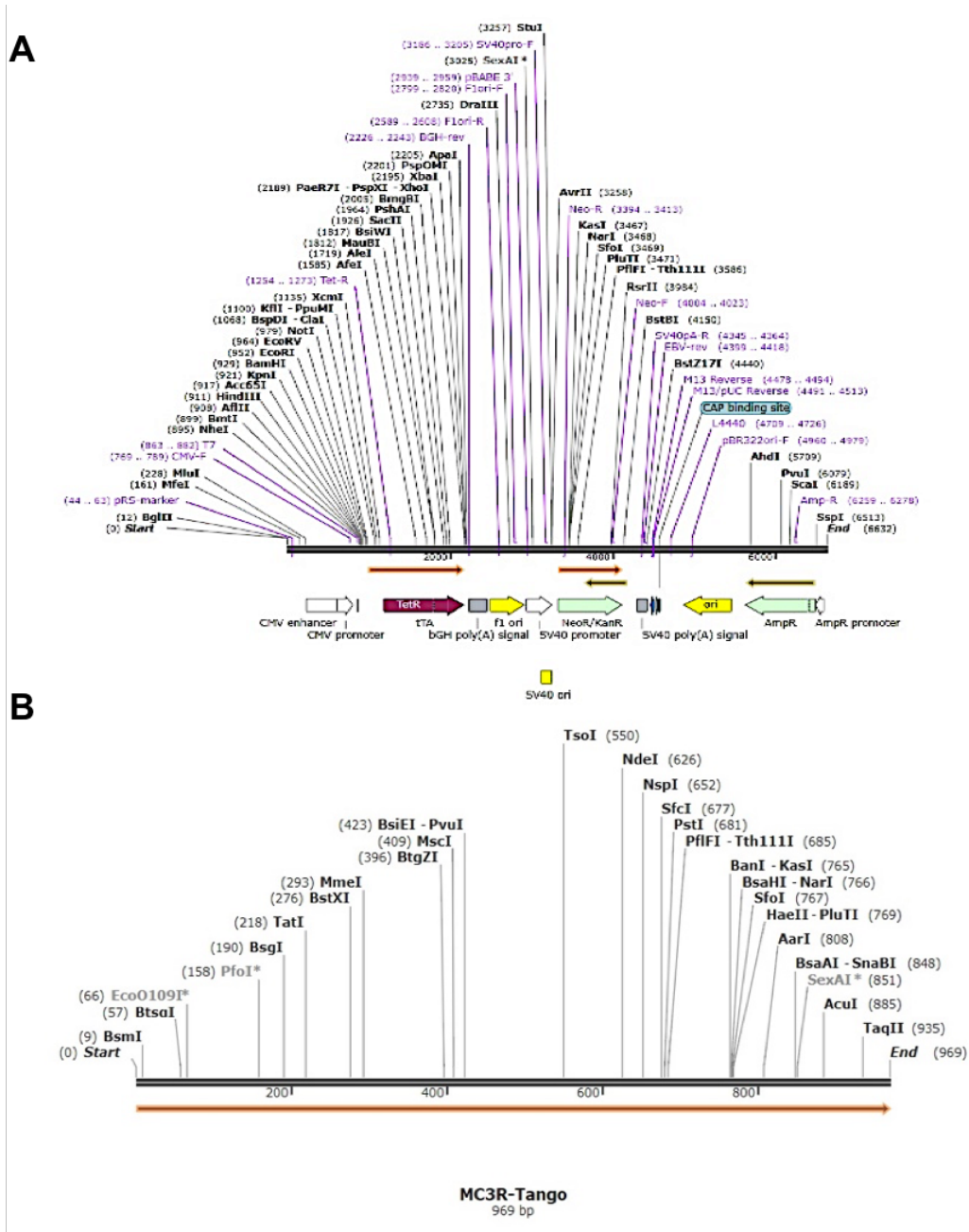


Figure 8.5: The Sequences map of the MC₃-Tango. A: The sequence of the empty Tango; the plasmid size without the insert is 6632 bp. B: The sequence of the MC₃ insert; the size of the insert is 969 bp. (MC₃R-Tango catalogue no. 66429, Addgene, USA).

Adding the ligands on the third-day post-transfection was determined having previously characterised plates with HTLA cells stimulated 24 hours and 48 hours post-transfection. See appendix 7 for duration graphs. Table 8. 2 lists the ligands used to treat the MC₃-Tango transfected HTLA cells in the PRESTO-Tango assay.

Table 8-2: The ligands used to treat the MC₃-Tango in the PRESTO-Tango assay.

Agonist / antagonist or ligand	Molecular weight (g/mol)	Company	Catalogue number
<i>ACTH₁₋₃₉(H-Ser-Tyr-Ser-Met-Glu-His-Phe-Arg-Trp-Gly-Lys-Pro-Val-Gly-Lys-Lys-Arg-Arg-Pro-Val-Lys-Val-Tyr-Pro-Asn-Gly-Ala-Glu-Asp-Glu-Ser-Ala-Glu-Ala-Phe-Pro-Leu-Glu-Phe-OH trifluoroacetate salt)</i>	4541.5	Bachem	H-1160.1000
<i>α-MSH (α-MSH trifluoroacetate salt Ac-Ser-Tyr-Ser-Met-Glu-His-Phe-Arg-Trp-Gly-Lys-Pro-Val-NH₂ trifluoroacetate salt)</i>	1664.907	Bachem	H-1075.0005
* [Nle ⁴ , D-Phe ⁷]-α-MSH or NDP-MSH (melanotan I) - MTI	1646.86	Tocris	Cat. No. 3013
* PG990 (Ac-Nle-c[Asp-Pro-Pro-DNal(2)-Arg-Trp-Lys]-NH ₂) (non-commercial MC ₃ agonist)	1134.35	*	*
* γ ₁ -MSH (H ₂ N- YVMGHFRWDRF-NH ₂)	1512.74	Tocris	3424
*(D-Trp ⁸)-γ-MSH	1570.81	Tocris	4272
SHU9119 (MC _{3,4} antagonist and agonist at MC _{1,5})	1074.258	Tocris	3420/1
* BMS-470539 (MC ₁ selective agonist)	559.70	Tocris	4053

The dose-response curve for each ligand 1 pM – 1uM (all prepared in phenol red-free DMEM supplemented with 1% BSA). ACTH: adrenocorticotrophic hormone; α-MSH: α-melanocyte stimulating hormone; γ₁-MSH: gamma 1 – melanocyte stimulating hormone; NDP-MSH: synthetic α-MSH; PG990: non-commercial MC₃ agonist; SHU9119: synthetic MC₃ and MC₄ antagonist. *: Ligands were a kind gift from Dr Stephen Getting.

8. 2. 5 MC₃-Tango and MRAP1 or MRAP2 transfection

After examining the effects of ligands on MC₃ β -arrestin recruitment, experiments were repeated to examine the activity of the same ligands with MC₃-Tango in the presence of the accessory proteins, MRAP1 or MRAP2. The same transfection protocol in 3.6.3 was followed, and the cells were co-transfected with either hMRAP1-pCDNA3.1 or hMRAP2-pCDNA3.1-myc, kind gifts from Dr Paul Le Tissier and Dr Joanne F Murray (University of Edinburgh) and Dr Li Chan (William Harvey Research Centre), respectively.

Transfections reactions started with a total volume of 50 ng of plasmid in 100 μ l per well of 96- a well plate divided as follows:

- a. MC₃-Tango (5 ng) +control vector (45 ng) only.
- b. MC₃-Tango (5 ng) +MRAP1 (5 ng) +control vector (40 ng).
- c. MC₃-Tango (5 ng) +MRAP2 (5 ng) +control vector (40 ng).

8. 2. 6 PRESTO-Tango data analysis

After reading the luminescence using the Glomax[®] Multi System plate reader the data is exported into an Excel worksheet, labelled and then imported into GraphPad (Prism, USA).

1. Using column statistics in GraphPad, the mean of five observations for each concentration of the ligand was calculated.
2. The experimental values were base-corrected by subtracting unstimulated values of MC₃-Tango which represents the background noise values (this is auto-luminescence from either the samples, the substrate or the culture media).
3. The concentrations used were then transformed into logarithmic values (log 10) and the log (dose) versus response non-linear regression curve produced. The EC₅₀ and logEC₅₀ standard errors were included in generating the curves. Each curve fit represents a summary of five Glomax[®] observations per well reading, each

concentration of the stimulant was added in 2-3 technical replicates on the same plate; and the curve fit was also generated from a summary of 3-5 experiments.

The curve fit for comparison treatments (ACTH₍₁₋₃₉₎/ MTI/ (D-Trp⁸)- γ -MSH; MTI with or without SHU9119; MC₃-Tango with or without MRAP1 or MRAP2 using the different ligands) is showing a representative experiment.

Statistical analysis using one-way ANOVA was carried out in the treatment comparison experiments to check significance following MC₃-Tango stimulation or inhibition. This was established by comparing each concentration of the different stimuli using ANOVA (analysis of variance); including post-hoc a multiple comparison to ACTH₍₁₋₃₉₎.

Unpaired two-tailed t-test analyses were also carried out on curves comparing MC₃-Tango stimulation alone to that with either MRAP1 or MRAP2 co-transfection to check statistical significance of stimulation and inhibition.

8. 2. 7 HTLA cells Viability test (MTT assay)

MTT assay (MTT is an abbreviation for 3-(4,5-Dimethylthiazol-2-yl)-2,5-diphenyltetrazolium bromide) was used to check the viability of the HTLA cells after the transfection with MC₃-Tango, MC₃-Tango with MRAP1 and MC₃-Tango with MRAP2. Through the mitochondrial activity of viable cells, the MTT compound is converted into purple formazan crystals. Therefore, it reflects the effect of different compounds on the growth and viability of cells in vitro (van Meerloo *et al.*, 2011). The transfected cells (100 μ l) were seeded in 96-well clear plate and were incubated at 37°C overnight. On the following day, 100 μ l of MTT solution (a final concentration of 0.2 mg/ml) were added to cells and incubated for 30 minutes (until the intracellular formazan crystals are visible under light microscope) at 37°C; then the media containing MTT were aspirated and replaced with 100 μ l of 10% DMSO (dimethylsulfoxide) prepared in phosphate buffered saline (PBS) and mixed by pipetting to dissolve the formazan crystals. Plates were incubated at 37°C for 15 minutes and then read using a spectrophotometer plate reader at 540 nm and then 630 nm as a reference which was subtracted from the 540 nm reading to remove the cellular debris and other background noise.

8. 3 Results

Preliminary PRESTO-Tango experiments were conducted to verify the transfection of the HTLA cells with the MC₃-Tango plasmid. Figure 8. 6 illustrates a bar chart of relative luminescence readings of HTLA cells with only luciferin, HTLA cells transfected with MC₃-Tango but with no stimulation and HTLA cells transfected with MC₃-Tango treated with 100 nM ACTH₍₁₋₃₉₎. The luminescence light units were significantly higher ($p < 0.0001$) in the MC₃-Tango transfected HTLA cells treated with 100 nM ACTH₍₁₋₃₉₎ compared to both cells with luciferin only, and the un-treated MC₃-Tango transfected HTLA cells. Cells with the luciferin alone were also significantly lower ($p = 0.05$) than the untreated MC₃-Tango HTLA cells.

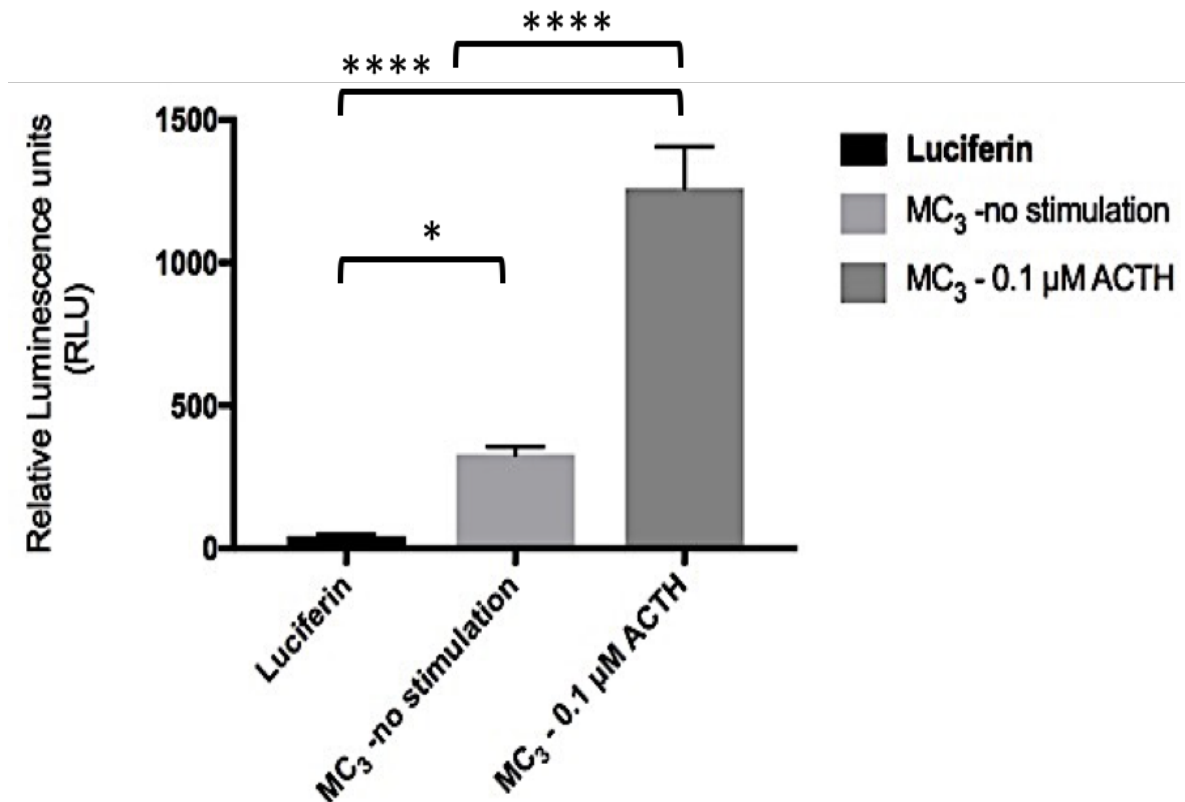


Figure 8.6: Bar chart of PRESTO-Tango assay of MC₃ in HTLA cells. A significant rise in the relative luminescence units (RLU) observed in the MC₃-Tango transfected HTLA cells treated with 0.1 μM (100 nM) of ACTH₍₁₋₃₉₎ ($p < 0.0001$) compared untreated MC₃-Tango transfected HTLA cells and cells with the only luciferin. The Bar chart was generated using GraphPad (Prism 7.04, USA).

8. 3. 1 MC₃-Tango stimulation with the melanocortin ligands

The MC₃-Tango transfected cells were incubated with different melanocortin ligands, resulting in different β -arrestin transcriptional response. The concentration of 1 μ M of Melanotan I (MTI, NDP- α -MSH) produced significantly higher RLU readings compared to D-Trp⁸- γ -MSH ($p=0.001$) followed by ACTH₍₁₋₃₉₎ ($p= 0.05$) while a lower concentration of MTI (0.1 μ M) was significantly higher than only D-Trp⁸- γ -MSH ($p=0.01$). Figure 8. 7 shows the response-curve of HTLA treatment with either ACTH₍₁₋₃₉₎, NDP- α -MSH or D-Trp⁸- γ -MSH. Table 8. 3 lists the maximal response, EC₅₀, logEC₅₀ \pm standard error, the coefficient of determination (R^2) and the number of experiments (n).

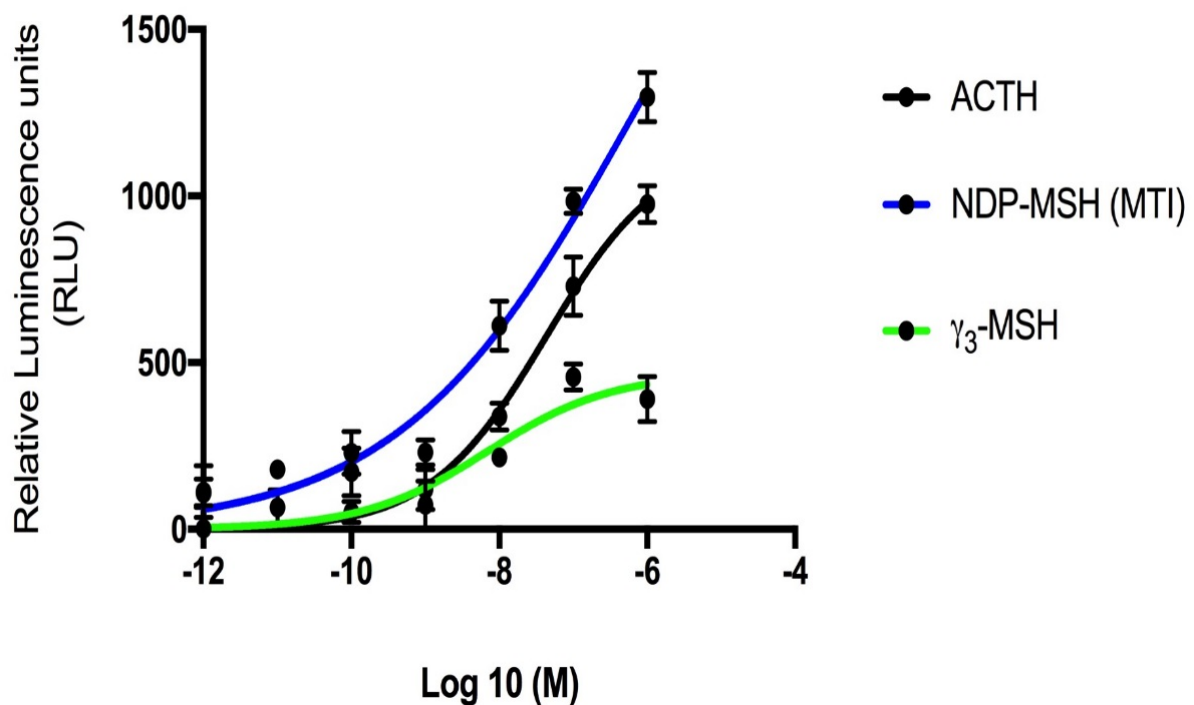


Figure 8.7: PRESTO-Tango dose-response curve of MC₃ in the HTLA cells. The HTLA treated with ACTH₍₁₋₃₉₎ (black curve fit); NDP- α -MSH (blue curve fit) and D-Trp⁸- γ -MSH (green curve fit). The β -arrestin response of D-Trp⁸- γ -MSH was significantly lower than ACTH₍₁₋₃₉₎ ($p = 0.003$) and NDP- α -MSH ($p = 0.001$). The Curve fit generated using GraphPad (Prism 7.04, USA).

Table 8-3: PRESTO-Tango of MC₃ response to the melanocortin peptides.

Ligand	Maximum response	LogEC ₅₀ ± st. error	EC ₅₀ (nM)	R ²	n
ACTH ₍₁₋₃₉₎	1155	-7.37±0.339	43.0	0.93	6
NDP- α -MSH	2465	-6.217±1.479	606.4	0.96	4
D-Trp ^{β} - γ -MSH	468.3	-8.155±0.6852	7	0.69	3

The table represents a summary of 5 readings per well recorded by Glomax[®] multisystem plate reader of ACTH₍₁₋₃₉₎ (n = 6, EC₅₀ = 43 nM), NDP- α -MSH (n = 4, EC₅₀ = 606.4) and D-Trp ^{β} - γ -MSH (n = 3, EC₅₀ = 7). The data in the table was generated using the log (dose) vs. response non-linear regression curve in GraphPad (Prism 7.04, USA).

8. 3. 2 MC₃-Tango stimulation with the melanocortin antagonist SHU9119

To test the antagonistic activity in the PRESTO-Tango β -arrestin recruitment assay, the MC₃-Tango transfected HTLA cells were treated with NDP- α -MSH and the MC_{3/4} synthetic antagonist SHU9119. Compared to NDP- α -MSH treatment, the addition of SHU9119 either alone or with NDP- α -MSH produced minimal or entirely blocked the β -arrestin transcriptional response respectively as seen in Figure 8. 8 which showed no recorded luminescence activity in both types of treatments. Table 8. 4 lists the maximal response, EC₅₀, logEC₅₀ ± standard error, the coefficient of determination (R²) and the number of experiments (n).

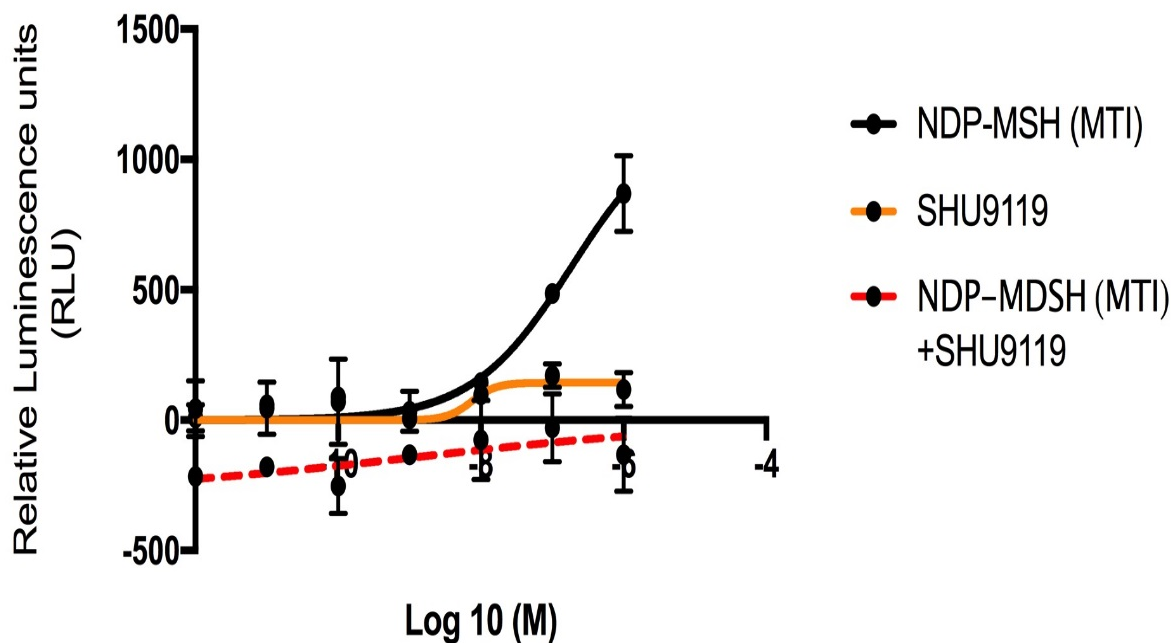


Figure 8.8: PRESTO-Tango dose-response curve of MC₃ in the HTLA cells. The HTLA treated with either NDP- α -MSH (black curve fit) or SHU9119 (orange curve fit) or NDP- α -MSH+SHU9119 (dotted red curve fit). The β -arrestin response of SHU9119 produced negligible luminescence activity. Luminescence activity was blocked entirely with NDP- α -MSH+SHU9119 treatment. The Curve fit generated using GraphPad (Prism 7.04, USA).

Table 8-4: PRESTO-Tango of MC₃ response to antagonistic SHU9119 treatment.

Ligand	Maximum response	LogEC ₅₀ \pm st. error	EC ₅₀ (nM)	R ²	n
NDP- α -MSH	1178	-6.729 \pm 0.6025	186.5	0.94	6
SHU9119	143.7	-8.128 \pm 1.89	7.444	0.098	6
NDP- α -MSH + SHU9119	-283.8	-8.911 \pm 8.262	1.227	0.1799	6

The table represents a summary of 5 observations per well recorded by Glomax[®] multisystem plate reader of NDP- α -MSH (n = 6, EC₅₀ = 186.5 nM), SHU9119 (n = 6, EC₅₀ = 7.444) and NDP- α -MSH+SHU9119 (n = 6, EC₅₀ = 1.227). The data in the table was generated using the log (dose) vs. response non-linear regression curve in GraphPad (Prism 7.04, USA).

The treatment of MC₃ transfected HTLA cells with the MC₃ selective agonist, PG990 and the MC₁ selective agonist (BMS-470539) blocked β -arrestin recruitment as the luminescence activity was below the level of detection compared to ACTH₍₁₋₃₉₎ as seen in Figure 8.9 A and B respectively.

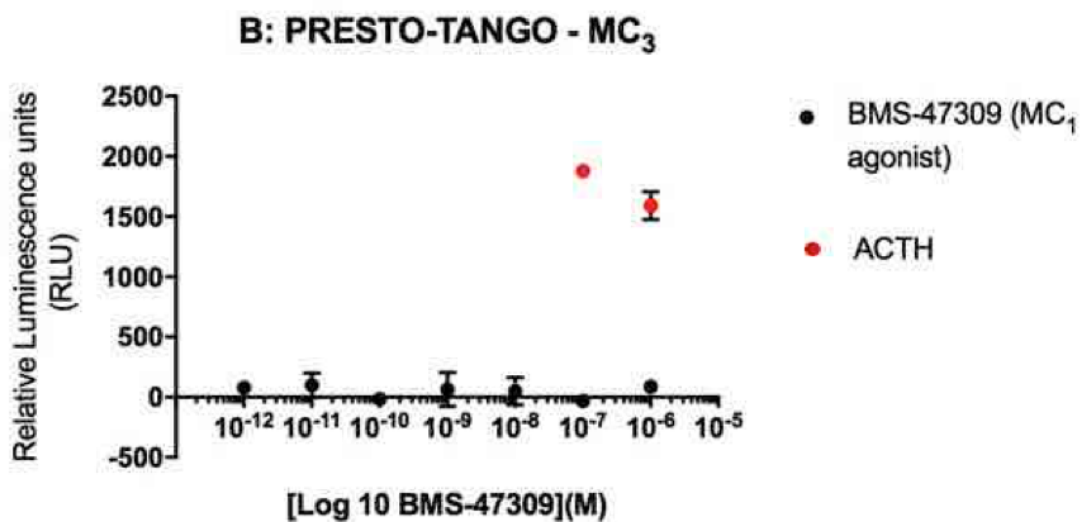
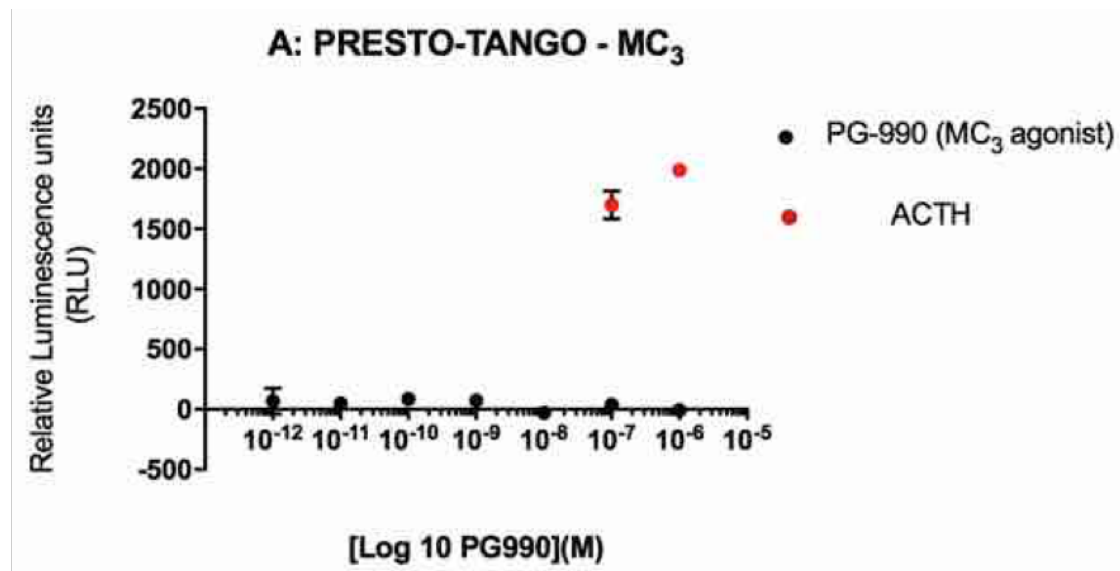


Figure 8.9: PRESTO-Tango dose-response curve of MC₃ in the HTLA cells. The HTLA treated with either the MC₃ selective agonist (PG990) (A) or MC₁ selective against (BMS-470539) (B). No luminescence activity recorded for either of the treatments compared to ACTH₍₁₋₃₉₎. The Curve fit generated using GraphPad (Prism 7.04, USA).

8. 3. 3 The regulation of MC₃ response with MRAP1 and MRAP2

Preliminary PRESTO-Tango experiments were conducted to verify the co-transfection of the HTLA cells with either MC₃-Tango/MRAP1-pCDNA3.1 or MC₃-Tango/MRAP2-myc plasmids. Figure 8. 10 illustrates a bar chart of relative luminescence readings of HTLA cells with MC₃-Tango alone, HTLA cells co-transfected with MC₃-Tango/MRAP1-pCDNA3.1 and HTLA cells co-transfected with MC₃-Tango/MRAP2-myc (all treated with no stimulation). The luminescence light units were significantly lower ($p = 0.004$) in the MC₃-Tango/MRAP1 co-transfected HTLA cells and MC₃-Tango/MRAP2-myc co-transfected cells ($p = 0.001$) compared MC₃-Tango transfected HTLA cells.

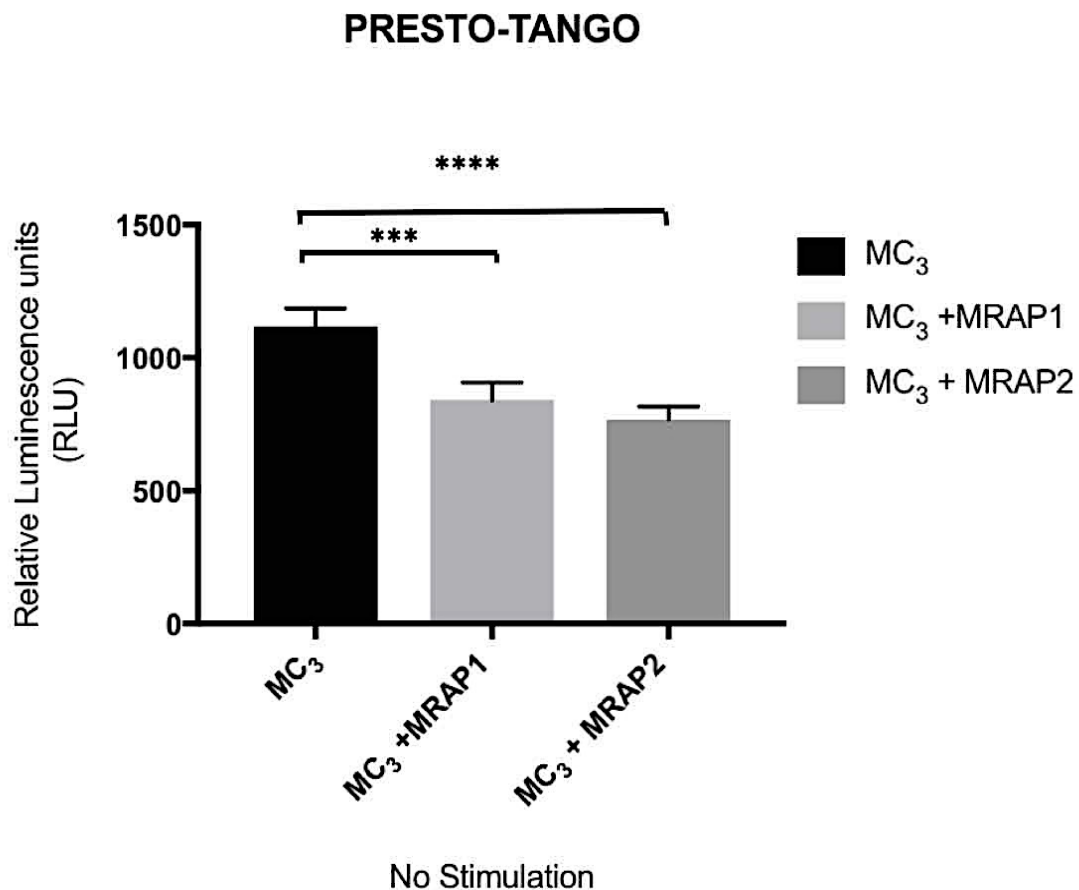


Figure 8.10: Bar chart of PRESTO-Tango assay of MC₃-Tango/MRAP1-pCDNA3.1 or MC₃-Tango/ MRAP2-myc co-transfected HTLA cells. Significant fall in the relative luminescence units (RLU) observed in the MC₃-Tango/MRAP1-pCDNA3.1 and MC₃-Tango/MRAP2-myc co-transfected HTLA cells ($P = 0.004$ and $p = 0.001$ respectively) compared to MC₃-Tango transfected HTLA. The Bar chart was generated using GraphPad (Prism 7.04, USA).

8. 3. 4. The regulation of MC₃ response with MRAP1

The β -arrestin transcriptional activities generated by MC₃ when treated with the melanocortin peptides in the PRESTO-Tango assays were repeated and tested in the presence of MRAP1. The response of the β -arrestin recruitment assays was found to produce different activities with the different melanocortin peptides. HTLA cells co-transfected with MC₃-Tango and MRAP1-pCDNA3.1 and treated with 1 μ M of ACTH₍₁₋₃₉₎ produced a significant rise in the β -arrestin response compared to HTLA cell transfected with MC₃-Tango alone ($p = 0.02$; Figure 8. 11. A). Also, the presence of MRAP1 appeared to increase the sensitivity of MC₃ to ACTH₍₁₋₃₉₎ as a lower concentration of ACTH₍₁₋₃₉₎ (100 nM) increased the response significantly ($p = 0.01$).

Although the treatment with NDP- α -MSH in the presence of MRAP1 had an overall comparable response to that in the absence of MRAP1, lower NDP- α -MSH concentrations (10 nM and 1nM) produced significantly higher luminescence light units compared to higher NDP- α -MSH concentrations (1 μ M and 0.1 μ M) ($p = 0.02$ and $p = 0.02$). Figure 8. 11. B shows the curve fit of NDP- α -MSH treated MC₃-Tango transfected HTLA cells with and without MRAP1 co-transfection.

The same pattern of β -arrestin response was observed when HTLA cells, co-transfected with MC₃-Tango and MRAP1-pCDNA3.1, were treated with D-Trp⁸- γ -MSH compared to NDP- α -MSH treatment. Figure 8. 11. C shows the lower concentrations of D-Trp⁸- γ -MSH (10 nM and 1 nM) caused a significant rise in the β -arrestin activity ($p = 0.002$ and $p = 0.03$ respectively) compared to the D-Trp⁸- γ -MSH treatment of HTLA cells transfected with MC₃-Tango without MRAP1. Table 8. 5 lists the maximal response, EC₅₀, logEC₅₀ \pm standard error, the coefficient of determination (R^2) and the number of experiments (n).

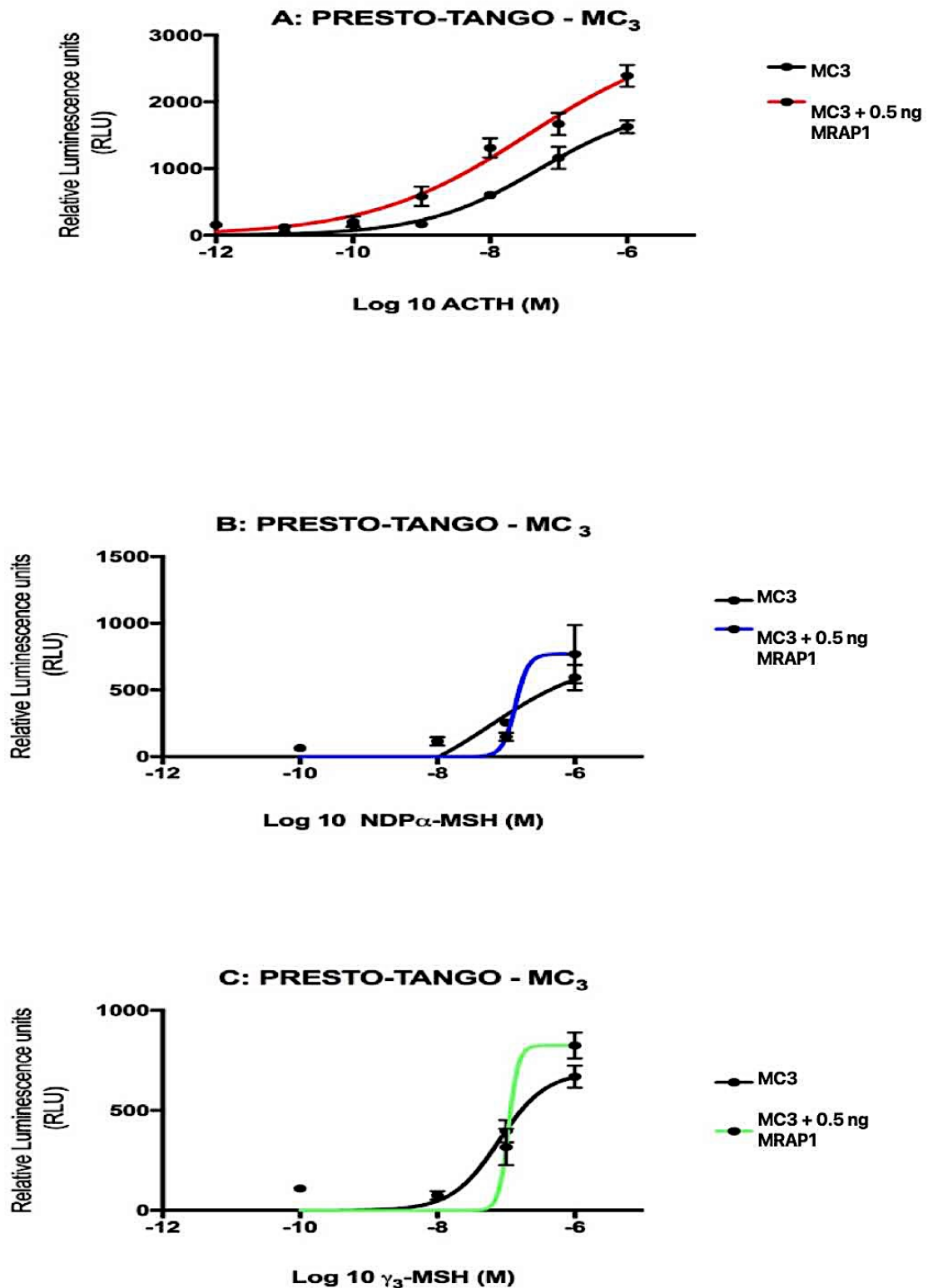


Figure 8.11: PRESTO-Tango dose-response curve MC₃-Tango and MRAP1- pCDNA3.1 co-transfection in HTLA cells. The luminescence activity was increased in with ACTH₍₁₋₃₉₎ (1 μ M and 100 nM, $p = 0.02$ and $p = 0.01$ respectively) (A); NDP- α -MSH (10 nM and 1 nM, $p = 0.02$ and $p = 0.002$ respectively) and (B) and D-Trp⁸- γ -MSH (10 nM and 1 nM, $p = 0.002$ and $p = 0.03$ respectively) (C). The Curve fit generated using GraphPad (Prism 7.04, USA).

Table 8-5: PRESTO-Tango of MC₃ response with or without MRAP1-pCDNA3.1 co-transfection.

Ligand	Maximum response	LogEC ₅₀ ± st. error	EC ₅₀ (nM)	R ²	n
MC ₃ -ACTH ₍₁₋₃₉₎	1978	-7.29± 0.311	51.24	0.96	6
MC ₃ /MRAP1- ACTH ₍₁₋₃₉₎	3016	-7.451± 0.538	35.43	0.94	6
MC ₃ -NDP- α -MSH	676.4	-6.814±1.006	153.3	0.648	4
MC ₃ /MRAP1-NDP- α -MSH	768.7	-6.866±755.8	136.3	0.472	4
MC ₃ - D-Trp ⁸ - γ -MSH	694	-7.106±0.235	78.32	0.83	4
MC ₃ /MRAP1- D-Trp ⁸ - γ -MSH	824.6	-6.966±934.1	108.1	0.66	4

The table represents a summary of 5 observations per well recorded by Glomax[®] multisystem plate reader of MC₃-ACTH₍₁₋₃₉₎ (n = 6, EC₅₀ = 51.24 nM), MC₃/MRAP1- ACTH₍₁₋₃₉₎ (n = 6, EC₅₀ = 35.43), MC₃-NDP- α -MSH (n = 6, EC₅₀ = 153.3), MC₃/MRAP1-NDP- α -MSH (n = 6, EC₅₀ = 136.3), MC₃- D-Trp⁸- γ -MSH (n = 6, EC₅₀ = 78.32) and MC₃/MRAP1- D-Trp⁸- γ -MSH (n = 6, EC₅₀ = 108.1). The data in the table was generated using the log (dose) vs. response non-linear regression curve in GraphPad (Prism 7.04, USA).

8. 3. 4. B The regulation of MC₃ response with MRAP2

Before examining the β -arrestin recruitment to MC₃ treated with the different melanocortin peptides in the presence of MRAP2, different concentrations of the MRAP2-myc plasmid were investigated and were shown to have interestingly paradoxical effects. The co-transfection of HTLA cells with 5 ng of MC₃-Tango and a low concentration of MRAP2-myc (0.5 ng) was found to increase the β -arrestin recruitment response when the co-transfected HTLA cells were treated with 1 μ M of ACTH₍₁₋₃₉₎ (p = 0.04) (see Figure 8. 12). Whereas, co-transfecting the HTLA cells with 5 ng of MC₃-Tango and a higher concentration of MRAP2-myc (5 ng) had reduces response significantly when treated with 1 μ M (p = 0.02), 0.1 μ M (p = 0.03) and 100 nM (p = 0.02) of ACTH₍₁₋₃₉₎ as seen in Figure 8. 12 and 8. 13. A.

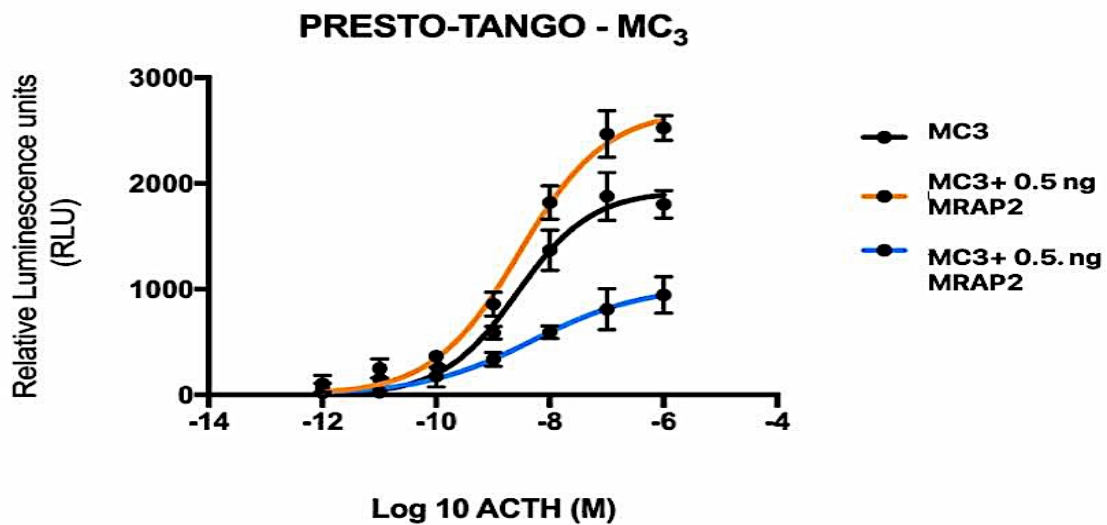


Figure 8.12: PRESTO-Tango dose-response curve of MC₃-Tango- HTLA cells co-transfected with different concentrations of MRAP2-myc. The HTLA treated with ACTH_{(1-39)}}. The luminescence activity was significantly higher when MC₃-HTLA cells with 0.5 ng MRAP2-myc (orange curve fit) and treated with 1 μ M of ACTH_{(1-39)}} ($p = 0.04$). Higher concentration of MRAP2-myc (5 ng) had reduced the luminescence activity in the HTLA cells when treated with 1 μ M ($p = 0.02$), 0.1 μ M ($p = 0.03$) and 100 nM ($p = 0.02$) of ACTH_{(1-39)}}. The Curve fit generated using GraphPad (Prism 7.04, USA).

The sensitivity of MC₃ to NDP- α -MSH in the presence of MRAP2 was significantly increased in the lowest concentration of NDP- α -MSH (10 pM and 1 pM, $p = 0.04$ and $p = 0.04$) compared to HTLA cells transfected with MC₃-Tango alone. Whereas, the response of the co-transfected HTLA cells was comparable to the HTLA cells transfected with MC₃-Tango alone as seen in Figure 8.13. B.

The treatment of the MC₃-Tango/ MRAP2-myc HTLA cells with different concentrations of D-Trp⁸- γ -MSH did not change the β -arrestin recruitment response from that seen with HTLA cells transfected with MC₃-Tango alone as shown in Figure 8. 13. C. Table 8. 6 lists the maximal response, EC₅₀, logEC₅₀ \pm standard error, the coefficient of determination (R^2) and the number of experiments (n).

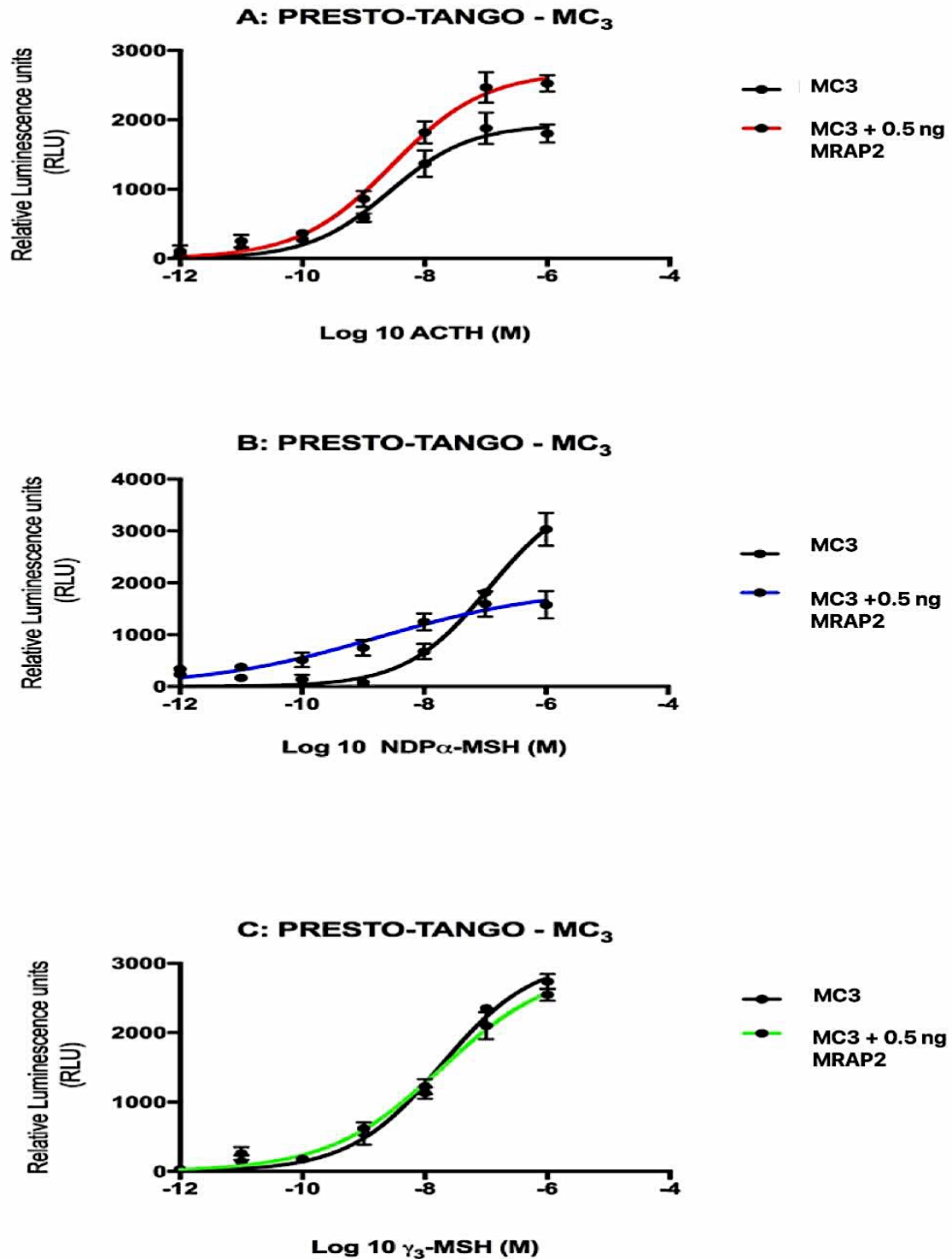


Figure 8.13: PRESTO-Tango dose-response curve MC₃-Tango and 0.5 ng of MRAP2- myc co-transfection in HTLA cells. The luminescence activity was increased with 1 μ M of ACTH₍₁₋₃₉₎ ($p = 0.04$) (A). The co-transfected HTLA cells' luminescence activity was lowered with NDP- α -MSH (10 pM and 1 pM, $p = 0.04$ and $p = 0.04$) (B) and was not changed when treated with D-Trp⁸- γ -MSH (C). The Curve fit generated using GraphPad (Prism 7.04, USA).

Table 8-6: PRESTO-Tango of MC₃ response with or without MRAP2-pCDNA3.1- myc co-transfection.

Ligand	Maximum response	LogEC ₅₀ ± st. error	EC ₅₀ (nM)	R ²	n
MC ₃ -ACTH ₍₁₋₃₉₎	1930	-8.576 ± 0.182	2.65	0.93	4
MC ₃ /MRAP2 (0.5 ng) - ACTH ₍₁₋₃₉₎	2695	-8.534 ± 0.163	2.921	0.98	4
MC ₃ /MRAP2 (5 ng) ACTH ₍₁₋₃₉₎	1033	-8.297 ± 0.585	5.051	0.81	4
MC ₃ -NDP- α -MSH	3437	-7.016 ± 0.191	96.37	0.97	1
MC ₃ /MRAP2 (0.5 ng)- NDP- α -MSH	1903	-8.746 ± 0.767	1.79	0.88	1
MC ₃ - D-Trp ⁸ - γ -MSH	3072	-7.73 ± 0.159	18.64	0.99	1
MC ₃ /MRAP2 (0.5 ng)- D-Trp ⁸ - γ -MSH	2964	-7.738 ± 0.244	18.27	0.98	1

The table represents a summary of 5 observations per well recorded by Glomax[®] multisystem plate reader of MC₃-ACTH₍₁₋₃₉₎ (n = 4, EC₅₀ = 2.65 nM), MC₃/MRAP2 (5 ng) - ACTH₍₁₋₃₉₎ (n = 4, EC₅₀ = 5.051) MC₃/MRAP2 (0.5 ng) - ACTH₍₁₋₃₉₎ (n = 4, EC₅₀ = 2.921), MC₃-NDP- α -MSH (n = 1, EC₅₀ = 96.37), MC₃/MRAP1-NDP- α -MSH (n = 1, EC₅₀ = 1.79), MC₃- D-Trp⁸- γ -MSH (n = 1, EC₅₀ = 18.64) and MC₃/MRAP1- D-Trp⁸- γ -MSH (n = 1, EC₅₀ = 18.27). The data in the table was generated using the log (dose) vs. response non-linear regression curve in GraphPad (Prism 7.04, USA).

8. 3. 5 HTLA cell viability

The MTT assay was carried out to check the cytotoxicity of the MC₃-transfection and co-transfection with either MRAP1-pCDNA3.1 or MRAP2-myc. The MTT assay reflects the metabolic activity of the HTLA cells. This is through the reduction of tetrazolium compound to the purple formazan crystals that then is solubilised using DMSO. Therefore, the more purple crystals, the more viable cells.

As seen in Figure 8.14, the viability assays showed, although insignificant, an increased percentage of cell viability in the transfected and co-transfected unstimulated cells. The viability percentages were 122.2% for MC₃-Tango transfected HTLA cells. The co-transfection had increased this percentage furthermore to 175.8% for MC₃-Tango/ MRAP1-pCDNA3.1 and about 168% MC₃-Tango/ (0.5 ng or 5 ng) MRAP2-myc.

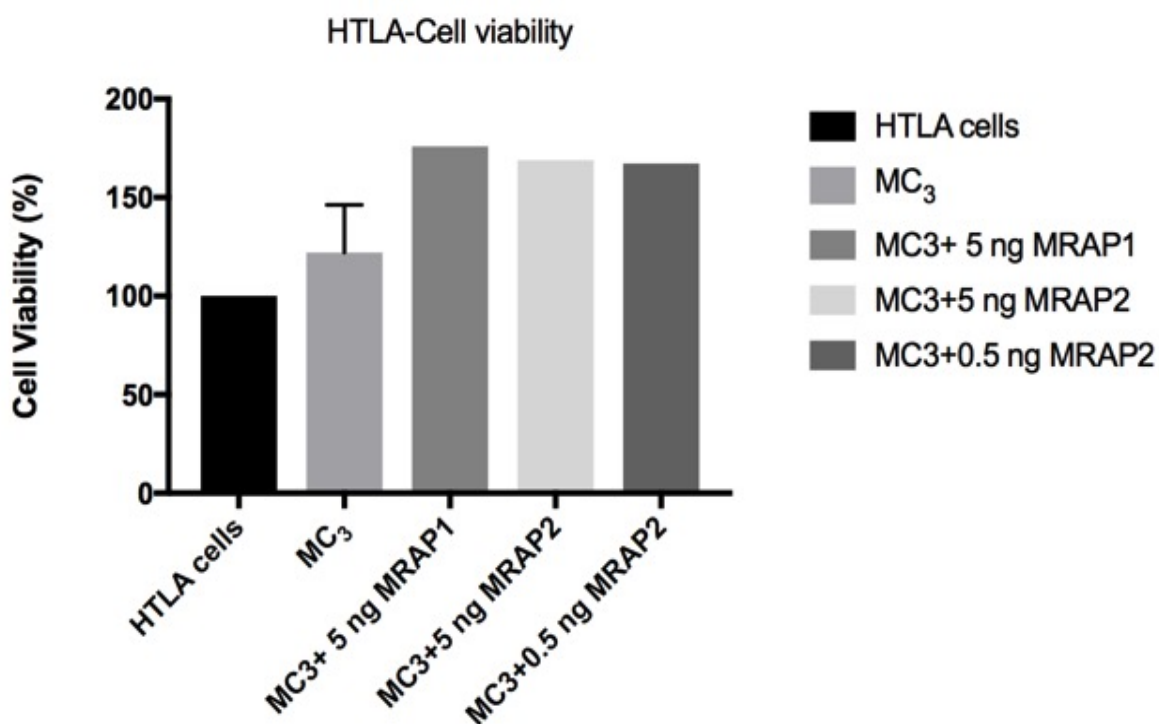


Figure 8.14: Cell viability of transfected and co-transfected HTLA cells. The bar charts a for MC₃-Tango transfected cells (n = 3), MC₃-Tango/ MRAP1-pCDNA3.1 co-transfection (n = 1) and MC₃-Tango/ (0.5 ng or 5 ng) MRAP2-myc co-transfection. The absorbance readings were obtained using SPECTROstar^{Nano} microplate reader (BMG LABTECH, UK) and the Bar chart was generated using GraphPad (Prism 7.04, USA).

8. 4 Discussion

The PRESTO-Tango assays revealed MC₃ has different responses to the melanocortin analogues depending on the presence or absence of MRAPs. The highest β -arrestin response was observed when MC₃ was stimulated with NDP- α -MSH (MTI), followed by ACTH₍₁₋₃₉₎ and then D-Trp⁸- γ -MSH. Interestingly, the efficacy and potency of MTI and ACTH₍₁₋₃₉₎ was markedly increased when MC₃ was co-expressed with MRAP1 in the HTLA cells compared to MC₃ alone. Although the efficacy of D-Trp⁸- γ -MSH appeared to increase with MC₃/ MRAP1 co-expression, the potency was found to be reduced (about 30 nM increase in the EC₅₀ values). The co-expression of MC₃/ MRAP2 had different effects on the ligand potencies depending on the amount of MRAP2 introduced into the cells. A low MRAP2 concentration (0.5 ng) did not cause a substantial change in the potency of ACTH₍₁₋₃₉₎, and the same effect was observed with D-Trp⁸- γ -MSH. The potency of NDP- α -MSH was reduced in the presence of low MRAP2 concentration by about 5 nM. The co-transfection of higher amounts of MRAP2 (5 ng) caused a decline in both the efficacy and the potency of ACTH₍₁₋₃₉₎ by about 900 RLU and 3 nM respectively. The β -arrestin recruitment activity was absent when the MC₃ transfected cells were treated with either SHU9119 alone or together with NDP- α -MSH.

The surface expression of the MC₃-Tango was confirmed by immunohistochemistry using an anti-flag antibody by Dr Kroeze and colleagues in 2015. This is the first report of validating MC₃-Tango activity in recruiting β -arrestin by bypassing activation of the G-subunits signalling cascades (PRESTO-Tango assays); using different melanocortin ligands, including the peptides that were not be validated previously (ACTH₍₁₋₃₉₎, D-Trp⁸- γ -MSH and SHU9119). The main purpose of developing such a platform was to establish a functional screening of the GPCR-ome in parallel independent of the diverse second messenger activation pathways. However, this platform also enables the investigation of the efficacy and potency of ligands of almost all the GPCR family members as well as being useful in the identification of new ligands for the orphan receptors. In addition, the PRESTO-Tango assay could also be used in studying the effect of the heterodimerisation of different GPCR either of the same sub-family (such as the five melanocortin receptors) or different members of the larger GPCR family members that are known to recruit the β -arrestin as part of their different activated signalling pathways.

Stimulating β -arrestin recruitment via most of the GPCRs occurs through the activation of GPCR dependent kinases (GRKs). This leads to the phosphorylation of the intracellular domains (either the C-terminal or the third intercellular loop) of the GPCR leading to the desensitisation of the receptor and at the same time activating β -arrestin dependent signalling pathway, finally resulting in uncoupling of the G-protein and internalisation of the receptor through clathrin-coated vesicles (Lohse and Hoffmann, 2014). MC₃ was found to be co-localised in endocytic lysosomal vesicles after γ_2 -MSH treatment. This internalisation was claimed to be mediated by PKC (Wachira *et al.*, 2006) and this could be the pathway adopted by the other γ -MSH analogue, D-Trp⁸- γ -MSH used in this research. However, other phosphorylation pathways were reported to be activated by the melanocortin receptors. These include β -arrestin recruitment via activation of the Pi3K/ERK1/2 and GRKs dependent pathways after α -MSH analogue treatment (Sánchez-Laorden *et al.*, 2007; Rodrigues *et al.*, 2012) Therefore, there are different pathways that could be activated by the different melanocortin ligands used in this research, since MC₃ is known to have an affinity to all the melanocortin peptides (see table 8.1 for details of MC₃ affinity). Stimulating the MC₃-transfected cells with the selective agonist PG990 did not recruit β -arrestin and this might require further optimisation or suggest that the stimulation of MC₃-transfectant cells with PG990 requires the co-transfection of either of the MRAPs, this could not be achieved in this thesis as time did not allow.

The efficacy of the melanocortin ligands was found to be modulated by the co-expression of MC₃ with MRAP1. Previously, MRAP1 was thought to mainly regulate the expression and signalling of MC₂ in the adrenal gland (Metherell *et al.*, 2005). After that, different studies had reported different MRAP1 effects on other melanocortin receptors such as MC₅, which was found to have less surface expression in the presence of MRAP1 (Chan *et al.*, 2009; Sebag and Hinkle, 2009). In this current study, MRAP1 was found to increase the efficacy of all three tested melanocortin ligands (ACTH₍₁₋₃₉₎, NDP- α -MSH and D-Trp⁸- γ -MSH), although the potency of D-Trp⁸- γ -MSH was found to be reduced. The decreased potency could be as a result of MRAP1 affecting the number of MC₃ receptors binding D-Trp⁸- γ -MSH.

In contrast to the high dependency of MC₂ expression and signalling on the colocalization with MRAP1, MC₃ was found expressed on the cell surface after cell

transfection and without being co-expressed with any of the MRAPs (Kroeze *et al.*, 2015). These findings are consistent with (Chan *et al.*, 2009) data that reported unchanged MC₃ surface expression in MC₃/MRAP1 or MRAP2 co-transfectant CHO cells. Also, MC₃ did not appear to rely entirely on MRAP1 for recruiting β -arrestin when stimulated with the different melanocortin analogues. However, MRAP1 did increase the sensitivity to these ligands and this could be translated to the requirement of the MRAP1 in pathophysiological conditions that cause alterations in the expression of MC₃.

Using different concentrations of MRAP1 in co-transfecting the HTLA cells with MC₃, only 5 ng of MRAP1-pCDNA3.1-FLAG caused a significant increase in the luminescence activity when the MC₃-Tango: MRAP1 co-transfected cells were stimulated with ACTH₍₁₋₃₉₎. Lower (2.5 ng) or higher concentrations (10 ng and 20 ng) of MRAP1-pCDNA3.1-FLAG caused a reduction in the luminescent activity of activated MC₃-Tango: MRAP1 co-transfected cells (see appendix 8 for MRAP1 different concentrations graphs).

As already mentioned, MRAP2 did have different regulatory effects on the potency ACTH₍₁₋₃₉₎ which was reduced with a high concentration of MRAP2. This is in agreement with previous studies that also used higher concentrations of MRAP2 in co-expression studies with either MC₂, MC₄ and/or MC₅ (Sebag and Hinkle, 2010, 2009; Kay *et al.*, 2015). Whereas, a relative low amount of MRAP2 plasmid co-transfected with MC₃ increased the latter's sensitivity to ACTH₍₁₋₃₉₎ and NDP- α -MSH. Some physiological conditions, such as pregnancy, may cause alterations in the responses to the melanocortin peptides by the melanocortin receptors (Ladyman *et al.*, 2016). The findings by Ladyman and colleagues might be attributed to fluctuation in MRAP2 expression and its effect on melanocortin and non-melanocortin receptors' responses to their ligands based on the physiological requirements. Recent data that reported the regulation of non-melanocortin receptors by MRAP2, support this claim; for instance, GHSR1-a had increased response when co-expressed with MRAP2 (Srisai *et al.*, 2017).

One unanticipated finding was the increased cell viability of MC₃-transfected cells after the introduction of either of the MRAPs. Increased cell viability in the MTT assays could be related to increased mitochondrial enzymatic activity by the transfected cells.

However, as this group of studies was conducted only twice, further repetition of the MTT assay should be considered to rule out experimental errors. If the data obtained afterwards were matching the current study's finding, further investigations are required to identify the effect exerted by the MRAPs on the HTLA cellular proliferation.

This research study had shown the MC₃ response is regulated by both MRAP1 and MRAP2. This regulation appeared to be dependent on the specific melanocortin peptides used in the PRESTO-Tango assay. Also, the introduction of MRAP2 plasmid DNA at different amounts was found to differently affect the sensitivity of MC₃ to the melanocortin analogues.

Some of the objectives planned, but could not be accomplished because of lack of time, were to investigate MC₃ sensitivity to the different melanocortin peptides when co-expressed with both of the melanocortin accessory proteins, MRAP1 and MRAP2, as (Chan *et al.*, 2009) has reported dimerisation of both accessory proteins. As mentioned earlier, the PRESTO-Tango assay permits examination of the coupling of different GPCRs and if the time and sufficient budget allowed, this research study would have included examining the melanocortin analogues' response after the dimerisation of MC₃ with the other melanocortin receptors as previous studies reported MC₁ and MC₅ dimerisation (Kobayashi *et al.*, 2016). This series of studies would also have examined the response of the MCs dimerisation in the presence of either of MRAP1 or MRAP2. Furthermore, the PRESTO-Tango studies could have also aimed to investigate the dimerisation of the melanocortin receptors with other GPCR such as corticotropin hormone receptor (CRHR), dopamine receptors (DRD1 and DRD2) and somatostatin receptors (SSTR2) which might help identification of the mechanisms through which specific regulatory networks (such as the paracrine anterior and intermediate pituitary gland network) control different physiological functions.

9 Discussion and future recommendations

9. 1 General Discussion

This research was set out to characterise the MC system in the reproductive axis of the female C57BL/6 mouse and to examine the effect of age and pregnancy on the expression of the MC system. The RT-qPCR expression studies have demonstrated the expression of most of the MC system members at all levels of the female mouse reproductive axis (the hypothalamus, the pituitary gland and the ovary) as well as the uterus. This research reports, for the first time, the expression of MRAP1 in the hypothalamus and the pituitary gland. The hypothalamus and the pituitary gland of the female mouse had higher expression levels of the MC system compared to the ovary and the uterus. Age and pregnancy were shown to regulate the expression of some of the MC system member in female reproductive axis (MC₅ and POMC) and the uterus. The RNAscope[®] identified the expression of MC₃, MC₅ and MRAP2 in the hypothalamus, the pituitary gland, the ovary and the uterus providing information about expression in specific cell types and areas related to controlling the reproductive function in organ. The RNAscope[®] confirmed MC₃ (although non- significant), MC₅ and MRAP2 expression to be affected by age and pregnancy. The RNAscope[®] studies enabled double expression of MC₃/MRAP2 in these tissues which indicated a potential regulatory role of MC₃ by MRAP2. Following the expression studies, in vitro cell studies focussed on MC₃ utilising the PRESTO-Tango GPCRome screening assay which showed firstly that MC₃ responded differently to the melanocortin analogues and secondly that MC₃ responsiveness was affected by MRAPs.

The gene expression of the MC system studies was preceded by GeNorm reference genes expression stability analyses to select the most stable reference gene(s) for each tissue. The GeNorm analysis had shown a fluctuation in the expression of some of the most commonly used reference genes such as ACTB and 18S, in agreement with previous studies suggesting the requirement to select stable reference genes according to experimental conditions and tissues (Siegert and Nitsche, 2004; Pfaffl *et al.*, 2004; Andersen *et al.*, 2004). Furthermore, the expression stability of each of the reference genes varied between the hypothalamus, the pituitary gland, the ovary and the uterus. The most stable reference genes were CANX and YWHAZ in both the hypothalamus and the pituitary gland; ATP5B and GAPDH in the ovary and ACTB, ATP5B and YWHAZ in the uterus. These genes were used in the normalisation of the data obtained from the RT-qPCR expression studies of the MC system and are

recommended for future RT-qPCR analyses of these tissues over the commonly used ACTB, GAPDH and 18S.

In the hypothalamus, the cellular characterisation of MC₃, MC₅ and MRAP2 revealed expression in the preoptic areas and the arcuate nucleus. These areas are known to contain functionally different GnRH cell populations and the preoptic area is known to mediate the ovulatory function of GnRH by stimulating the LH surge (Herbison, 2014). A direct role of α -MSH in mediating the medial preoptic GnRH firing activity was suggested after the detection of MC₄ in the mPOA GnRH cells (Israel *et al.*, 2012). This function could also be mediated by either of the melanocortin receptors identified in the current research, as Israel and colleagues were using non-selective melanocortin peptides. The arcuate was also reported to control the pulsatile release of GnRH through kisspeptin (Clarkson *et al.*, 2017). However, a recent study reports the inadequacy of kisspeptin to control the GnRH pulse generator by itself (León *et al.*, 2016) which might indicate the requirement of other neuropeptides and their receptors, such as the melanocortin receptors, to maintain the pulsatility of the GnRH. The RNAscope[®] assays had shown the consistency of the MC₃ data with that of the RT-qPCR and in both studies neither age nor pregnancy affected MC₃ expression.

MC₅ had much lower expression in all areas of the hypothalamus compared to MC₃ and the results were consistent with low expression detected by RT-qPCR. Murray *et al.* (2006) reported that LH release stimulated by the administration of MCH in the preoptic areas was mediated by activation of MC₅, further investigations are required to elucidate the exact role of MC₅. A developmental, behavioural or weaning role might be mediated by MC₅, since MC₅ expression was higher in pre-weaned female mice (2 weeks) than older animals.

Global hypothalamic expression of MRAP2 was observed at the level of the mPOA and was higher in pre-weaned and pregnant female mice. The co-expression studies showed a high number of cells expressing MRAP2 alone, as well as cells with double expression of MRAP2 with MC₃; this possibly implicates novel regulatory pathways mediated by MRAP2 in the hypothalamus which might be MC independent, as reported by (Chaly *et al.*, 2016; Srisai *et al.*, 2017).

Expression of the melanocortin system suggests it has a regulatory role within both the anterior and intermediate pituitary gland. Both MC₃ and MRAP2 mRNA transcripts

were co-localized in both somatotrophs and gonadotrophs indicating direct communication between the melanocortin system and the anterior pituitary cells. A previous study had reported the expression of MC₃ in the lactotrophs of immature rat (Lorsignol *et al.*, 1999) and more studies had identified different roles of the melanocortin peptides in the anterior pituitary (Lorsignol *et al.*, 1999; Matsumura *et al.*, 2003, 2004). The detection of MC₃ in the gonadotrophs support a role for MC₃ regulating of LH and FSH expression (Jiang *et al.*, 2017). However, Jiang and colleagues had hypothesised this role to be mediated through a paracrine mechanism via lactotrophs: the results described herein suggest a more direct role.

Age and pregnancy were found to regulate MRAP2 expression, with a rise seen in older female animals and during pregnancy, indicating increasing demand for MRAP2 by different receptors during those stages. A mild reduction in the double expression of MC₃ / MRAP2 during pregnancy was observed, which might indicate a role for MRAP2 independent to that of MC₃. (Chan *et al.*, 2009) had reported that MC₃ expression was not affected by the absence of both of the MRAPs. The detection of MC₃ and MRAP2 in the intermediate lobe of the pituitary glands implies an autoregulatory pathway of MC₃ on melanotroph functions. In contrast to the hypothalamus RNAscope[®] expression study, the pituitary RNAscope[®] showed MC₅ to be higher in older females. Previous studies had shown expression of MC₅ in the GH3 cell lines and rat pituitary (Langouche *et al.*, 2004, 2001) but an exact role mediated by the MC₅ had not been determined.

RT-qPCR, revealed relatively high levels of POMC expression; the pituitary gland produces POMC through two different cells, the melanotrophs and corticotrophs, and both produce different POMC fragments (α -MSH and ACTH respectively) (Mollard *et al.*, 2012). Interestingly, AgRP was found expressed in the pituitary gland, which supports the previous report of AgRP stimulation on prolactin release (Langouche *et al.*, 2004).

Compared to the hypothalamus and the pituitary gland, the ovary and the uterus had lower expression of melanocortin receptors. Interestingly in both ovary and uterus, MC₅ expression was detected in all compartments. In the ovary, MC₅ was detected in the follicular cells and in the interstitial tissue of the stroma. RT-qPCR showed a mild rise in the expression of MC₅, and to a lesser extent MC₄, in the pre-weaned animals,

which might indicate its contribution in the ovarian proliferation during the postnatal period. Furthermore, MC₄ and MC₅ could be involved in ovarian steroidogenesis and this is supported by reports of the lipolytic action of both receptors through their selective agonists LY2112688 and PG-901 respectively (Møller *et al.*, 2015). In pregnancy MC₄ was detected at very low levels whilst MC₅ was not detected at all.

The detection of MC₂ in the ovary, with a significant reduction in pregnancy might imply a role in regulating the corpus luteum function through progesterone as reported by (Guelfi *et al.*, 2011) in pseudopregnant rabbits. Since the expression profile of MRAP1 was opposite to that of MC₂, the regulation of MC₂ might have been mediated by MRAP2 which does not appear to be affected during pregnancy. The Guelfi study had also detected MC₁ and MC₃ in the ovaries of those rabbits. These findings bring back the argument about the specificity of the antibodies used against MC₁ and MC₃ in several studies (Kathpalia *et al.*, 2011; Ahmed, 2014; Dowejko, 2014; Holloway *et al.*, 2015) and the use of anti-MC₁ and anti-MC₃ should be carefully considered.

The uterus had few members of the MC system expressed, and those detected were at low levels; however, both MC₄ and MC₅ had a similar pattern of expression (with MC₅ showing a significant rise in the pre-weaned animals) implicating a similar role that is either mediated separately or through dimerisation; considering MC₄ is known to form heterodimers (Kobayashi *et al.*, 2016). Several functions could be mediated by MC₅, including the proliferation of the endometrial epithelia and stroma through either the activation of growth factors released from the uNK cells as suggested by (Lantang *et al.*, 2015); or through the Pi3K signalling pathway, essential for uterine gland development as reported by (Chang *et al.*, 2018). Even though the RT-qPCR analysis could not detect MC₃ in the uterus, the RNAscope[®] showed MC₃ in all compartments of the uterus of neonatal mice but at lower levels compared to that of MC₅. The roles suggested for MC₄ and MC₅ might also be mediated by MC₃.

In the mouse ovary and uterus, full-length POMC gene was not detected by RT-qPCR study, a shorter 5'-truncated gene transcript of POMC was detected at low levels in both tissues. This POMC variant is devoid of the signal sequence that directs the transcribed mRNA to the endoplasmic reticulum to be translated into functional protein (Ivell, 1994). Therefore, the MCs expressed in the ovary and systemically derived

melanocortin peptides most likely activate the uterus but more investigations are required to outline the function of truncated POMC in the ovary and the uterus.

The PRESTO-Tango assay (Kroeze *et al.*, 2015) has revealed interesting effects of MRAP1 on the MC₃ receptor; differences in MC₃ responses to the melanocortin analogues were observed, with NDP- α -MSH having the highest potency, followed by ACTH₍₁₋₃₉₎ and D-Trp ^{δ} - γ -MSH had the lowest potency. Those effects were altered in the presence of MRAP1 or MRAP2. The co-expression of MC₃ with MRAP1 caused a significant increase in the sensitivity of MC₃ to lower doses of NDP- α -MSH, ACTH₍₁₋₃₉₎ and D-Trp ^{δ} - γ -MSH. The co-expression with MRAP2 had a different effect on MC₃ than MRAP1; the level of the expression of the MRAP2 with 5 ng of MC₃ affected the response of MC₃ to ACTH₍₁₋₃₉₎ with a higher amount of transfected MRAP2 causing a significant decrease in the potency and efficacy of ACTH₍₁₋₃₉₎, whilst lower MRAP2 DNA in transfections caused a mild rise in NDP- α -MSH and ACTH₍₁₋₃₉₎ compared to the responsiveness of MC₃ alone contradicting (Chan *et al.*, 2009) findings. In MC₃ / MRAP2 co-expressing cells NDP- α -MSH elicited half the maximal response seen in the cells expressing MC₃ alone, this may indicate that the MRAP2 alters the saturation of the MC₃.

In conclusion, both RT-qPCR and RNAscope[®] demonstrated the expression of the melanocortin system in all levels of the HPO controlling female fertility. These findings provide further support for a role of the melanocortin system, potentially through stimulating GnRH activity, in modulating the anterior and intermediate pituitary functions, stimulating folliculogenesis, steroidogenesis, stimulating uterine proliferation and modulating an anti-inflammatory function. The exact mechanism of these processes is still a mystery. This research project is the first comprehensive study conducted to examine the MC system family members at all levels of the C57BL/6 female mouse reproductive axis. This series of studies has provided further understanding of the functions of the melanocortin system and lays the groundwork for future research into the functional analysis of the MC system in the C57BL/6 female mouse.

9. 2 Recommendations for future work

Further expression (both the RT-qPCR and the RNAscope®) studies are required in these tissues using more stages of the reproductive cycle to include different stages of the mouse estrous cycle; earlier and later stages of pregnancy, lactation and post weaning maternal samples. The localisation of the non-examined melanocortin receptors (MC₁, MC₂, MC₄ and MRAP1) using the RNAscope® expression studies either by singleplex or duplex to determine the localisation and the colocalization of MC₁, MC₂, MC₄ and MRAP1 in the mouse hypothalamus, pituitary, ovary and uterus. The RNAscope® duplex expression assay would be enhanced if MC probes could be used in conjunction with well-known cell-specific probes, which could include: GnRH in the hypothalamus; prolactin, TSH and POMC in the pituitary gland; CD31, CD56⁺ and *B4galt2* in the ovary; and VEGF, PI3K, CD10 and CD56⁺ in the uterus.

Finally, the PRESTO-Tango assay was established to study the regulation of MC₃ by the MRAPs. Additionally, this assay could be used with cells co-expressing other melanocortin receptors, particularly MC₅, and with either of the MRAPs the expression of which has been characterised here but, still has many questions left unanswered about its role and regulation. These studies could also include imaging studies using confocal microscopy to examine the receptors' expression and protein-protein interactions since the PRESTO-Tango constructs contain FLAG-tag epitopes which lend themselves to such studies. Future studies should also be conducted on human tissue samples to determine the melanocortin system expression in women.

References

- Abdel-Malek, Z.A. (2001). Melanocortin receptors: Their functions and regulation by physiological agonists and antagonists *Cellular and Molecular Life Sciences*. 58 (3), 434–441.
- Ahmed, T.J. (2014) *Translational research in rheumatoid arthritis: exploiting melanocortin receptors*. [Online]. Queen Mary, University of London.
- Amleh, A. and Dean, J. (2002). Mouse genetics provides insight into folliculogenesis, fertilization and early embryonic development *Human Reproduction Update*. 8 (5), 395–403.
- Amweg, A.N., Paredes, A., Salvetti, N.R., Lara, H.E. and Ortega, H.H. (2011). Expression of melanocortin receptors mRNA, and direct effects of ACTH on steroid secretion in the bovine ovary *Theriogenology*. 75 (4), 628–637.
- Andersen, G.M., Meyer, M.K., Nagaev, I. Nagaeva, O., Wikberg, J.E.S, *et al.* (2017). Regulated melanocortin receptor 1-5 gene expressions in CD56+ NK cells from two rheumatoid arthritis patients treated with adalimumab *J Immunol Infect Inflamm Dis*. 2 (1), 1–6.
- Andersen, C.L., Jensen, J.L. and Ørntoft, T.F. (2004). Normalization of real-time quantitative reverse transcription-PCR data: A model-based variance estimation approach to identify genes suited for normalization, applied to bladder and colon cancer data sets *Cancer Research*. 64 (15), 5245–5250.
- Asai, M., Ramachandrapa, S., Joachim, M., Shen, Y. and Zhang, R. *et al.* (2013). Loss of function of the melanocortin 2 receptor accessory protein 2 is associated with mammalian obesity *Science*. 341 (6143), 275–278.
- Avtanski, D., Novaira, H.J., Wu, S. and Romero, C.J. Kineman, R. *et al.* (2014). Both estrogen receptor α and β stimulate pituitary GH gene expression. *Molecular endocrinology (Baltimore, Md.)*. 28 (1), 40–52.
- Bachelot, A. and Binart, N. (2005). Corpus Luteum Development: Lessons from Genetic Models in Mice *Current Topics in Developmental Biology*. 68,49–84.

- Backholer, K., Bowden, M., Gamber, K., Bjørbæk, C. and Iqbal, J. *et al.* (2010). Melanocortins mimic the effects of leptin to restore reproductive function in lean hypogonadotropic ewes *Neuroendocrinology*. 91 (1), 27–40.
- Backholer, K., Smith, J. and Clarke, I.J. (2009). Melanocortins may stimulate reproduction by activating orexin neurons in the dorsomedial hypothalamus and kisspeptin neurons in the preoptic area of the ewe *Endocrinology*. 150 (12), 5488–5497.
- Bagnol, D., Lu, X.Y., Kaelin, C.B., Day, H.E. and Ollmann, M. *et al.* (1999). Anatomy of an endogenous antagonist: relationship between Agouti-related protein and proopiomelanocortin in brain. *The Journal of neuroscience : the official journal of the Society for Neuroscience*. 19 (18), RC26.
- Barnea, G., Strapps, W., Herrada, G., Berman, Y. and Ong, J. *et al.* (2008). The genetic design of signaling cascades to record receptor activation *Proceedings of the National Academy of Sciences*. 105 (1), 64–69.
- Barnett, K.R., Schilling, C., Greenfeld, C.R., Tomic, D. and Flaws, J.A. (2006). Ovarian follicle development and transgenic mouse models *Human Reproduction Update*. 12 (5), 537–555.
- Bartke, A. (1999). Role of growth hormone and prolactin in the control of reproduction: What are we learning from transgenic and knock-out animals? *Steroids*. 64 (9), 598–604.
- Bauer-Danton, A.C., Hollenberg, A.N. and Jameson, J.L. (1993). Dynamic regulation of gonadotropin-releasing hormone receptor mRNA levels in the anterior pituitary gland during the rat estrous cycle *Endocrinology*. 133 (4), 1911–1914.
- Beleche, T., Fairris, D. and Marks, M. (2012). Do course evaluations truly reflect student learning? Evidence from an objectively graded post-test *Economics of Education Review*. 31 (5), 709–719.
- Bhurke, A.S., Bagchi, I.C. and Bagchi, M.K. (2016). Progesterone-Regulated Endometrial Factors Controlling Implantation *American Journal of Reproductive Immunology*. 75 (3), 237–245.

- Bicknell, A.B. (2008). The tissue-specific processing of pro-opiomelanocortin *Journal of Neuroendocrinology*. 20 (6), 692–699.
- Binder, A.K., Winuthayanon, W., Hewitt, S.C., Couse, J.F. and Korach, K.S. (2014) 'Steroid Receptors in the Uterus and Ovary', in J. D Neill (ed.) *Knobil and Neill's Physiology of Reproduction: Two-Volume Set*. 4th edition. Elsevier. pp. 1099–1193.
- Bjelobaba, I., Janjic, M.M., Tavcar, J.S., Kucka, M. and Tomić, M. *et al.* (2016). The relationship between basal and regulated Gnhrh expression in rodent pituitary gonadotrophs *Molecular and Cellular Endocrinology*. 437,302–311.
- De Bond, J.A.P. and Smith, J.T. (2014). Kisspeptin and energy balance in reproduction *Reproduction*. 147 (3), R63.
- Boston, B.A. and Cone, R.D. (1996). Characterization of melanocortin receptor subtype expression in murine adipose tissues and in the 3T3-L1 cell line *Endocrinology*. 137 (5), 2043–2050.
- Bouzo-Lorenzo, M., Santo-Zas, I., Lodeiro, M., Nogueiras, R. and Casanueva, F.F. *et al.* (2016). Distinct phosphorylation sites on the ghrelin receptor, GHSR1a, establish a code that determines the functions of β -arrestins *Scientific Reports*. 6 (1), 22495.
- Breen, K.M., Thackray, V.G., Hsu, T., Mak-McCully, R.A. and Coss, D. *et al.* (2012). Stress Levels of Glucocorticoids Inhibit LH β -Subunit Gene Expression in Gonadotrope Cells *Molecular Endocrinology*. 26 (10), 1716–1731.
- Breit, A., Wolff, K., Kalwa, H., Jarry, H. and Büch, T. *et al.* (2006). The natural inverse agonist agouti-related protein induces arrestin-mediated endocytosis of melanocortin-3 and -4 receptors *Journal of Biological Chemistry*. 281 (49), 37447–37456.
- Bronson, F.H., Dagg, C.P. and Snell, G.D. (1968). *Chapter 11: Reproduction*. 2nd edition. E. L. Green (ed.). Dover.
- Budry, L., Lafont, C., El Yandouzi, T., Chauvet, N. and Conejero, G. *et al.* (2011). Related pituitary cell lineages develop into interdigitated 3D cell networks *Proceedings of the National Academy of Sciences*. 108 (30), 12515–12520.
- Buggy, J.J. (1998). Binding of α -melanocyte-stimulating hormone to its G-protein-coupled receptor on B-lymphocytes activates the Jak/STAT pathway *Biochemical Journal*. 331 (1), 211–216.

- Burger, H.G. (2002). Hormonal Changes in the Menopause Transition *Recent Progress in Hormone Research*. 57 (1), 257–275.
- Butler, A.A. and Cone, R.D. (2002). The melanocortin receptors: Lessons from knockout models *Neuropeptides*. 36 (2–3), 77–84.
- De Camilli, P., Macconi, D. and Spada, A. (1979). Dopamine inhibits adenylate cyclase in human prolactin-secreting pituitary adenomas [14] *Nature*. 278 (5701), 252–254.
- Cardoso, R.C., Alves, B.R.C., Prezotto, L.D., Thorson, J.F. and Tedeschi, L.O. *et al.* (2014). Reciprocal changes in leptin and NPY during nutritional acceleration of puberty in heifers *Journal of Endocrinology*. 223 (3), 289–298.
- Catania, A., Garofalo, L., Cutuli, M., Gringeri, A. and Santagostino, E. *et al.* (1998). Melanocortin peptides inhibit production of proinflammatory cytokines in blood of HIV-infected patients *Peptides*. 19 (6), 1099–1104.
- Catania, A., Gatti, S., Colombo, G. and Lipton, J.M. (2004). Targeting melanocortin receptors as a novel strategy to control inflammation. *Pharmacological reviews*. 56 (1), 1–29.
- Cerdá-Reverter, J.M., Ling, M.K., Schiöth, H.B. and Peter, R.E. (2003). Molecular cloning, characterization and brain mapping of the melanocortin 5 receptor in the goldfish *Journal of Neurochemistry*. 87 (6), 1354–1367.
- Cerda-Reverter, J.M., Ringholm, A., Schioth, H.B. and Peter, R.E. (2003). Molecular cloning, pharmacological characterization, and brain mapping of the melanocortin 4 receptor in the goldfish: involvement in the control of food intake *Endocrinology*. 144 (6), 2336–2349.
- Cha, J., Dey, S.K. and Lim, H. (2014) 'Embryo Implantation', in J.D. Neill (ed.) *Knobil and Neill's Physiology of Reproduction: Two-Volume Set*. 4th edition. Elsevier. pp. 1697–1739.
- Chai, B., Li, J.Y., Zhang, W., Ammori, J.B. and Mulholland, M.W. (2007). Melanocortin-3 receptor activates MAP kinase via PI3 kinase *Regulatory Peptides*. 139 (1–3), 115–121.

- Chaly, A.L., Srisai, D., Gardner, E.E. and Sebag, J.A. (2016). The melanocortin receptor accessory protein 2 promotes food intake through inhibition of the prokineticin receptor-1 *eLife*. 5,e12397.
- Chan, L.F., Webb, T.R., Chung, T.T., Meimaridou, E. and Cooray, S.N. *et al.* (2009). MRAP and MRAP2 are bidirectional regulators of the melanocortin receptor family *Proceedings of the National Academy of Sciences*. 106 (15), 6146–6151.
- Chang, H.J., Shin, H.S., Kim, T.H., Yoo, J.Y. and Teasley, H.E. *et al.* (2018). Pik3ca is required for mouse uterine gland development and pregnancy *PLoS ONE*. 13 (1), e0191433.
- Chen, W.-P., Witkin, J.W. and Silverman, A.-J. (1989). Beta-endorphin and gonadotropin-releasing hormone synaptic input to gonadotropin-releasing hormone neurosecretory cells in the male rat *The Journal of Comparative Neurology*. 286 (1), 85–95.
- Chen, X., Huang, L., Tan, H.Y., Li, H. and Wan, Y. *et al.* (2017). Deficient melanocortin-4 receptor causes abnormal reproductive neuroendocrine profile in female mice *Reproduction*. 153 (3), 267–276.
- Chhajlani, V. (1996). Distribution of cDNA for melanocortin receptor subtypes in human tissues. *Biochemistry and molecular biology international*. 38 (1), 73–80.
- Chhajlani, V., Muceniece, R. and Wikberg, J.E.S. (1993). Molecular cloning of a novel human melanocortin receptor *Biochemical and Biophysical Research Communications*. 195 (2), 866–873.
- Chhajlani, V. and Wikberg, J.E.S. (1992). Molecular cloning and expression of the human melanocyte stimulating hormone receptor cDNA *FEBS Letters*. 309 (3), 417–420.
- Childs, G. V. and Unabia, G. (2001). Epidermal growth factor and gonadotropin-releasing hormone stimulate proliferation of enriched population of gonadotropes *Endocrinology*. 142 (2), 847–853.
- Clark, A.J.L. (2016). The proopiomelanocortin gene: Discovery, deletion and disease *Journal of Molecular Endocrinology*. 56 (4), T27–T37.

Clarkson, J., Han, S.Y., Piet, R., McLennan, T. and Kane, G.M. *et al.* (2017). Definition of the hypothalamic GnRH pulse generator in mice *Proceedings of the National Academy of Sciences*. 114 (47), 201713897.

Clemson, C.M., Yost, J. and Taylor, A.W. (2017). The Role of Alpha-MSH as a Modulator of Ocular Immunobiology Exemplifies Mechanistic Differences between Melanocortins and Steroids *Ocular Immunology and Inflammation* 25 (2) p.179–189.

Cone, R.D. (2005). Anatomy and regulation of the central melanocortin system : Article : *Nature Neuroscience* *Nature neuroscience*. 8 (5), 571–578.

Cone, R.D. (1999). The central melanocortin system and its role in energy homeostasis *Annales d'endocrinologie*. 60 (1), 3–9.

Cooke, P.S., Nanjappa, M.K., Medrano, T.I., Lydon, J.P. and Bigsby, R.M. (2015). Role of estrogen and progesterone receptors in neonatal uterine cell proliferation in the mouse *Anim. Reprod* 12 (1).

Cottrell, E.C., Campbell, R.E., Han, S.-K. and Herbison, A.E. (2006). Postnatal Remodeling of Dendritic Structure and Spine Density in Gonadotropin-Releasing Hormone Neurons *Endocrinology*. 147 (8), 3652–3661.

Cowley, M.A., Smart, J.L., Rubinstein, M., Cerdán, M.G. and Diano, S. *et al.* (2001). Leptin activates anorexigenic POMC neurons through a neural network in the arcuate nucleus *Nature*. 411 (6836), 480–484.

Cowley, M.A., Smith, R.G., Diano, S., Tschöp, M. and Pronchuk, N. *et al.* (2003). The distribution and mechanism of action of ghrelin in the CNS demonstrates a novel hypothalamic circuit regulating energy homeostasis *Neuron*. 37 (4), 649–661.

Czieselsky, K., Prescott, M., Porteous, R., Campos, P. and Clarkson, J. *et al.* (2016). Pulse and Surge Profiles of Luteinizing Hormone Secretion in the Mouse *Endocrinology*. 157 (12), 4794–4802.

Denef, C. (2008). Paracrinicity: The story of 30 years of cellular pituitary crosstalk *Journal of Neuroendocrinology*. 20 (1), 1–70.

Denef, C. and Andries, M. (1983). Evidence for paracrine interaction between gonadotrophs and lactotrophs in pituitary cell aggregates *Endocrinology*. 112 (3), 813–822.

- Denzel, A., Molinari, M., Trigueros, C., Martin, J.E. and Velmurgan, S. *et al.* (2002). Early postnatal death and motor disorders in mice congenitally deficient in calnexin expression. *Molecular and cellular biology*. 22 (21), 7398–7404.
- Dowejko, M. (2014) *Characterization of MC3 and the other melancortin receptors (MC) in the hypothalamo-pituitary-gonadal system of the mouse*. [Online]. University of Westminster.
- Du, H. and Taylor, H.S. (2016). The role of hox genes in female reproductive tract development, adult function, and fertility *Cold Spring Harbor Perspectives in Medicine*. 6 (1), a023002.
- Dubois, S.L., Acosta-Martinez, M., DeJoseph, M.R., Wolfe, A. and Radovick, S. *et al.* (2015). Positive, but not negative feedback actions of estradiol in adult female mice require estrogen receptor alpha in kisspeptin neurons *Endocrinology*. 156 (3), 1111–1120.
- Dubois, S.L., Wolfe, A., Radovick, S., Boehm, U. and Levine, J.E. (2016). Estradiol restrains prepubertal gonadotropin secretion in female mice via activation of ER α in kisspeptin neurons *Endocrinology*. 157 (4), 1546–1554.
- Ducrest, A.L., Keller, L. and Roulin, A. (2008). Pleiotropy in the melanocortin system, coloration and behavioural syndromes *Trends in Ecology and Evolution*. 23 (9), 502–510.
- Durlinger, A.L.L., Kramer, P., Karels, B., De Jong, F.H. and Uilenbroek, J.T.J. *et al.* (1999). Control of primordial follicle recruitment by anti-mullerian hormone in the mouse ovary *Endocrinology*. 140 (12), 5789–5796.
- Egan, O.K., Inglis, M.A. and Anderson, G.M. (2017). Leptin Signaling in AgRP Neurons Modulates Puberty Onset and Adult Fertility in Mice *The Journal of Neuroscience*. 37 (14), 3875–3886.
- Eisinger, M., Li, W.H., Anthonavage, M., Pappas, A. and Zhang, L. *et al.* (2011). A melanocortin receptor 1 and 5 antagonist inhibits sebaceous gland differentiation and the production of sebum-specific lipids *Journal of Dermatological Science*. 63 (1), 23–32.

- Elias, C.F., Aschkenasi, C., Lee, C., Kelly, J. and Ahima, R.S. *et al.* (1999). Leptin differentially regulates NPY and POMC neurons projecting to the lateral hypothalamic area *Neuron*. 23 (4), 775–786.
- Espey, L. and Richards, J. (2006) 'Ovulation', in Jimmy D Neill (ed.) *Knobil and Neill's Physiology of Reproduction*. 3rd edition [Online]. Academic Press. pp. 425–474.
- Eyal, O., Jomain, J.-B., Kessler, C., Goffin, V. and Handwerger, S. (2007). Autocrine Prolactin Inhibits Human Uterine Decidualization: A Novel Role for Prolactin1 *Biology of Reproduction*. 76 (5), 777–783.
- Farkas, I., Vastagh, C., Sárvári, M. and Liposits, Z. (2013). Ghrelin Decreases Firing Activity of Gonadotropin-Releasing Hormone (GnRH) Neurons in an Estrous Cycle and Endocannabinoid Signaling Dependent Manner *PLoS ONE*. 8 (10), .
- Filant, J., DeMayo, F.J., Pru, J.K., Lydon, J.P. and Spencer, T.E. (2014). Fibroblast Growth Factor Receptor Two (FGFR2) Regulates Uterine Epithelial Integrity and Fertility in Mice *Biology of Reproduction*. 90 (1), .
- Filant, J., Zhou, H. and Spencer, T.E. (2012). Progesterone Inhibits Uterine Gland Development in the Neonatal Mouse Uterus1 *Biology of Reproduction*. 86 (5), .
- Freeman, M.E. (2006) 'Neuroendocrine control of the ovarian cycle of the rat', in Jimmy D Neill (ed.) *Knobil and Neill's Physiology of Reproduction*. 3rd edition [Online]. Elsevier. pp. 2327–2388.
- Furukawa, S., Kuroda, Y. and Sugiyama, A. (2014). A Comparison of the Histological Structure of the Placenta in Experimental Animals *Journal of Toxicologic Pathology*. 27 (1), 11–18.
- Gantz, I. and Fong, T.M. (2003). The melanocortin system: Table 1. *American Journal of Physiology - Endocrinology And Metabolism*. 284 (3), E468–E474.
- Gantz, I., Konda, Y., Tashiro, T., Shimoto, Y. and Miwa, H. *et al.* (1993). Molecular cloning of a novel melanocortin receptor. *The Journal of biological chemistry*.
- Gantz, I., Miwa, H., Konda, Y., Shimoto, Y. and Tashiro, T. *et al.* (1993). Molecular cloning, expression, and gene localization of a fourth melanocortin receptor *Journal of Biological Chemistry*. 268 (20), 15174–15179.

- Gantz, I., Shimoto, Y., Konda, Y., Miwa, H. and Dickinson, C.J. *et al.* (1994). Molecular cloning, expression, and characterization of a fifth melanocortin receptor. *Biochemical and biophysical research communications*. 200 (3), 1214–20.
- Gaynor, L.M. and Colucci, F. (2017). Uterine natural killer cells: Functional distinctions and influence on pregnancy in humans and mice *Frontiers in Immunology* 8 (4).
- Gellersen, B., Fernandes, M.S. and Brosens, J.J. (2009). Non-genomic progesterone actions in female reproduction *Human Reproduction Update*. 15 (1), 119–138.
- Getting, S.J. (2006). Targeting melanocortin receptors as potential novel therapeutics *Pharmacol. Ther.* 111 (1), 1–15.
- Getting, S.J., Kaneva, M., Bhadresa, Y., Renshaw, D. and Leoni, G. *et al.* (2009). Melanocortin peptide therapy for the treatment of arthritic pathologies *TheScientificWorldJournal*. 91394–1414.
- Gong, H., Chen, Y., Xu, J., Xie, X. and Yu, D. *et al.* (2017). The regulation of ovary and conceptus on the uterine natural killer cells during early pregnancy *Reproductive Biology and Endocrinology* 15 (1).
- Gonzalez, M.I., Kalia, V., Hole, D.R. and Wilson, C.A. (1997). alpha-Melanocyte-stimulating hormone (alpha-MSH) and melanin-concentrating hormone (MCH) modify monoaminergic levels in the preoptic area of the rat. *Peptides*. 18 (3), 387–392.
- Grandison, L. and Guidotti, A. (1977). Stimulation of food intake by muscimol and beta endorphin *Neuropharmacology*. 16 (7–8), 533–536.
- Grattan, D.R., Jasoni, C.L., Liu, X., Anderson, G.M. and Herbison, A.E. (2007). Prolactin regulation of gonadotropin-releasing hormone neurons to suppress luteinizing hormone secretion in mice *Endocrinology*. 148 (9), 4344–4351.
- Grattan, D.R. and Le Tissier, P. (2014) 'Hypothalamic Control of Prolactin Secretion, and the Multiple Reproductive Functions of Prolactin', in Jimmy D Neill (ed.) *Knobil and Neill's Physiology of Reproduction: Two-Volume Set*. 4th edition. Elsevier. pp. 469–526.
- Gray, C.A., Bartol, F.F., Tarleton, B.J., Wiley, A.A. and Johnson, G.A. *et al.* (2001). Developmental Biology of Uterine Glands *Biology of Reproduction*. 65 (5), 1311–1323.

Greenwald, G.S. and Rothchild, I. (1968). Formation and maintenance of corpora lutea in laboratory animals. *Journal of animal science* 27 p.139–162.

Griffin, J.E. and Ojeda, S.R. (2004) '*Textbook of endocrine physiology*', in S.R. Griffin, J.E. and Ojeda (ed.) 5th edition. Oxford University Press. pp. 209–260.

Gruenewald, D.A. and Matsumoto, A.M. (1991). Age-related decrease in proopiomelanocortin gene expression in the arcuate nucleus of the male rat brain. *Neurobiology of aging*. 12 (2), 113–121.

Guelfi, G., Zerani, M., Brecchia, G., Parillo, F. and Dall'Aglio, C. *et al.* (2011). Direct actions of ACTH on ovarian function of pseudopregnant rabbits *Molecular and Cellular Endocrinology*. 339 (1–2), 63–71.

Gutiérrez-pascual, E., Martínez-fuentes, A.J., Pinilla, L., Tena-Sempere, M. and Malagón, M.M. *et al.* (2007). Direct pituitary effects of kisspeptin: Activation of gonadotrophs and somatotrophs and stimulation of luteinising hormone and growth hormone secretion *Journal of Neuroendocrinology*. 19 (7), 521–530.

Han, S.Y., McLennan, T., Czieselsky, K. and Herbison, A.E. (2015). Selective optogenetic activation of arcuate kisspeptin neurons generates pulsatile luteinizing hormone secretion *Proceedings of the National Academy of Sciences*. 112 (42), 13109–13114.

Hayashi, K., Yoshioka, S., Reardon, S.N., Rucker, E.B. and Spencer, T.E. *et al.* (2011). WNTs in the Neonatal Mouse Uterus: Potential Regulation of Endometrial Gland Development *Biology of Reproduction*. 84 (2), 308–319.

He, W., Li, X., Adekunbi, D., Liu, Y. and Long, H. *et al.* (2017). Hypothalamic effects of progesterone on regulation of the pulsatile and surge release of luteinising hormone in female rats *Scientific Reports*. 7 (1), .

Henagan, T.M., Phillips, M.D., Cheek, D.J., Kirk, K.M. and Barbee, J.J. *et al.* (2011). The Melanocortin 3 receptor: A novel mediator of exercise-induced inflammation reduction in postmenopausal women? *Journal of Aging Research*. 2011.

Henderson, H.L., Townsend, J. and Tortonesi, D.J. (2008). Direct effects of prolactin and dopamine on the gonadotroph response to GnRH *Journal of Endocrinology*. 197 (2), 343–350.

Herbison, A.E. (2016). Control of puberty onset and fertility by gonadotropin-releasing hormone neurons *Nature Reviews Endocrinology*. 12 (8), 452–466.

Herbison, A.E. (2014) 'Physiology of the Adult Gonadotropin-Releasing Hormone Neuronal Network', in Jimmy D Neill (ed.) *Knobil and Neill's Physiology of Reproduction: Two-Volume Set*. 4th edition. Elsevier. pp. 399–467.

Herbison, A.E., Porteous, R., Pape, J.R., Mora, J.M. and Hurst, P.R. (2008). Gonadotropin-releasing hormone neuron requirements for puberty, ovulation, and fertility *Endocrinology*. 149 (2), 597–604.

Herraiz, C., Journé, F., Abdel-Malek, Z., Ghanem, G. and Jiménez-Cervantes, C. *et al.* (2011). Signaling from the Human Melanocortin 1 Receptor to ERK1 and ERK2 Mitogen-Activated Protein Kinases Involves Transactivation of cKIT *Molecular Endocrinology*. 25 (1), 138–156.

Hill, J.W., Elmquist, J.K. and Elias, C.F. (2008). Hypothalamic pathways linking energy balance and reproduction *American Journal of Physiology-Endocrinology and Metabolism*. 294 (5), E827–E832.

Hohlweg, W. and Junkmann, K. (1932). Die Hormonal-Nervöse Regulierung der Funktion des Hypophysenvorderlappens *Klinische Wochenschrift*. 11 (8), 321–323.

Hohmann, J.G., Teal, T.H., Clifton, D.K., Davis, J. and Hruby, V.J. *et al.* (2000). Differential role of melanocortins in mediating leptin's central effects on feeding and reproduction. *American journal of physiology. Regulatory, integrative and comparative physiology*. 278 (1), R50–R59.

Holloway, P.M., Durrenberger, P.F., Trutschl, M., Cvek, U. and Cooper, D. *et al.* (2015). Both MC1 and MC3 receptors provide protection from cerebral ischemia-reperfusion-induced neutrophil recruitment *Arteriosclerosis, Thrombosis, and Vascular Biology*. 35 (9), 1936–1944.

Hsu, K.F., Pan, H.A., Hsu, Y.Y., Wu, C.M. and Chung, W.J. *et al.* (2014). Enhanced myometrial autophagy in postpartum uterine involution *Taiwanese Journal of Obstetrics and Gynecology*. 53 (3), 293–302.

Huang, C.C., Orvis, G.D., Wang, Y. and Behringer, R.R. (2012). Stromal-to-epithelial transition during postpartum endometrial regeneration *PLoS ONE*. 7 (8), e44285.

Humphreys, M.H. (2004). γ -MSH, sodium metabolism, and salt-sensitive hypertension *American Journal of Physiology-Regulatory, Integrative and Comparative Physiology*. 286 (3), R417–R430.

Illytska, O. and Argyropoulos, G. (2008). The role of the Agouti-Related Protein in energy balance regulation. *Cellular and molecular life sciences : CMLS*. 65 (17), 2721–31.

Iqbal, J., Pompolo, S., Dumont, L.M., Wu, C.S. and Mountjoy, K.G. *et al.* (2001). Long-term alterations in body weight do not affect the expression of melanocortin receptor-3 and -4 mRNA in the ovine hypothalamus *Neuroscience*. 105 (4), 931–940.

Israel, D.D., Sheffer-Babila, S., De Luca, C., Jo, Y.H. and Liu, S.M. *et al.* (2012). Effects of leptin and melanocortin signaling interactions on pubertal development and reproduction *Endocrinology*. 153 (5), 2408–2419.

Ivell, R. (1994). The proopiomelanocortin gene is expressed as both full-length and 5'truncated transcripts in rodent Leydig cells *Reproduction, fertility and development*. 6 (6), 791–794.

Jackson, D.S., Ramachandrappa, S., Clark, A.J. and Chan, L.F. (2015). Melanocortin receptor accessory proteins in adrenal disease and obesity *Frontiers in Neuroscience*. 9 (5), 213.

Jaffer, S., Shynlova, O. and Lye, S. (2009). Mammalian target of rapamycin is activated in association with myometrial proliferation during pregnancy *Endocrinology*. 150 (10), 4672–4680.

Jennes, L., Stumpf, W.E. and Sheedy, A.E. (1985). Ultrastructural Characterization of Gonadotropin-Releasing Hormone (GnRH)-Producing Neurons *The Journal of Comparative Neurology*. 232 (4), 534–547.

Jiang, D.N., Li, J.T., Tao, Y.X., Chen, H.P. and Deng, S.P. *et al.* (2017). Effects of melanocortin-4 receptor agonists and antagonists on expression of genes related to reproduction in spotted scat, *Scatophagus argus* *Journal of Comparative Physiology B: Biochemical, Systemic, and Environmental Physiology*. 187 (4), 603–612.

Johnson, M.J. (2013) 'Essential Reproduction', in *Animal Reproduction Science*. 7th edition [Online]. Wiley-Blackwell. pp. 173–206.

- Kadokawa, H., Suzuki, S. and Hashizume, T. (2008). Kisspeptin-10 stimulates the secretion of growth hormone and prolactin directly from cultured bovine anterior pituitary cells *Animal Reproduction Science*. 105 (3–4), 404–408.
- Kanasaki, H., Oride, A. and Miyazaki, K. (2011). Paracrine Control of Gonadotrophs by Somatolactotrophs through TRH- induced Follistatin Production *The Open Neuroendocrinology Journal*. 4102–110.
- Kaneva, M.K., Kerrigan, M.J.P., Grieco, P., Curley, G.P. and Locke, I.C. *et al.* (2012). Chondroprotective and anti-inflammatory role of melanocortin peptides in TNF- α activated human C-20/A4 chondrocytes *British Journal of Pharmacology*. 167 (1), 67–79.
- Karch, F.J., Dierschke, D.J., Weick, R.F., Yamaji, T. and Hotchkiss, J. *et al.* (1973). Positive and negative feedback control by estrogen of luteinizing hormone secretion in the rhesus monkey *Endocrinology*. 92 (3), 799–804.
- Kathpalia, P.P., Charlton, C., Rajagopal, M. and Pao, A.C. (2011). The natriuretic mechanism of Gamma-Melanocyte-Stimulating Hormone *Peptides*. 32 (5), 1068–1072.
- Kay, E.I., Botha, R., Montgomery, J.M. and Mountjoy, K.G. (2013). hMRAP α increases α MSH-induced hMC1R and hMC3R functional coupling and hMC4R constitutive activity *Journal of Molecular Endocrinology*. 50 (2), 203–215.
- Kay, E.I., Botha, R., Montgomery, J.M. and Mountjoy, K.G. (2015). HMRAP α , but not hMRAP2, enhances hMC4R constitutive activity in HEK293 cells and this is not dependent on hMRAP α induced changes in hMC4R complex N-linked glycosylation *PLoS ONE*. 10 (10), e0140320.
- Kazi, A.A., Molitoris, K.H. and Koos, R.D. (2009). Estrogen rapidly activates the PI3K/AKT pathway and hypoxia-inducible factor 1 and induces vascular endothelial growth factor A expression in luminal epithelial cells of the rat uterus *Biol Reprod*. 81 (2), 378–387.
- Khorram, O., Castro, J.C.B. De, McCann, S.M. and De Castro, J.C.B. (1985). Stress-induced secretion of α -melanocyte-stimulating hormone and its physiological role in

modulating the secretion of prolactin and luteinizing hormone in the female rat *Endocrinology*. 117 (6), 2483–2489.

Kim, J., Bagchi, I.C. and Bagchi, M.K. (2009). Control of ovulation in mice by progesterone receptor-regulated gene networks *Molecular Human Reproduction*. 15 (12), 821–828.

Kimber, S.J. (2005). Leukaemia inhibitory factor in implantation and uterine biology *Reproduction* 130 (2) p.131–145.

Kluge, M., Schüssler, P., Schmidt, D., Uhr, M. and Steiger, A. (2012). Ghrelin suppresses secretion of Luteinizing Hormone (LH) and Follicle-Stimulating Hormone (FSH) in women *Journal of Clinical Endocrinology and Metabolism*. 97 (3), E448–E451.

Kobayashi, Y., Hamamoto, A., Takahashi, A. and Saito, Y. (2016). Dimerization of melanocortin receptor 1 (MC1R) and MC5R creates a ligand-dependent signal modulation: Potential participation in physiological color change in the flounder *General and Comparative Endocrinology*. 230–231 (5), 103–109.

Kokay, I.C., Petersen, S.L. and Grattan, D.R. (2011). Identification of prolactin-sensitive GABA and kisspeptin neurons in regions of the rat hypothalamus involved in the control of fertility *Endocrinology*. 152 (2), 526–535.

Konda, Y., Gantz, I., Delvalle, J., Shimoto, Y. and Miwa, H. *et al.* (1994). Interaction of dual intracellular signaling pathways activated by the melanocortin-3 receptor *The Journal of Biological Chemistry*. 269 (18), 13162–13166.

Korbonits, M., Bustin, S.A., Kojima, M., Jordan, S. and Adams, E.F. *et al.* (2001). The Expression of the Growth Hormone Secretagogue Receptor Ligand Ghrelin in Normal and Abnormal Human Pituitary and Other Neuroendocrine Tumors *The Journal of Clinical Endocrinology & Metabolism*. 86 (2), 881–887.

Kroeze, W.K., Sassano, M.F., Huang, X.P., Lansu, K., McCorvy, J.D., Giguère, P.M., Sciaky, N. and Roth, B.L. (2015). PRESTO-Tango as an open-source resource for interrogation of the druggable human GPCRome *Nature Structural and Molecular Biology*. 22 (5), 362–369.

- Krude, H. and Grüters, A. (2000). Implications of proopiomelanocortin (POMC) mutations in humans: The POMC deficiency syndrome *Trends in Endocrinology and Metabolism*. 11 (1), 15–22.
- Labbé, O., Desarnaud, F., Eggerickx, D., Vassart, G. and Parmentier, M. (1994). Molecular Cloning of a Mouse Melanocortin 5 Receptor Gene Widely Expressed in Peripheral Tissues *Biochemistry*. 33 (15), 4543–4549.
- Ladyman, S.R., Augustine, R.A., Scherf, E., Phillipps, H.R. and Brown, C.H. *et al.* (2016). Attenuated hypothalamic responses to α -melanocyte stimulating hormone during pregnancy in the rat *Journal of Physiology*. 594 (4), 1087–1101.
- Langouche, L., Hersmus, N., Papageorgiou, A., Vankelecom, H. and Deneef, C. (2004). Melanocortin peptides stimulate prolactin gene expression and prolactin accumulation in rat pituitary aggregate cell cultures *Journal of Neuroendocrinology*. 16 (8), 695–703.
- Langouche, L., Roudbaraki, M., Pals, K. and Deneef, C. (2001). Stimulation of intracellular free calcium in GH3 cells by γ 3-melanocyte-stimulating hormone. Involvement of a novel melanocortin receptor? *Endocrinology*. 142 (1), 257–266.
- Lantang, A.M., Innes, B.A., Gan, E.H., Pearce, S.H. and Lash, G.E. (2015). Expression of melanocortin receptors in human endometrium *Human Reproduction*. 30 (10), 2404–2410.
- Lee, Y.S., Challis, B.G., Thompson, D.A., Yeo, G.S.H. and Keogh, J.M. *et al.* (2006). A POMC variant implicates beta-melanocyte-stimulating hormone in the control of human energy balance *Cell Metabolism*. 3 (2), 135–140.
- León, S., Barroso, A., Vázquez, M.J., García-Galiano, D. and Manfredi-Lozano, M. *et al.* (2016). Direct Actions of Kisspeptins on GnRH Neurons Permit Attainment of Fertility but are Insufficient to Fully Preserve Gonadotropic Axis Activity *Scientific Reports*. 6 (1), 19206.
- Levine, J.E. (2014) 'Neuroendocrine Control of the Ovarian Cycle of the Rat', in Jimmy D Neill (ed.) *Knobil and Neill's Physiology of Reproduction: Two-Volume Set*. 4th edition. Elsevier. pp. 1199–1257.
- Levine, J.E. (1997). New concepts of the neuroendocrine regulation of gonadotropin surges in rats. *Biology of reproduction*. 56 (2), 293–302.

- Li, B., Matter, E.K., Hoppert, H.T., Grayson, B.E. and Seeley, R.J. *et al.* (2014). Identification of optimal reference genes for RT-qPCR in the rat hypothalamus and intestine for the study of obesity *International Journal of Obesity*. 38 (2), 192–197.
- Liang, J., Li, L., Jin, X., Xu, B. and Pi, L. *et al.* (2018). Pharmacological effect of human melanocortin-2 receptor accessory protein 2 variants on hypothalamic melanocortin receptors *Endocrine*. 61 (1), 94–104.
- Livak, K.J. and Schmittgen, T.D. (2001). Analysis of relative gene expression data using real-time quantitative PCR and *Methods*. 25 (4), 402–408.
- Lloyd, J.M., Scarbrough, K., Weiland, N.G. and Wise, P.M. (1991). Age-related changes in proopiomelanocortin (POMC) gene expression in the periarculate region of ovariectomized rats *Endocrinology*. 129 (4), 1896–1902.
- Loes, D.J., Barloon, T.J., Yuh, W.T.C., DeLaPaz, R.L. and Sato, Y. (1991). MR anatomy and pathology of the hypothalamus *American Journal of Roentgenology*. 156 (3), 579–585.
- Lohse, M.J. and Hoffmann, C. (2014). Arrestin interactions with G protein-coupled receptors *Handbook of Experimental Pharmacology*. 21915–56.
- Lorsignol, A., Vande Vijver, V., Ramaekers, D., Vankelecom, H. and Deneef, C. (1999). Detection of melanocortin-3 receptor mRNA in immature rat pituitary: Functional relation to gamma-3-MSH-induced changes in intracellular Ca²⁺ concentration? *Journal of Neuroendocrinology*. 11 (3), 171–179.
- Luckenbach, J.A., Dickey, J.T. and Swanson, P. (2010). Regulation of pituitary GnRH receptor and gonadotropin subunits by IGF1 and GnRH in prepubertal male coho salmon *General and Comparative Endocrinology*. 167 (3), 387–396.
- Machelon, V. and Emilie, D. (1997). Production of ovarian cytokines and their role in ovulation in the mammalian ovary. *European cytokine network*. 8 (2), 137–43.
- Magiakou, M.A., Mastorakos, G., Webster, E. and Chrousos, G.P. (1997). The hypothalamic-pituitary-adrenal axis and the female reproductive system *Adolescent Gynecology and Endocrinology: Basic and Clinical Aspects*. 816,42–56.
- Malik, S., Dolan, T.M., Maben, Z.J. and Hinkle, P.M. (2015). Adrenocorticotrophic hormone (ACTH) responses require actions of the melanocortin-2 receptor accessory

protein on the extracellular surface of the plasma membrane *Journal of Biological Chemistry*. 290 (46), 27972–27985.

Mandrika, I., Petrovska, R. and Wikberg, J. (2005). Melanocortin receptors form constitutive homo- and heterodimers *Biochemical and Biophysical Research Communications*. 326 (2), 349–354.

Manfredi-Lozano, M., Roa, J., Ruiz-Pino, F., Piet, R. and Garcia-Galiano, D. *et al.* (2016). Defining a novel leptin–melanocortin–kisspeptin pathway involved in the metabolic control of puberty *Molecular Metabolism*. 5 (10), 844–857.

Matsumura, R., Takagi, C., Kakeya, T., Okuda, K. and Takeuchi, S. *et al.* (2003). α -Melanocyte-Stimulating Hormone Stimulates Prolactin Secretion Through Melanocortin-3 Receptors Expressed in Mammotropes in the Mouse Pituitary *Neuroendocrinology*. 78 (2), 96–104.

Matsumura, R., Takeuchi, S. and Takahashi, S. (2004). Effect of estrogen on melanocortin-3 receptor mRNA expression in mouse pituitary glands in vivo and in vitro. *Neuroendocrinology*. 80 (3), 143–51.

McGee, E.A. and Hsueh, A.J.W. (2000). Initial and cyclic recruitment of ovarian follicles *Endocrine Reviews*. 21 (2), 200–214.

McNeilly, A.S. (2006) 'Suckling and the control of gonadotropin secretion', in Jimmy D Neill (ed.) *Knobil and Neill's Physiology of Reproduction*. 3rd edition [Online]. Academic Press. pp. 2511–2551.

Van Meerloo, J., Kaspers, G.J.L. and Cloos, J. (2011). Cell sensitivity assays: The MTT assay *Methods in Molecular Biology*. 731, 237–245.

Messinisi, I.E. (2006). Ovarian feedback, mechanism of action and possible clinical implications *Human Reproduction Update*. 12 (5), 557–571.

Metherell, L.A., Chapple, J.P., Cooray, S., David, A. and Becker, C. *et al.* (2005). Mutations in MRAP, encoding a new interacting partner of the ACTH receptor, cause familial glucocorticoid deficiency type 2 *Nature Genetics*. 37 (2), 166–170.

Millington, G.W.M., Tung, Y.C.L., Hewson, A.K., O'Rahilly, S. and Dickson, S.L. (2001). Differential effects of α -, β - and γ 2-melanocyte-stimulating hormones on

hypothalamic neuronal activation and feeding in the fasted rat *Neuroscience*. 108 (3), 437–445.

Millington, W.R., Rosenthal, D.W., Unal, C.B. and Nyquist-Battie, C. (1999). Localization of pro-opiomelanocortin mRNA transcripts and peptide immunoreactivity in rat heart *Cardiovascular Research*. 43 (1), 107–116.

Mitchner, N.A., Garlick, C. and Ben-Jonathan, N. (1998). Cellular Distribution and Gene Regulation of Estrogen Receptors α and β in the Rat Pituitary Gland *Endocrinology*. 139 (9), 3976–3983.

Moga, M.M., Saper, C.B. and Gray, T.S. (1990). Neuropeptide organization of the hypothalamic projection to the parabrachial nucleus in the rat *Journal of Comparative Neurology*. 295 (4), 662–682.

Molitch, M.E. (2000). *Pituitary and Adrenal Disorders of Pregnancy*. Feingold KR, Anawalt B, Boyce A, et al. (ed.). MDText.com, Inc.

Mollard, P., Hodson, D.J., Lafont, C., Rizzoti, K. and Drouin, J. (2012). A tridimensional view of pituitary development and function *Trends in Endocrinology and Metabolism*. 23 (6), 261–269.

Møller, C.L., Pedersen, S.B., Richelsen, B., Conde-Frieboes, K.W. and Raun, K. et al. (2015). Melanocortin agonists stimulate lipolysis in human adipose tissue explants but not in adipocytes Obesity *BMC Research Notes*. 8 (1), 559.

Morales, C. (2000). Different patterns of structural luteolysis in the human corpus luteum of menstruation *Human Reproduction*. 15 (10), 2119–2128.

Morgan, C. and Cone, R.D. (2006). Melanocortin-5 receptor deficiency in mice blocks a novel pathway influencing pheromone-induced aggression *Behavior Genetics*. 36 (2), 291–300.

Morley, A.A. (2014). Digital PCR: A brief history *Biomolecular Detection and Quantification*. 1 (1), 1–2.

Mountjoy, K.G., Robbins, L.S., Mortrud, M.T. and Cone, R.D. (1992). The cloning of a family of genes that encode the melanocortin receptors *Science*. 257 (5074), 1248–1251.

- Muceniece, R., Zvejniece, L., Kirjanova, O., Liepinsh, E. and Krigere, L. (2004). Beta- and Gamma -Melanocortins Inhibit Lipopolysaccharide Induced Nitric Oxide Production in Mice Brain *Brain research*. 995 (1), 7–13.
- Murray, J.F., Baker, B.I., Levy, A. and Wilson, C.A. (2000). The influence of gonadal steroids on pre-pro melanin-concentrating hormone mRNA in female rats *Journal of Neuroendocrinology*. 12 (1), 53–59.
- Murray, J.F., Hahn, J.D., Kennedy, A.R., Small, C.J. and Bloom, S.R. *et al.* (2006). Evidence for a stimulatory action of melanin-concentrating hormone on luteinising hormone release involving MCH1 and melanocortin-5 receptors *Journal of Neuroendocrinology*. 18 (3), 157–167.
- Nakanishi, S., Nakamura, M., Cohen, S.N., Numa, S. and Chang, A.C.Y. *et al.* (1979). Nucleotide sequence of cloned cDNA for bovine corticotropin- β -lipotropin precursor *Nature*. 278 (5703), 423–427.
- Nelson, J.F., Bender, M. and Schachter, B.S. (1988). Age-related changes in proopiomelanocortin messenger ribonucleic acid levels in hypothalamus and pituitary of female c57bl/6 j mice *Endocrinology*. 123 (1), 340–344.
- Neumann, E., Khawaja, K. and Müller-Ladner, U. (2014). G protein-coupled receptors in rheumatology *Nature Reviews Rheumatology*. 10 (7), 429–436.
- Nijenhuis, W.A.J. (2001). AgRP(83-132) Acts as an Inverse Agonist on the Human-Melanocortin-4 Receptor *Molecular Endocrinology*. 15 (1), 164–171.
- Nimura, M., Udagawa, J., Hatta, T., Hashimoto, R. and Otani, H. (2006). Spatial and temporal patterns of expression of melanocortin type 2 and 5 receptors in the fetal mouse tissues and organs *Anatomy and Embryology*. 211 (2), 109–117.
- Niswender, G.D., Juengel, J.L., Silva, P.J., Rollyson, M.K. and McIntush, E.W. (2000). Mechanisms controlling the function and life span of the corpus luteum. *Physiological reviews*. 80 (1), 1–29.
- Nocetto, C., Cragolini, A.B., Schiöth, H.B. and Scimonelli, T.N. (2004). Evidence that the effect of melanocortins on female sexual behavior in preoptic area is mediated by the MC3 receptor: Participation of nitric oxide *Behavioural Brain Research*. 153 (2), 537–541.

- Novoselova, T. V., Jackson, D., Campbell, D.C., Clark, A.J.L. and Chan, L.F. (2013). Melanocortin receptor accessory proteins in adrenal gland physiology and beyond *Journal of Endocrinology*. 217 (1), 1.
- Novoselova, T. V., Larder, R., Rimmington, D., Lelliott, C. and Wynn, E.H. *et al.* (2016). Loss of Mrap2 is associated with Sim1 deficiency and increased circulating cholesterol *Journal of Endocrinology*. 230 (1), 13–26.
- Okutsu, K., Ojima, F., Shinohara, N., Taniuchi, S. and Mizote, Y. *et al.* (2015). Functional characterization of the mouse melanocortin 3 receptor gene promoter *Gene*. 562 (1), 62–69.
- Özen, S., Özcan, N., Uçar, S.K., Gökşen, D. and Darcan, S. (2015). Unexpected clinical features in a female patient with proopiomelanocortin (POMC) deficiency *Journal of Pediatric Endocrinology and Metabolism*. 28 (5–6), 691–694.
- Padilla, S.L., Qiu, J., Nestor, C.C., Zhang, C. and Smith, A.W. *et al.* (2017). AgRP to Kiss1 neuron signaling links nutritional state and fertility *Proceedings of the National Academy of Sciences*. 114 (9), 2413–2418.
- Palombella, S., Pirrone, C., Cherubino, M., Valdatta, L. and Bernardini, G. *et al.* (2017). Identification of reference genes for qPCR analysis during hASC long culture maintenance *PLoS ONE*. 12 (2), e0170918.
- Parent, A.S., Lebrethon, M.C., Gérard, A., Vandersmissen, E. and Bourguignon, J.P. (2000). Leptin effects on pulsatile gonadotropin releasing hormone secretion from the adult rat hypothalamus and interaction with cocaine and amphetamine regulated transcript peptide and neuropeptide Y *Regulatory Peptides*. 92 (1–3), 17–24.
- Patel, H.B., Bombardieri, M., Sampaio, A.L.F., D'Acquisto, F. and Gray, M. *et al.* (2010). Anti-inflammatory and antiosteoclastogenesis properties of endogenous melanocortin receptor type 3 in experimental arthritis *The FASEB Journal*. 24 (12), 4835–4843.
- Paxinos, G. and Franklin, K.B.J. (2008). *The Mouse Brain in Stereotaxic Coordinates, Compact, Third Edition: The coronal plates and diagrams*. Amsterdam: Elsevier Academic Press.

- Peters, H. (1969). the Development of the Mouse Ovary From Birth To Maturity *European Journal of Endocrinology*. 62 (1), 98–116.
- Pfaffl, M.W. (2001). A new mathematical model for relative quantification in real-time RT-PCR *Nucleic Acids Research*. 29 (9), 45e–45.
- Pfaffl, M.W., Tichopad, A., Prgomet, C. and Neuvians, T.P. (2004). Determination of stable housekeeping genes, differentially regulated target genes and sample integrity: BestKeeper-Excel-based tool using pair-wise correlations. *Biotechnology letters*. 26 (6), 509–15.
- Piekorz, R.P., Gingras, S., Hoffmeyer, A., Ihle, J.N. and Weinstein, Y. (2005). Regulation of Progesterone Levels during Pregnancy and Parturition by Signal Transducer and Activator of Transcription 5 and 20 α -Hydroxysteroid Dehydrogenase *Molecular Endocrinology*. 19 (2), 431–440.
- Pilgrim, C. (1974). Histochemical Differentiation of Hypothalamic Areas *Progress in Brain Research*. 41 (C), 97–110.
- Pivonello, R., Ferone, D., De Herder, W.W., Kros, J.M. and Del Basso De Caro, M.L. *et al.* (2004). Dopamine Receptor Expression and Function in Corticotroph Pituitary Tumors *Journal of Clinical Endocrinology and Metabolism*. 89 (5), 2452–2462.
- Plant, T.M., Terasawa, E. and Witchel, S.F. (2014) 'Puberty in Non-human Primates and Man', in J. D. Neill (ed.) *Knobil and Neill's Physiology of Reproduction: Two-Volume Set*. 4th edition. Elsevier. pp. 1487–1536.
- Prevot, V. (2014) 'Puberty in Mice and Rats', in *Knobil and Neill's Physiology of Reproduction: Two-Volume Set*. 3rd edition. Elsevier. pp. 1395–1439.
- Puelles, L. and Rubenstein, J.L.R. (2015). A new scenario of hypothalamic organization: rationale of new hypotheses introduced in the updated prosomeric model *Frontiers in Neuroanatomy*. 9 (27), 10.3389.
- Rajkovic, A., Pangas, S.A. and Matzuk, M.M. (2006) 'Follicular development: Mouse, sheep, and human models', in *Knobil and Neill's Physiology of Reproduction*. [Online]. pp. 383–423.
- Ramathal, C.Y., Bagchi, I.C., Taylor, R.N. and Bagchi, M.K. (2010). Endometrial decidualization: Of mice and men *Seminars in Reproductive Medicine* 28 (1) p.17–26.

- Ramírez, D., Saba, J., Carniglia, L., Durand, D. and Lasaga, M. *et al.* (2015). Melanocortin 4 receptor activates ERK-cFos pathway to increase brain-derived neurotrophic factor expression in rat astrocytes and hypothalamus *Molecular and Cellular Endocrinology*. 411 (8), 28–37.
- Ratajczak, C.K. and Muglia, L.J. (2008). Insights into parturition biology from genetically altered mice *Pediatric Research* 64 (6) p.581–589.
- Rediger, A., Piechowski, C.L., Yi, C.X., Tarnow, P. and Strotmann, R. *et al.* (2011). Mutually opposite signal modulation by hypothalamic heterodimerization of ghrelin and melanocortin-3 receptors *Journal of Biological Chemistry*. 286 (45), 39623–39631.
- Redmann, S.M. and Argyropoulos, G. (2006). AgRP-deficiency could lead to increased lifespan *Biochemical and Biophysical Research Communications*. 351 (4), 860–864.
- Regard, J.B., Sato, I.T. and Coughlin, S.R. (2008). Anatomical Profiling of G Protein-Coupled Receptor Expression *Cell*. 135 (3), 561–571.
- Reichenbach, A., Steyn, F.J., Sleeman, M.W. and Andrews, Z.B. (2012). Ghrelin receptor expression and colocalization with anterior pituitary hormones using a GHSR-GFP mouse line *Endocrinology*. 153 (11), 5452–5466.
- Reinick, C.L., Liang, L., Angleson, J.K. and Dores, R.M. (2012). Identification of an MRAP-independent melanocortin-2 receptor: Functional expression of the cartilaginous fish, *Callorhynchus milii*, melanocortin-2 receptor in CHO cells *Endocrinology*. 153 (10), 4757–4765.
- Ren, J., Li, Y., Xu, N., Li, H. and Li, C. *et al.* (2017). Association of estradiol on expression of melanocortin receptors and their accessory proteins in the liver of chicken (*Gallus gallus*) *General and Comparative Endocrinology*. 240 (1), 182–190.
- Roberts, J.L. and Herbert, E. (1977). Characterization of a common precursor to corticotropin and beta-lipotropin: identification of beta-lipotropin peptides and their arrangement relative to corticotropin in the precursor synthesized in a cell-free system. *Proceedings of the National Academy of Sciences of the United States of America*. 74 (12), 5300–5304.

- Rocha, M., Bing, C., Williams, G. and Puerta, M. (2003). Pregnancy-induced hyperphagia is associated with increased gene expression of hypothalamic agouti-related peptide in rats *Regulatory Peptides*. 114 (2–3), 159–165.
- Rodrigues, A.R., Almeida, H. and Gouveia, A.M. (2012). Melanocortin 5 receptor signaling and internalization: Role of MAPK/ERK pathway and β -arrestins 1/2 *Molecular and Cellular Endocrinology*. 361 (1–2), 69–79.
- Rodrigues, A.R., Pignatelli, D., Almeida, H. and Gouveia, A.M. (2009). Melanocortin 5 receptor activates ERK1/2 through a PI3K-regulated signaling mechanism *Molecular and Cellular Endocrinology*. 303 (1–2), 74–81.
- Rønnekleiv, O.K., Fang, Y., Zhang, C., Nestor, C.C. and Mao, P. *et al.* (2014). Research Resource: Gene Profiling of G Protein–Coupled Receptors in the Arcuate Nucleus of the Female *Molecular Endocrinology*. 28 (8), 1362–1380.
- Roselli-Reh fuss, L., Mountjoy, K.G., Robbins, L.S., Mortrud, M.T. and Low, M.J. *et al.* (1993). Identification of a receptor for gamma melanotropin and other proopiomelanocortin peptides in the hypothalamus and limbic system. *Proceedings of the National Academy of Sciences*. 90 (19), 8856–8860.
- Rossi, S., Maisto, R., Gesualdo, C., Trotta, M.C. and Ferraraccio, F. *et al.* (2016). Activation of Melanocortin Receptors MC1 and MC5 Attenuates Retinal Damage in Experimental Diabetic Retinopathy *Mediators of Inflammation*. 2016,1–13.
- Rouault, A.A.J., Lee, A.A. and Sebag, J.A. (2017). Regions of MRAP2 required for the inhibition of orexin and prokineticin receptor signaling *Biochimica et Biophysica Acta - Molecular Cell Research*. 1864 (12), 2322–2329.
- Rowland, N.E., Schaub, J.W., Robertson, K.L., Andreasen, A. and Haskell-Luevano, C. (2010). Effect of MTII on food intake and brain c-Fos in melanocortin-3, melanocortin-4, and double MC3 and MC4 receptor knockout mice *Peptides*. 31 (12), 2314–2317.
- Russell, D.L. and Robker, R.L. (2007). Molecular mechanisms of ovulation: Coordination through the cumulus complex *Human Reproduction Update*. 13 (3), 289–312.

Sánchez-Laorden, B.L., Jiménez-Cervantes, C. and García-Borrón, J.C. (2007). Regulation of human melanocortin 1 receptor signaling and trafficking by Thr-308 and Ser-316 and its alteration in variant alleles associated with red hair and skin cancer *Journal of Biological Chemistry*. 282 (5), 3241–3251.

Sánchez, F. and Smitz, J. (2012). Molecular control of oogenesis *Biochimica et Biophysica Acta - Molecular Basis of Disease* 1822 (12) p.1896–1912.

Sandrock, M., Schulz, A., Merkwitz, C., Schöneberg, T. and Spaniel-Borowski, K. *et al.* (2009). Reduction in corpora lutea number in obese melanocortin-4-receptor-deficient mice *Reproductive Biology and Endocrinology*. 7 (7), 24.

Scarlett, J.M., Zhu, X., Enriori, P.J., Bowe, D.D. and Batra, A.K. *et al.* (2008). Regulation of agouti-related protein messenger ribonucleic acid transcription and peptide secretion by acute and chronic inflammation *Endocrinology*. 149 (10), 4837–4845.

Schellekens, H., Van Oeffelen, W.E.P.A., Dinan, T.G. and Cryan, J.F. (2013). Promiscuous dimerization of the growth hormone secretagogue receptor (GHS-R1a) attenuates ghrelin-mediated signaling *Journal of Biological Chemistry*. 288 (1), 181–191.

Schiöth, H.B. and Watanobe, H. (2002). Melanocortins and reproduction *Brain Research Reviews*. 38 (3), 340–350.

Scully, K.M. and Rosenfeld, M.G. (2002). Pituitary development: Regulatory codes in mammalian organogenesis *Science*. 295 (5563), 2231–2235.

Sebag, J.A. and Hinkle, P.M. (2009). Opposite effects of the melanocortin-2 (MC2) receptor accessory protein MRAP on MC2 and MC5 receptor dimerization and trafficking *Journal of Biological Chemistry*. 284 (34), 22641–22648.

Sebag, J.A. and Hinkle, P.M. (2010). Regulation of G protein-coupled receptor signaling: Specific dominant-negative effects of melanocortin 2 receptor accessory protein2 *Science Signaling*. 3 (116), ra28.

Sebag, J.A., Zhang, C., Hinkle, P.M., Bradshaw, A.M. and Cone, R.D. (2013). Developmental control of the melanocortin-4 receptor by MRAP2 proteins in zebrafish *Science*. 341 (6143), 278–281.

- Sherman, B.M. and Korenman, S.G. (1975). Hormonal characteristics of the human menstrual cycle throughout reproductive life *Journal of Clinical Investigation*. 55 (4), 699–706.
- Shin, S.H., Song, J.H. and Ross, G.M. (2010). Regulation of prolactin secretion: Dopamine is the prolactin-release inhibiting factor (PIF), but also plays a role as a releasing factor (PRF) *Korean Journal of Biological Sciences*. 3 (2), 103–113.
- Shynlova, O., Dorogin, A. and Lye, S.J. (2010). Stretch-induced uterine myocyte differentiation during rat pregnancy: involvement of caspase activation *Biology of reproduction*. 82 (6), 1248–1255.
- Shynlova, O., Lee, Y.H., Srikhajon, K. and Lye, S.J. (2013). Physiologic uterine inflammation and labor onset: Integration of endocrine and mechanical signals *Reproductive Sciences*. 20 (2), 154–167.
- Siegert, W. and Nitsche, A. (2004). Guideline to reference gene selection for quantitative real-time PCR *Biochemical and biophysical research communications*. 313 (4), 856–862.
- Silva, L.E.C.M., Castro, M., Amaral, F.C., Antunes-Rodrigues, J. and Elias, L.L.K. (2010). Estradiol-induced hypophagia is associated with the differential mRNA expression of hypothalamic neuropeptides *Brazilian Journal of Medical and Biological Research*. 43 (8), 759–766.
- Simamura, E., Shimada, H., Shoji, H., Otani, H. and Hatta, T. (2011). Effects of melanocortins on fetal development *Congenital Anomalies*. 51 (2), 47–54.
- Smith, A.I. and Funder, J.W. (1988). Proopiomelanocortin processing in the pituitary, central nervous system, and peripheral tissues *Endocrine Reviews*. 9 (1), 159–179.
- Snegovskikh, V., Park, J.S. and Norwitz, E.R. (2006). Endocrinology of parturition *Endocrinology and Metabolism Clinics of North America*. 35 (1), 173–191.
- Soloff, M.S., Jeng, Y.J., Izban, M.G., Sinha, M. and Luxon, B.A. *et al.* (2011). Effects of progesterone treatment on expression of genes involved in uterine quiescence *Reproductive Sciences*. 18 (8), 781–797.

- Spencer, T.E., Dunlap, K.A. and Filant, J. (2012). Comparative developmental biology of the uterus: Insights into mechanisms and developmental disruption *Molecular and Cellular Endocrinology*. 354 (1–2), 34–53.
- Spies, H.G. and Norman, R.L. (1975). Interaction of estradiol and lhrh on lh release in rhesus females: Evidence for a neural site of action *Endocrinology*. 97 (3), 685–692.
- Srisai, D., Yin, T.C., Lee, A.A., Rouault, A.A.J. and Pearson, N.A. *et al.* (2017). MRAP2 regulates ghrelin receptor signaling and hunger sensing *Nature Communications*. 8 (1), 713.
- Stefaneanu, L. (2001). Regulatory circuits of the pituitary gland *NeuroImmune Biology*. 1 (C), 99–113.
- Stefaneanu, L., Kovacs, K., Lloyd, R. V., Scheithauer, B.W. and Young, W.F. *et al.* (1992). Pituitary lactotrophs and somatotrophs in pregnancy: a correlative in situ hybridization and immunocytochemical study *Virchows Archiv B Cell Pathology Including Molecular Pathology*. 62 (1), 291–296.
- Stocco, C., Telleria, C. and Gibori, G. (2007). The molecular control of corpus luteum formation, function, and regression *Endocrine Reviews* 28 (1) p.117–149.
- Sugino, N. and Okuda, K. (2007). Species-related differences in the mechanism of apoptosis during structural luteolysis. *The Journal of reproduction and development*. 53 (5), 977–86.
- Sutton, B.S., Langefeld, C.D., Williams, A.H., Norris, J.M. and Saad, M.F. *et al.* (2005). Association of proopiomelanocortin gene polymorphisms with obesity in the IRAS family study *Obesity Research*. 13 (9), 1491–1498.
- Syrovatkina, V., Alegre, K.O., Dey, R. and Huang, X.Y. (2016). Regulation, Signaling, and Physiological Functions of G-Proteins *Journal of Molecular Biology*. 428 (19), 3850–3868.
- Takeuchi, S., Teshigawara, K. and Takahashi, S. (2000). Widespread expression of Agouti-related protein (AGRP) in the chicken: A possible involvement of AGRP in regulating peripheral melanocortin systems in the chicken *Biochimica et Biophysica Acta - Molecular Cell Research*. 1496 (2–3), 261–269.

- Tan, J., Paria, B.C., Dey, S.K. and Das, S.K. (1999). Differential uterine expression of estrogen and progesterone receptors correlates with uterine preparation for implantation and decidualization in the mouse *Endocrinology*. 140 (11), 5310–5321.
- Thomas, F.H. and Vanderhyden, B.C. (2006). Oocyte-granulosa cell interactions during mouse follicular development: Regulation of kit ligand expression and its role in oocyte growth *Reproductive Biology and Endocrinology*. 4 (19), .
- Tibbetts, T. a, Conneely, O.M. and O'Malley, B.W. (1999). Progesterone via its receptor antagonizes the pro-inflammatory activity of estrogen in the mouse uterus. *Biology of reproduction*. 60 (5), 1158–1165.
- Le Tissier, P.R., Hodson, D.J., Lafont, C., Fontanaud, P. and Schaeffer, M. *et al.* (2012). Anterior pituitary cell networks *Frontiers in Neuroendocrinology*. 33 (3), 252–266.
- Tong, Y. and Pelletier, G. (1992). Prolactin regulation of pro-opiomelanocortin gene expression in the arcuate nucleus of the rat hypothalamus *Neuroendocrinology*. 56 (4), 561–565.
- Tortonese, D.J. (2016). Intrapituitary mechanisms underlying the control of fertility: key players in seasonal breeding *Domestic Animal Endocrinology*. 56 (7), S191–S203.
- Vandesompele, J., De Preter, K., Pattyn, I., Poppe, B. and Van Roy, N. *et al.* (2002). Accurate normalization of real-time quantitative RT-PCR data by geometric averaging of multiple internal control genes *Genome Biology*. 3 (711), 34–1.
- Vastagh, C., Rodolosse, A., Solymosi, N. and Liposits, Z. (2016). Altered Expression of Genes Encoding Neurotransmitter Receptors in GnRH Neurons of Proestrous Mice *Frontiers in Cellular Neuroscience*. 10,230.
- Vongs, A., Lynn, N.M. and Rosenblum, C.I. (2004). Activation of MAP kinase by MC4-R through PI3 kinase *Regulatory Peptides*. 120 (1–3), 113–118.
- Wachira, J.M., Uradu, L. and Hughes-Darden, C. (2006). Activation and endocytic internalization of melanocortin 3 receptor in neuronal cells *The FASEB Journal*. 20 (4), A116–A116.
- Wachira, S.J., Hughes-Darden, C.A., Nicholas, H.B., Taylor, C. V. and Robinson, T.J. (2004). Neural melanocortin receptors are differentially expressed and regulated by

stress in rat hypothalamic-pituitary-adrenal axis. *Cellular and molecular biology (Noisy-le-Grand, France)*. 50 (6), 703–713.

Wang, H., Eriksson, H. and Sahlin, L. (2000). Estrogen receptors alpha and beta in the female reproductive tract of the rat during the estrous cycle. *Biology of reproduction*. 63 (5), 1331–1340.

Wang, L., DeFazio, R.A. and Moenter, S.M. (2016). Excitability and Burst Generation of AVPV Kisspeptin Neurons Are Regulated by the Estrous Cycle Via Multiple Conductances Modulated by Estradiol Action *eNeuro*. 3 (3), .

Wang, X., Wu, S.P. and DeMayo, F.J. (2017). Hormone dependent uterine epithelial-stromal communication for pregnancy support *Placenta*. 60,S20–S26.

Ward, D.R., Dear, F.M., Ward, I.A., Anderson, S.I. and Spergel, D.J. *et al.* (2009). Innervation of gonadotropin-releasing hormone neurons by peptidergic neurons conveying circadian or energy balance information in the mouse Paul A. Bartell (ed.) *PLoS ONE*. 4 (4), e5322.

Ward, R.D., Stone, B.M., Raetzman, L.T. and Camper, S.A. (2006). Cell Proliferation and Vascularization in Mouse Models of Pituitary Hormone Deficiency *Molecular Endocrinology*. 20 (6), 1378–1390.

Wassarman, P.M. and Josefowicz, W.J. (1978). Oocyte development in the mouse: An ultrastructural comparison of oocytes isolated at various stages of growth and meiotic competence *Journal of Morphology*. 156 (2), 209–235.

Watanobe, H., Schiöth, H.B., Wikberg, J.E.S. and Suda, T. (1999). The melanocortin 4 receptor mediates leptin stimulation of luteinizing hormone and prolactin surges in steroid-primed ovariectomized rats *Biochemical and Biophysical Research Communications*. 257 (3), 860–864.

Watson, E.D. (2005). Development of Structures and Transport Functions in the Mouse Placenta *Physiology*. 20 (3), 180–193.

Webb, T.R. and Clark, A.J.L. (2010). Minireview: The Melanocortin 2 Receptor Accessory Proteins *Molecular Endocrinology*. 24 (3), 475–484.

- De Wied, D. (1999). Behavioral pharmacology of neuropeptides related to melanocortins and the neurohypophyseal hormones *European Journal of Pharmacology*. 375 (1–3), 1–11.
- Wikberg, J.E.S., Muceniece, R., Mandrika, I., Prusis, P. and Lindblom, J. *et al.* (2000). New aspects on the melanocortins and their receptors *Pharmacological Research*. 42 (5), 393–420.
- Wilfonger, W.W., Larsen, W.J., Downs, T.R. and Wilbur, D.L. (1984). An in vitro model for studies of intercellular communication in cultured rat anterior pituitary cells *Tissue and Cell*. 16 (4), 483–497.
- Wilson, C.A., Thody, A.J., Hole, D.R., Grierson, J.P. and Celis, M.E. (1991). Interaction of Estradiol, Alpha-Melanocyte-Stimulating Hormone, and Dopamine in the Regulation of Sexual Receptivity in the Female Rat *Neuroendocrinology*. 54 (1), 14–22.
- Winterhoff, B. and Konecny, G.E. (2017). Targeting fibroblast growth factor pathways in endometrial cancer *Current Problems in Cancer*. 41 (1), 37–47.
- Wolf Horrell, E.M., Boulanger, M.C. and D’Orazio, J.A. (2016). Melanocortin 1 receptor: Structure, function, and regulation *Frontiers in Genetics*. 7 (5), .
- Wood, G.A., Fata, J.E., Watson, K.L.M. and Khokha, R. (2007). Circulating hormones and estrous stage predict cellular and stromal remodeling in murine uterus *Reproduction*. 133 (5), 1035–1044.
- Xia, L., Vanvugt, D., Alston, E.J., Luckhaus, J. and Ferin, M. (1992). A surge of gonadotropin-releasing hormone accompanies the estradiol-induced gonadotropin surge in the rhesus monkey *Endocrinology*. 131 (6), 2812–2820.
- Xia, Y., Wikberg, J.E.S. and Chhajlani, V. (1995). Expression of melanocortin 1 receptor in periaqueductal gray matter *Neuroreport*. 6 (16), 2193–2196.
- Xu, Y., Kim, E.R., Fan, S., Xia, Y. and Xu, Y. *et al.* (2014). Profound and rapid reduction in body temperature induced by the melanocortin receptor agonists *Biochemical and Biophysical Research Communications*. 451 (2), 184–189.
- Xu, Y., Nedungadi, T.P., Zhu, L., Sobhani, N. and Irani, B.G. *et al.* (2011). Supplemental Information Distinct Hypothalamic Neurons Mediate Estrogenic Effects on Energy Homeostasis and Reproduction *Cell Metab*. 14 (4), 453–465.

- Yang, Y. (2011). Structure, function and regulation of the melanocortin receptors *European Journal of Pharmacology*. 660 (1), 125–130.
- Yang, Z., Kong, B., Mosser, D.M. and Zhang, X. (2011). TLRs, macrophages, and NK cells: Our understandings of their functions in uterus and ovary *International Immunopharmacology*. 11 (10), 1442–1450.
- Yeo, S.H. and Herbison, A.E. (2014). Estrogen-negative feedback and estrous cyclicity are critically dependent upon estrogen receptor-alpha expression in the arcuate nucleus of adult female mice *Endocrinology*. 155 (8), 2986–2995.
- Yeung, C.M., Chan, C.B., Leung, P.S. and Cheng, C.H.K. (2006). Cells of the anterior pituitary *International Journal of Biochemistry and Cell Biology*. 38 (9), 1441–1449.
- Zapletal, E., Kraus, O., čupić, B. and Gabrilovac, J. (2013). Differential expression of proopiomelanocortin (POMC) transcriptional variants in human skin cells *Neuropeptides*. 47 (2), 99–107.
- Zhang, J., Li, X., Zhou, Y., Cui, L. and Li, J. *et al.* (2017). The interaction of MC3R and MC4R with MRAP2, ACTH, α -MSH and AgRP in chickens *Journal of Endocrinology*. 234 (2), 155–174.
- Zhang, L., Li, W.H., Anthonavage, M. and Eisinger, M. (2006). Melanocortin-5 receptor: A marker of human sebocyte differentiation *Peptides*. 27 (2), 413–420.
- Zhang, X., Jin, B. and Huang, C. (2007). The PI3K/Akt pathway and its downstream transcriptional factors as targets for chemoprevention. *Current cancer drug targets*. 7 (4), 305–16.
- Zhou, H., Wang, X., Ko, W.K.W. and Wong, A.O.L. (2004). Evidence for a novel intrapituitary autocrine/paracrine feedback loop regulating growth hormone synthesis and secretion in grass carp pituitary cells by functional interactions between gonadotrophs and somatotrophs *Endocrinology*. 145 (12), 5548–5559.

Appendices

Appendix 1: Example of the RT-qPCR expression analysis the MC system (POMC in pituitary gland)

Calculating ΔCT (normalised raw data) by subtracting the geometric mean of the CT values of the reference genes:

$$\Delta CT = CT_{\text{gene of interest}} - CT_{\text{reference genes geometric mean}}$$

$$\Delta CT = CT_{\text{POMC}} - CT_{\text{geometric mean of YWHAZ, and CANX}}$$

$$= 19.46 - 22.58$$

$$= -3.12$$

As there are no control samples used, two-week samples were used as a reference sample or a calibrator; this was used to calculate $\Delta\Delta CT$ by subtracting ΔCT of the gene of interest from the calibrator:

$$\Delta\Delta CT = \Delta CT_{\text{gene of interest}} - \Delta CT_{\text{calibrator}}$$

$$= (-3.2916) - (-5.17)$$

$$= 2.05$$

Converting the $\log^{-2} \Delta\Delta CT$ to a linear scale was used to calculate the fold change which is the measure of the relative expression used to compare between the examined age groups and the pregnant samples.

$$\text{Fold change} = 2^{-(\Delta\Delta CT)}$$

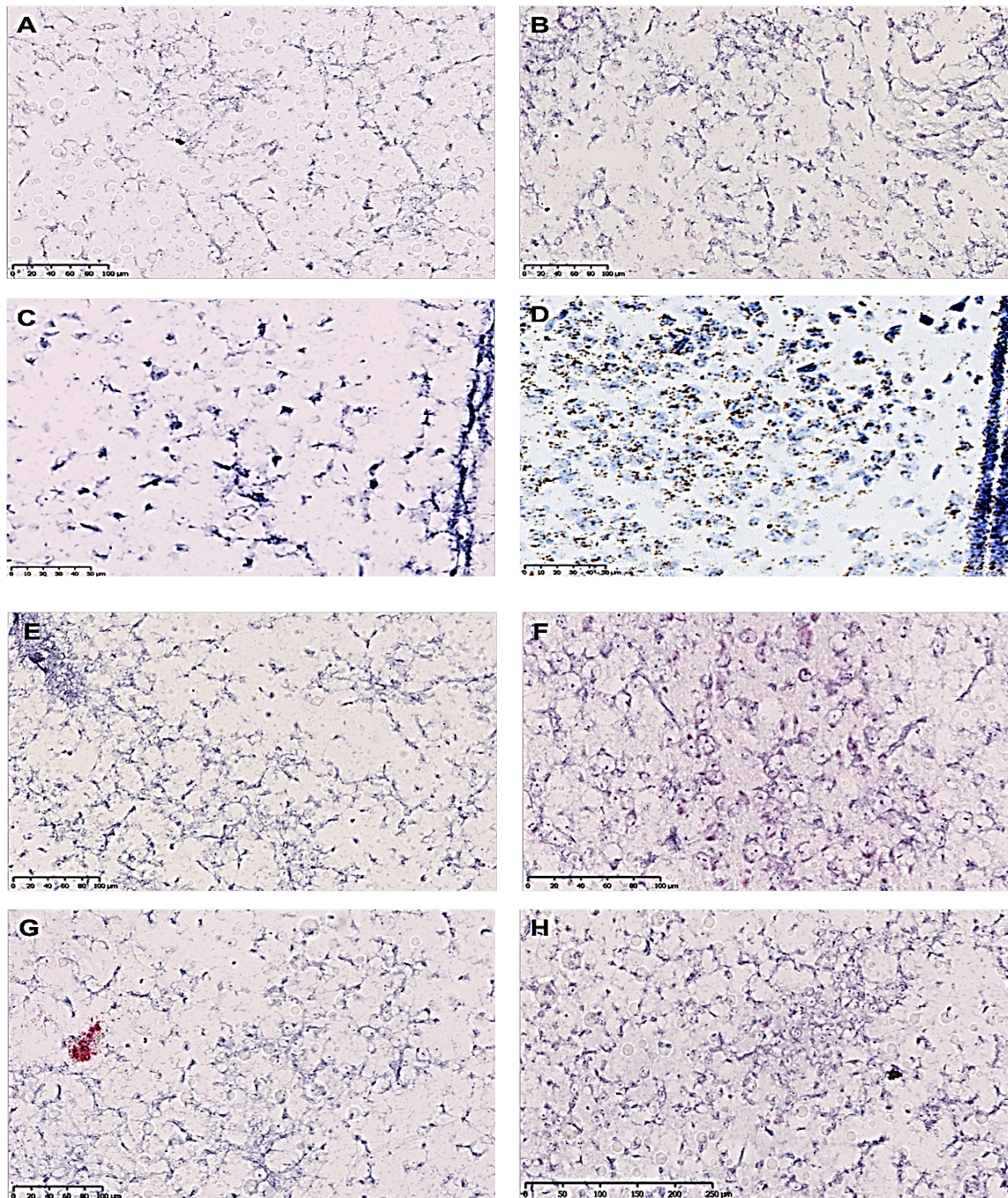
$$= 2^{(-2.05)}$$

$$= 0.241484$$

To carry out statistical analyses for expression significance assessment, the $\log^2 \Delta CT$ of the replicates were converted to the linear scale; that is, equal to $2^{-\Delta CT}$

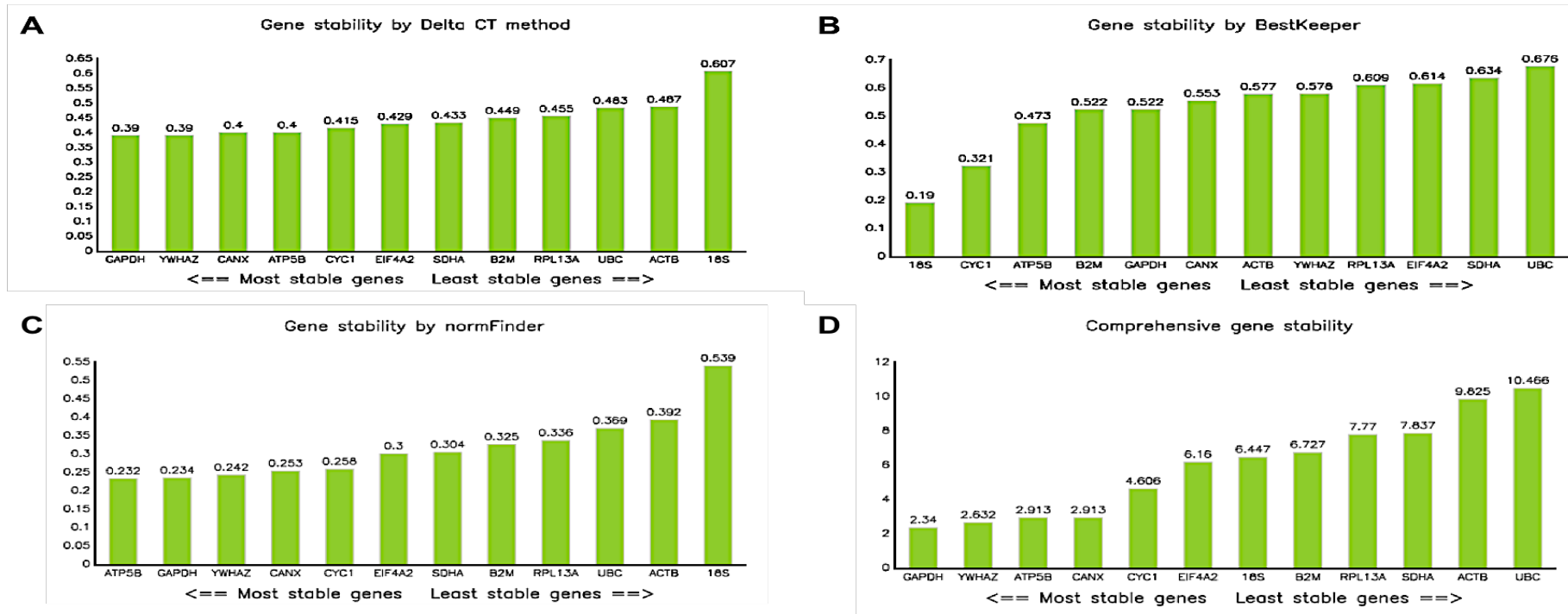
$$2^{-\Delta CT} = 8.693879$$

Appendix 2: RNAscope® pre-treatment optimisation for the hypothalamus



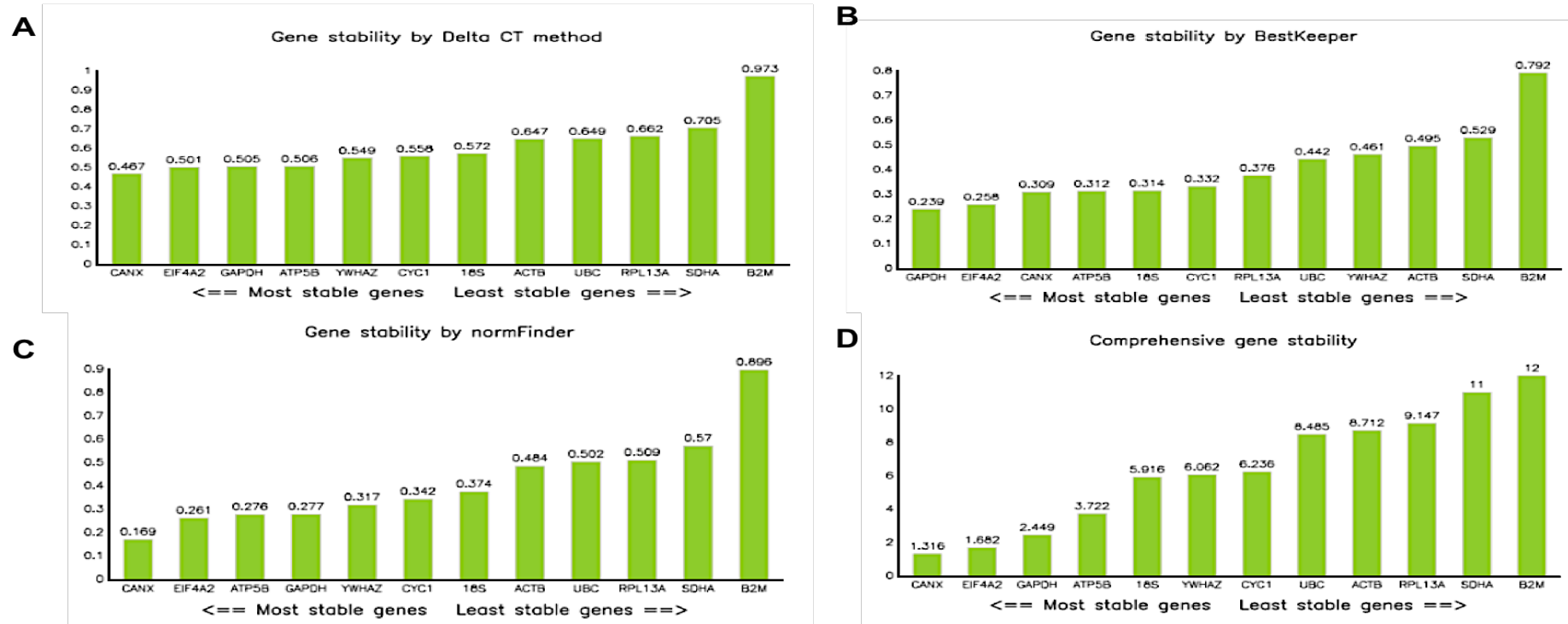
The optimisation of the pre-treatment conditions of the RNAscope® included different incubation periods of the hypothalamus sections (negative control- left side panel Figures) and positive control – right panel Figures) in the slowly boiling RNAscope® target retrieval reagent. Those time periods included 15 minutes (A and B), 17 minutes (C and D), 20 minutes (E and F) and 25 minutes (G and H). Incubating the slides for 17 minutes generated the most specific expression signal in the positive control section with no background staining in the negative control sections. Images were taken using a Nanozoomer slide scanner (Hamamatsu Photonics) at King's College London.

Appendix 3. A: Reference genes expression stability- C57BL/6 female mouse hypothalamus



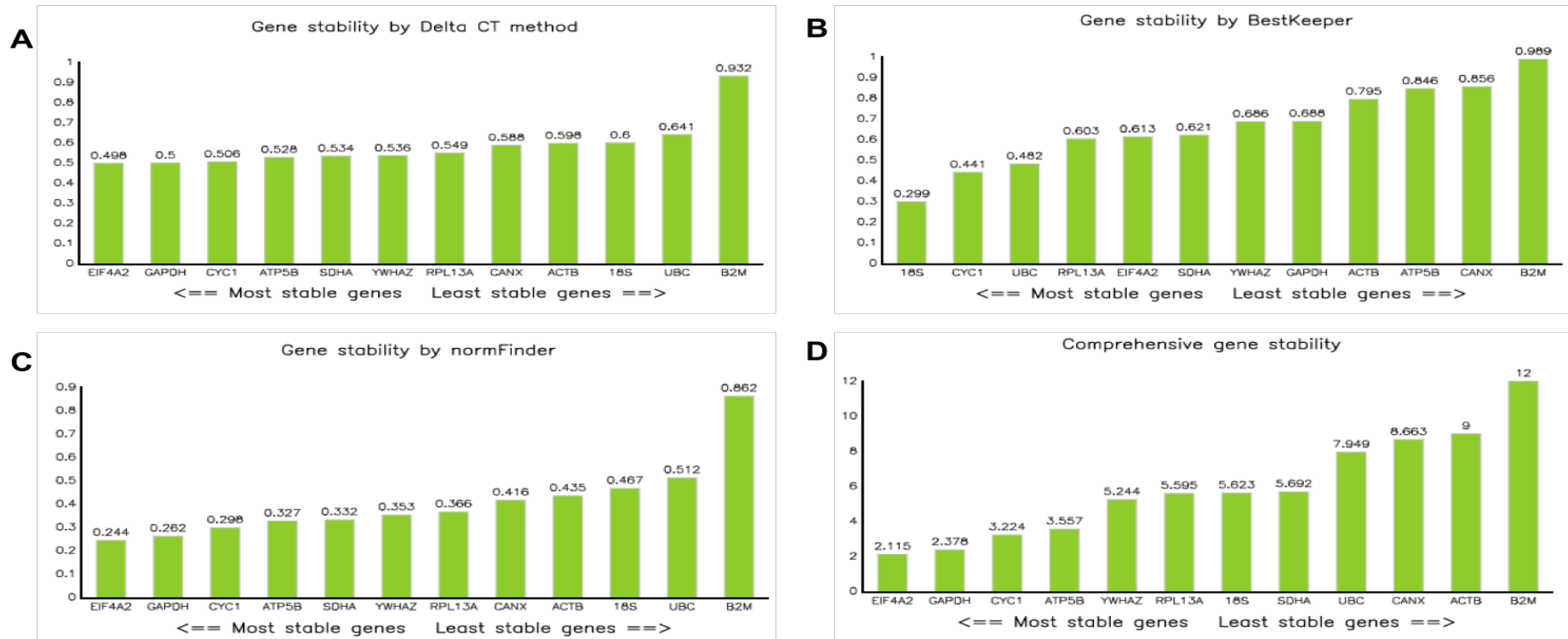
The analysis of reference genes expression stability in the C57BL/6 female mouse hypothalamus was examined in hypothalami of mice aged 2, 6, 9, 10 and 14 weeks old and pregnant (14 ± 1 dpc) mice. The results were different according to the analysis software used. **A:** Delta CT method showed GAPDH and YWHAZ to be the most stable whereas ACTB and 18S were the least stable. **B:** BestKeeper software showed 18S and CYC1 to be the most stable whereas SDHA and UBC were the least stable. **C:** NormFinder software showed ATP5B and GAPDH to be the most stable genes whereas ACTB and 18S as the least stable. The last graph shows the comprehensive ranking of the reference genes expression stability after analysing data collected from the mentioned software as well as GeNorm with GAPDH and YWHAZ being the most stable whereas ACTB and UBC the least stable (**D**). The software Delta CT, BestKeeper, NormFinder and Comprehensive ranking is available from <http://150.216.56.64/referencegene.php?type=reference>.

Appendix 3. B: Reference genes expression stability- C57BL/6 female mouse pituitary gland



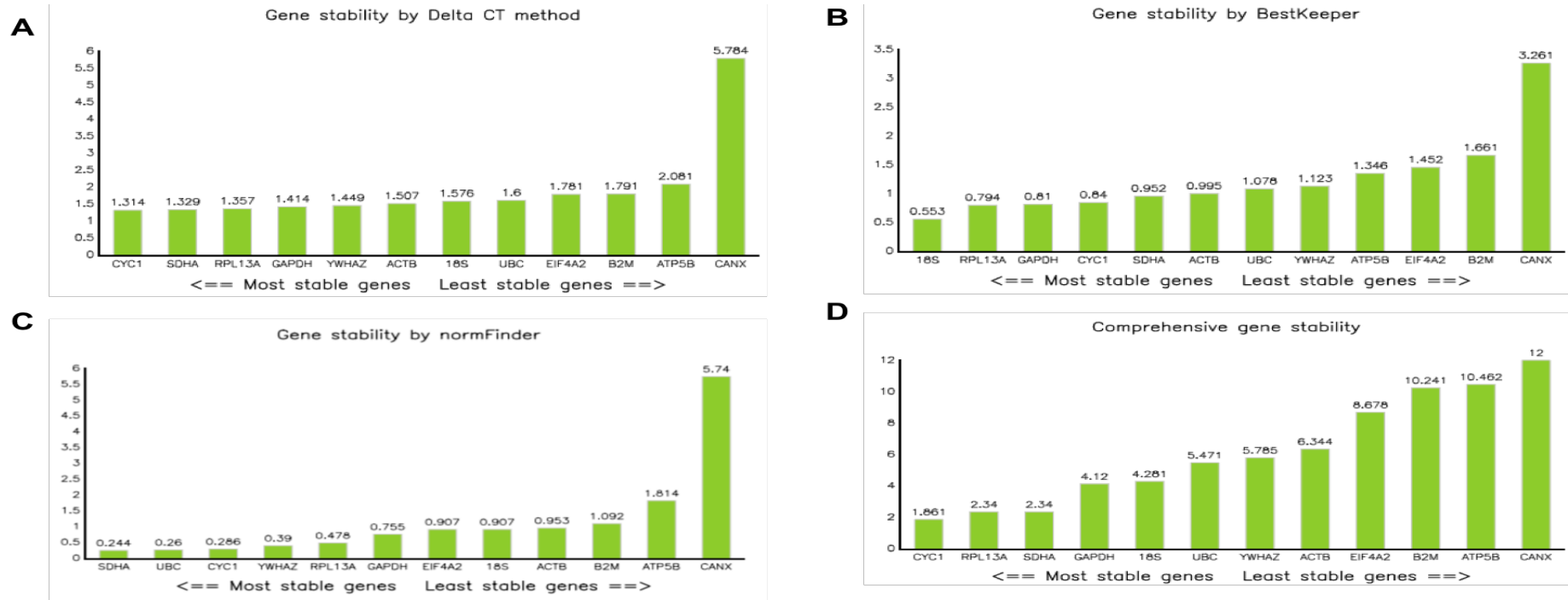
The analysis of reference genes expression stability in the C57BL/6 female mouse pituitary gland was examined in pituitaries of mice aged 2, 6, 9, 10 and 14 weeks old and pregnant (14 ± 1 dpc) mice. The results were different according to the analysis software used. **A:** Delta CT method showed CANX and EIF4A2 to be the most stable whereas SDHA and B2M were the least stable. **B:** BestKeeper software showed GAPDH and EIF4A2 to be the most stable whereas SDHA and B2M were the least stable. **C:** NormFinder software showed CANX and EIF4A2 to be the most stable genes whereas SDHA and B2M as the least stable. The last graph shows the comprehensive ranking of the reference genes expression stability after analysing data collected from the mentioned software as well as GeNorm with CANX and EIF4A2 being the most stable whereas SDHA and B2M the least stable (**D**). The software Delta CT, BestKeeper, NormFinder and Comprehensive ranking is available from: <http://150.216.56.64/referencegene.php?type=reference>.

Appendix 3. C: Reference genes expression stability- C57BL/6 female mouse ovary



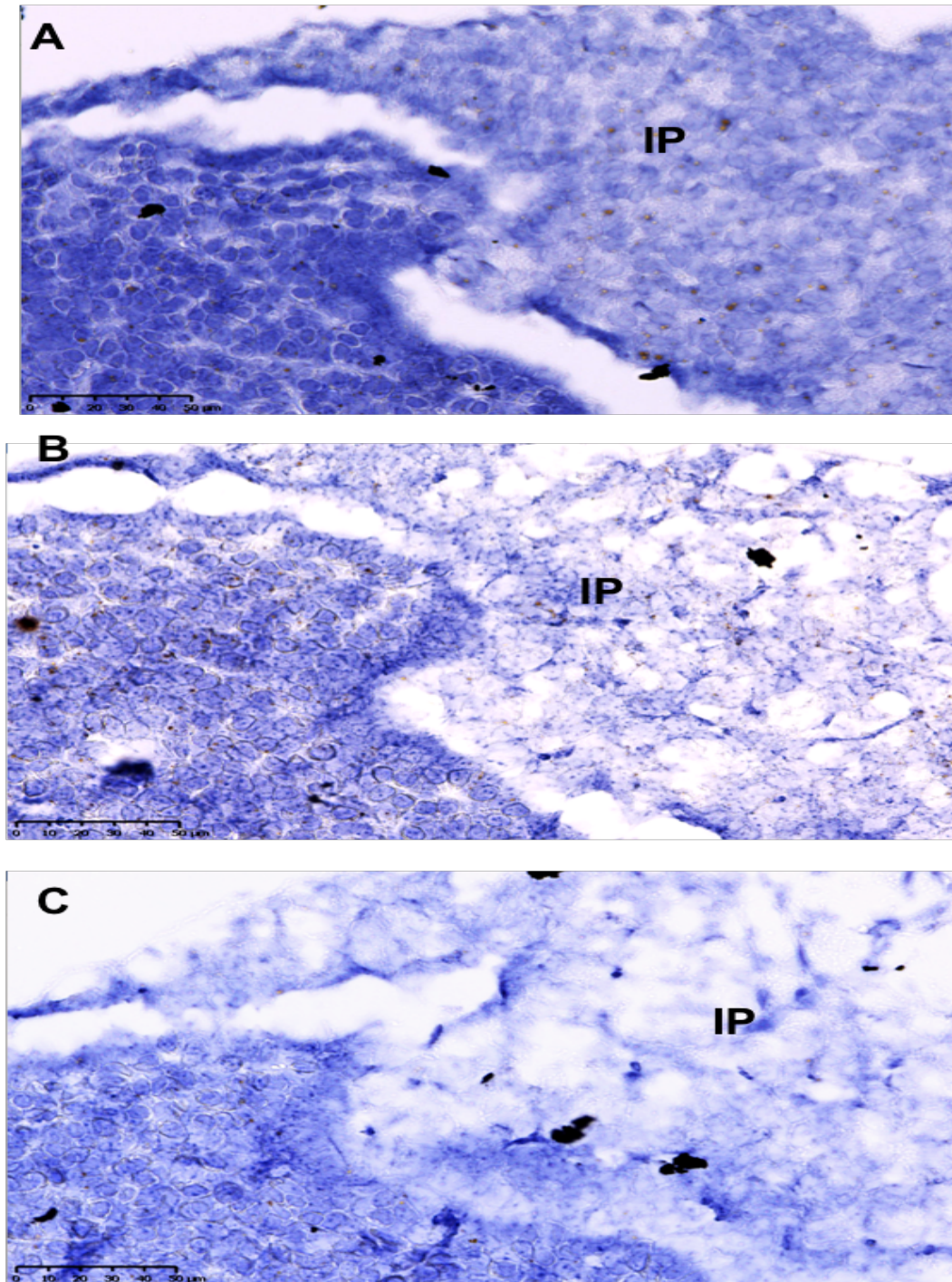
The analysis of reference genes expression stability in the C57BL/6 female mouse ovary was examined in ovaries of mice aged 2, 6, 9, 10 and 14 weeks old and pregnant (14 ± 1 dpc) mice. The results were different according to the analysis software used. **A:** Delta CT method showed EIF4A2 and GAPDH to be the most stable whereas UBC and B2M were the least stable. **B:** BestKeeper software showed 18S and CYC1 to be the most stable whereas CANX and B2M were the least stable. **C:** NormFinder software showed EIF4A2 and GAPDH to be the most stable genes whereas UBC and B2M as the least stable. The last graph shows the comprehensive ranking of the reference genes expression stability after analysing data collected from the mentioned software as well as GeNorm with EIF4A2 and GAPDH being the most stable whereas ACTB and B2M the least stable (**D**). The software Delta CT, BestKeeper, NormFinder and Comprehensive ranking is available from: <http://150.216.56.64/referencegene.php?type=reference>.

Appendix 3. D: Reference genes expression stability- C57BL/6 female mouse uterus



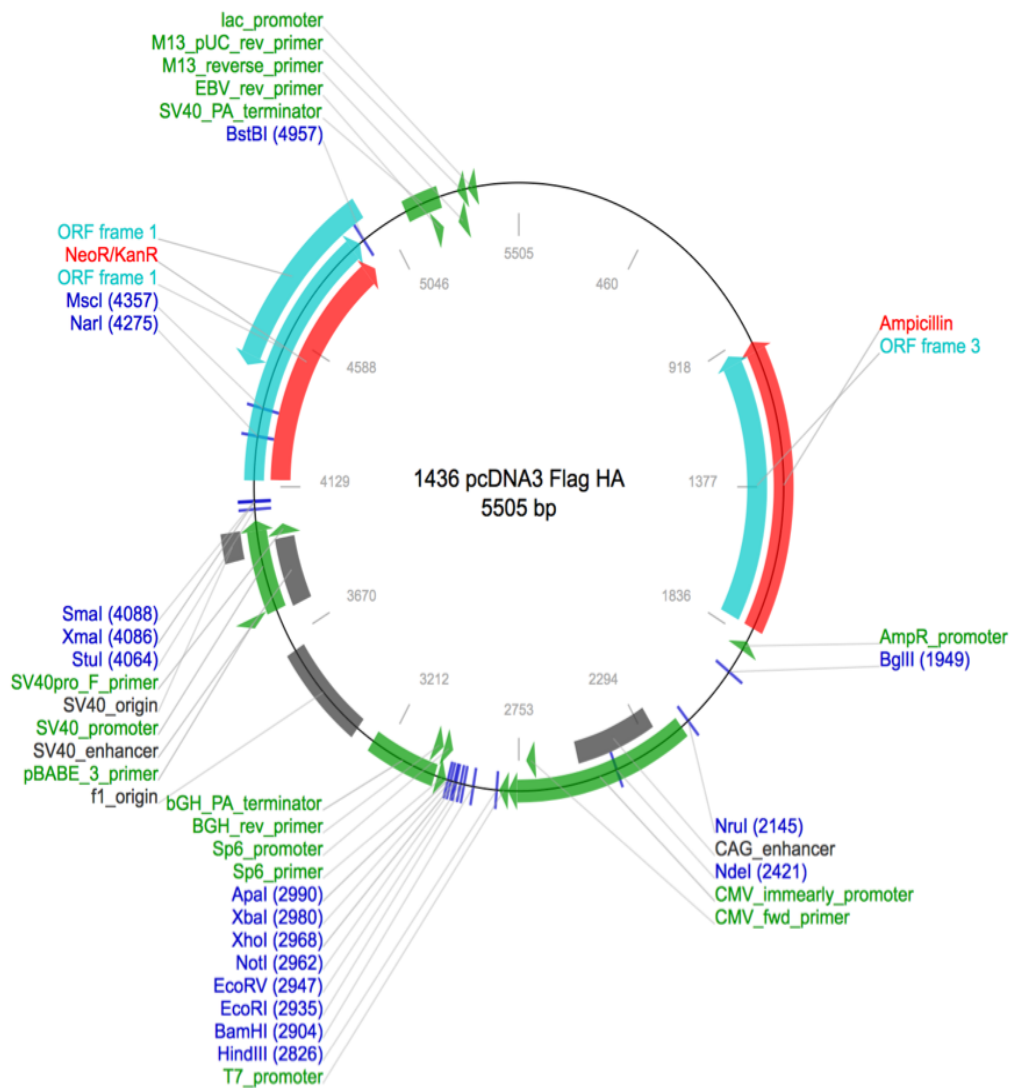
The analysis of reference genes expression stability in the C57BL/6 female mouse uterus was examined in uteri of mice aged 2, 6, 9, 10 and 14 weeks old and pregnant (14 ± 1 dpc) mice. The results were different according to the analysis software used. **A:** Delta CT method showed CYC1 and SDHA to be the most stable whereas ATP5B and CANX were the least stable. **B:** BestKeeper software showed 18S and RPL13A to be the most stable whereas B2M and CANX were the least stable. **C:** NormFinder software showed SDHA and UBC to be the most stable genes whereas CYC1 and RPL13A as the least stable. The last graph shows the comprehensive ranking of the reference genes expression stability after analysing data collected from the mentioned software as well as GeNorm with CANX and EIF4A2 being the most stable whereas SDHA and B2M the least stable (**D**). The GeNorm was substantially different from the results of the other three software in the reference genes expression stability analysis in the uterus. The software Delta CT, BestKeeper, NormFinder and Comprehensive ranking is available from: <http://150.216.56.64/referencegene.php?type=reference>.

Appendix 4: The RNAscope® 2.5HD brown assay: the expression of MC3, MC5 and MRAP2 in the intermediate lobe of the female mouse pituitary gland



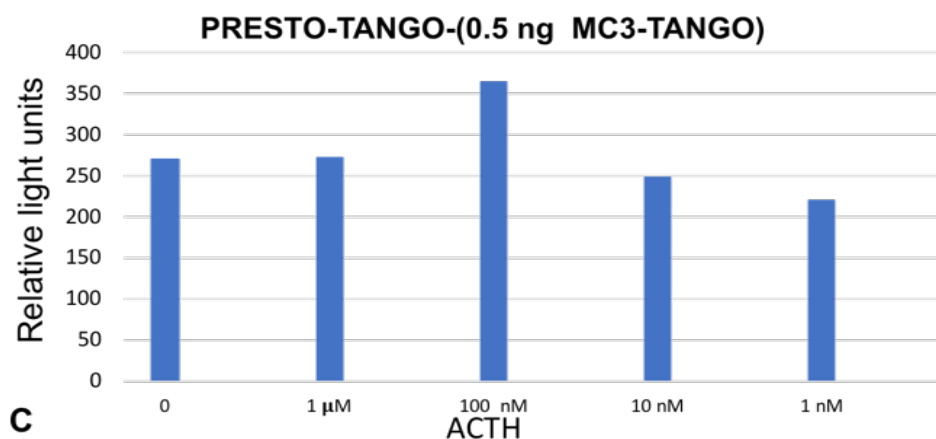
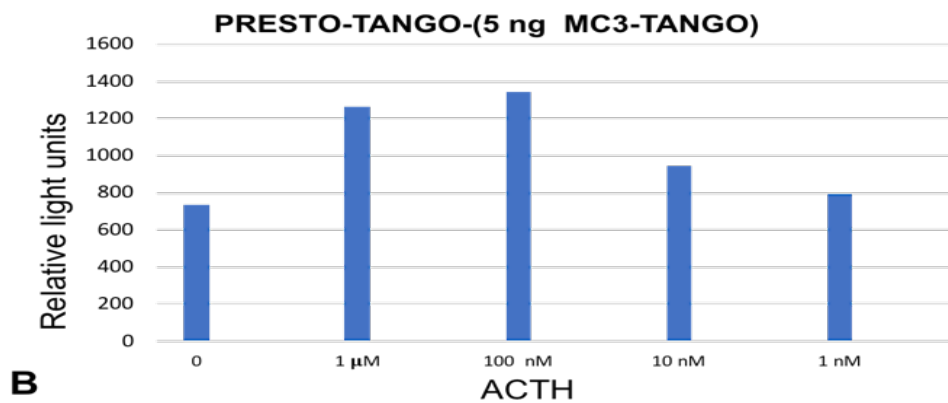
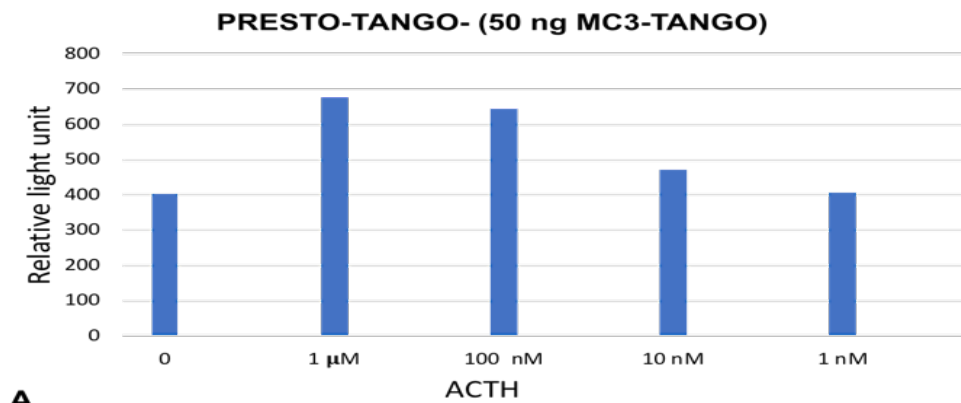
The RNAscope® 2.5HD brown assay in the C57BL/6 female mouse pituitary gland had revealed the expression as brown expression signals in the intermediate lobe of the pituitary gland (IP) of mice aged 2, 10 weeks old and pregnant (14 ± 1 dpc) mice. A: Expression of *MC3* in the intermediate pituitary. B: Expression of *MC5* in the intermediate pituitary (outlined in the black circles). C: Expression of *MRAP2* in the intermediate pituitary. Images were taken using a NanoZoomer slide scanner (Hamamatsu Photonics) at King's College London.

Appendix 5: The Full Sequence Map for 1436 pcDNA3 Flag HA



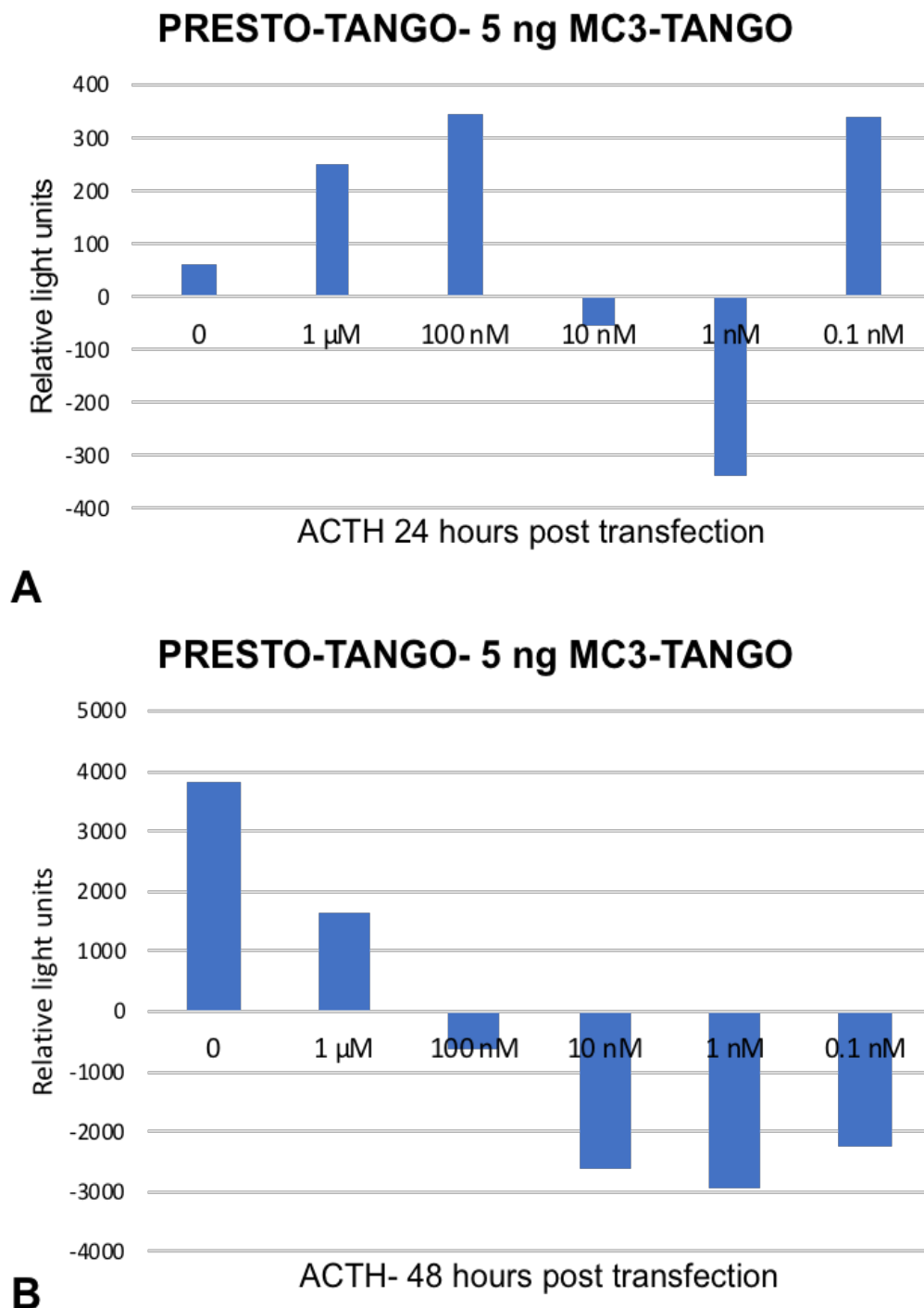
Mammalian expression vector (empty backbone) pCDNA3 vector with added FLAG tag epitope. The backbone empty vector size is 5446 bp. Sequence map obtained from Addgene (USA).

Appendix 6: PRESTO-Tango: choosing a transfection concentration for MC₃-Tango



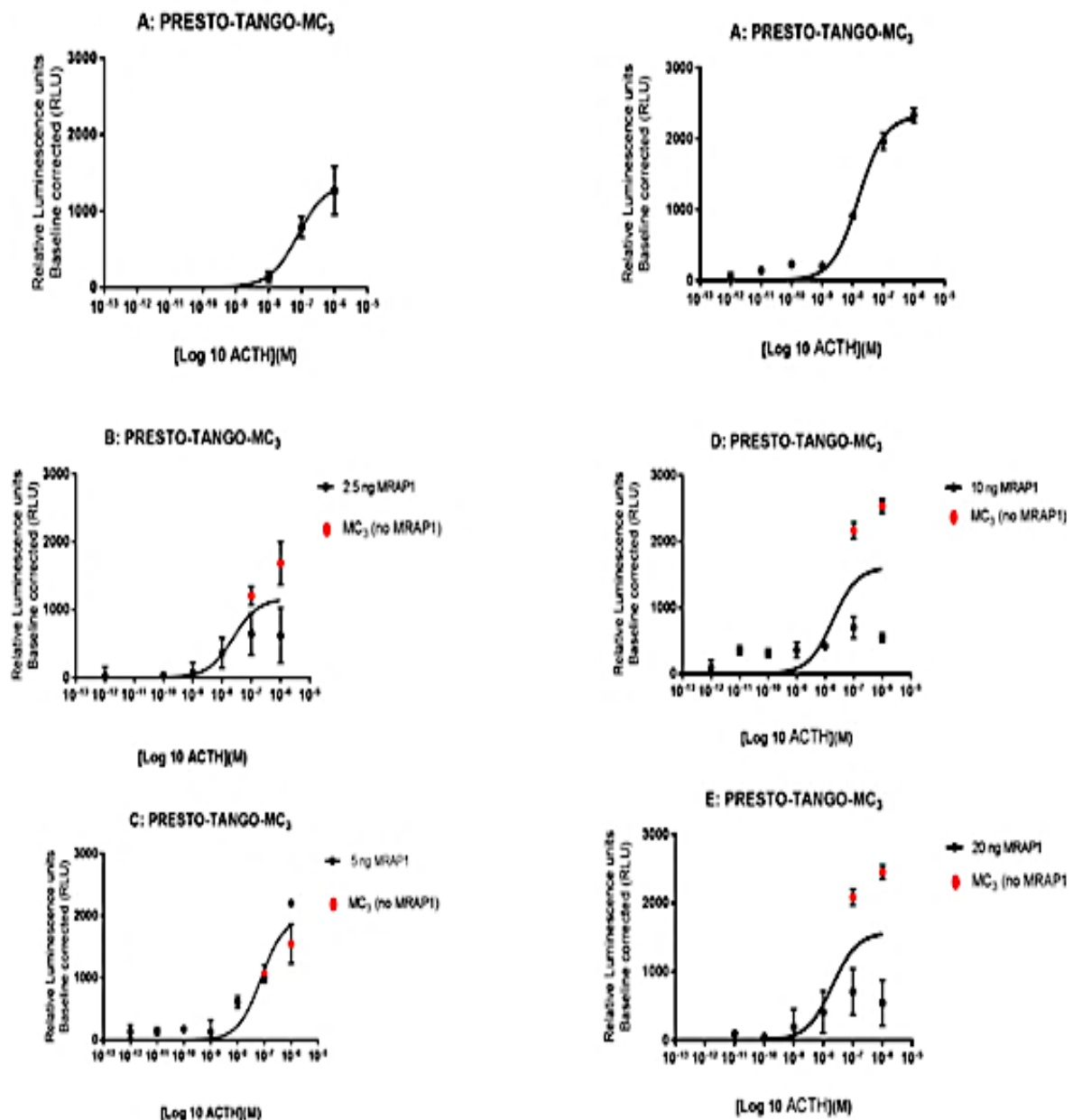
The luminescence activity of different concentrations of MC₃-Tango used in the transfection of the HTLA cells. All of the reactions had a total reaction of 50 ng (B and C were supplemented with 45 ng and 49.5 ng of pCDNA3.1 respectively). The MC₃-Tango concentration of 5 ng (B) was the concentration to be used in the PRESTO-Tango assay due to optimal luminescence activity compared to the luminescence activity generated in A and C. This was repeated twice and summary of results are represented in these graphs

Appendix 7: PRESTO-Tango: Determination of HTLA incubation period post-transfection and addition of stimulants



After transfection with MC3-Tango the HTLA cells were incubated for either 24 hours (A) or 48 hours (B) before adding the stimulants (ACTH in these experiments) in humidified atmosphere at 37°C. The luminescence activity produced by MC₃ stimulated 48 hours (B) was about 10 folds higher than that of the MC₃ stimulated 24 hours after HTLA transfection. Therefore, the stimulants in the subsequent PRESTO-Tango experiments were to be added 48 hours post transfection.

Appendix 8: PRESTO-Tango: Determining MRAP1 concentrations to be used in the co-transfection with MC3-Tango



Prior to co-transfecting the HTLA cells with MC₃-Tango and MRAP1, the concentration of *MRAP1-pCDNA3.1-FLAG* needed to be determined for the co-transfection. A range of concentrations [2.5 ng (B), 5 ng (C), 10 ng (D) and 20 ng (E)] of the plasmid was used in co-transfection with MC₃-Tango. The luminescence activity was found to be higher with only 5 ng of *MRAP1-pCDNA3.1-FLAG* compare to MC₃-Tango (As) alone and to other examined concentrations. This was conducted twice and summary of results are represented in these graphs. The concentration of 5 ng of *MRAP1-pCDNA3.1-FLAG* was determined to be used in the co-transfection of MC₃-Tango and *MRAP1*.